I-A3a

CRREL / Monograph I-A3a

COLD REGIONS SCIENCE AND ENGINEERING

Part I: Environment

Section A3: Climatology

INTRODUCTION
NORTHERN HEMISPHERE I

by

C. Wilson

20080813 369

JUNE 1967

U.S. ARMY MATERIEL COMMAND

COLD REGIONS RESEARCH & ENGINEERING LABORATORY

HANOVER, NEW HAMPSHIRE

AD-656447

COLD REGIONS SCIENCE AND ENGINEERING

Part I: Environment

Section A3: Climatology

INTRODUCTION
NORTHERN HEMISPHERE I

by

C. Wilson

JUNE 1967

U.S. ARMY MATERIEL COMMAND
COLD REGIONS RESEARCH & ENGINEERING LABORATORY
HANOVER, NEW HAMPSHIRE

DA Project IVO25001A130

PREFACE

This report on the climatology of the cold regions is presented in four separate parts for the sake of convenience. It is essentially one monograph.

Part a contains a general introduction to the cold regions, and a discussion of the geographical controls, the atmospheric circulation, the net radiation, and the heat balance of the Northern Hemisphere.

Part b concludes the study of the Northern Hemisphere with a survey of the resulting temperature, humidity and wind conditions, and a list of general references and data sources.

Part c is devoted to the Southern Hemisphere.

Part d is on radioactive fallout in the northern regions. The treatment is mainly geographical, with emphasis on spatial distributions and their variation in time. Specific references were selected from over 2,000 publications used in preparation of the monograph.

Some physical aspects of micrometeorology are dealt with by Dr. R.F. Scott in Heat Exchange at the Ground Surface, II-A1 in this series.

The author, Cynthia V. Wilson, wrote the monograph while on the faculties of McGill University, and of Laval University, where she lectures in climatology with a background of geography and meteorology.

This is a review summary and the "reviewer" is indebted to many people and organizations who have granted permission for work to be reproduced and, in some cases, have made available unpublished work. Special thanks are due to Dr. F.K. Hare of London University, Dr. S. Orvig and Dr. E. Vowinckel of McGill University, Montreal, and Dr. R.J. Reed of the University of Washington, whose regional studies have provided basic references; and to Dr. R.W. Gerdel and others of the staff of USA CRREL for their help and criticism.

USA CRREL is an Army Materiel Command laboratory.

CONTENTS

ILLUSTRATIONS

CONTENTS (Cont'd)

TABLES

EDITOR'S FOREWORD

"Cold Regions Science and Engineering" consists of a series of monographs written by specialists to summarize existing knowledge and provide selected references on the Cold Regions, defined here as those areas of the earth where the freezing and thawing of soils is an essential consideration in engineering.

Sections of the work are being published as they become ready, not necessarily in numerical order but fitting into this plan, which may be amended as the work proceeds:

I. <u>Environment</u>

- A. General
  1. Geology and physiography
  2. Permafrost
  3. Climatology
     - a. General and Northern Hemisphere 1
     - b. Northern Hemisphere 2
     - c. Southern Hemisphere
     - d. Radioactive fallout in the Northern Hemisphere
  4. Vegetation
     - a. Patterns of vegetation
     - b. Regional descriptions
     - c. Utilization of vegetation
- B. Regional
  1. The Antarctic ice sheet
  2. The Greenland ice sheet

II. <u>Physical Science</u>

- A. Geophysics
  1. Heat exchange at the earth's surface
  2. Exploration geophysics
- B. Physics and mechanics of snow as a material
- C. Physics and mechanics of ice
  1. Snow and ice on the earth's surface
  2. Ice as a material
  3. The mechanical properties of sea ice
- D. Physics and mechanics of frozen ground

EDITOR'S FOREWORD (Cont'd)

III. Engineering

A. Snow engineering

1. Engineering properties of snow
2. Construction
3. Technology
   a. Explosions and snow
   b. Snow removal and ice control
   c. Blowing snow
   d. Avalanches
4. Oversnow transportation

B. Ice engineering

C. Frozen ground engineering

1. Site exploration and excavation
2. Buildings, utilities and dams
3. Roads, railroads and airfields
4. Foundations
5. Sanitary engineering
   a. General and water supply
   b. Sewerage and waste disposal
6. Cold weather construction

D. General

F.J. SANGER

CLIMATOLOGY OF THE COLD REGIONS

Part a. Introduction. Northern Hemisphere I

by

Cynthia Wilson

INTRODUCTION

The Limits of the Cold Regions

Climate involves the integration of many variables, and classifications will differ widely according to the criteria chosen. Köppen[6,7] * and Thornthwaite[8,9] have provided the two most widely used schemes, both based on the vegetation cover, which Köppen saw as a resultant of climate and Thornthwaite as an active agent in the process of energy exchanges at the earth's surface. The major differences between them[3] concern the combination of the moisture and heat elements; in the cold regions, however, the moisture content of the air is so low at saturation point that temperature is the predominant factor and the two systems converge.

Figures 1a and 1b show the limits of cold climates using Köppen's criteria:

(a) a mean temperature of less than -3C for the coldest month (the highest value at which a snow cover can persist for an appreciable period during the winter season), and

(b) not more than four months with a mean temperature of 10C.

The breakdown based on the severity of the winter and the seasonal distribution of precipitation is indicated and explained in the key to Figure 1a, b. In both hemispheres the limits extend toward the equator as far as latitude 45°; however, the influence of the meridional distribution of land and sea and of major topography in the northern hemisphere is reflected in the poleward (60°N) embayments off the west coast of America and Eurasia, and in the southern extension over the continents.

The vertical limit of land areas included in this study has been fixed arbitrarily at approximately 3000m (700 mb). This is roughly the surface level of both the Greenland and Antarctic ice sheets; elsewhere it is representative of the general circulation of the free atmosphere, above the major effects of the interaction of the earth's surface and the lowest layer of the atmosphere (Fig. 1c, d), which are restricted for the most part to the lowest 1500m (850 mb). Cold regions in lower latitudes, which are due to elevation, have been omitted. The meteorological conditions differ from those in high latitudes and from one locality to another.

---

* Reference numbers refer to the bibliography at the end of each section. See also Landsberg, H.E. et al. "World Maps of Climatology," Springer-Verlag, New York, Inc., 1965.

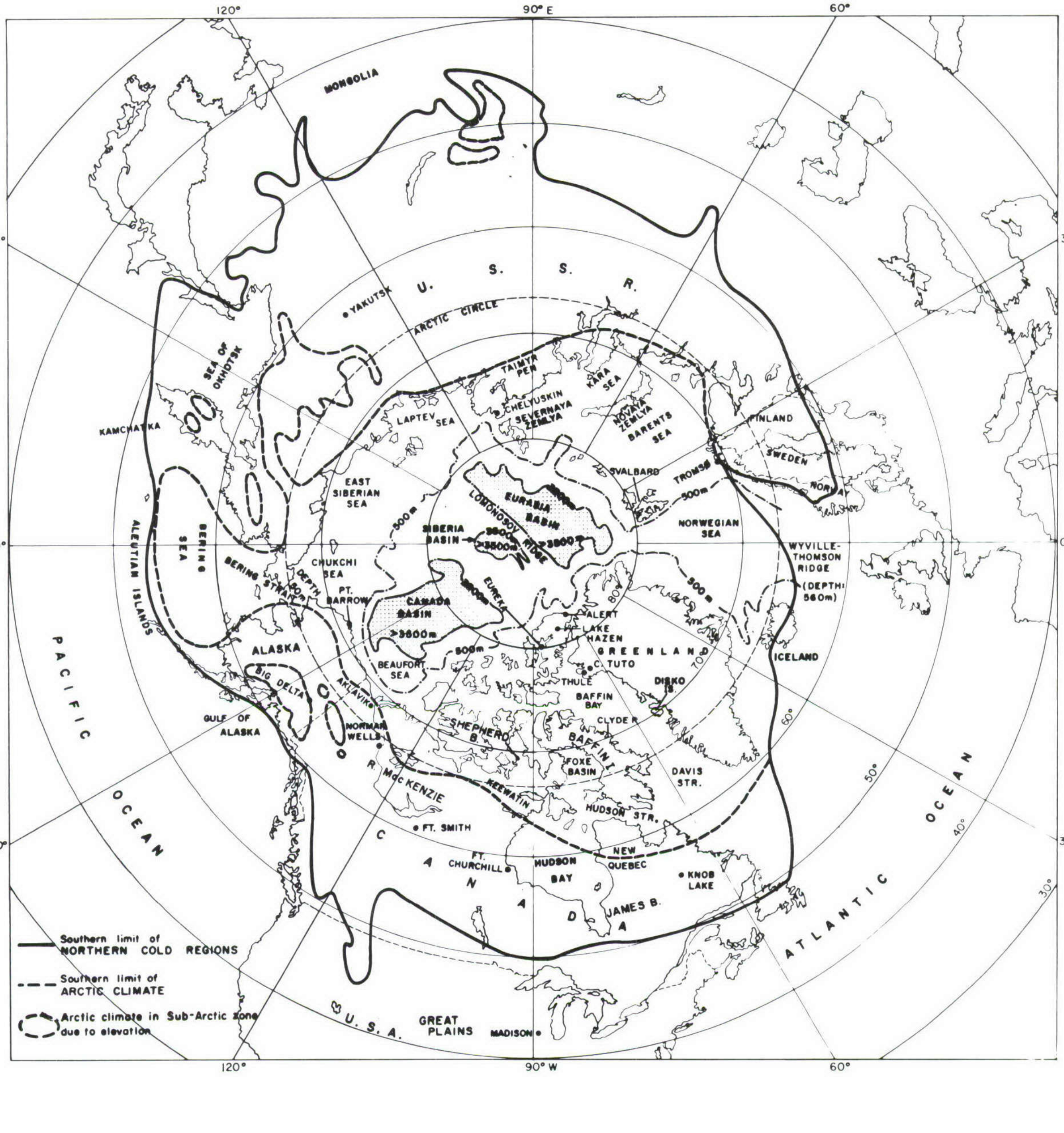

Figure 1a. Northern Cold Regions: key map.

Climatic limits - key to Figures 1a, b (After Köppen, cf. Haurwitz and Austin.[4])

1. Major climatic types

   E Polar (snow) climates. Mean temperature for warmest month below 10C.

   D Cold, snow-forest climates. Mean temperature for coldest month less than -3C and warmest month above 10C.

2. Subdivisions

   - E
     - ET (tundra) Mean temperature of warmest month above zero C (but below 10C).
     - EF (frost) Mean temperature of every month below freezing. Permanent snow.
     - E (Falkland) Mean temperature of coldest month greater than -3C. (But warmest month less than 10C.)
     - EH (mountain) Mountain type of lower latitudes (greater than 1500 m).
   - D
     - Seasonal precipitation distribution
       - f No dry season. Precipitation of wettest month in cold season less than 3 times that of driest month in warm season.
       - w Dry winters. Driest month of cold season less than or equal to 1/10 precipitation of wettest month in warm season.
     - Severity of winter temperature
       - c Mean temperature of coldest month between -38C and -3C. (Only 1 to 4 months with mean temperature greater than 10C and not more than 22C.)
       - d Mean temperature of coldest month less than -38C. (Only 1 to 4 months with mean temperature greater than 10C, and not more than 22C.)

3. Summary

EF	Frost or Ice Cap	
ET	Tundra	
E	Falkland Type	
EH	Mountain Type	
Dfc	Cold winters, no dry season	Cold snow-forest (cool short summers)
Dfd	Severe winters, no dry season	
Dwc	Cold dry winters, moist summers	
Dwd	Severe dry winters, moist summers	

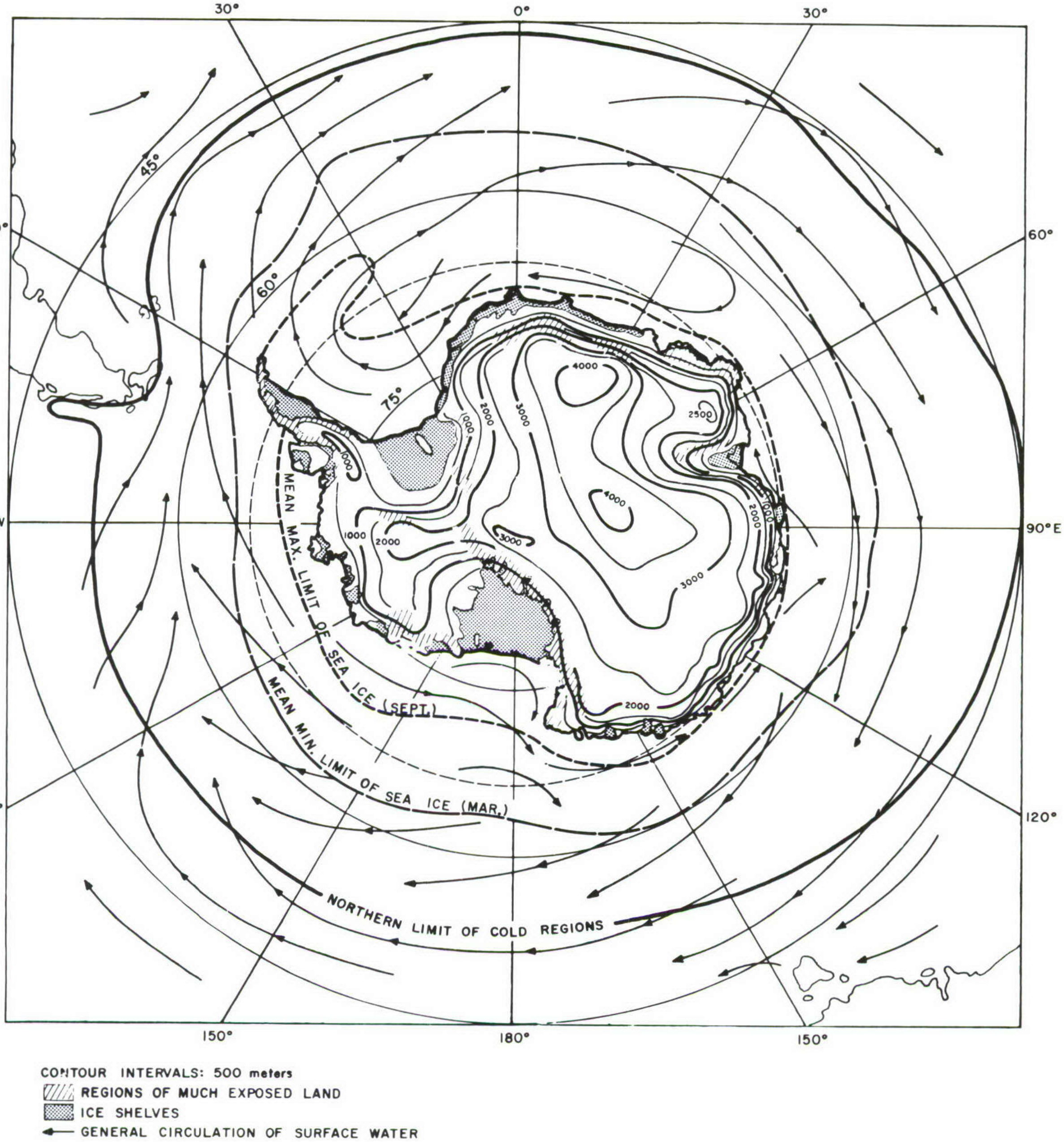

Figure 1b. Southern Cold Regions: general map.

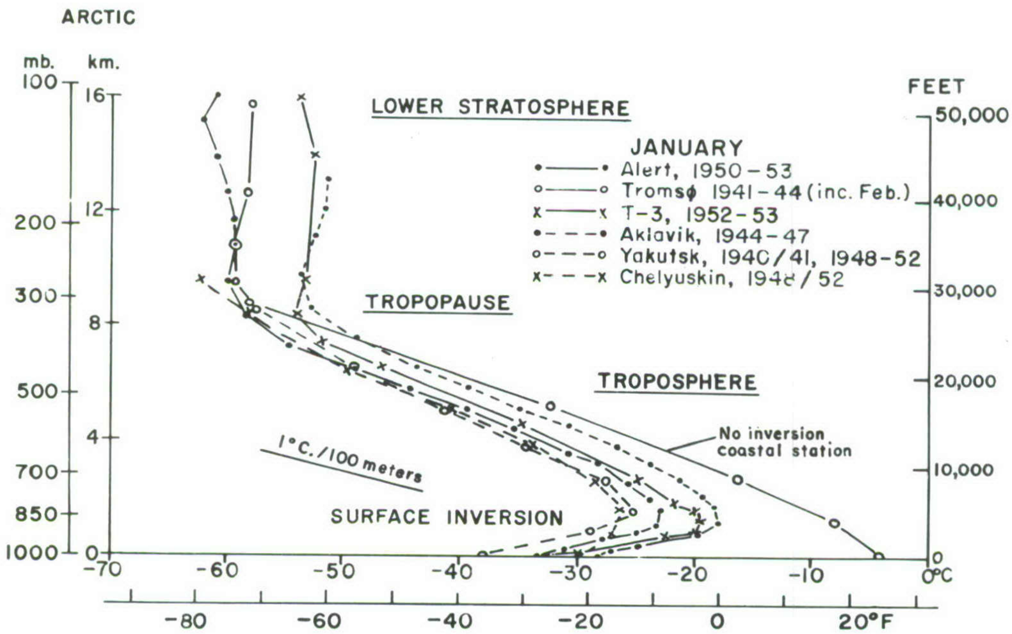

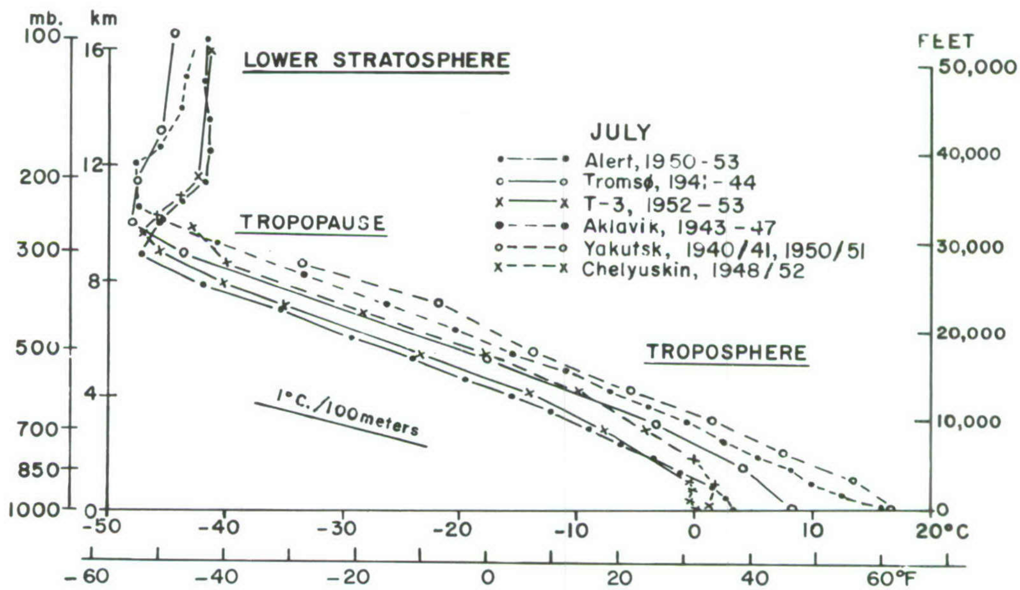

Figure 1c. Northern Cold Regions: mean temperature profiles (after Hare and Orvig, 1958).

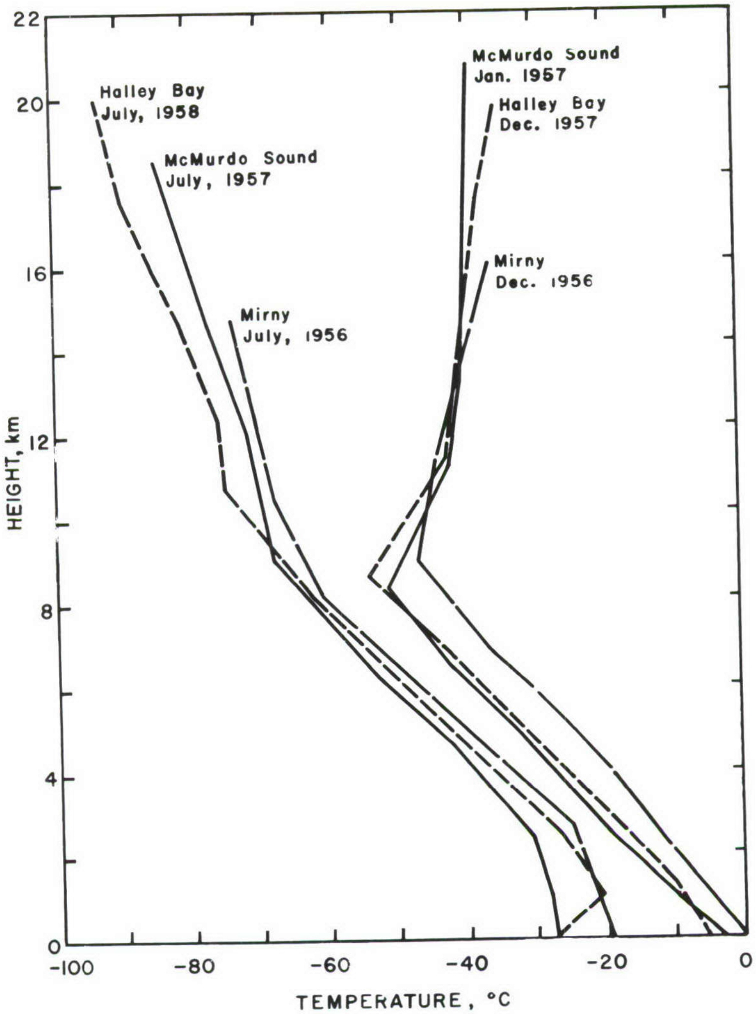

Figure 1d. Southern Cold Regions: mean temperature profiles.

A major criticism of the Köppen limits, based on mean temperature values, is their static quality. This is especially true over the northern continental masses, where outbreaks of frigid Arctic air can extend Arctic conditions into mid-latitudes. Such circulation patterns can be highly persistent, and the southern extent of the regions varies widely within each winter and from year to year, depending on their frequency and intensity. A partial solution to this problem is offered in a recent alternative definition of cold regions based on the frequency of occurrence of low temperatures.[2] In this case the 1% occurrence of -25F (-32C) in January was chosen as significant; that is, those areas where -25F (-32C) or lower occurs in January more often than once in 3 years are classified as cold. With the increasing amount of data available and modern high speed processing, such an approach is becoming realistic (cf. monograph I-A3 b).

Major differences between the Arctic and Antarctic are brought about by the reversed distributions of the oceans and continental masses, and the two areas will therefore be treated separately.

The General Nature of Cold Climates

Cold climates in high latitudes are characterized by:

(a) A distinctive regime of daylight and darkness together with low solar elevation, which give rise to a prolonged period of radiational loss from the earth's surface.

(b) Surface weather systems associated with the large-scale, cold-cored circumpolar vortex* present in the free atmosphere of each hemisphere – a function of the differential heating between the equator and poles and the earth's rotation. Already apparent at 1500 m (850 mb), these upper air flow patterns reach their greatest intensity near 10,000 m (200 mb). Surface cyclones and anticyclones responsible for much of the weather are embedded in and steered by this flow, so that changes in the shape and position of the vortex can radically affect regional conditions.

(c) A snow/ice cover during at least an appreciable part of the year. In cold regions the nature of the surface is largely a question of whether or not there is a snow/ice cover. The difference in the percentage of absorbed solar radiation is as great as 60% (< 20% absorption with a fresh snow surface compared with > 80% in most snow-free regions). The immediate effect of changes in this cover on the heat exchange at the surface is so great that these regions can be said to have two seasons only, with a swift transition of a week or two at the spring thaw and the fall freeze-up. Over the permanent ice caps and the polar pack ice during the brief summer, the ice maintains the air temperature at about zero C, while temperatures in snow/ice-free areas can reach 21C or 27C. Towards mid-latitudes in the periglacial zone, as the length of the snow-free period increases, variations from winter to winter in the timing and continuity of the snow cover become more important, and the number of freeze-thaw cycles in the year increases rapidly. The continental subarctic can experience minimum temperatures as low as the central Arctic Basin, but on approaching the total winter darkness at the pole, the persistence of low temperatures increases. With the "reversed" topography of the Antarctic, factors of continentality, elevation and outgoing radiation are strongest in the general vicinity of the pole itself and lowest temperatures are recorded over the central Antarctic ice cap – including the extreme lowest temperature on record, -126.9F (-88.3C) at Vostok.

The presence of a snow/ice cover plays an important role in the modification of airmasses crossing these regions. Cyclones depend on temperature contrast and generally speaking their intensity and frequency are closely allied to the sharp gradients at the margins of the snow/ice cover and open water; over the central polar regions they stagnate and fill. The distribution of precipitation is largely related to the passage of

---

* A cyclonic vortex in which, in the middle latitudes, the movement is predominantly from west to east.

cyclones over open water, and the occasional open leads in winter become important heat and moisture sources. However, the cooling of the airmasses over the snow and ice reduces the water-holding capacity of the air to such an extent that the greater part of polar regions is virtually a desert. This coldness of the air leads to the characteristic precipitation of small, dry, hard snow particles, which are easily redistributed by the wind to produce blowing snow storms. Middle and high clouds are also associated with cyclonic activity, but, owing to the dryness of the air, the clouds tend to be less dense over the central Arctic. Low cloud and fog, characteristic of coastal areas and the broken pack ice in summer, are essentially linked with the distribution of snow/ice and open water. The combination of overcast sky and an unbroken snow/ice surface produces the optical phenomenon of whiteout.

It is characteristic of snow and ice conditions that once a certain critical growth is reached, they tend to be self-perpetuating. However, where there is a snow/ice-free period, the relationship between the earth's surface and the atmosphere is finely balanced and any induced changes resulting in a crossing of the freeze-thaw threshold can significantly alter the complex association. Animal and human destruction of the natural cover and additions to the heat and moisture sources have set off irreversible chain reactions.

(d) A strong temperature inversion* above the snow/ice surface, the result of strong radiational cooling. In winter, the average depth of this inversion layer is 1200 to 1500 m (850 mb). Development is most intense under calm, clear anticyclonic conditions, when outgoing radiation is unhindered; extremely low temperatures can occur. Inherently a stable feature under conditions of negative radiation balance at the surface in winter, it is only temporarily or partially cleared by the strong winds, cloud cover or precipitation associated with cyclonic activity, and rapidly re-forms. In summer this type of inversion is confined to the pack ice and ice cap surfaces. It is less intense at this season and is frequently "lifted" off the surface by the presence of a shallow "mixing layer" over the ice itself. The configuration of the surface plays an important role in the local intensity and persistence of the inversion. Where the dense cold air is trapped in hollows and valleys, as for example in the Yukon and northeastern Siberia, some of the lowest temperatures have been recorded. Over the curved surfaces of the ice caps, the dense cold air appears to drain off in surges under gravitation (katabatic winds). Recent study suggests that these may be triggered by flow conditions in the free atmosphere. The strong density gradients associated with the inversion frequently give rise to optical effects such as mirages, while the supersaturation of air below about -40C through human or animal activity or combustion processes leads to the spontaneous formation of persistent ice fogs.

---

* An increase in temperature with height, a reversal of the normal conditions.

Meteorological Observation at High Latitudes

Until the Second World War, meteorological observations at polar latitudes were mainly confined to sporadic expedition data, and for many regions these remain the only first-hand knowledge of local conditions. In high northern latitudes there were only a few stations where regular observations had been taken over several decades. Since the war, defense interests in the Arctic and the stimulus of the International Geophysical Year have led to a rapid increase in the knowledge of cold climates.

Broad-scale features of the general circulation and associated weather systems

Aided by improved instrumentation and communications, a network of stations has been set up to record standard observations simultaneously at set hours, and so extend the synoptic data coverage from mid-latitudes to the polar regions. In 1952 the first reasonably reliable daily weather charts for sea level and upper air levels could be drawn over the Arctic and subarctic, forming the basis both of daily operational forecasting and a climatological record. With the IGY, daily synoptic analysis was attempted over Antarctica and the neighboring oceans. In general, the station density over polar latitudes remains sparse and uneven, and communication failure through radio fadeout at times of strong solar flare activity can disrupt the forecasters' much needed continuity. The distance between stations north of 60°N averages about 500 km, but some areas fall well below this average, which is largely the result of a higher density over Eurasia. The Arctic Ocean and the Greenland Ice Cap remain the least known, and Keegan[5] has shown the amount of error that can result on the daily weather chart when a single ice-island report is missing. At the moment the Arctic forecaster is working with only about 1/50 of the information available at mid-latitudes. In the Southern Hemisphere, the problems in setting up stations on the ocean and ice cap are accentuated by the insular geography of the region and the isolation from major centers of population. Shipping reports supplement those of the sparse island stations; on the continent itself the greater part of the record is confined to the coastal stations. The introduction of automatic stations may solve some of these problems.

The synoptic observations aim to obtain measurements representative of the large-scale airmasses. Upper air soundings are taken twice daily. At the surface, the main observations are made at 6 or 12-hour intervals and consist of temperature and humidity readings (taken in a shaded, well-ventilated shelter (screen) approximately 5 ft above a light vegetation cover and away from buildings); station pressure (later reduced to sea level); pressure tendency; precipitation amount, type, and duration (a problem with respect to snow); wind direction, speed and gustiness (by anemometer on a roof or other exposed position); sunshine hours; state of sky and height of cloud base; visibility; and past weather. In addition, some stations take three-hourly observations and many record hourly temperature values.

Over the Arctic and subarctic there is now an accumulation of 10 to 12 years of reliable synoptic data and charts. This information used in conjunction with that from stations of longer records, expedition data, and explorers' journals has resulted in a good knowledge for each month of the year of the average large-scale surface pressure patterns and upper air flow, of the areas and tracks most frequented by cyclones and anticyclones, and the distribution of mean surface and upper air temperature.* Surface winds, humidity, cloud cover, and precipitation offer greater problems. Although this period is too short to give a reliable estimate of the large-scale variations, within a season, from year to year or from region to region, and to provide significant information on the frequency and absolute values of extreme conditions†, this daily record of weather and flow patterns has provided considerable understanding of the structure, flow and process of the Arctic atmosphere, of the nature of the variations and of the factors involved in the occurrence of extremes, to allow a more intelligent weighting of the available data and interpolation between stations. For the Antarctic, knowledge of even the average patterns is still highly tenuous, but already differences can be seen between northern and southern polar climates.

Local climates and microclimatology

While the synoptic view provides the overall picture from which the local conditions can be seen in context, the synoptic observation purposely filters out the local small-scale features. The frequency of severe weather† - strong winds, windchill, blowing snow, cloud cover and fog - can change within a mile or two, or even less, and local weather can rapidly deteriorate or clear in less than an hour. It is largely a question of the interaction of local topography, the nature of the surface, and the main weather systems.

Few rigorous studies of local climate based on systematic measurements have been undertaken. Local forecasters have written down their accumulated experience of the occurrence of hazardous local conditions in order to leave some rules of thumb for their successors and occasional local studies have been made of specific phenomena. Expeditions on drifting stations on the pack ice, and on the ice caps and glaciers, have samples the special local climates linked with these surface conditions. Gradually, with the growing knowledge of the relationship of all these local events to the better known broad flow patterns and of the physical processes involved, it has become possible to make at least a working estimate of local climatic variations from the climatology of the regional

* According to the World Meteorological Organization, standard "normals" (long-term averages) are for a 30-year period, updated each decade. Current normals cover the period 1931-1960.

† When conditions are extreme, and in the winter darkness, human and instrumental difficulties are greatest, so that observations are frequently missing (M). There is also the predilection for selecting (and so sampling) sheltered or less exposed sites. Even in the United States with its dense observing network, the most severe rainfall in an area can be at least three times that measured at the official meteorological stations. In their descriptions of severe weather, the diaries of explorers can be of considerable value.

flow patterns, weather systems and temperature distribution, a broad knowledge of the seasonal variation of snow/ice cover and open water, and a detailed knowledge of the site and setting of the locality itself.

Over polar regions, microclimates – i.e. the conditions in the boundary layer between the earth and atmosphere – take on a special significance. In the small-scale interaction of earth and atmosphere, processes are so interdependent that to measure any one is to disturb the balance of the whole. Knowledge of the combined frequencies and co-variation of many elements is necessary. There is no organization to collect data simultaneously and systematically from this layer. Measurements are confined to a very few stations and to special field expeditions and projects, where sample studies have been made for a limited period of time over various types of surface. Such observations concern the heat budget and energy exchange at the earth's interface and include temperature, humidity and wind profiles, surface and subsurface temperatures, moisture content of the soil and evaporation, evapotranspiration and net radiation. These data are related to the small-scale variations in surface roughness, aspect, slope, orientation, color, and wetness, to the water-holding capacity of the soil, the degree of saturation and drainage, the presence and depth of permafrost and to the transpiration of the plant cover as well as its shading effect and its interception of snowfall.

Radiation measurement

With the regime of polar day and polar night, the long periods of twilight, the generally low solar angle, the cloud cover, and the highly contrasted and varying surface conditions, the radiation balance over the polar regions is a highly complex factor to measure. Until the post-war period there were few direct radiation data over high latitudes. Even with modern instrumentation there are still many problems in measuring the various components, above all the long-wave radiation emitted by the earth's surface and the separation of direct and scattered incoming radiation. Much of the present knowledge is estimated; the calculations are based on data from the standard synoptic observation and a broad knowledge of the state of the surface, with the limited direct measurements acting as controls. A major difficulty in estimating radiation is the tentative nature of the humidity and cloud data over Arctic regions, on which these calculations must depend. Over the western hemisphere there are still very few stations recording radiation on a regular basis; there are, however, many sample data covering short periods for a variety of surface conditions.

The recent development of weather satellites has opened up new possibilities in cloud observation and radiation measurement. Of possible significance in polar regions are the variations beyond the visible range of the spectrum, in which the solar radiation received at the outer limits of the earth's atmosphere is considered constant at 1.98 ly/min.* The possibility of variations in ultraviolet and solar corpuscular radiation was first suggested by the correlation of such phenomena as intense

---

* 1 ly = 1 cal/cm^2 = 7.3 Btu/ft^2

geomagnetic disturbances, aurorae and airglow, sudden ionospheric disturbances, and ozone variations with the shape, size, and brightness of disturbances on the solar surface. Recent satellite data have confirmed these variations.

Ultraviolet radiation is absorbed in the upper layers of the atmosphere where it creates the ionized layer above 60 km and the ozone in the 35 to 50-km region. Increased absorption in the lower (D) layer of the ionosphere during sudden ionosphere disturbances bring about radio fadeout in certain wavelengths – a frequent and inconvenient phenomenon in high latitudes which can last up to about 2 weeks.

The variation in solar corpuscular radiation is of special interest in high latitudes. Under the influence of the earth's magnetic field, the stream of high-energy particles is apparently funneled into narrow rings aroung 67°N and S geomagnetic latitude. Here, maximum penetration of the atmosphere seems to occur, manifested in the form of aurorae which extend in height from about 90 to 120 km. A periodicity of some 27 days has been suggested, coinciding with the apparent solar rotation.

Although these variations in the incoming solar energy represent a small fraction of the total, and no efficient mechanism is yet known by which the variations are transferred to the lower atmosphere, it is possible that they may trigger off new events in the general circulation. This has important implications in long-range forecasting at high latitudes.

SELECTED BIBLIOGRAPHY

1. Geiger, R. (1965) The climate near the ground. Harvard University Press.

2. Gerdel, R. W. (1964) Meteorology and climatology of the cold regions, mimeographed, U. S. Army Cold Regions Research and Engineering Laboratory.

3. Hare, F. K. (1951) "Climate classification" in London essays in Geography, L. D. Stamp and G. W. Wooldridge, editors.

4. Haurwitz, B. and Austin, J. M. (1944) Climatology. New York: McGraw Hill.

5. Keegan, T. J. (1958) "The wintertime circulation in the arctic troposphere" in Contributions to the study of the arctic circulation, Publication in Meteorology, No. 9, McGill University, Montreal, p. 22-47.

6. Köppen, D. W. (1936) The geographical system of climate, Handbuch der Klimatologie, vol. 1, part C, p. C5-C44.

7. ______ (1954) Köppen-Geiger map of the world's climatic zones, revised 1953 by R. Geiger and W. Pohl.

8. Thornthwaite, C. W. (1931) The climate of North America according to a new classification, Geographical Review, vol. 21, p. 633-655.

9. ______ (1948) An approach toward a rational classification of climate, Geographical Review, vol. 38, p. 55-94.

10. World Meteorological Organization (1960) Guide to climatological pra tices, WMO Publication no. 100, TP 44. See also Guide to mete ological instrument and observing practices, no. 8, TP3, and Guide to agricultural meteorological practices, no. 134, TP 61, Geneva.

NORTHERN HEMISPHERE - THE NATURE OF THE SURFACE

The features of the earth's surface that have most bearing on the diversity of the climate are the distribution of land and sea, the major relief, and the nature of the surface cover - its roughness, texture, wetness, and color. These last qualities change comparatively little within each of the two seasons of the cold regions, but considerably from one season to the next.

Configuration and Relief

The Arctic Ocean

Northern waters extend over some five and a half million square miles (Fig. la) and the configuration of the basins[3, 68] and coasts plays an important role climatically. In the central Arctic Sea depths below 5,000 meters have been measured and in the Greenland and Norwegian Seas, depths exceed 3,000 meters. These basins are separated by well-defined ridges.[2, 16] On the Pacific side, the Arctic Ocean is almost land-locked since the narrow Bering Strait is only 50 km wide; over the Atlantic sector, the Wyville Thomson submarine ridge, running from Scotland to Iceland and southern Greenland, separates the deep waters from those of the North Atlantic, but allows free entry of the warm surface waters of the Gulf Stream and exit of the ice-laden Arctic waters. To the north of Siberia, the continental shelf is broad, and the bordering seas - the Barents, Kara, Laptev and East Siberian Seas - relatively shallow. On the North American side, the ocean floor drops away rapidly to the depths, while to the south there is an interpenetration of Arctic waters and land as far as mid-latitudes.

The general circulation at the surface of the Arctic Ocean is given in Figure 2a. Over the "Pacific" sector a clockwise flow exists over the Arctic Sea, exemplified by the drift of ice island T3 (Fig. 2b); over the "Atlantic" sector, beyond the Lomonosov Ridge, the flow is generally counterclockwise. The origin and nature of the surface water carried by these currents has a profound effect not only on the climate of the oceanic areas, but on the Arctic and subarctic coastal regions.

In the surface layer of the polar oceans there are two major types of water,[32] different in their origin, temperature, and salinity. Arctic water is formed in the Arctic Sea and extends from the surface to an average depth of 200 meters. Of low salinity (< 34 ^{o}/oo), and low temperature (close to the freezing point at this salinity, -1.5 to -1.8C), it comprises fresh water draining from the surrounding land masses (some 8300 km^3 of water per year) and water from the melting ice, mixed with water from below of Atlantic origin. The largest single exit of Arctic water is in the East Greenland current, a cold, ice-laden stream which is a key factor in the climate of Greenland's east coast. A second outlet lies through the channels of the Canadian Archipelago, through Smith, Lancaster and Jones Sounds and southward along the eastern shores of Baffin Island (the Canadian current) or via Foxe Basin, Hudson Bay and Hudson Strait. Off the coast of Labrador, both branches join and continue southward as the cold Labrador current.

The Gulf Stream - Atlantic Drift water enters the Arctic to the west and east of Svalbard, and to the north of these islands begins to sink beneath the surface, where it forms a layer 500 to 600 m thick below the Arctic water.

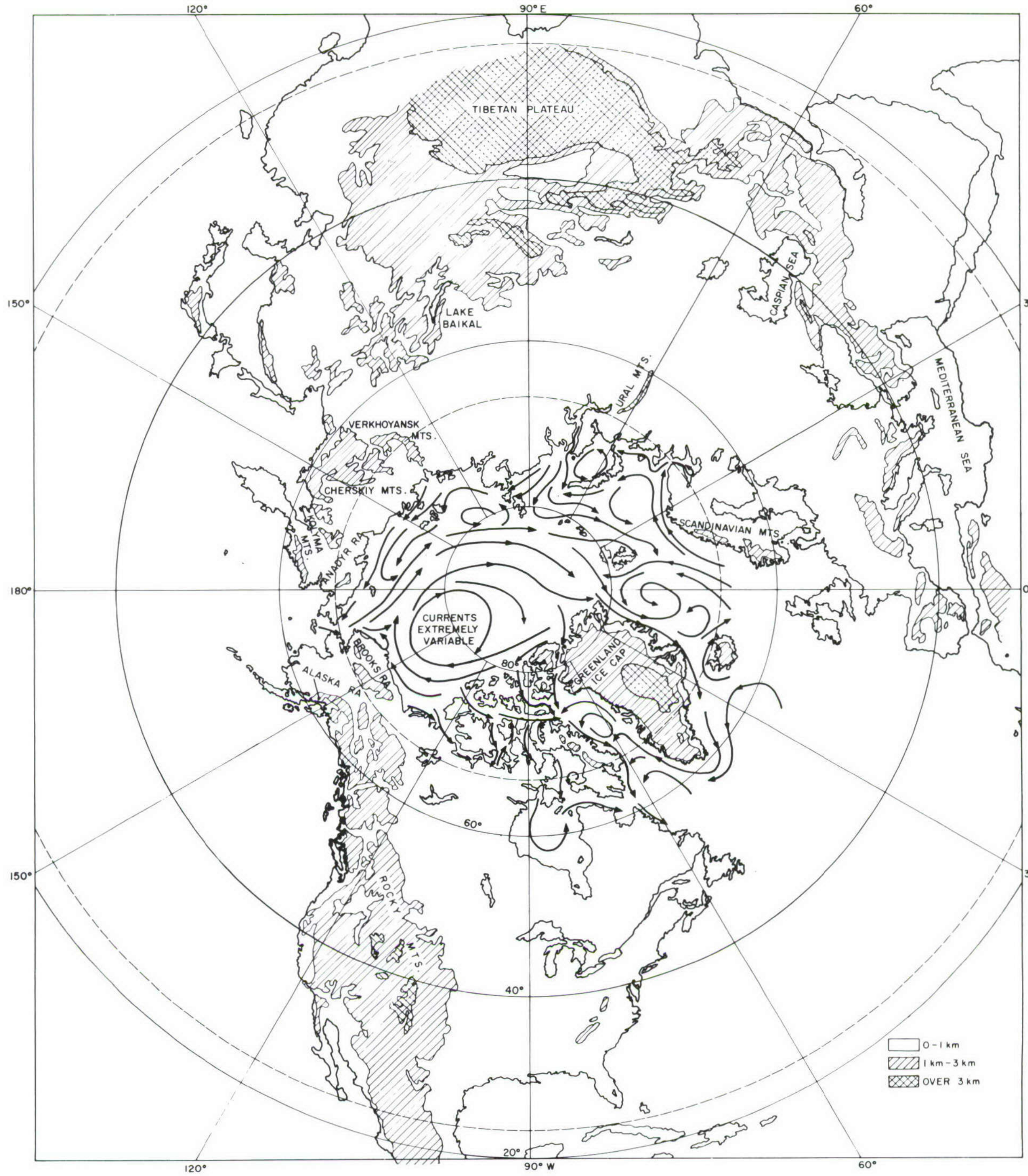

Figure 2a. Northern Cold Regions: major relief and ocean currents.

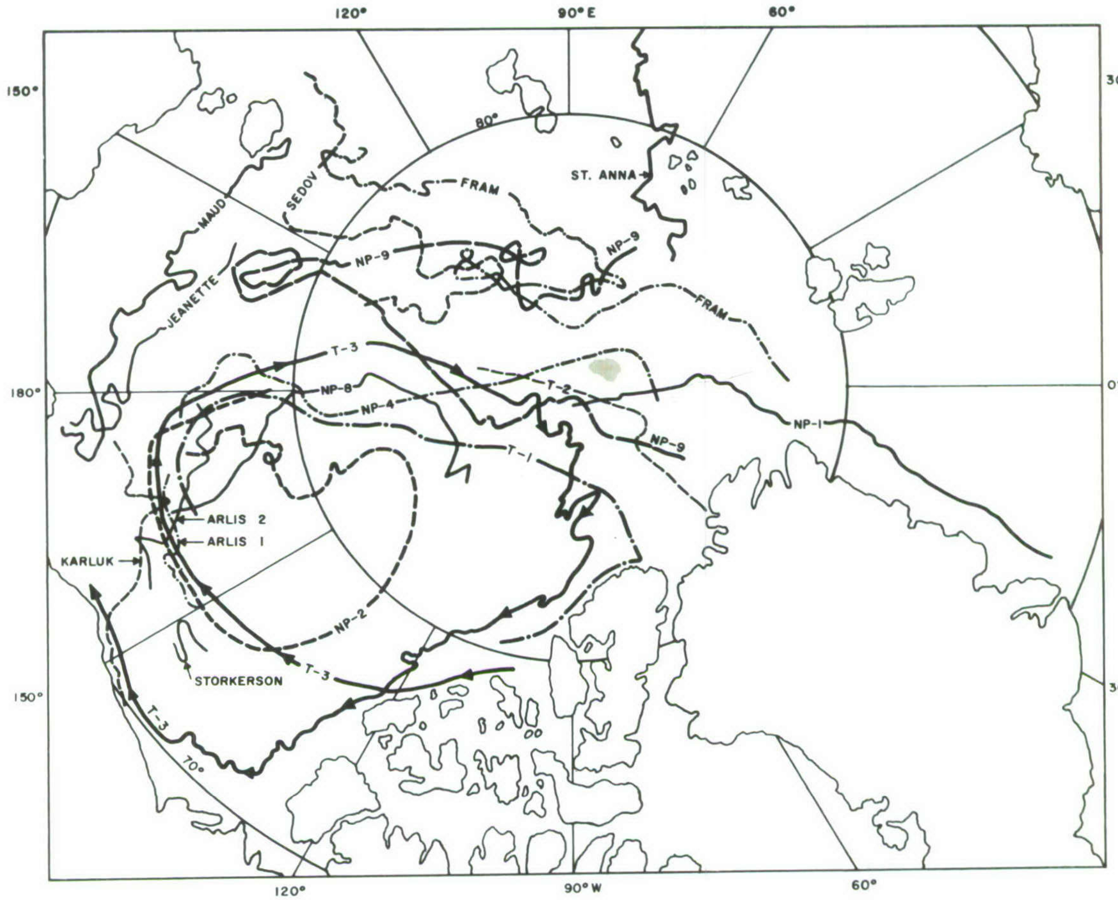

Figure 2b. Drifts of various expeditions and of the largest ice islands (incl. floes) in the Arctic Ocean through 1961.[3]

North of Svalbard, a salinity of 35.10 ⁰/oo and a temperature of 3 to 4C have been measured at 75-400 m; nearer to the pole, the salinity of the layer drops to a little less than 35, and the temperature to 0.79C. There is another entry of warm Atlantic Drift water along the coast of northern Norway into the Barents Sea, and the amount of ice in the Barents Sea appears to be related to the fluctuations in the Gulf Stream. There is still some controversy as to how much these Atlantic waters affect the surface conditions of the Kara and Laptev Seas, with their semipermanent polynyas;[35,47] and in turn the winter climates along the Taimyr Peninsula and neighboring islands. There is certainly frequent regeneration of storms over this region.

A branch of the Atlantic Drift diverges south of Iceland (the Irminger current) and travels westward to Greenland, where, owing to its higher salinity, it sinks below the East Greenland current. Around the tip of Greenland, turbulence and mixing occurs and the composite current is joined by Atlantic water from the Labrador Sea as it continues northward along the west Greenland coast. Near the latitude of Disko Island, a section of this West Greenland current curves west and joints the southflowing cold Canadian current, while the remainder continues northward into Baffin Bay. Hare and Montgomery[42] discuss the presence of open water in winter over Davis Strait, Baffin Bay (North Water), Hudson Strait, and Lancaster Sound, and its effect on winter climate. Their publication includes monthly mean maps of the surface temperature over the eastern Arctic of North America, which show the considerable difference in temperature between the coasts of western Greenland and eastern Baffin Island, due to these contrasting currents. In December, Disko Island can record temperatures 14C higher than Clyde River, 600 km across the bay, and contrasts remain strong until April.

Through the narrow Bering Strait, water from the Pacific westerly drift flows northward into the Arctic Basin, at least in summer; it continues in part westward past northeastern Siberia, and in part to the east off the Alaskan coast towards Point Barrow. In the Pacific subarctic there is again a climatic difference between the coastal areas of Siberia and those of southern Alaska, which are washed by warm surface drift.

The continents

Much of the northern land surface is of low elevation. Important mountain barriers do exist however and play a significant role in the development, deflection and stagnation of storms, the distribution of clouds and precipitation, and the origin of such local phenomena as the föhn and katabatic winds.

The areas of highest relief are in Greenland and Alaska (Fig. 1b). The Greenland Ice Cap[5], a solid north-south barrier to westerly atmospheric circulation, 2400 km long and 1000 km wide, averages 2100 m in height, surpassing 3000 m at its highest point. The mountains of southern Alaska, another north-south obstacle, project 2500 m into the upper air flow, with peaks rising from 4500 to 6000 m. The rise is abrupt from the coast, and a sharp climatic divide results between coastal and interior regions. In summer, the Brooks Range of northern Alaska, averaging 1500 m with peaks to 3000 m, forms a similar divide between the cold air to the north and the warmer Yukon Valley to the south.

Over Eurasia, the mountains of Scandinavia and the Urals present two less marked north-south barriers, both generally rising to 1200 m with peaks of 2400 m. In northeastern Siberia, the Verkhoyansk, Cherskiy, and Anadyr' Ranges and the Kolyma mountains emerge in a complex from plateau country of a few hundred meters; their average elevation is 1500 m, but some peaks reach 3000 m.

Vegetation Zones[41, 26]*

Tundra

The tundra borders the Arctic Ocean. North of the tree line (Fig. 2c) the vegetation consists of low creeping shrubs, tufted grass-like plants and thick growths of lichen and mosses. The tundra is mostly underlain by perennially frozen ground, with an active layer which freezes and thaws in a thickness depending on latitude, exposure, surface and soil conditions. In spite of the low precipitation, the impermeability of the underlying frozen layer leads to poor drainage and abundant surface water at this season.

* Refer to I-A4 in the monograph series.

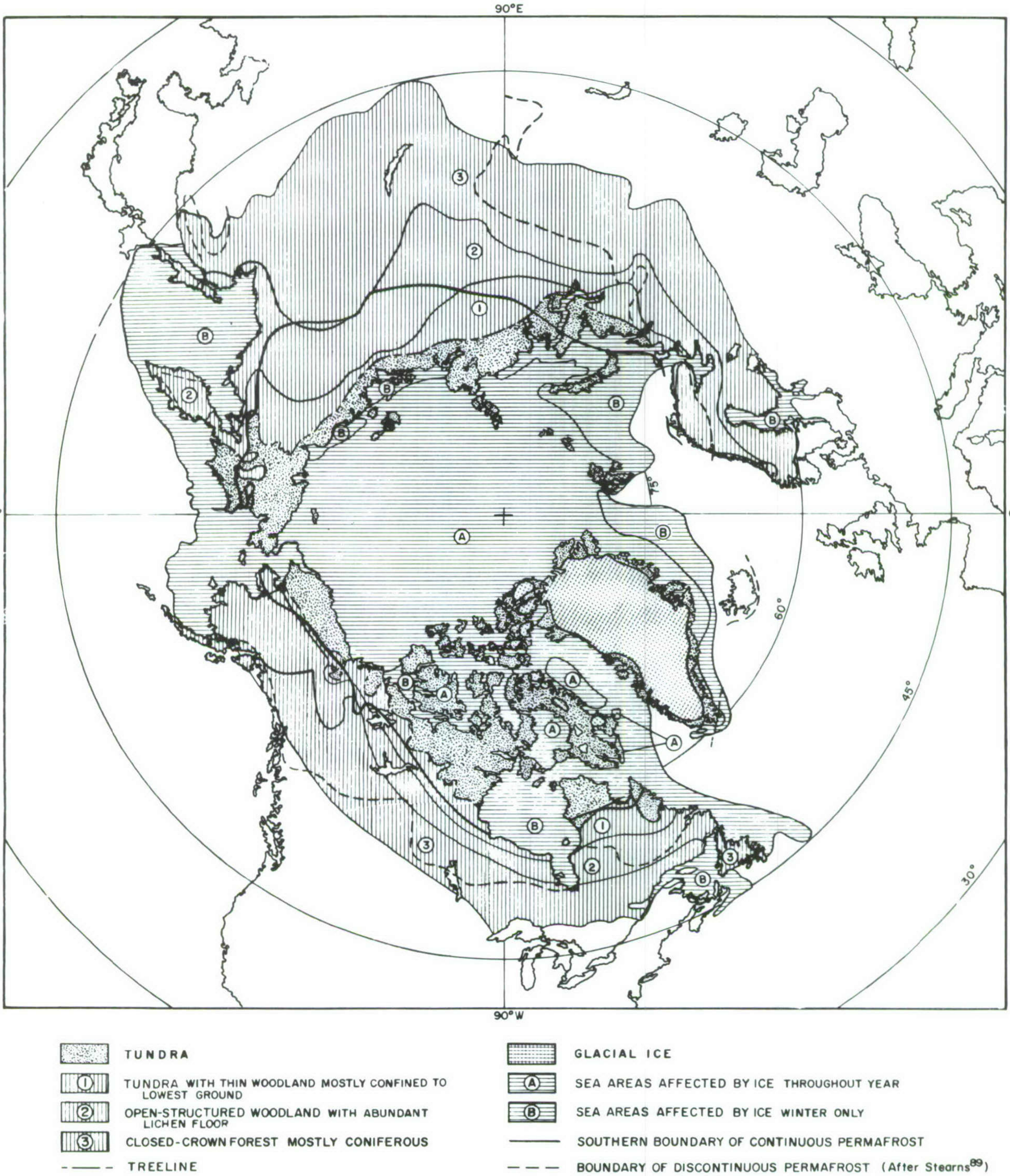

Figure 2c. Northern Cold Regions: surface conditions (after Hare, 1958).

Lichen-woodland

To the south of the tree line there is a gradual transition to the boreal forest of the subarctic. At first the tundra is interspersed with thin woodland, confined to the more favored areas (zone 1); farther south, the tundra becomes relegated to the colder or more adverse sites and an open-structured lichen-woodland is characteristic of zone 2. Permafrost or isolated patches of permafrost also exist throughout much of this region and large areas are waterlogged, forming lakes and muskeg. Hare[41] suggests that 50% of northern Canada has a water rather than a land surface in summer.

Boreal forest

The boreal forest (zone 3) grades into lichen-woodland to the north. It is a closed-crown forest, with unbroken stretches of tall and mostly coniferous trees with scattered shrubs and herbs and a well-developed moss layer. In European Russia and Scandinavia, much of the forest has been cleared south of 60°N.

Permanent and Seasonal Ice and Snow

Sea ice (pack ice)

Figure 2c shows the normal extent of the ice in mid-winter (Febrary - March) and late summer (August). At the maximum, in March, it covers approximately 15 million km^2; at the September minimum the area is reduced to a half. The Arctic Ocean is affected all year; the ice covers about 95% of the surface.

The pack ice averages about 3 m in thickness, but broad expanses of flat ice surface are broken by ridges and hummocks which occasionally rise to 10 m above the general level. In winter, thermal and wind stresses cause fracturing and the formation of open leads, which soon freeze over but often melt open again in summer. The ice attains its maximum thickness just before the summer melt period in June. From June to late August, about a meter of the ice may melt both underneath and on top. Water drains into the ocean through cracks orremains in pools on the ice.

The distribution of open water in summer is largely influenced by the prevailing winds, and large fluctuations occur within a season and from year to year. In the U.S.S.R., observation and research have been carried out for many years by the Northern Sea Route Authority and the Hydrometeorological Service, and in 1949 the United States and Canada collaborated in the development of a program for observing and forecasting sea ice[6] over the American Arctic. In general, the southern parts of the Chukchi, East Siberian and Laptev Seas are open from late June or July through August or September, the Kara Sea into October. Over North America, the largest penetration of open water in high latitudes is in the Baffin Bay region, most of which is ice-free from August to October. Along the coast of the Beaufort Sea, there are only a few weeks in late August and September when there is an ice-free passage. Even Hudson Bay, frozen over from January to June, can count on only a short shipping season from mid-July to mid-October. During the melt season, while thawing ice is present, sea surface temperatures remain low.

Ice caps and glaciers[60]

The Greenland Ice Cap[5] which covers about 1.8 million km^2 comprises 80% of the area occupied by land ice. The influence of this ice mass as a relief barrier has already been discussed. As a region of refrigeration it appears to have little influence on the general climatic conditions over the Arctic and subarctic as a whole. In the winter, this elevated snow-ice surface is subject to strong radiational cooling and surface temperatures fall to -50C and below, while in summer the glacier efficiently holds surface temperatures below or close to freezing. In general the effect of this frozen surface is remarkably shallow, and the air aloft is frequently warmer than that, for example, over the Canadian Archipelago. The influence of the outflow under gravity of the cold dense air in the lowest layer above the ice cap on the climate of the coastlands and coastal waters has yet to be fully assessed.

Other ice caps and valley glaciers are found on the islands of the Canadian Archipelago, notably Ellesmere and Baffin, on Iceland, Svalbard, Franz Josef Land, Novaya Zemlya, and in the mountains of Scandinavia, Alaska and western Canada.[60] The climatic effect of these smaller areas of permanent ice cover is local.

Seasonal ice and snow[60]

With the exception of the comparatively restricted areas covered by ice caps and glaciers, the continental surfaces of the Arctic and subarctic are free from ice and snow for some weeks during the warm season; this period varies from two months near the shores of the Arctic Ocean to five to six months over the subarctic. The dates of the occurrence and disappearance of a snow cover[18,24,72,80] and of the freeze-up and break-up of rivers[1,14,44,58,75] and lakes are not only difficult to define and measure, but are also highly variable from year to year, and according to local conditions.[10,14]

In September in the high Arctic, and in late October or November in the subarctic, the surface waters of lakes and rivers begin to freeze over, and land and ice is blanketed with a snow cover. Sea ice forms during the following weeks[75] so that, during midwinter, one vast, continuous, highly homogeneous ice and snow surface caps the Northern Hemisphere as far as mid-latitudes. These conditions persist until the end of April in the subarctic and to the end of June or early July along the shores of the Arctic Ocean. Spring is brief in northern latitudes; the sun is already near its zenith in the high Arctic, daylight is continuous, the snow cover meager and the thaw rapid, except for occasional protected drifts which may last all summer. For river, lake, and sea ice, the break-up season is longer, lasting from four to six weeks, so that during two or three weeks the land may be snow-free with the ice tracing out the drainage patterns and coastlines. It is mid-July before the northern lakes are clear.

The snow cover over the central Arctic is thin and uneven. The total snowfall averages only 50 to 100 cm a year with a maximum depth in late spring of 30 to 60 cm. (Rare exceptions with a total fall from 200 to over 250 cm a year are found in northern Quebec and eastern Baffin Island owing to their position with respect to Atlantic storms.) The roughness of the tundra at this season (late spring) is very similar to that of the neighboring ocean and seas, and wind action is severe. The fine dry snow grains are easily redistributed, until the snow surface itself becomes compacted by the wind at these low temperatures. Exposed areas and smooth ice surfaces are frequently blown clear of snow; drifts build up around obstacles, and dunes and sastrugi are formed. The exposure of the tundra makes this an exceptionally inhospitable region; even the caribou and reindeer winter on the softer snows sheltered by the stunted trees of the forest margin.

To the south, as the woodland becomes denser and merges into the boreal forest, new sets of surface conditions are created.[39] The tree crown intercepts the falling snow and wind action is at a minimum in the forest, but the ground is also sheltered from direct solar radiation in the spring and early summer which lengthens the melt period considerably. In the subarctic, snowfall is generally light in the continental interior, but in areas under maritime influence it can exceed 250 cm; the maximum depth over Labrador, for example, is more than 150 cm.

A major factor in the radiation balance of the forested zone is the variability in the albedo of the surface, from 70 to 80% with an unbroken ice or new snow surface to approximately 25% for these snow-covered evergreen forests.[65] To the north of the tree line, when the frozen continental and sea surfaces are buried under an insulating cover of snow, they behave similarly as far as energy transfer is concerned.

SELECTED BIBLIOGRAPHY

1. Allen, W.T.R. (1964) Break-up and freeze-up dates in Canada, Canadian Meteorological Branch, CIR 4116, ICE 17, Toronto.

2. Anon (1954) New Soviet researches, explorations and discoveries in the central Arctic, Izv. Akad. Nauk. Ser. Geog., vol. 5, p. 3-6, trans. E.R. Hope, Defence Research Board, Canada, T165R.

3. Arctic Institute of North America (1963) Proceedings of the Arctic Basin Symposium, Oct. 1962, Tidewater Publishing Corp., Centreville, Md.

4. Armstrong, T.C. (1958) Sea ice north of the U.S.S.R., Part I, Frequency charts, Hydrographic Department of the Admiralty, London.

5. Bader, H. (1961) The Greenland ice sheet, U. S. Army Cold Regions Research and Engineering Laboratory, Monograph I-B2.

6. Bates, C.C. (1958) "Current status of sea ice reconnaissance and forecasting for the American Arctic," In Polar Atmosphere Symposium, Part I, Pergamon Press, p. 285-322.

7. Berkofsky, L. and Bertoni, E.A. (1960) Topographic charts at one-degree intersections for the entire earth, G. R. 3 Research Notes, No. 42, Bedford, Mass.

8. Bilello, M. (1957) A survey of Arctic snow-cover properties as related to climatic conditions, U. S. Army Snow Ice and Permafrost Research Establishment, Research Report 39.

9. ________ (1961) Formation, growth and decay of sea-ice in the Canadian Arctic Archipelago, Arctic, vol. 14, p. 2-25. Also U.S.A. SIPRE Research Report 65, July 1960. (See also USA CRREL Research Report 135, Growth, structure and strength of sea-ice, A. Assur and W. F. Weeks, October 1964.)

SELECTED BIBLIOGRAPHY (Cont'd)

10. Bilello, M. A. (1964) Method for predicting river and lake ice formation, Journal of Applied Meteorology, vol. 3, p. 38-44. Also USA CRREL Research Report 129.

11. British Admiralty, Hydrographic Office: Arctic pilot, volumes for various coastal areas, H. M. Stationery Office, London.

12. Brown, J. and Johnson, P. L. (1965) Pedo-ecological investigations, Barrow, Alaska, USA CRREL Technical Report 159.

13. Burbidge, F.E. (1951) The modification of continental polar air over Hudson Bay, Quarterly Journal of the Royal Meteorological Society, vol. 77, p. 365-374.

14. ______________ and Lauder, J. R. (1957) A preliminary investigation into break-up and freeze-up conditions in Canada, Meteorological Branch, Canada, CIR-2939, TEC-252.

15. Burkhanov, V.F. (1956) "Achievements of Soviet geographic exploration and research in the Arctic," in Cherez okeanna dreifuyushchikh l'dakh, Moscow. Translation E. R. Hope, Defence Research Board, Canada, T253R, 1957.

16. ______________ (1957) Arctic scientific research in the Soviet Union, Priroda, vol. 5, p. 21-30. Translation by E. R. Hope, Defence Research Board, Canada, T265R.

17. Callaway, E.B. (1954) An analysis of environmental factors affecting ice growth, U. S. Navy Hydrographic Office, Technical Report TR-7.

18. Canadian Department of Mines and Technical Surveys (1957) Atlas of Canada, Geographical Branch, Ottawa.

19. Canadian Hydrographic Service (1959) Pilot of Arctic Canada, Vol. I, Ottawa.

20. Canadian Meteorological Branch: Aerial ice observing and reconnaissance (sea ice), annual technical circulars covering the eastern Canadian seaboard from 1958, the Hudson Bay route from 1960 and the western Arctic from 1957. Ice conditions on the eastern Canadian seaboard during winter 1960-1961, and winter and spring 1961-1962 are summarized in CIR 3651, TEC-407 and CIR 3835, TEC-467 respectively; an account of the sea-ice distributions in Canadian Arctic waters summer 1962 is contained in CIR 3824, TEC-463.

21. ______________: Aerial ice observing and reconnaissance (lake ice), nnual technical circulars for the lower MacKenzie River area from 1961.

22. ______________ (1959) Break-up and freeze-up dates of rivers and lakes in Canada, CIR-3156, ICE-2.

23. ______________: Ice thickness data for selected Canadian stations, 1958-1961, CIR-3537, ICE-5; 1961-62, CIR-3711, ICE-6; 1962-63, CIR-3918, ICE-11.

24. ______________: Snow cover data, Eastern Canada, published annually from winter 1954-55. For earlier years, request from Eastern Snow Conference.

SELECTED BIBLIOGRAPHY (Cont'd)

25. Corton, E.D. (1954) The ice budget of the Arctic pack and its application to ice forecasting, U. S. Navy Hydrographic Office, Technical Report no. 6.

26. Dansereau, P. (1955) "Biogeography of the land and inland waters," in Geography of the Northlands, G.H.T. Kimble and D. Good, editors. American Geographical Society, John Wiley, New York.

27. Dansk Meteorologisk Institut, The state of ice in the Arctic seas, Copenhagen; yearbooks.

28. DePercin, F. (1956) Topoclimatic study, Fort Churchill, Canada, H.Q. Quartermaster Research and Development Command, U. S. Army, Technical Report EP-38.

29. ____________ (1960) Microclimatology of a subarctic spruce forest and a clearing at Big Delta, Alaska, H.Q. Quartermaster Research and Development Command, U. S. Army, Technical Report EP-130.

30. Deutsches Hydrographisches Institut (1950) Atlas der Eisverhältnisse des Nordatlantischen Ozeans und Ubersichtskarten der Eisverhältnisse des Nord-und Südpolargebietes. Hamburg, Deutsches Hydrographisches Institut, 28 p.

31. Dickson, R.R. (1964) A synoptic characterization of the thermal nature of the earth's surface, Monthly Weather Review, vol. 92, p. 195-201.

32. Dunbar, M.J. (1955) "Watermasses, circulation, ice cover," in Geography of the Northlands, G.H.T. Kimble and D. Good, editors. American Geographical Society, John Wiley, New York.

33. ____________ and Greenway, K.R. (1957) Arctic Canada from the air, Defence Research Board, Ottawa.

34. Elliott, F.E. (1956) Some factors affecting the extent of ice in the Barents Sea area, Arctic, vol. 19, p. 249-257.

35. Eskin, F.I. (1960) The influence of Atlantic waters on upper levels of the Arctic seas, American Meteorological Society Translation, TR 315, by C. E. Townsend, from Leningradskii Universitet Vestnik, No. 6, p. 153-158.

36. Formozov, A.N. (1963) Snow cover as an integral factor of the environment and its importance in the ecology of mammals and birds, Translated from Russian by Prychodko and Pruitt, Boreal Institute, University of Alberta, Edmonton, Occas. Paper No. 1.

37. Forward, C.N. (1954) Ice distribution in the Gulf of St. Lawrence during the break-up season, Geographical Bulletin, vol. 6, p. 45-84, Ottawa.

38. ____________ (1956) Sea ice conditions along the Hudson Bay route, Geographical Bulletin, vol. 8, p. 22-50, Ottawa.

39. Gold, L.W. and Williams, G.P. (1957) Some results of the snow survey of Canada, National Research Council, Division of Building Research, Ottawa, Research paper no. 38.

SELECTED BIBLIOGRAPHY (Cont'd)

40. Hare, F.K. (1951) Some climatological problems of the Arctic and sub-arctic, Compendium of Meteorology, Americal Meteorological Society, Boston, p. 952-964.

41. __________ (1958) "Arctic geography and climate," in Polar Atmosphere Symposium, Part I, Pergamon Press, p. 3-8.

42. __________ and Montgomery, M. R. (1949) Ice, open water and winter climate in the Eastern Arctic of North America, Arctic, vol. 2, p. 78-89, and p. 149-64.

43. __________ and Orvig, S. (1958) The Arctic circulation, Publication in Meteorology No. 12, McGill University, Montreal, p. 128-199.

44. Hastings, A.D. (1961) Atlas of arctic environment, H.Q. Quartermaster Research and Engineering Command, U. S. Army, Research Study Report RER-33.

45. Holtsmark, B. E. (1955) Insulating effect of a snow cover on the growth of young sea ice, Arctic, vol. 8, p. 60-65.

46. Kimble, G. H. T. and Good, D. (editors) (1955) Geography of the North-lands, American Geographical Society, John Wiley and Sons, Inc., New York.

47. Kupetskii, V.N. (1960) Atlantic waters as a cause of certain features of the polar climate, American Meteorological Society, Translation TR319, by C.E. Townsend from Problemy Arktiki, No. 6, p. 60-65.

48. Lamb, H.H. (1955) Two-way relationship between the snow or ice limit and 1000-500-mb thicknesses in the overlying atmosphere, Quarterly Journal of the Royal Meteorological Society, vol. 81, p. 172.

49. Lee, A. (1961) Effect of wind on water movements in the Norwegian and Greenland seas, Symposium of Mathematics - Hydrodynamical Methods of Physical Oceanography Institute fur Meereskunde, Un. of Hamburg, p. 353-73.

50. Lee, O.S. and Simpson, L. S. (1954) A practical method of predicting sea-ice formation and growth, Technical Report 4, U. S. Hydrographic Office, 27 p.

51. Lobeck, A.K. (1950) Physiographic diagram of Asia and physiographic diagram of North America, The Geographical Press, Columbia University, New York.

52. Mackay, D.K. (1962) River ice conditions in the Nelson River drainage system, Geographical Paper no. 34, Geographical Branch, Canadian Department of Mines and Technical Surveys, Ottawa.

53. ____________ (1962) Trends and factors affecting break-up and freeze-up dates in the Nelson River drainage system, Geographical Paper no. 35, Geographical Branch, Canadian Department of Mines and Technical Surveys, Ottawa.

54. ____________ and Mackay, J. R. (1965) Historical records of freeze-up and break-up on Churchill and Hayes Rivers, Geographical Bulletin, vol. 7, p. 7-16, Geographical Branch, Canadian Department of Mines and Technical Surveys, Ottawa.

SELECTED BIBLIOGRAPHY (Cont'd)

55. Mackay, G.A. (1952) The effect of protracted spring thaws on ice conditions in Hudson Bay, Bulletin of American Meteorological Society, vol. 33, p. 101-106.

56. Mackay, J.R. (1963) River ice conditions in Canada, Proceedings of Eastern Snow Conference.

57. ______________ (1963) Progress of break-up and freeze-up along the MacKenzie River, Geographical Bulletin, vol. 19, p. 103-116, Ottawa.

58. Markham, W.E. (1962) Summer break-up patterns in the Canadian Arctic, Canadian Meteorological Branch, CIR 3586, TEC 389, Toronto.

59. ______________ (1963) A preliminary study of ice conditions in Barrow Strait and Lancaster Sound during June, July and August, Canadian Meteorological Branch, CIR 3900, TEC 481, Toronto.

60. Mellor, M. (1964) Snow and ice on the earth's surface, USA CRREL Monograph II-C1.

61. Munn, R.E. (1964) Forest meteorology, A survey of the literature, Canadian Meteorological Branch, CIR 4029, TEC 516, Toronto.

62. Nusser, F. (1958) "Distribution and character of sea ice in the European arctic sector," in Arctic sea ice, National Academy of Science, National Research Council, Washington, D.C., publication no. 598, p. 1-10.

63. Ostrekin, M. Ye. (1954) Recent study and exploration of the central Arctic, Priroda, vol. 12, p. 3-12, translated by E.R. Hope, Defence Research Board, Canada, 1955, T172R.

64. Pihlainen, J.A. (1963) A review of muskeg and its associated engineering problems, USA CRREL Technical Report 97.

65. Reed, R. J. (1962) Arctic forecast guide, U.S. Navy Weather Research Facility, Norfolk, Virginia, NWRF 16-0462-058.

66. Rodhe, B. (1952) On the relation between air temperatures and ice formation in the Baltic, Geografiska Annaler, vol. 34, p. 175-202.

67. ______________ (1955) A study of the correlation between the ice extent, the course of air temperature, and the sea surface temperature in the Aland Archipelago, Geografiska Annaler, vol. 35, p. 141-63.

68. Sater, J.E. (1963) The Arctic basin, Arctic Institute of North America, Tidewater Publishing Corporation, Md.

69. Suslov, S.P. (1947) Fizicheskaia Geografiia S.S.S.R., Pedagogicheskoe Izdatel' stvo Ministerstva Prosveshcheniia R.S.F.S.R., Moscow, 544 p. (Abstracted by W. Mandel, the Stefansson Library, New York, 1950, for SIPRE).

70. Swithinbank, C. (1960) Ice atlas of Canada, Scott Polar Research Institute, Cambridge, England, for Defence Research Board, Ottawa.

71. Sychev, K.A. (1960) The heat content of Atlantic waters and the expenditure of heat in the Arctic basin, American Meteorological Society, TR 336.

SELECTED BIBLIOGRAPHY (Cont'd)

72. U. S. Army Arctic Construction Frost Effects Laboratory (1954) Depth of snow cover in the Northern Hemisphere, U. S. Army Engineer Division, New England (including full bibliography to date).

73. U. S. Army Corps of Engineers (1954) Investigation of construction and maintenance of airdromes on ice: Fiscal year 1954, Contains "Compilation and study of ice thicknesses in the Northern Hemisphere, 1952-1953," by Theodore Ryder, American Geographical Society, New York, with extensive bibliography and ice thickness data tabulations.

74. Bilello, M. A. (1961, 1964) Ice thickness observations, North American Arctic and subarctic, 1958-1962, USA CRREL Special Report 43, Parts I and II.

75. U. S. Navy, Hydrographic Office (1946) Ice atlas of the Northern Hemisphere, Washington, D. C. (with extensive bibliography).

76. ______________: Sailing directions, volumes for various coastal areas, Washington, D. C.

77. ______________: Report of ice observations and forecasting (an annual publication).

78. U. S. Navy, Technical Assistant to the Chief of Naval Operations for Polar Projects (1956) The dynamic North, Book I, Washington, D. C.

79. U. S. S. R. (1954) Bolshoy, Sovetskiy atlas mira, Moscow.

80. ________ (1960) Agricultural atlas of the U. S. S. R, Moscow.

81. Vowinckel, E. and Orvig, S. (1951) Water balance and heat flux of the Arctic Ocean, Publication in Meteorology, No. 44, McGill University, Montral (with extensive bibliography).

82. Vowinckel, E. (1963) Ice transport between Greenland and Spitzbergen and its causes, Publication in Meteorology, No. 59, McGill University, Montreal, 24 p.

83. Williams, G. P. and Gold, L. W. (1963) The use of dust to advance the break-up of ice on lakes and rivers, Eastern Snow Conference, Annual Proceedings (list of references), p. 31-56.

84. Winchester, J. W. and Bates, C. C. (1958) "Meteorological conditions and associated sea ice distribution in the Chukchi Sea during the summer of 1955," in Polar Atmosphere Symposium, Part I, Pergamon Press, p. 323-334.

85. Zubov, N. N. and Somov, M. M. (1940) The ice drift of the central part of the Arctic Basin, Problemy Arktiki, vol. 2, p. 57-68. (American Meteorological Society, TR 274.)

86. Zubov, N. N. (1945) Arctic ice, Moscow, Izd. Glevs, 360 p.

87. __________ (1958) "Arctic ice and the warming of the Arctic" in In the centre of the Arctic, Northern Sea Route Directorate Press, Moscow-Leningrad. Translated by E. R. Hope, Defence Research Board, Canada, T14R, 1960.

SELECTED BIBLIOGRAPHY (Cont'd)

88. Miller, D. H. (1956) The influence of snow cover on local climate in Greenland, Journal of Meteorology, vol. 13 (1), p. 112-120.

89. Stearns, S. R. (1965) Selected aspects of geology and physiography of the cold regions, USA CRREL Monograph I-A1.

THE GENERAL CIRCULATION AND WEATHER SYSTEMS[30]

A brief outline of the general atmospheric circulation of high latitudes and the associated surface weather systems offers a more dynamic approach to the study of regional and local climates and the distribution and frequency of the individual climatic elements, although in winter the presence of a strong radiational temperature inversion in the lowest layers appears to restrict and retard the influence of upper flow on surface conditions, and in summer differential heating of open water, ice and continental surfaces greatly modifies the surface effects of the large-scale circulation patterns.

The Circumpolar Vortex

Considering both the descriptive and predictive aspects of climate at high latitudes, the dominant factor is the presence of a cold-cored westerly circumpolar vortex in the middle and upper atmosphere roughly from 3 to 10 km. This is a function of the temperature differential between equatorial and polar regions, and the earth's rotation. This north-south temperature gradient is generally steepest in mid-latitudes, where it increases with height to a maximum near 10 km and is associated with a zone of strong westerly flow.[10] The westerly jet streams at the periphery of the vortex play a vital role in the development and steering of the surface cyclones and anticyclones, so that variations in weather (and individual meteorological elements) from day to day, season to season, and year to year, and from one region to another are closely linked with deformations of this upper vortex. Those areas below the periphery of the vortex are generally characterized by a succession of eastward-moving frontal cyclones, whereas regions under the sluggish cold core of the vortex experience persistent "cold lows," cold, non-frontal systems resulting from the "occlusion" of the frontal storms; the majority of the storms are occluded before they reach the Arctic. Aloft, the cold low centers of the circumpolar vortex appear to be related to the upward growth of these occluded systems in which adiabatic cooling occurs.[25] The movements of these cold lows are slow, erratic and difficult to predict. Anticyclones are typically large, irregular areas of high pressure, without distinct centers and characterized by subsidence and stability. In the Arctic, they are frequently shallow surface systems, but when they are associated above with the northward ridging of the circumpolar vortex and are capped by warmer air of subtropical origin, they become deep and persistent. From time to time, smaller migratory anticyclones move out of the Arctic toward the southeast, directed by the upper flow, but more characteristically these sytems are very slow-moving and tend to oscillate around preferred positions or to change shape rather than to follow clearly defined paths (see Table Ib, constancy factor).

Table Ia. Means, extremes and variation of cyclonic data.

Sector	I	II	III	IV	V	VI	VII	Total
No. of cases	129	223	251	344	94	190	135	1366
Pressure								
Mean	993	977	984	993	997	998	996	990
Maximum	1024	1023	1023	1024	1024	1023	1018	1024
Minimum	968	938	949	954	968	973	964	938
Velocity	NNE 190	NE 260	E 250	E 215	NE 260	E 210	NE 50	ENE 195
V.S.D.	485	480	390	390	450	395	385	435
Speed	440	440	385	385	450	425	310	400
Constancy	43	58	64	55	57	50	17	49

Table Ib. Means, extremes and variation of anticyclonic data.

Sector	I	II	III	IV	Total
No. of cases	172	119	267	220	778
Pressure					
Mean	1028	1040	1041	1034	1036
Maximum	1063	1072	1072	1056	1072
Minimum	1006	1012	1012	1008	1006
Velocity	E 85	S 50	E 70	E 145	E 85
V.S.D.	380	355	365	430	390
Speed	315	275	305	365	320
Constancy	27	19	24	40	27

December, January, February, 1952-1957, North of 60°N (after Keegan,[14] p. 515).
Pressure – sea level pressure in center of cyclone (or anticyclone) (mb).
Velocity – mean velocity of cyclone (anticyclone) movement (n. mi. /day).
V.S.D. – Vector standard deviation of velocity (n. mi. /day).
Speed – mean speed of cyclones (anticyclones) without regard for direction (n. mi. /day).
Constancy – the mean "velocity" divided by the mean "speed" (percent).

Mean patterns of the vortex

Figure 3 shows the mean situation for January, April, July and October at approximately 3 km* above sea level. The vortex shows a marked three- to four-wave pattern which appears to reflect the influence of the earth's major topography and the differential heating of the continents and oceans.

In winter (Fig. 3a) the vortex shows three centers: over the Canadian Archipelago, Kamchatka, and Novaya Zemlya. There are two major troughs, over eastern North America and off the east coast of Asia, with a third weaker trough over eastern Europe. The main ridges lie over the eastern Pacific and Rocky Mountains and over the eastern Atlantic and Scandinavia, with the third weaker ridge over the Urals and western Siberia. The well-developed ridge over the longitudinal barrier of the Rocky Mountains and the deep trough downstream over eastern North America are quasi-permanent features of the general circulation throughout the year. In winter, however, they are most firmly established, as the equator-pole temperature gradient is greatest, the vortex most intense, and the westerly flow strongest. As the gradient builds up during the fall, the vortex expands and the belt of strongest westerlies shifts southwards. Over Asia, towards the end of October, this belt reaches the latitudes of the Tibetan plateau, some 5000 m high, which forms a latitudinal barrier approximately the same width as the current itself. The current splits, flowing around the barrier in northerly and southerly branches to reunite downstream in a deep trough off the coast of eastern Asia. The southern branch is remarkably steady and seems to be anchored by the massif until the vortex contracts again in the spring, so that the deep trough off Asia remains a highly stable feature of the winter circulation.[31] The ridge over the eastern Atlantic is more variable and is believed to be partially a resonance effect downstream from the Rockies.

Owing to these strong southerly and northerly components of the main westerly current, cold dry Arctic air is carried far to the south especially over central and eastern North America and eastern Asia, while warm, moist air over the oceans of lower latitudes is drawn northwards towards polar regions over the Atlantic and Pacific oceans. In the troughs over eastern North America and Asia, temperature gradients between continental and oceanic air are strongest, and here are located the major cyclogenetic regions of the hemisphere at this season, with a third associated with the European trough over the Mediterranean. The surface cyclonic disturbances are steered northeast towards polar latitudes in the direction of the upper air flow and frequently spiral in towards the upper vortex centers. As they approach high latitudes, they generally lose much of their temperature contrast and the warm air is undercut and lifted off the ground by the colder air (i.e. the cyclone becomes occluded). Over the north Pacific and Atlantic, there are the two main "graveyards" where many storms stagnate and fill; this shows up clearly on the mean surface pressure map (Fig. 5a). Occasionally cyclones are regenerated at the ice-water margin, and storms continue towards the central Arctic. Anticyclogenesis occurs just east of the major ridges, the Yukon showing a particularly high frequency;[2] while occasionally systems move out to the southeast, they can remain stationary for many days at a time.

---

*It is customary in the free atmosphere to work with standard pressure levels rather than standard heights above sea level. These charts show the mean height of the 700-mb pressure surface, which is approximately 3 km above sea level. The direction of flow is generally parallel to the contours of a constant pressure surface; the closer the contour spacing, the faster the flow.

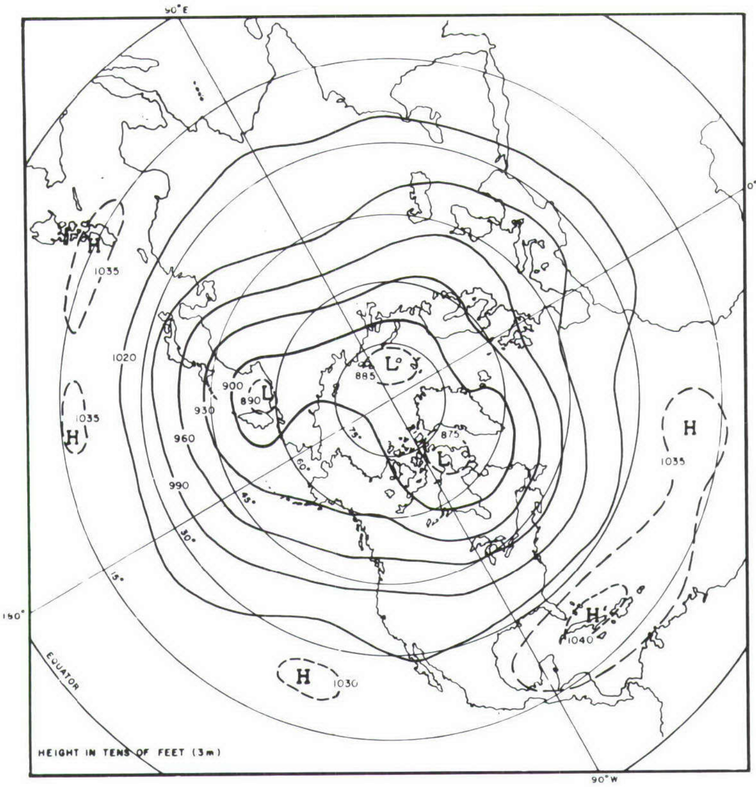

a. 12-year mean, January 1947 to 1958.

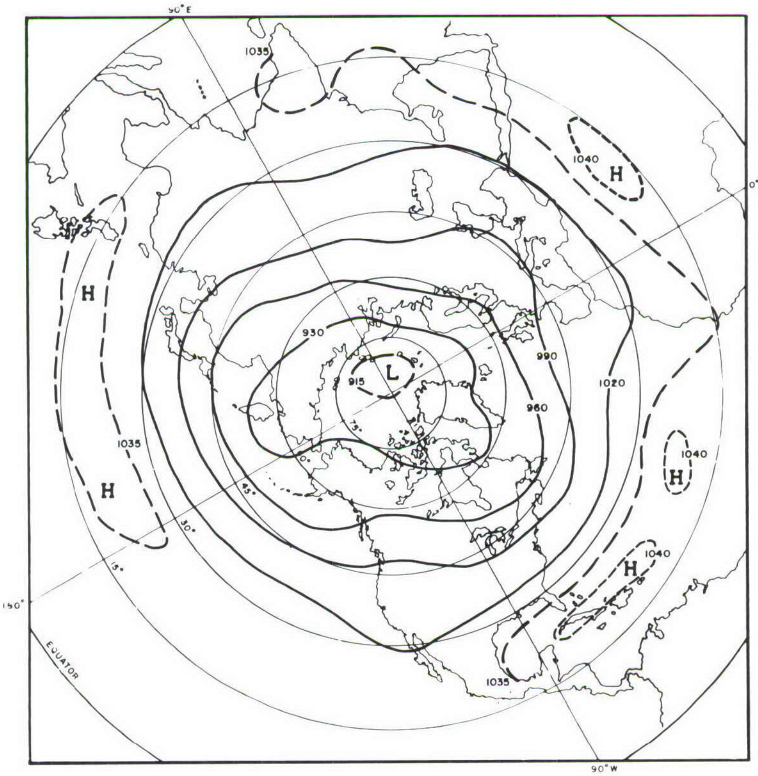

b. 12-year mean, April 1947 to 1958.

Figure 3. Mean height of the 700-mb surface (O'Connor, 1961.[21]).

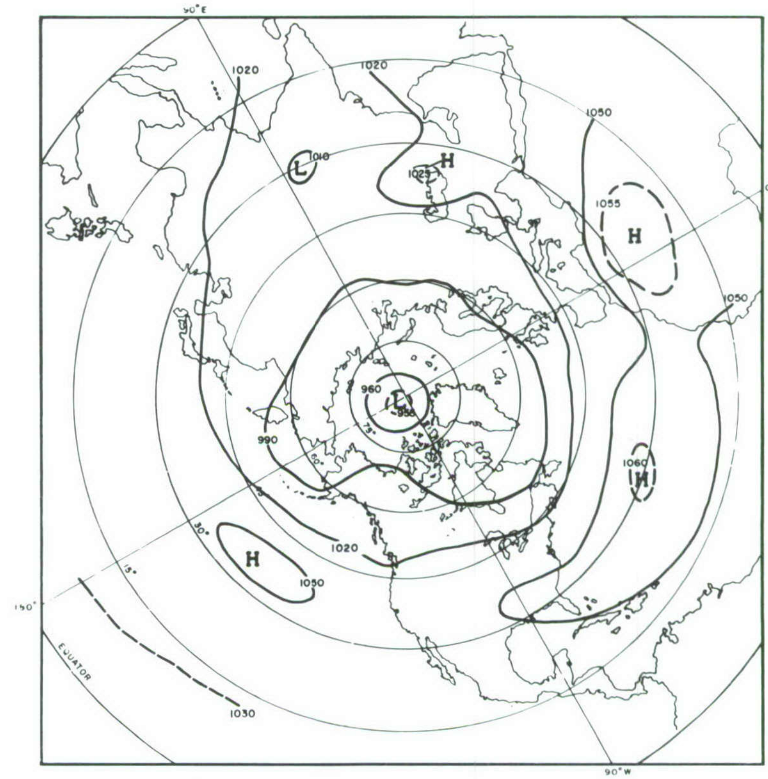

c. 12-year mean, July 1947 to 1958.

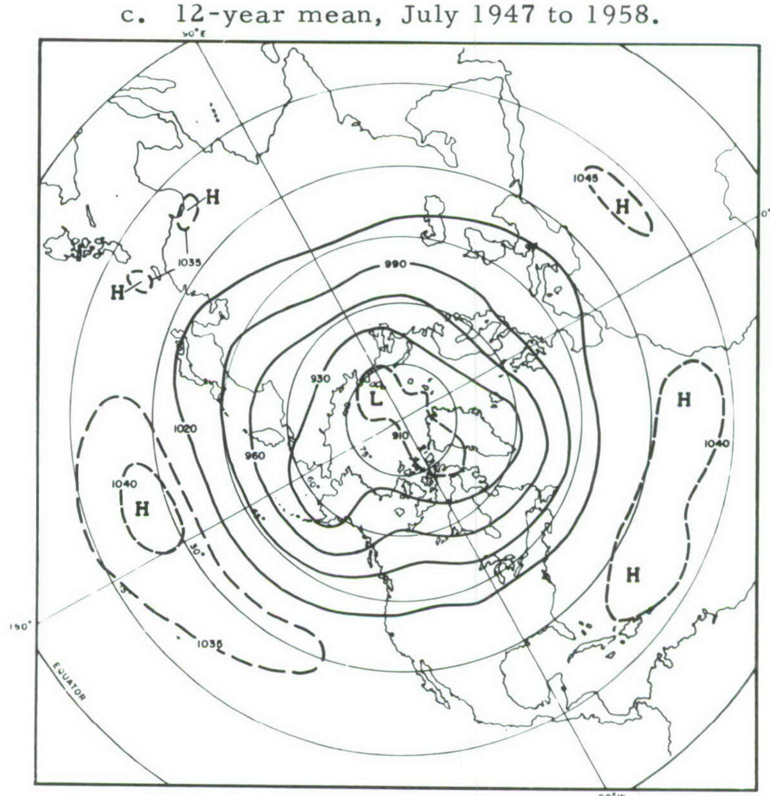

d. 12-year mean, October 1947 to 1958.

Figure 3 (Cont'd). Mean height of the 700-mb surface (O'Connor, 1961[21]).

Through the spring and in summer (Fig. 3b, c), as the north-south temperature gradient diminishes, the vortex weakens and contracts to a single mean center near the pole. The mean location of the belt of strongest westerly flow and the corresponding tracks of surface cyclones now lies over higher latitudes. With the lessening of the energy in the vortex and its contraction to the north of the Tibetan plateau, the wave pattern is weaker and the circulation tends to be more zonal (i.e. from west to east). With the heating of the snow-free land surfaces at this season, cyclogenesis is frequent inland over the subarctic and at the ice-water-land margin of the Arctic Ocean. The mean surface pressure chart for July (Fig. 9a) shows a weak amorphous circulation pattern, hiding the considerable small-scale fluctuations that can occur from day to day – the successions of weak, rapidly moving cyclones, and the oscillating cold lows that persist below upper level vortices over the central Arctic. In summer, cyclones predominate over the Arctic and subarctic, with the exception of the zone 70-75°N where anticyclones are more frequent.

With the exception of the Pacific trough, the autumn patterns both aloft (Fig. 3d) and at the surface (Fig. 11a) already closely resemble those of midwinter.

Variability of the vortex pattern

The change from a well-developed wave pattern with strong northerly and southerly components (a meridional situation) of easterly flow to a more zonal (west-east) flow pattern, already recognized in the seasonal means, is one of the most significant features of the northern circumpolar vortex with respect to Arctic and subarctic climates.[19] It is especially remarkable in the colder season, when the patterns are more strongly developed, that the vortex appears to undergo a cycle of deformation of a period of roughly a month from more zonal flow to strongly meridional conditions, when the long-wave pattern intensifies – the major cold troughs over the continents extend rapidly towards the Equator, while the warm ridges over the Pacific and Atlantic reach northwards, frequently as far as the inner Arctic Basin. One sector may experience a more zonal flow while meridional conditions exist at other longitudes, and the sequence and mechanism of these changes has still not been fully explored. During zonal flow, however, a slow progression of the long waves towards the east is characteristic; as the zonal flow "breaks down" the situation frequently becomes quasi-stationary, followed by an apparent slow retrogression towards the west.

The effect on Arctic and subarctic climate of these major changes in general circulation is best described with the aid of synoptic examples. Figures 4a, b illustrate a well-developed meridional circulation on January 6, 1959:

At approximately 5.5 km (500-mb surface), the pattern is dominated by a warm ridge extending northwestward from the Atlantic to the pole itself, with other major ridges over the Pacific and western Siberia, and a weaker ridge over North America; the cold vortex has four main centers located in the troughs over subpolar latitudes. The strongest westerly flow is associated with the strongest temperature gradient.

The sea-level pressure chart neatly reflects these circumstances. Strong anticyclonic conditions exist over the Arctic Basin and down over North America and Siberia – essentially a cap of very cold, dense dry Arctic air. These polar "outbreaks" over the continental masses temporarily extend the Arctic climate into middle latitudes. Frontal cyclones below the strong westerly currents are being steered around the troughs into graveyard areas where they stagnate and fill, on this occasion over the Gulf of Alaska, Labrador (with a characteristic extension of the trough over Davis Strait and Baffin Bay) and Scandinavia. The upper ridge over the Atlantic – Davis Strait region successfully blocks the main line of entry of storms into the Arctic Basin, but over northeastern Siberia weak cyclonic disturbances are being guided around the upper vortex from the Sea of Okhotsk northward to the Arctic Ocean, where they soon fill and disappear; * similarly storms moving towards the Barents Sea around the European trough rapidly weaken and fill in the vicinity of the upper low center over Novaya Zemlya.

Figure 4a also shows spot temperature reports and regions of falling snow. In general the anticyclonic areas with clear, calm conditions are the coldest, with continental temperatures lower than those over the Arctic basin. The lowest values (below -50C) are recorded in the valleys of the Yukon, Alaska, and northeastern Siberia and local fog (probably ice fog) is frequent where temperatures are below -40C. Blowing snow is reported where pressure gradients are particularly steep, for example over the northern Canadian Archipelago, where winds and a temperature of -33C also give a severe wind-chill effect. Higher temperatures and "storms" are associated with the four cyclonic centers of activity and with open water, where the strongest temperature and humidity contrasts and pressure gradients exist. Over northeastern Siberia and the Gulf of Alaska, these gradients are emphasized by the strong relief barriers which cut off the interior from the full effect of the open ocean. The 0C recorded on the western shore of Greenland, near the open water of Davis Strait, contrasts with the -50C on the same latitude in western Canada. Over northern Eurasia in general, the temperature distribution is a mirror image of that over North America, with temperatures near 0C at the Pacific coast falling rapidly to -50C in northeastern Siberia, then varying between -30C and -40C over the central section with a rapid rise to -20C over the White Sea and north Scandinavian coasts. Snow, cloud cover, blowing snow, high winds and high windchill are generally associated with these strong cyclonic centers.

Figures 4c, d illustrate a more zonal circulation on February 26, 1959.

At the 500-mb level the vortex shows a single major cell and is more nearly circumpolar, with a characteristic tendency towards asymmetry. The jet streams and associated storm tracks cross more northerly latitudes over northwestern Europe and west-central Siberia.

At sea-level, cyclonic circulation dominates the Arctic and subarctic, with the exception of the northeastern extension of the Siberian anticyclone linked by a narrow weak ridge to a small high pressure center south of Hudson Bay. Trains of frontal cyclones move eastward with the westerlies, spiraling in towards the upper vortex center. In general, circulation patterns are weaker over northern latitudes below the central vortex with less striking regional contrasts in weather than on January 6. The major difference lies in the weak ridge development over the Pacific and Atlantic; instead, there is a ridge of high pressure over central Europe and Scandinavia, and a series of Atlantic storms is being steered through the North Atlantic gateway and into the central Arctic under the vortex center.

---

* See Appendix A, Figure AI.

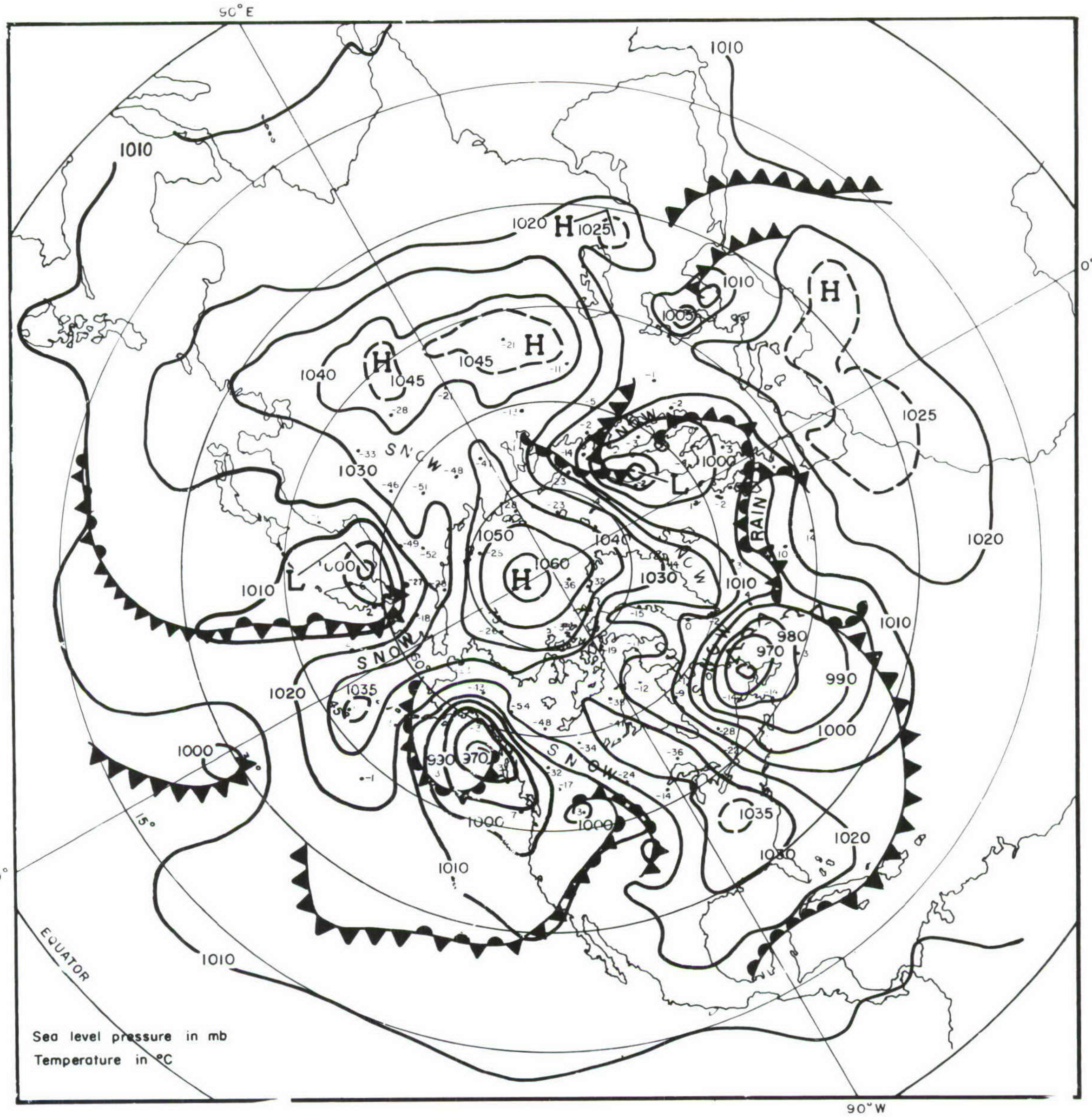

a. Sea level, 1230 GMT, 6 January 1959.

Figure 4. Selected daily synoptic charts for sea level and the 500-mb surface.

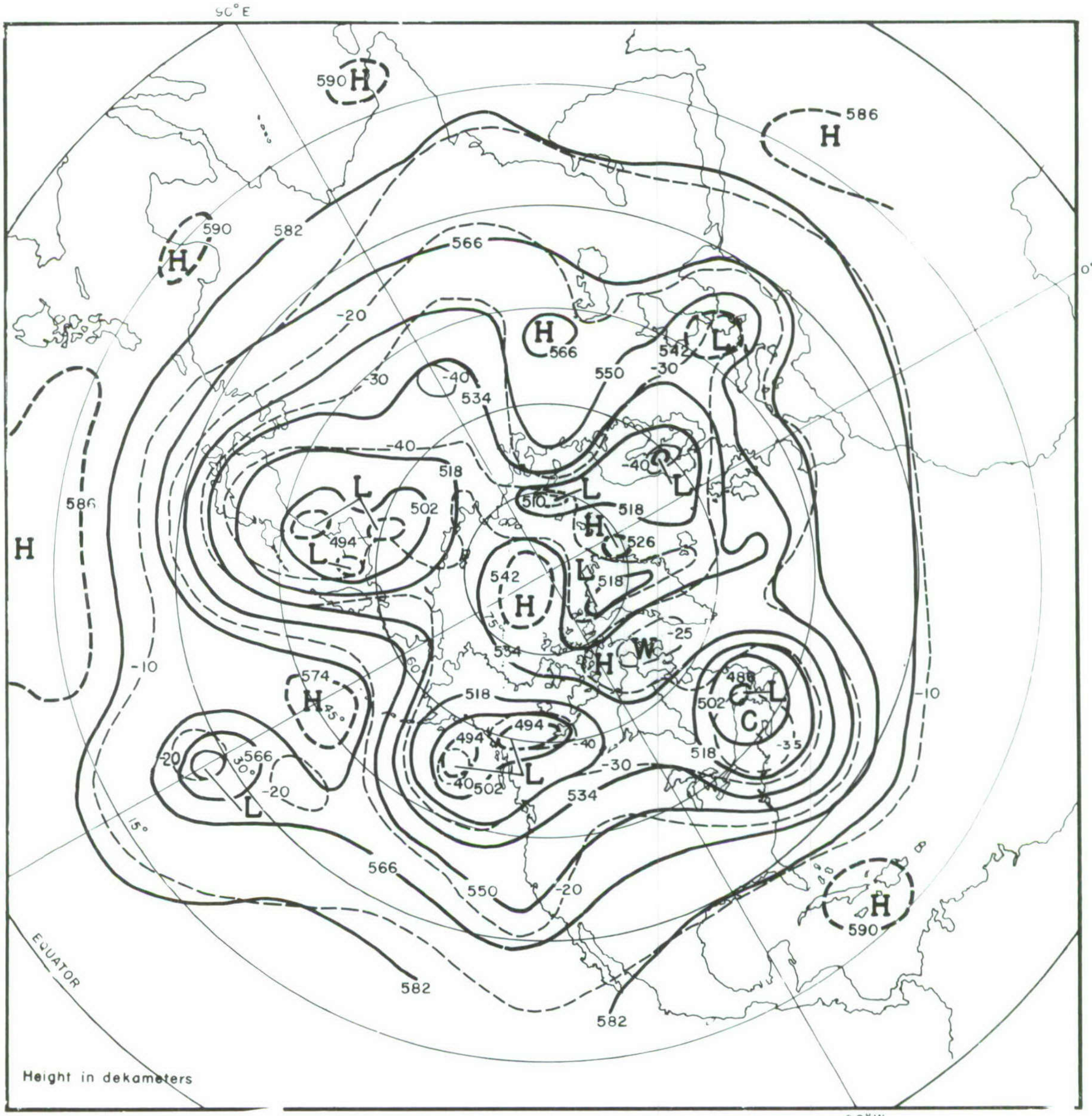

b. 500-mb level, 1200 GMT, 6 January 1959.

Figure 4 (Cont'd). Selected daily synoptic charts for sea level and the 500-mb surface.

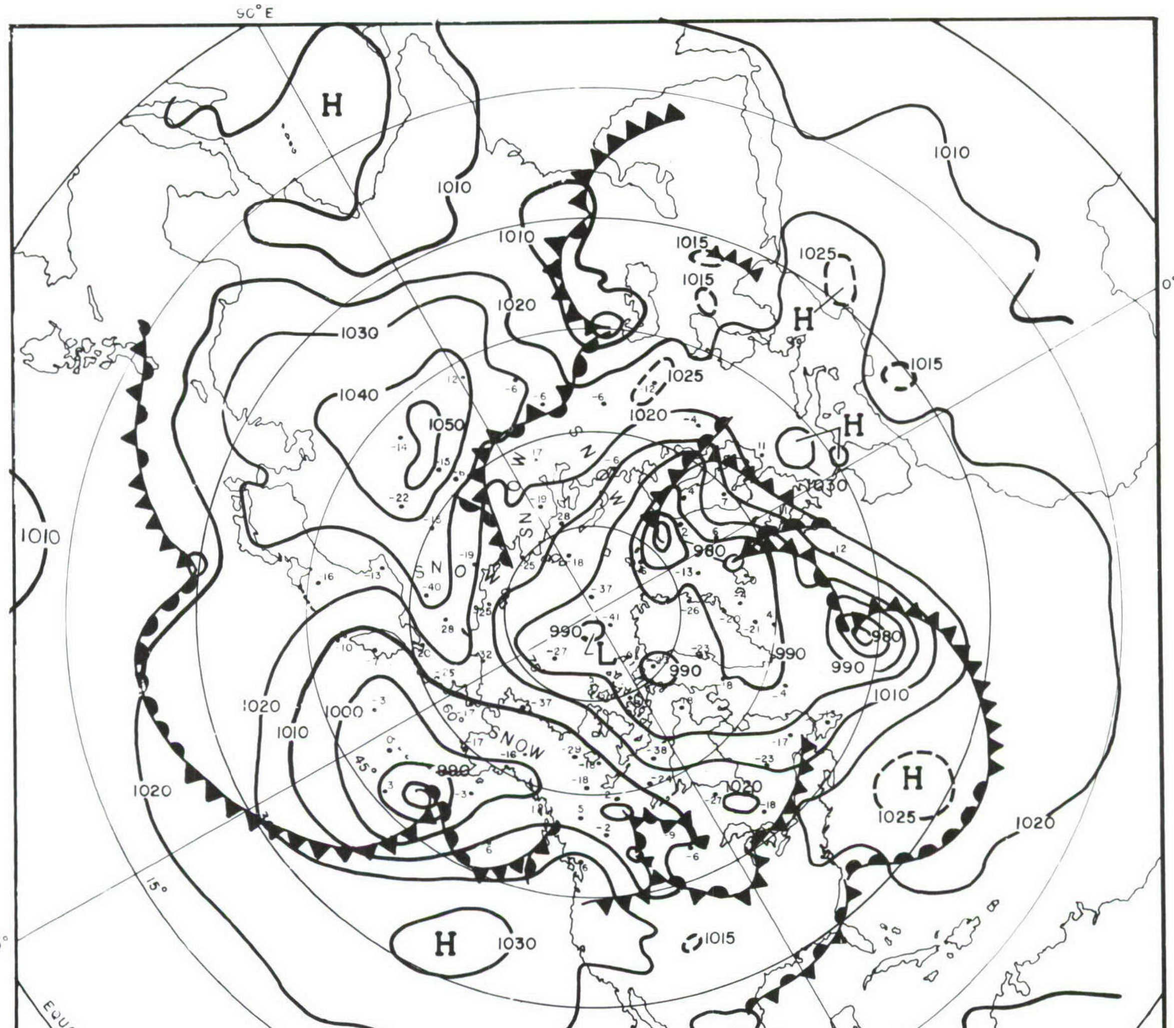

c. Sea level, 1230 GMT, 26 February 1959.

Figure 4 (Cont'd). Selected daily synoptic charts for sea level and the 500-mb surface.

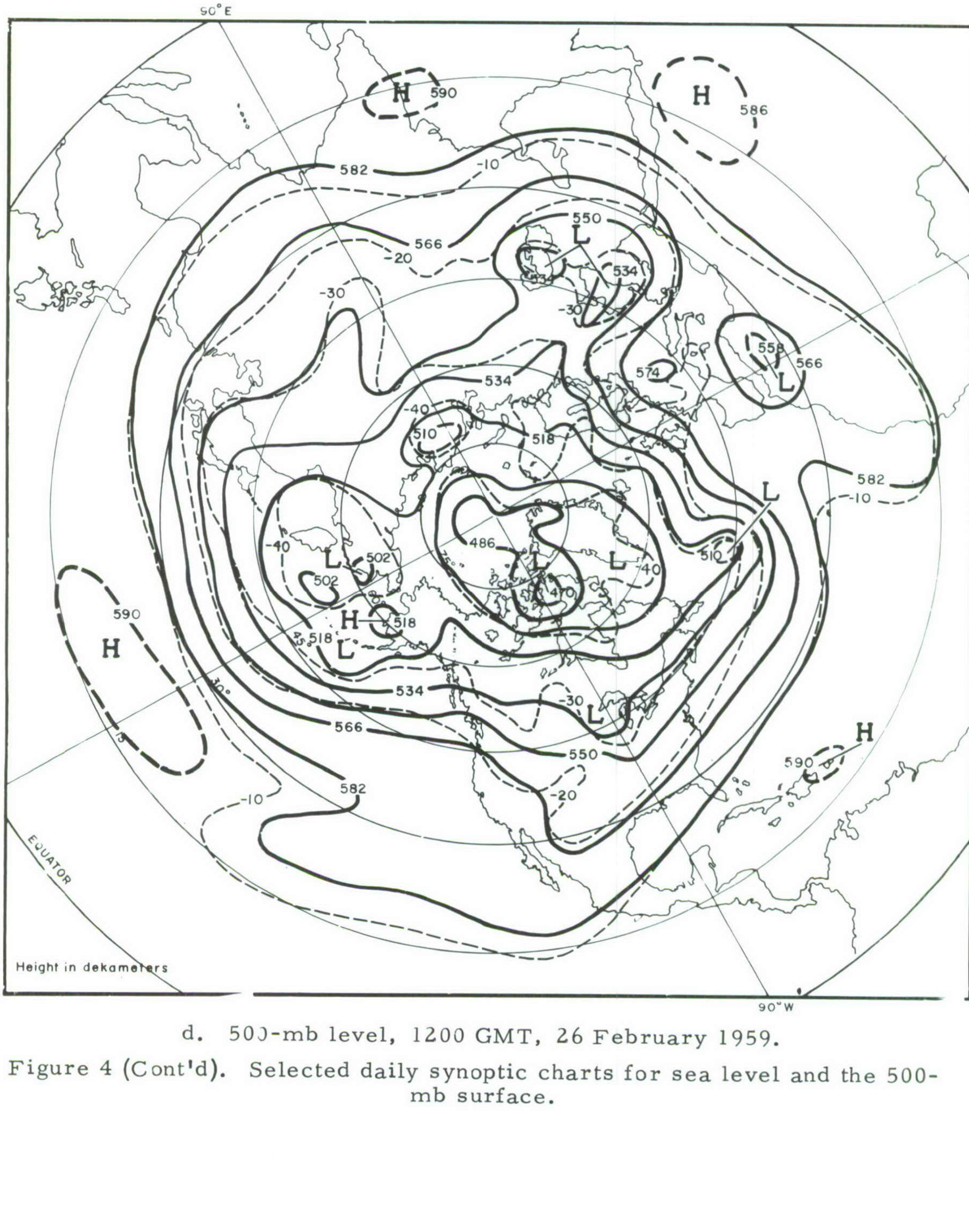

d. 50)-mb level, 1200 GMT, 26 February 1959.

Figure 4 (Cont'd). Selected daily synoptic charts for sea level and the 500-mb surface.

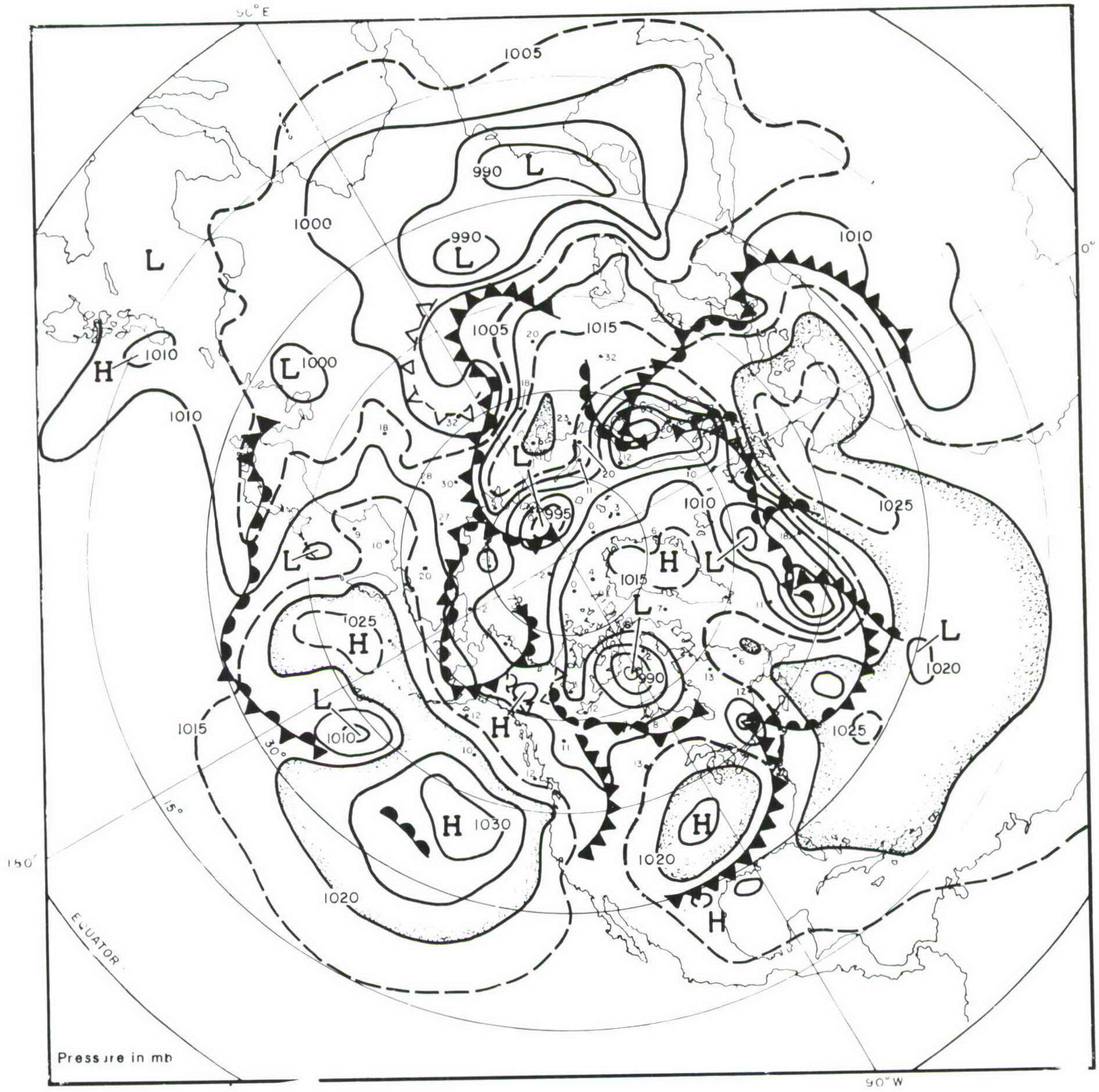

e. Sea level, 1230 GMT, 2 July 1959.

Figure 4 (Cont'd). Selected daily synoptic charts for sea level and the 500-mb surface.

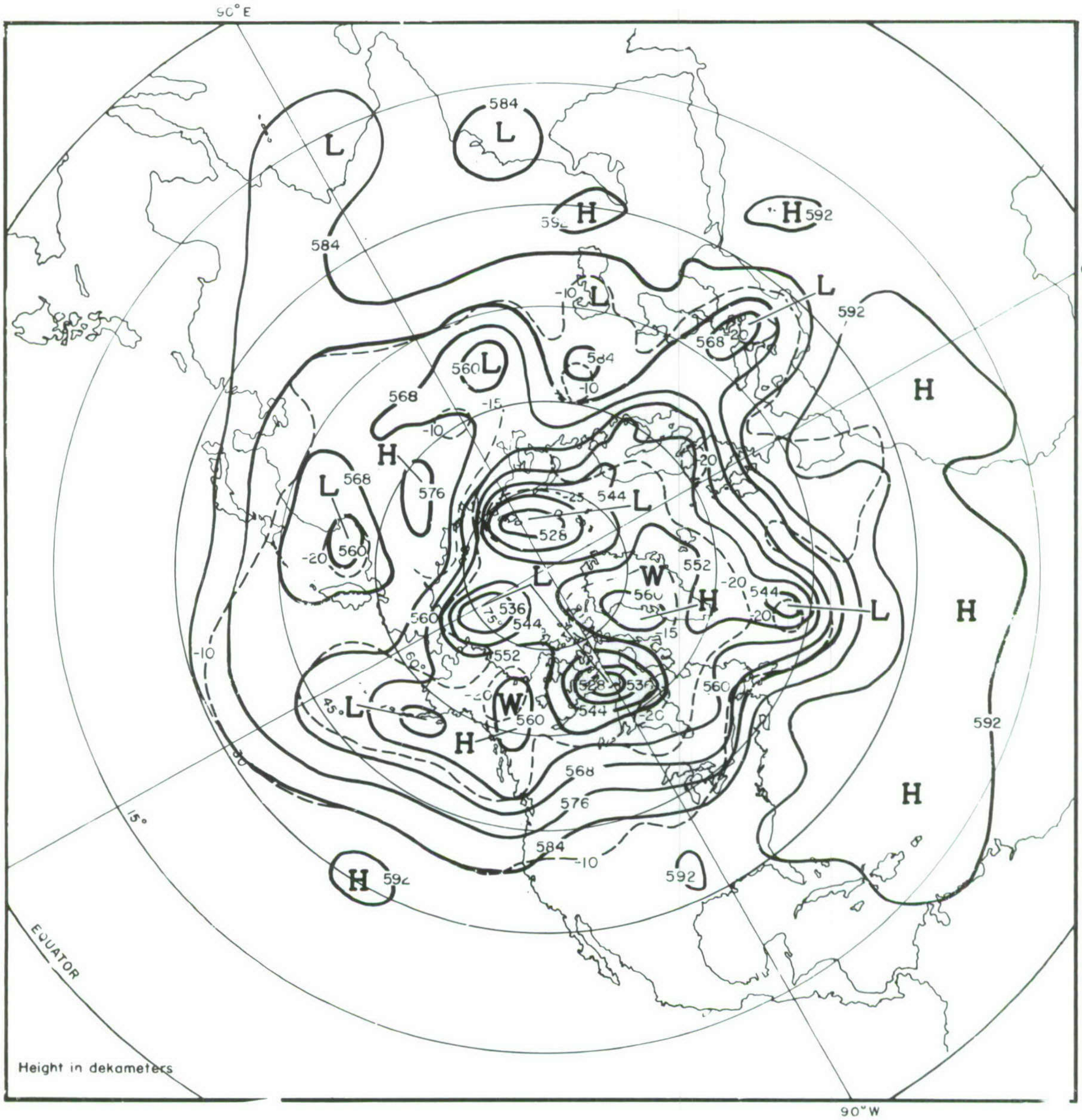

f. 500-mb level, 1200 GMT, 2 July 1959.

Figure 4 (Cont'd). Selected daily synoptic charts for sea level and the 500-mb surface.

The cold low center at the surface near the pole is giving neither cloud nor precipitation and winds are light, so that surface cooling is unhindered and temperatures as low as -37 and -41C are reported on ice islands near the pole. However, the active storms entering the Barents Sea are associated with cloud, snow and temperatures around the freezing point, and 48 hours later the temperature on one of the ice islands had risen to -19C as a storm approached the pole; an overcast sky with continuous light snow and 11 m/s winds were also reported. The Atlantic gulf of warmth shows up well on this chart.* It is the major source of warmth and humidity in the central Arctic at this season and is reflected in almost every climatic distribution.

Over North America, the eastern areas are now under the influence of northwesterly flow from the Arctic; and the cold dry conditions of New Quebec and Labrador contrast sharply with the abnormal warmth and heavy snowfall of January 6. On the other hand, western North America reports temperatures 20 to 30C higher than on the previous occasion as Pacific storms "jump" the mountain barrier, reappear as weaker centers and cross the plains. Over Eurasia, the upper trough previously over the Mediterranean now lies to the east over the Caspian Sea (Fig. 4d) and surface storms (Fig. 4c) are moving across central Siberia to the Arctic coast while the weakening anticyclone is now confined to eastern Siberia. As a result of this southerly flow, snow and cloud, temperatures are 20 to 30C higher over much of the region compared with January 6, while the eastern coast of Asia experiences colder weather under the cold northerly flow around the anticyclone cell. Northwestern Europe, in the warm southwesterly airstream, reports temperatures that are almost without exception above freezing.

Figures 4e, f, charts for July 2, 1959, illustrate a summer situation.

The 500-mb map shows the weaker, contracted vortex of the summer season; at the surface the broad scale patterns are less well-defined and the cyclonic and anticyclonic systems comparatively weak and shifting. Over Siberia, the strongest upper westerly flow and steepest temperature gradient are over the northern coastal region; on the North American side, this belt lies further south. A succession of small surface cyclones is moving eastwards in this flow to fill (eventually) below the shallow vortex centers aloft. At the surface, a very strong temperature contrast exists between the Arctic Ocean or coastal stations, where temperatures are close to 0C, and inland stations. Even at sheltered locations near the coast, temperatures soon rise to over 10C and by some 500 km inland reach values as high as +25 or even +30C. Reed[25] has remarked on the high frequency of frontal storms along this belt in summer, which he associates with these strong temperature gradients.

Over North America the 500-mb chart shows weak ridge development over the Davis Strait-Greenland area and the northwest, almost cutting off the cold vortex center over Keewatin.† At the surface, weak high pressure systems and a cold low center reflect this upper pattern, while weak frontal

---

*See Figure A3 for an excellent example of a sequence of cyclones from the Atlantic sector entering the Arctic Basin.

† Charts for July 19 and 22, 1956 (Fig. A4) show a situation with strong westerly flow over the North American Arctic.

systems are beginning to move down over Alaska and the Yukon as the upper flow strengthens in the next 48 hours and the cold low gradually fills. The reported temperatures over this sector are notably lower than those over Eurasia. This is largely a result of the complex interpenetration of land, ice and open water (Hudson Bay extending almost to 50°N), together with the fact that a fair proportion of these stations have coastal locations. A further factor of influence in the more southerly regions is the difference in the local time of observation; at 12:30 p.m. at the Greenwich meridian it is late afternoon near 90°E, and early morning at 90°W.

The main Atlantic storm track at this season typically crosses southern Scandinavia as in Figure 4e, while higher pressure is predominant over the Barents Sea. On July 2, temperatures as high as +12C were recorded on the north coast of Scandinavia, with +11C on Novaya Zemlya. It is a question not only of the warm southerly airstream on this occasion, but the general northward drift of relatively warm Atlantic waters. In turn, the coolness of the east coast of Greenland is also due to a large extent to the southward drift of the ice-laden waters offshore. Over the northeastern Pacific, the configuration of the coastline is not so favorable to the northward penetration of the warm surface waters into the central Arctic and temperatures on the north Alaskan coast remain near 0C.

Drizzle and light rain are reported from place to place in the vicinity of fronts; over the Beaufort Sea and Franz Josef land there is continuous snowfall and to the west of Lake Baikal, thunderstorm activity. Overcast skies and fog are widespread over northern coastal areas primarily as a result of the cooling effect on the air of the ice and cold northern waters. Here the local factors of station situation and wind direction play an important role.

Several basic considerations concerning the variability of northern climates arise from these three examples:

(1) Persistence of the large-scale patterns. The stalled large-scale circulation patterns on January 6, 1959 are characteristic of well-developed meridional situations, which can be highly persistent. Over the Western Hemisphere, the broad pattern remained essentially unchanged from early January, with the extension of the Atlantic ridge, to January 24, when there was a shift to the east and storms once again traveled northwards over the Atlantic. Regionally, these stalled situations can result in extended periods of abnormally cold or mild temperatures, drought or heavier than normal snowfall, high winds or other extreme conditions. Over the Eastern Hemisphere, there was a change to more zonal flow over Eurasia in the second half of the month, * and this pattern tended to persist well into February.

(2) Importance not only of relief barriers in the modification of the tracks and frequency of surface cyclones and anticyclones but of the dynamic barriers formed by persistent well-developed upper ridges and high centers. Areas of most frequent "blocking" are Scandinavia,[28, 29] Alaska, the Ural region and the Davis Strait-Greenland sector. Blocking is characteristic of the spring (March), when anticyclonic conditions are most frequent over the continental areas of the high Arctic. At this season the snow and ice cover

---

* See charts for January 14, 19, 21, 1959 (Fig. A1-2).

is still intact, the air is stable and visibility is good, so that flying conditions are generally at their best.

(3) Effect of the degree of expansion or contraction of the vortex and the subsequent abnormal displacement of the upper westerlies. In the summer this becomes a major factor over the Arctic and subarctic. In August 1955 the strongest westerly flow lay over the rim of the Arctic Basin and was associated with an unusually high frequency and intensity of cyclones. This has repercussions on the distribution of ice and open water, and seriously jeopardized the success of the supply mission to the Distant Early Warning (DEW) Line sites under construction between Point Barrow, Alaska and Shepherd Bay, Canada[38]*. It was not until the polar vortex began to break down about September 5 and storms took a more southerly track across the Bering Sea and Alaska, that an offshore lead was created permitting supply operations to continue along the coast of north Alaska. Here the steady offshore flow of cold moist air slowed down the disintegration of the pack ice in August and caused refreezing of the leads by thermal action, but sometimes offshore winds open leads by their dynamic effect.

In brief, since the tracks of surface disturbances are so closely related to the upper westerlies, the climate of any season or year, decade or epoch over the Arctic and subarctic depends to a large extent on the relative frequency of either zonal or meridional conditions, on the most favored location of blocking, and on the degree of contraction or expansion of the vortex. The southern limit of the polar region fluctuates accordingly. On a regional scale, the local shape, orientation and intensity of the vortex, the location of individual cells, and the changes in its morphology are basic considerations. In Scandinavia, Germany, and the United States there has been considerable study of these large-scale upper-air patterns and their changes over high latitudes, perticularly in connection with long-range forecasting and forecasting over "silent" areas. There appears to be a tendency for a particular type of large-scale circulation pattern to recur persistently in the same season after only a brief interruption. The nature of the pattern may differ considerably from one season to the same season of another year. Thus the average or normal conditions conceal several well-defined modes of general circulation, each remarkably stable[19] over the Arctic.

Mean Sea-Level Pressure and Frequency of Cyclones and Anticyclones

Winter

The distribution of mean sea-level pressure for January (Fig. 5a) summarizes the winter situation. The major semi-permanent features are the Icelandic and Aleutian lows and the Siberian and northwest Canadian highs linked by a ridge across the Arctic Ocean. The mean isobars give some indication of the general direction of flow. Klein's charts (Fig. 5b, c) supplement the mean map by indicating the most frequent areas of formation and "stagnation" of cyclones and anticyclones and their major tracks.

---

* The charts for July 19 and 22, 1956 (App. A) offer an example of a single strong vortex center over the Polar Basin; this pattern persisted throughout the month, while the center slowly revolved around the basin from west to east.

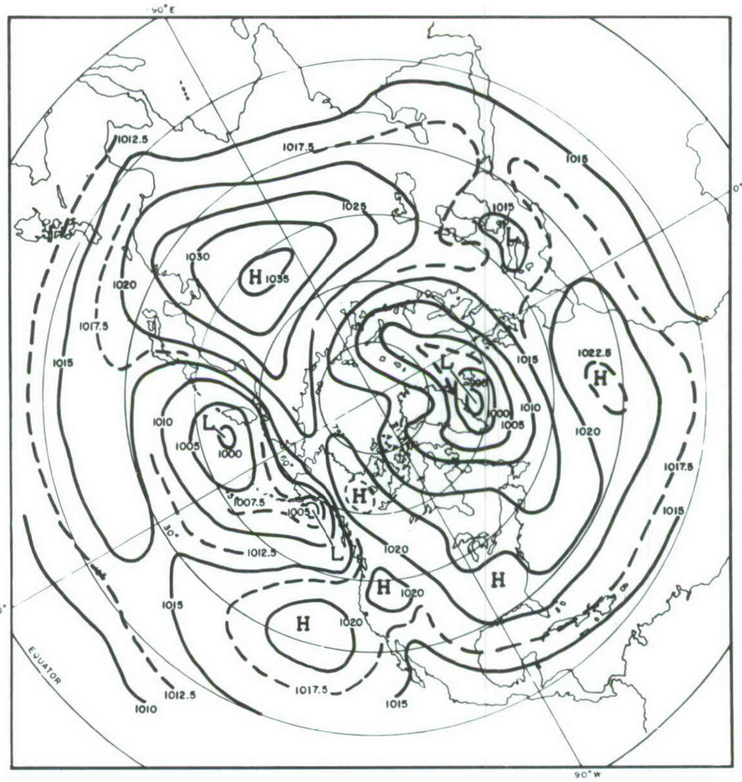

Figure 5a. Sea level pressure (mb), January (12-year mean)(O'Connor, 1961[21]).

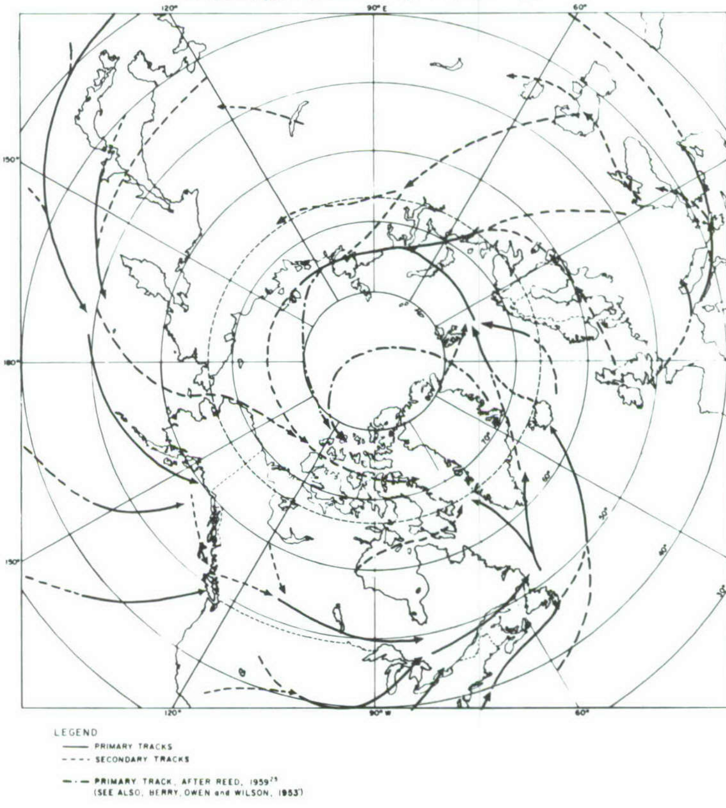

Figure 5b. Principal tracks of cyclones, January (after Klein, 1957[15]).

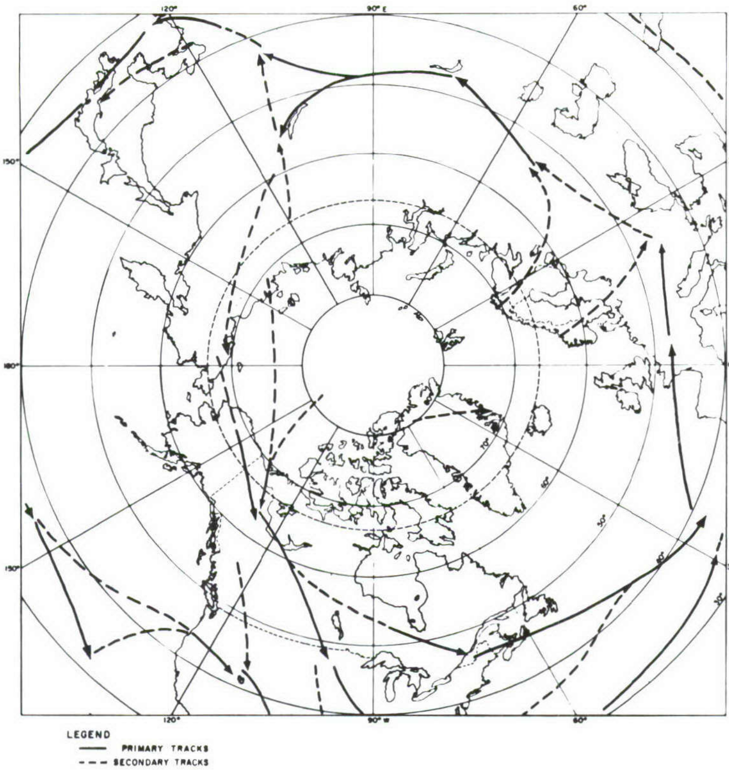

Figure 5c. Principal tracks of anticyclones, January (after Klein, 1957[15]).

Over North America most anticyclones form over Alaska and northwest Canada in relation to the upper Pacific ridge. Some travel southeastward, either continuing over the Great Plains of the United States or curving north of the Great Lakes towards Quebec. These systems are associated with the outbreaks of cold Arctic air that can extend as far south as Texas and Florida. Cyclogenesis occurs over Alberta, where systems from the Pacific produce closed surface lows on the eastern (lee) slope of the Rockies. These cyclones generally move east-southeast to a center of maximum frequency over the Great Lakes region, where tracks converge from the southwest and south. Most of these disturbances are then steered northeast to Newfoundland. Here they are joined by cyclones from the east coast, where thermal contrasts between the cold continental and warmer maritime air favor cyclogenesis. From Newfoundland storms generally migrate either towards Iceland (their high frequency resulting in the semi-permanent Iceland low), or along the west or east coasts of Greenland. A few disturbances also enter Davis Strait by way of Hudson Bay or drift in erratically from the west Canadian Arctic below the cold upper vortex center, and an area of high cyclonic frequency is located west of Greenland.

Over Eurasia, the westerly jet stream is split into northern and southern branches by the Himalayan massif. To the north of these mountains there is no cyclonic development comparable with that over continental North America, and the winter anticyclone over Siberia is persistent. Cyclones moving eastward over western Siberia are often old occluded storms and rapidly lose their intensity, although secondary cyclones occasionally form near Lake Baikal and deepen rapidly on moving towards the Pacific coast.

Major anticyclonic activity over western Siberia is related to the development and persistence of the strong upper ridge over the Urals. With the collapse of this "blocking", the surface centers move out to the southeast causing outbreaks of intensely cold air over China and Mongolia.[31] These outbreaks are associated with strong cyclogenesis off the east Asian coast. The majority of these east coast storms are steered northeastward toward the Aleutian semi-permanent low center, where they stagnate or curve south. Occasionally storms enter the Arctic Ocean over Northeastern Siberia or the Bering Straits; those that cross the Alaskan mountains appear to stagnate in less than 48 hours.[14] From time to time new storms develop on the north side of these mountains after primary storms have stagnated to the south. In general, storms over the Beaufort Sea appear to be largely of the cold low* type.

The daily charts of more recent years indicate that over the Polar Basin many cyclones spiral in toward the pole, and that cyclones outnumber anticyclones by 2 to 1.[14] Storms breaking off from the Icelandic low usually move northeast to the Norwegian-Barents Sea (an area of high frequency) and a primary track continues along latitude 75°N where "polynyas" or leads appear to exist in the Kara and East Laptev Seas. These frequent storms play an important role in the climate of the north European and Siberian coastlands. This primary track is joined by tracks from the Baltic, Black and Caspian Seas. Some storms stagnate near Novaya Zemlya, others regenerate and curve in toward the pole. However, intense anticyclones occur to the north of the Beaufort and Chukchi Seas, frequently in association with the extreme northward extension of the upper Pacific ridge. It is in March, at the time of the greatest frequency of blocking situations, that anticyclonic conditions are most frequent over the Arctic Basin. Keegan[14] has made frequency counts of the occurrence of low and high centers north of 60°N, per 100,000 sq mi (260,000 km^2) for the winter months, December, January and February, 1952-1957. The area was then divided into sectors, each containing a frequency maximum, and statistics on the frequency of centers and on the speed and direction of the 24-hour displacement were computed for each sector. The charts and statistics are reproduced in Figures 6 and 7, and Table I.

The most striking pattern to emerge north of 60°N is the predominance of cyclonic activity over the "Atlantic hemisphere" and of anticyclonic activity over the "Pacific hemisphere" (the Aleutian low center lies to the south of 60°N). Regions of highest cyclonic frequency extend:

(1) From a maximum south of Greenland to the north of Norway and Novaya Zemlya, spiraling into the central Arctic. Keegan has suggested that the frequency over the Arctic Basin would be greater if the observation network were closer and Gaigerov reports on the large number of cyclones passing over North Pole IV during the winter of 1955-56. These Atlantic storms are responsible for most of the weather and variation in the climatic elements over the Arctic Basin.

---

* A cold low is characterized by colder air near its center than around its periphery.

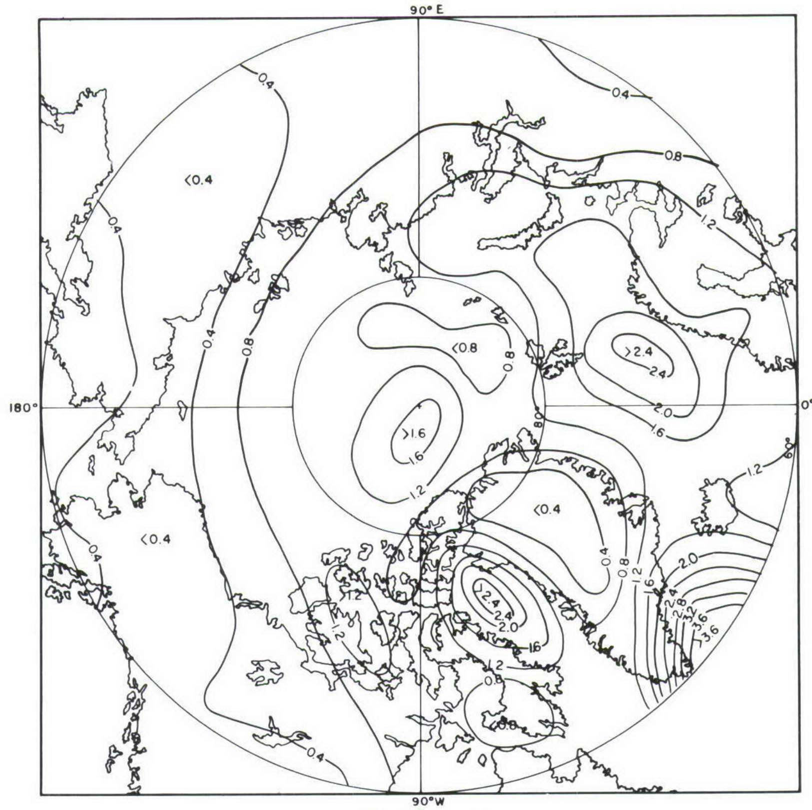

a. Cyclones

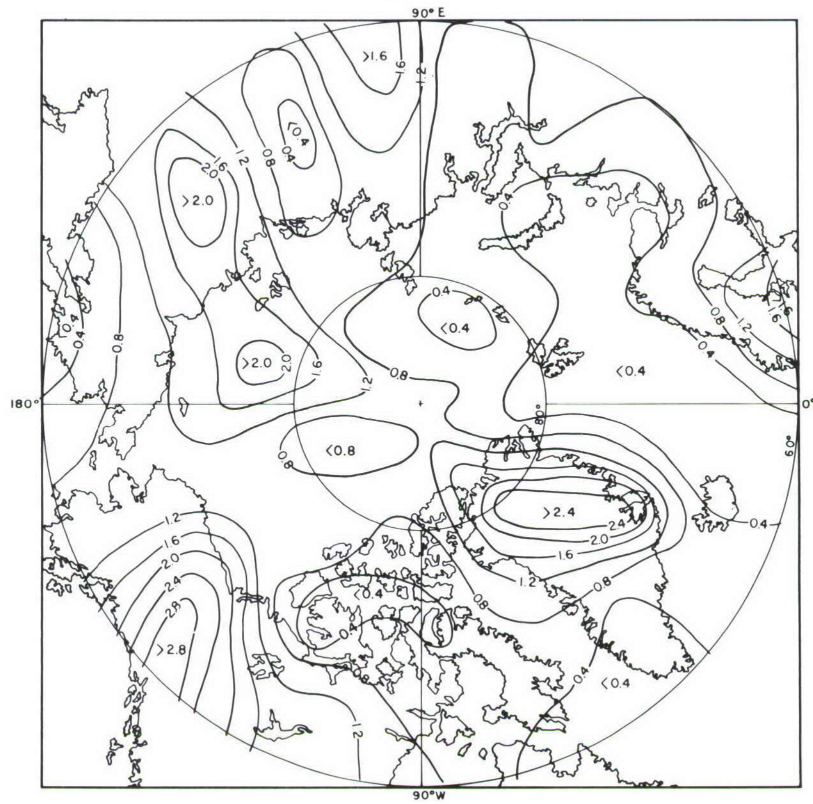

b. Anticyclones

Figure 6. Percent frequency of cyclonic and anticyclonic centers in winter north of 60°N, per 100,000 sq mi (260,000 km²). (Keegan, 1958[14]).

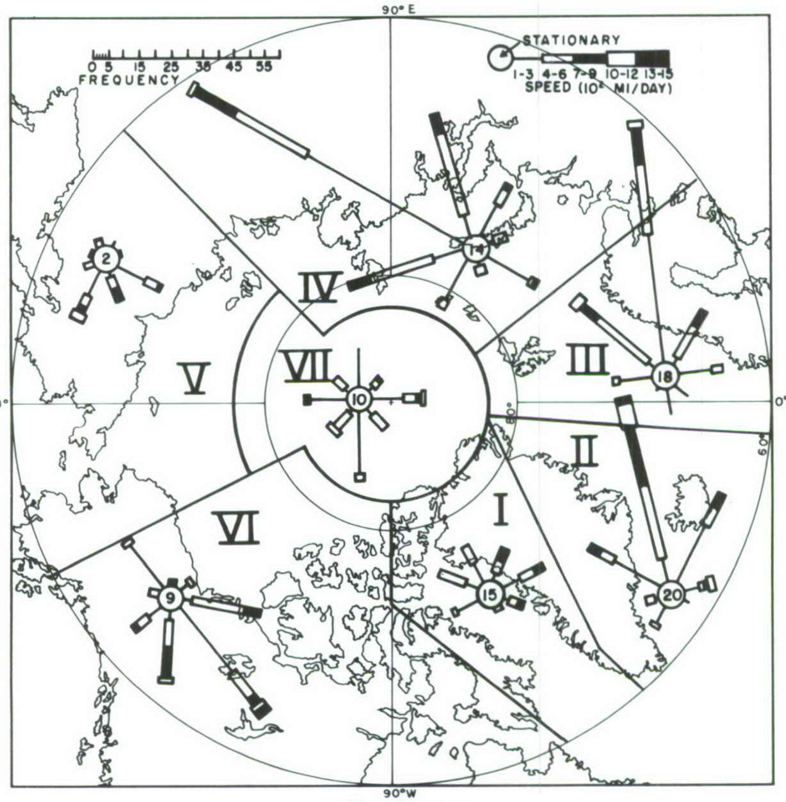

a. Cyclones

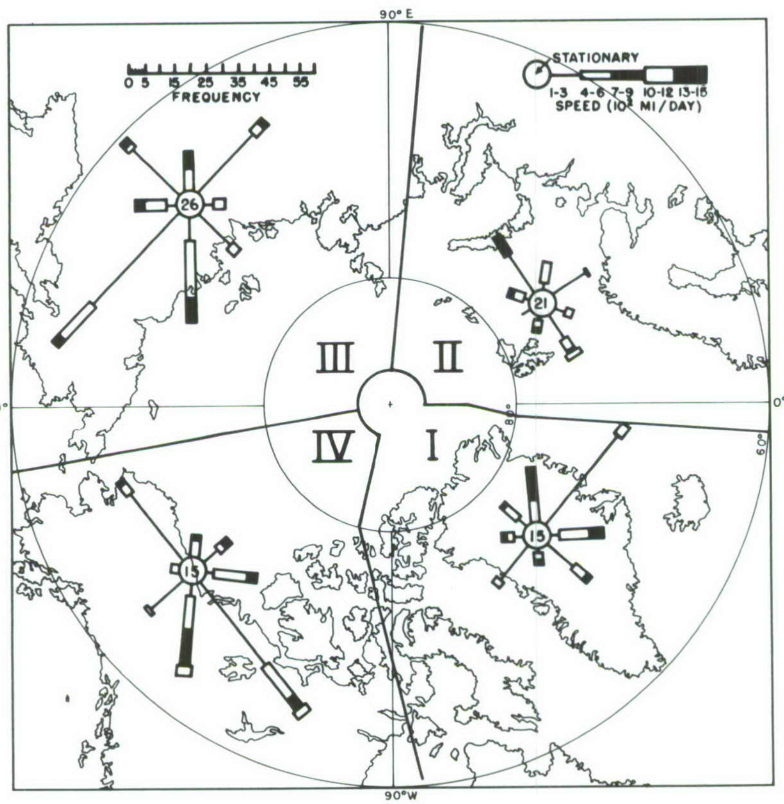

b. Anticyclones

Figure 7. Frequency of speed and direction of movement of cyclones and anticyclones in winter, by sectors. (After Keegan, 1958[14]).

(2) Over Davis Strait and Baffin Bay. The role played by the 2500 to 3000 m barrier of the Greenland Ice Cap is an important question. Evidence has shown[9,23] that the upper manifestations (700 mb) of the surface disturbances and fronts frequently cross the Greenland Ice Cap with significant effect on the weather. These upper-level features can often be identified with renewed surface systems on the eastern side of Greenland. Again, when deep lows lie near southern Greenland or Iceland and there is easterly flow across the plateau, rapid development or intensification occurs to the west (in the lee) over Baffin Bay. The cyclonic activity of this region is the dominating factor in the weather of much of the Canadian Archipelago.

Regions of highest anticyclonic frequency extend:

(1) In an arc from eastern Siberia, over the East Siberian and Beaufort Seas to Alaska and northwest Canada, a reflection of blocking associated with the upper Pacific ridge; there are maxima over the Yukon,[2] the Arctic Ocean and northeastern Siberia. (The very high pressures frequently mapped over northeastern Siberia are due to an overcorrection in the reduction to sea level, though the anticyclonic frequency maximum may still be real.)

(2) Over Greenland. Again, the centers of very high pressure that frequently appear on sea-level charts are due to the reduction of reported surface pressures to sea-level. More than a third of the Ice Cap surface is above 850 mb (1500 m) and the crest over 700 mb (3000 m); mean charts at 700 mb show no sign of such centers at any season, although there is always a ridge due to the topographic barrier. However, the frequency maximum is real. It is composed of both small, shallow systems lying between predominantly cyclonic regions to the east and west, and large systems related to the extension of the main upper Atlantic ridge over Greenland during blocking situations.[10] An analysis of the 12 years 1947-1958 shows a tendency towards more frequent blocking over this region compared with past years.[21]

(3) Over southern Scandinavia – again a favored location of the northward extensions of the Atlantic ridge.[28]

(4) Near 90°E, a northern extension of the main west Siberian anticyclone, which generally lies to the south of 60°N, a maximum linked with the frequent upper ridge development in the vicinity of the Ural Mountains.

Spring

A comparison of the mean pressure charts for January and April (Fig. 5a and 8a) shows the general weakening of the mean systems in spring, the northeast shift in the mean center of the Icelandic low, and the new high pressure centers which are the dominant feature of the high Arctic at this season. In April, the mean 700-mb chart shows a single circumpolar cell, although the axis of the main westerly belt is still far to the south (Fig. 3b); during May and June, however, it shifts rapidly to the north.

During spring there is a reduction in frequency of the anticyclone tracks over western Canada (Fig. 8c), while the primary track shifts eastward towards Hudson Bay. These "Hudson Bay" highs[13] are characteristic of this season when there is more anticyclonic activity in eastern than in western Canada. Over the Arctic portion of North America and Siberia there is a maximum intensification of anticyclonic conditions, and cyclonic activity is at a minimum.

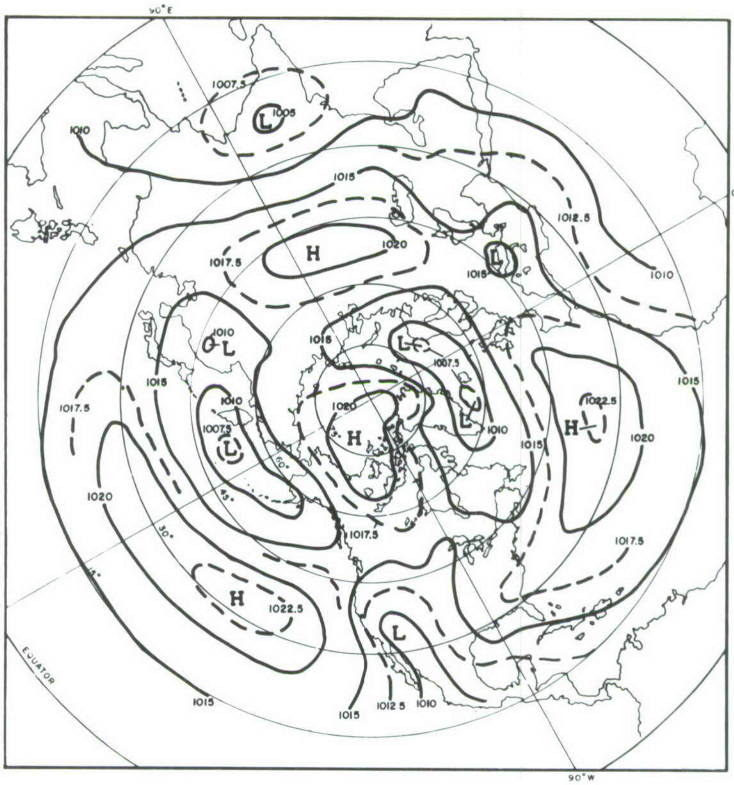

Figure 8a. Sea level pressure (mb), April (12-year mean)(O'Connor, 1961[21]).

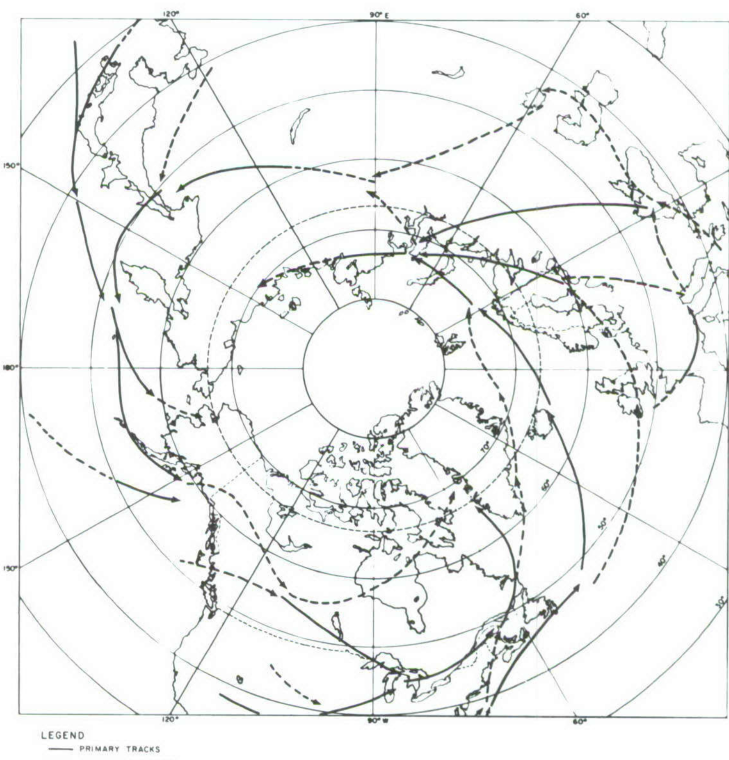

Figure 8b. Principal tracks of cyclones, April (after Klein, 1957[15]).

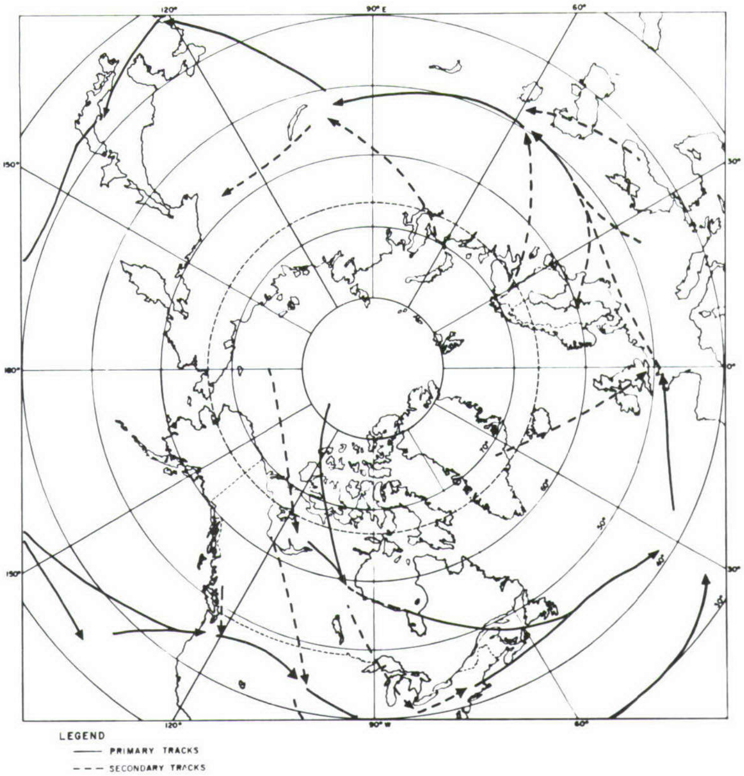

Figure 8c. Principal tracks of anticyclones, April (after Klein, 1957[21]).

An effect of the increasing insolation is to shift the areas of cyclogenesis from water to land regions (Fig. 8b). In Siberia, spring is marked by increasing cyclonic activity which reaches a maximum in May; secondary cyclonic developments over Lake Baikal and northeast China reach maximum frequency and intensity at this season. The cyclone track over the Arctic Ocean becomes a secondary feature in May, and primary tracks shift inland over the northeast part of Eurasia. Over North America, the cyclone paths shift poleward, to the north of the Great Lakes, and by June cyclonic frequency in Alberta reaches a maximum for the hemisphere.

Summer

The mean sea-level pressure chart for July (Fig. 9a) shows the remarkable fall in mean pressure in summer and the rather amorphous mean pattern which results from the relatively weak, shifting systems over the central Arctic. There appears to be considerable variation in the mean summer pressure from year to year, depending on the frequency and intensity of cyclonic activity. The main characteristics of the mean July pressure chart are the marked east-west extension of the Pacific and Atlantic ridges, the absence of a low center over the Gulf of Alaska, the westward shift of the weak Icelandic center, and the major low center over the heart of Siberia.

A comparison of the January and July mean height charts at 700 mb (Fig. 3a, c) shows the weakening of the upper westerly circulation in summer and the contraction of the vortex to a single major center over the

Arctic Ocean. In July and August, the peripheral zone of strong westerlies and the associated surface disturbances are furthest north (Fig. 9b), and over Asia this zone now lies to the north of the Himalayan massif. The primary cyclone tracks are at approximately 60°N with a further zone of high frequency between 70° and 80°N.

Over North America, the most marked change at this season is the northern displacement of the track of the Alberta lows. In summer the Prairie Provinces have one of the highest frequencies of cyclonic activity in the Northern Hemisphere; most of the storms cross Hudson Bay to the Davis Strait-Baffin Bay area where they stagnate. Over the Atlantic, to the east of the Icelandic "graveyard," the primary track is more zonal in July with a drop in frequency of the storms entering the Polar Basin. A well-defined path now extends from the eastern Atlantic into Siberia at about 60°N.

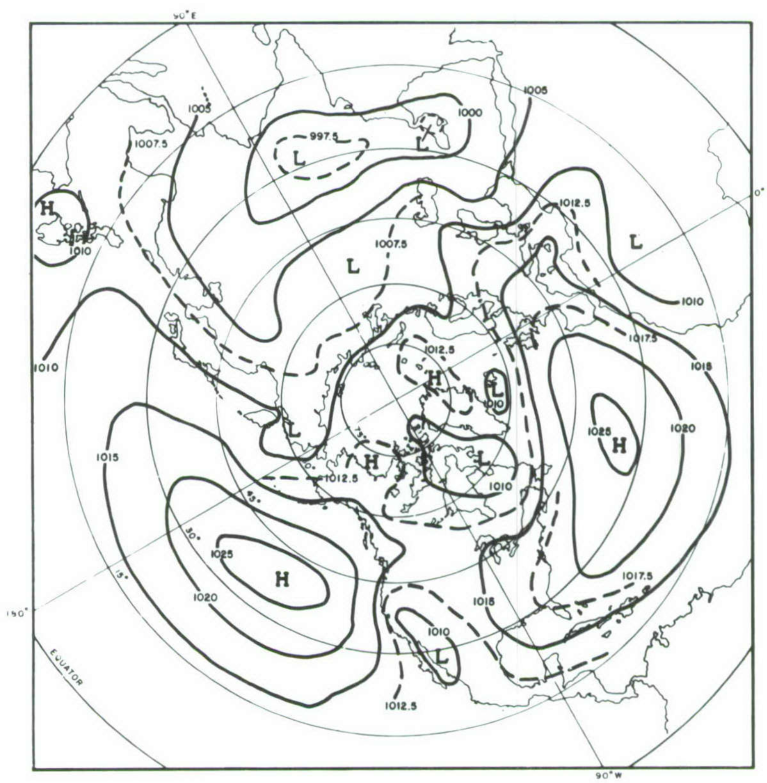

Figure 9a. Sea level pressure (mb), July (12-year mean)(O'Connor, 1961[21]).

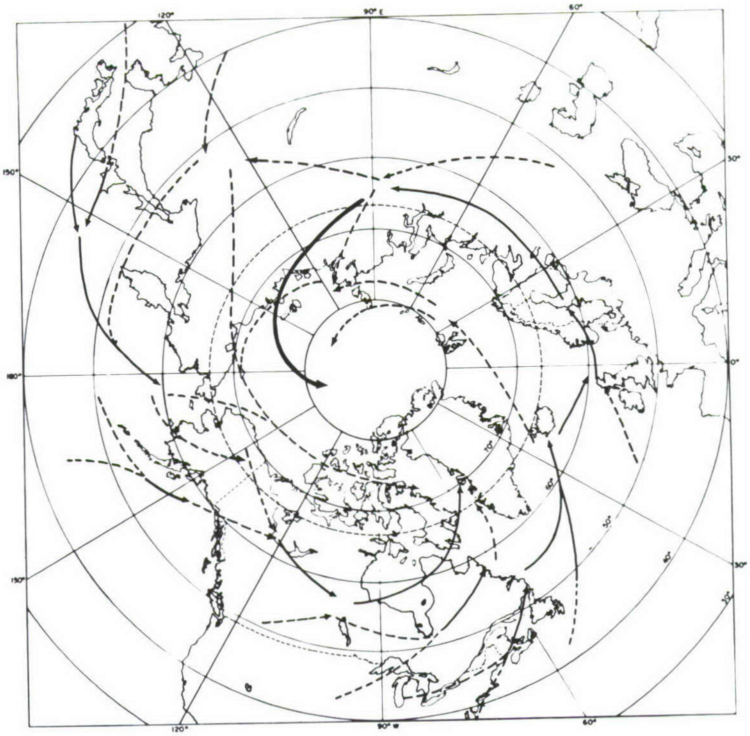

LEGEND
PRIMARY TRACKS
SECONDARY TRACKS
PRIMARY TRACK (REED, 1959[25])

Figure 9b. Principal tracks of cyclones, July (after Klein, 1957[15]).

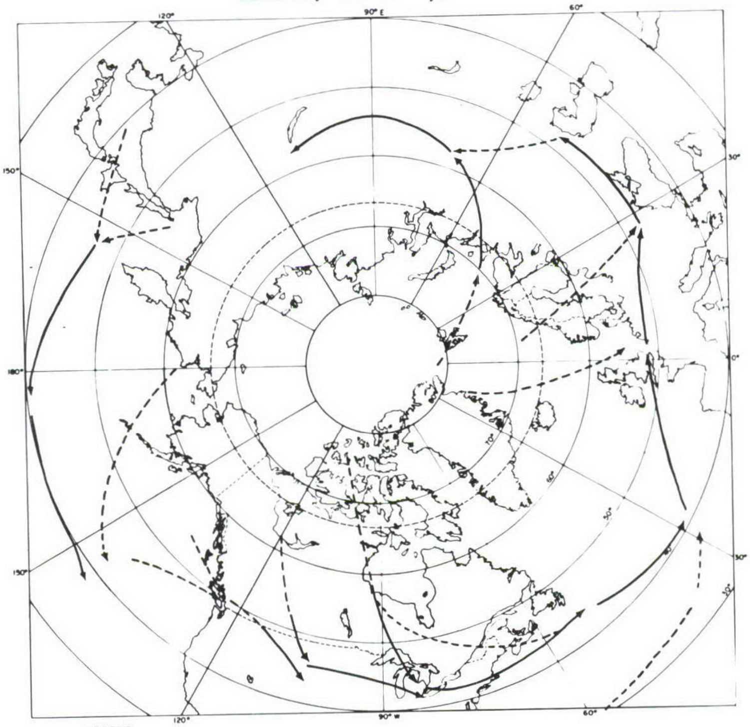

LEGEND
PRIMARY TRACKS
SECONDARY TRACKS

Figure 9c. Principal tracks of anticyclones, July (after Klein, 1957[15]).

In the Pacific sector the main track is well to the north of the Aleutians in summer, with storminess reaching an annual maximum over the Bering Sea and Bering Strait. Although fewer Atlantic storms enter the Polar Basin at this season, * there is a high frequency of traveling disturbances along the northern coastal regions of Siberia which appear to be related at least in part to the strong temperature gradients at the margin of the heated land and the melting Arctic ice. The storms move mainly to the northeast, spiraling into the central Arctic where they stagnate. Approximately one third of the lows that enter the Beaufort Sea are from northern Siberia.

The primary anticyclone tracks lie mostly to the south of the subarctic in summer (Fig. 9c). Anticyclones form to the west of Hudson Bay and move southeast to a region of maximum frequency over the Great Lakes; in August, however, this major track of polar highs shifts westward to the Beaufort Sea-Mackenzie area, although some centers still form in Manitoba. Another important primary track in summer extends from the Barents Sea southeast into Central Siberia. Anticyclone frequency reaches an annual minimum in eastern Siberia.

Reed and Kunkel[26] have published a study of the frequency of cyclone and anticyclone centers over the Arctic and subarctic for the summers of 1952-1956 (Fig. 10a, b). This whole region is the scene of considerable cyclonic activity, but maximum cyclonic frequency occurs:

(1) from southern Greenland to Iceland and to the north of Baffin Bay – the graveyards for both continental and east coast storms. The center west of Greenland is partially explained by the presence of the Greenland mass as a barrier to progress, although Hamilton's[8] study of the summer records over the ice cap revealed that frequent upper air disturbances (700 mb) cross the plateau during the summer, as in winter.

(2) over the Arctic Basin, where the high frequency reflects slow-moving, stagnating systems.

Anticyclonic frequency maxima occur over Greenland, the western Canadian Archipelago and Taimyr Peninsula – in general a belt between 70° – 75°N. The decreased frequency of cyclonic centers in this belt is not only due to the tendency for quasi-stable anticyclones to develop, especially over Greenland and near the Beaufort Sea, but also because of the greater mobility of the traveling cyclones in this zone.

A spot-check of the frequency of cyclones during 1952-56 against earlier expedition data for 1894-5 (Fram), 1904-5 (Ziegler Expedition) and 1923-4 (Maud), indicated no significant difference in the number of cyclones; therefore, these results are probably representative of a longer period of time.

Autumn

The autumn is marked by the intensification and southward expansion of the upper circumpolar vortex, and the mean October maps both for the 700 mb (Fig. 3) and surface levels (Fig. 11a) already show many of the major features of winter. Following this southern shift in the zone of maximum upper westerlies, the primary storm tracks move south. By November the belt of strongest westerly flow is again in the latitude of the Himalayan massif and the major winter features of the circulation are set up and held during the following 5 or 6 months.

---

* When the circulation is more meridional, storms from the Atlantic and the Pacific may penetrate well into the Arctic.

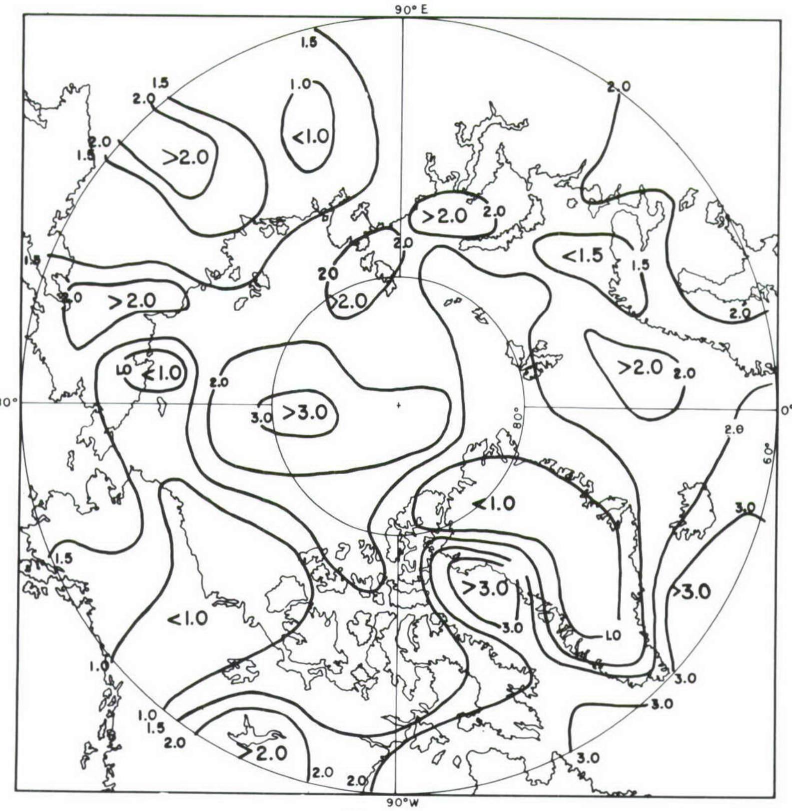

a. Cyclones

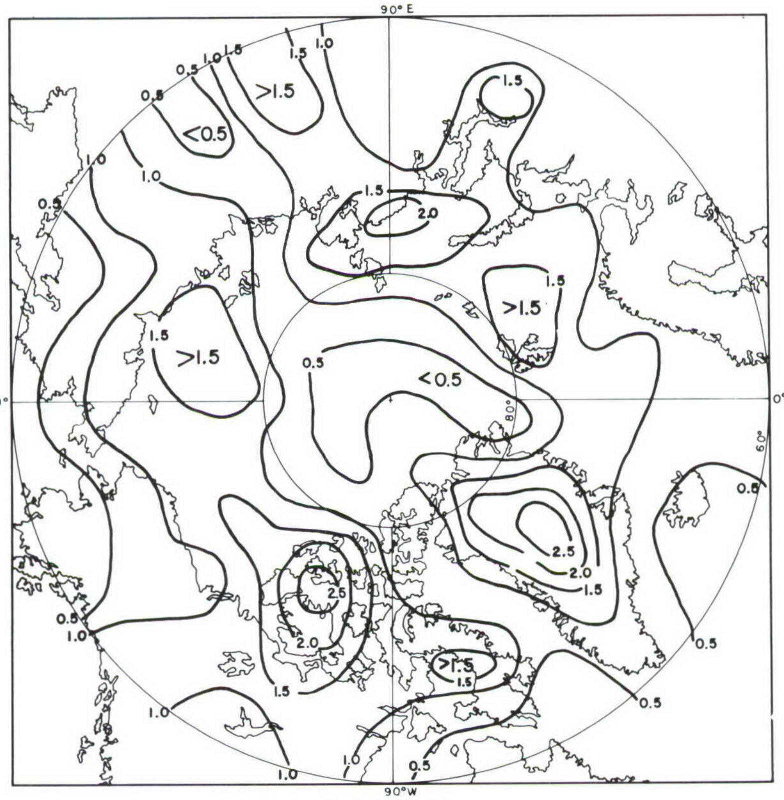

b. Anticyclones

Figure 10. Percent frequency of cyclonic and anticyclonic centers in squares of 100, 000 km².

A second feature of the autumn is the relative warmth of open water bodies compared with the rapidly cooling land. The October track charts (Fig. 11b, c) show areas of maximum cyclonic activity over the Sea of Okhotsk, the Barents Sea, the Gulf of Alaska, James Bay, and the Kara Sea. Primary cyclones enter the Arctic Basin from the Atlantic and the Baltic Sea and the frequency reaches an annual maximum over the Kara Sea, from which a primary track follows the coastal margin. In November, primary storm tracks from Alberta and Colorado again merge in a center of maximum frequency over the Great Lakes. Over the Atlantic the primary track shifts from the east to the west side of Iceland and the southern Davis Strait track reappears and intensifies.

During this season, anticyclonic frequency increases over eastern Asia and centers of high pressure appear at sea-level over Siberia. Over North America, the trajectory of polar highs over western Canada becomes of primary importance by November and remains so until March.

Persistence of Large-Scale Sea-Level Circulation Systems

The tendency to persist shown by various upper vortex patterns has been recognized as an important feature of the general circulation over the Arctic and subarctic, but comparatively little work has been done to investigate the broad regional forms of the sea-level circulation on this scale.

A study of the day-to-day persistence of the large-scale sea-level pressure patterns for the year 1955[37] gave the following results:

(i) Well-defined periods of stable large-scale situations existed, averaging 6 days and twice extending over 11 days.

(ii) Twenty-eight of these persistent periods were isolated in 1955, but the study was too restricted to attempt to classify these broad circulation patterns into types.

(iii) These periods of persistence were most marked from December to May and were separated by brief interludes of abrupt change, when the circulation seemed to flip from one pattern of stability to another.

(iv) From June to November the general level of persistence was lower and the changes less clear-cut than with the intense patterns of winter.

(v) Frequently, smaller-scale traveling disturbances were very active during these large-scale stable situations.

Examples of persistent situations in winter and summer are given in Figures 12 and 13.

(1) Figure 12 illustrates two dramatic changes of the sea-level patterns in March and April 1955. During the week prior to March 14, the Arctic circulation had been dominated by cyclonic activity. The pressure change that followed in the 48 hours, March 12-14, amounted to a sudden reversal in the flow patterns as an anticyclone moved into the Arctic Basin under a warm ridge aloft. This system intensified and essentially persisted until the beginning of April, when it was replaced equally suddenly between April 5 and 7 by a cyclonic system over the central Arctic.

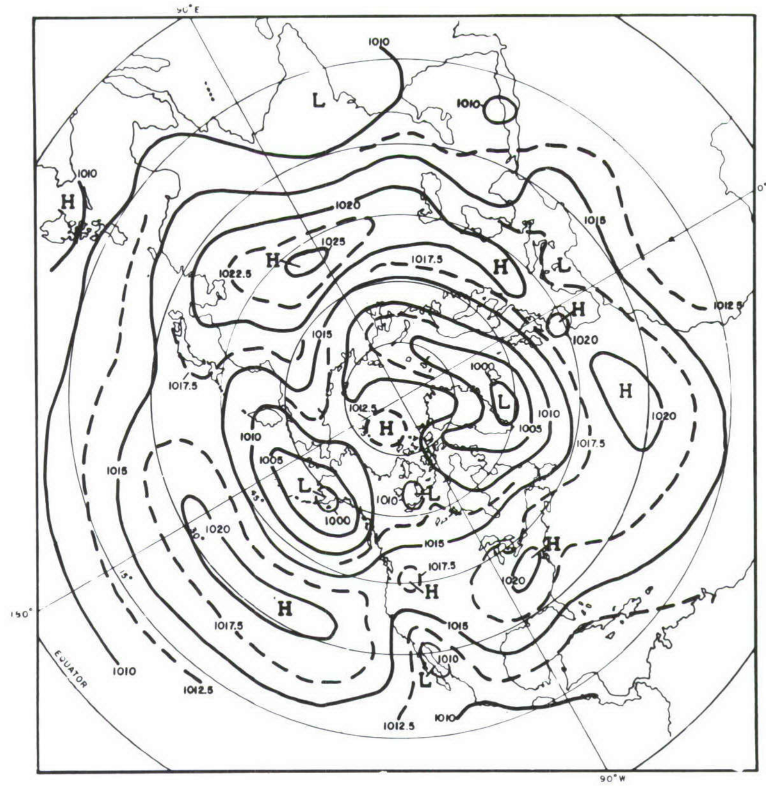

Figure 11a. Sea level pressure (mb), October (12-year mean)(O'Connor, 1961[21]).

(2) Figure 13a shows a well-defined, highly persistent mid-winter circulation pattern that lasted for 10 days in mid-January and was characterized by intensive smaller-scale cyclonic activity. After 3 days of rapid re-organization, a new pattern emerged and persisted during the next 11 days.

(3) Although the situations were less coherent after early June, when a rapid slackening of the circulation occurred, in August (Fig. 13b) there was a temporary intensification of the vortex over high latitudes, the belt of strongest westerlies was further north than normal and persistence briefly attained a mid-winter level after which it rapidly dropped off again.

The existence of two distinct regimes from December to May and June to November suggests the combined influence of the strong radiational cooling over the snow and ice cover and of the intensity of the general circulation on the persistence and change of the sea-level patterns.

For climatological purposes, regional knowledge of the frequency of large-scale "weather types" is useful. The multi-modal or skewed distributions of many weather elements can be explained by the existence of a number of patterns of stability.

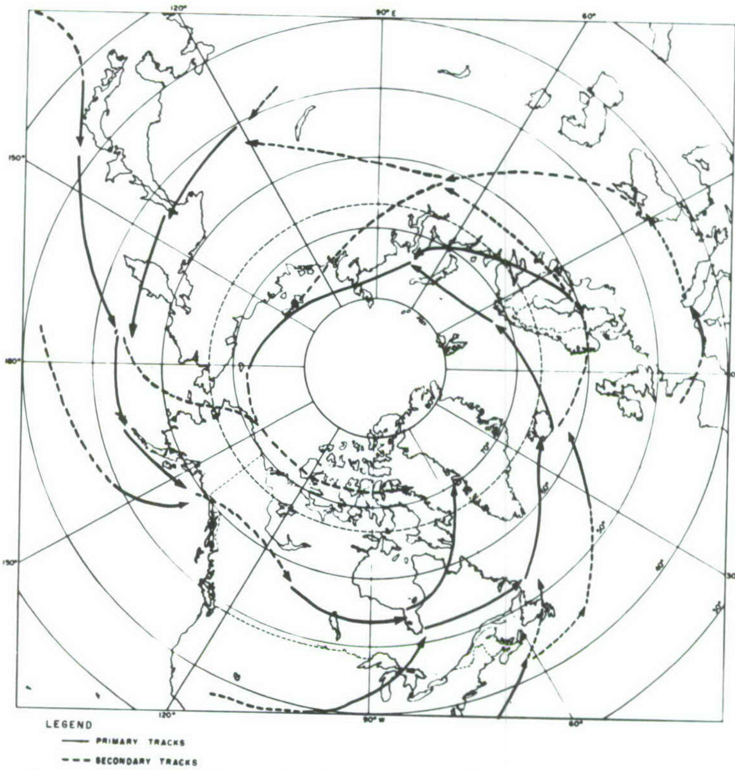

Figure 11b. Principal tracks of cyclones, October (after Klein, 1957[15]).

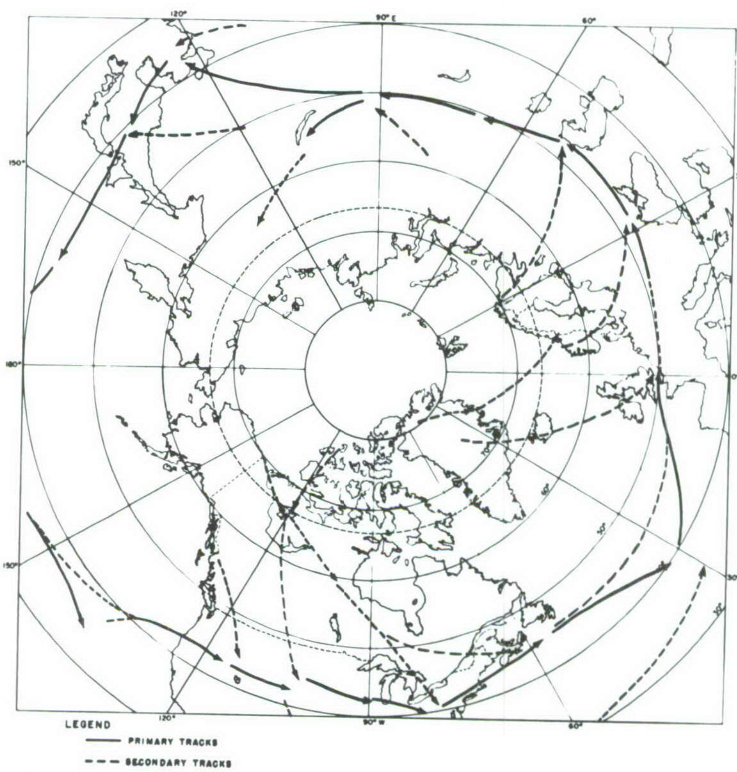

Figure 11c. Principal tracks of anticyclones, October (after Klein, 1957[15]).

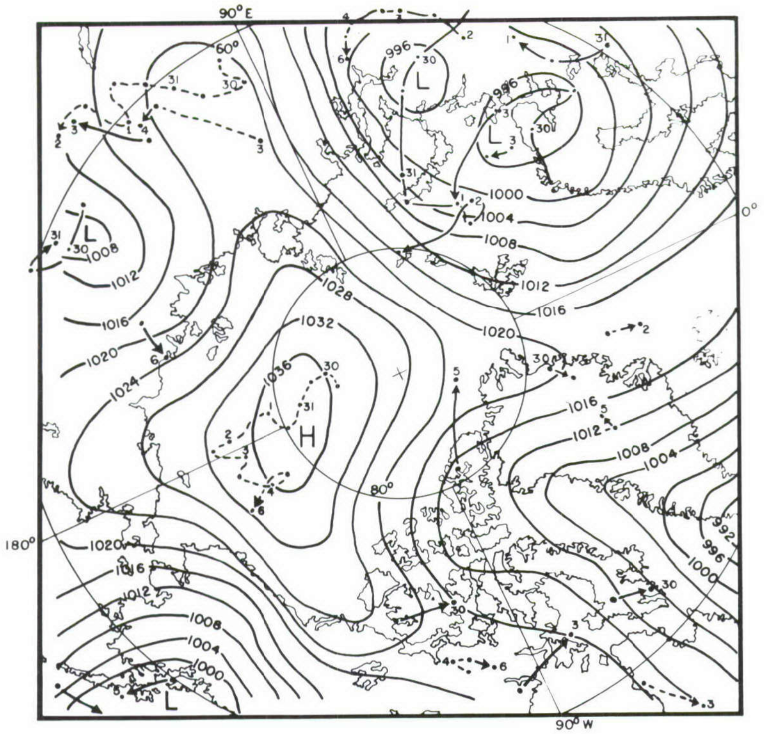

CENTERS AND APPARENT DISPLACEMENT OF CYCLONES (12-HR INTERVALS)
REGENERATION OR DOUBTFUL DISPLACEMENT
CENTERS AND APPARENT DISPLACEMENT OF ANTICYCLONES

a. 30 March – 5 April, 1230Z.

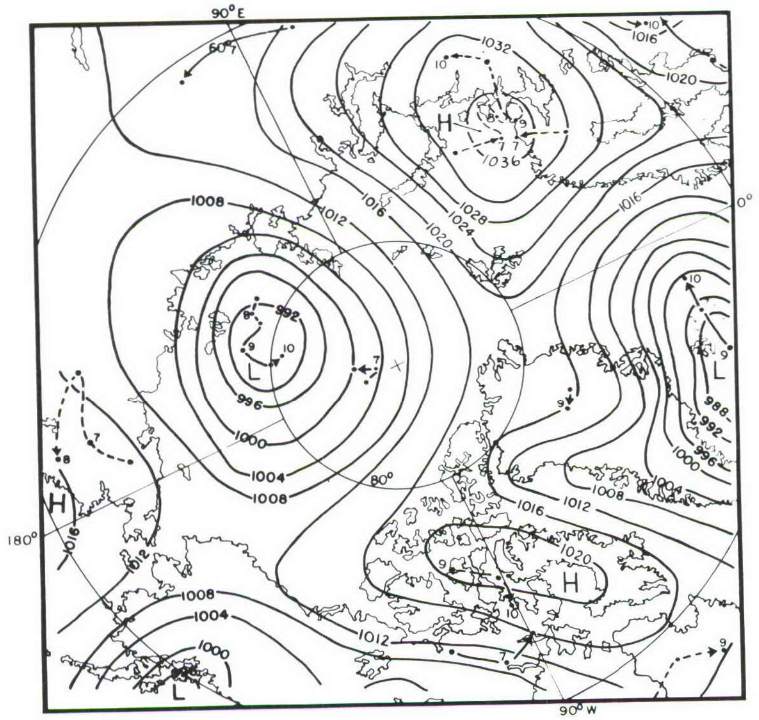

b. 7 – 10 April, 1230Z.

Figure 12. Persistence and rapid change of the large-scale mean sea level pressure patterns in spring 1955 (Wilson, 1958[37]).

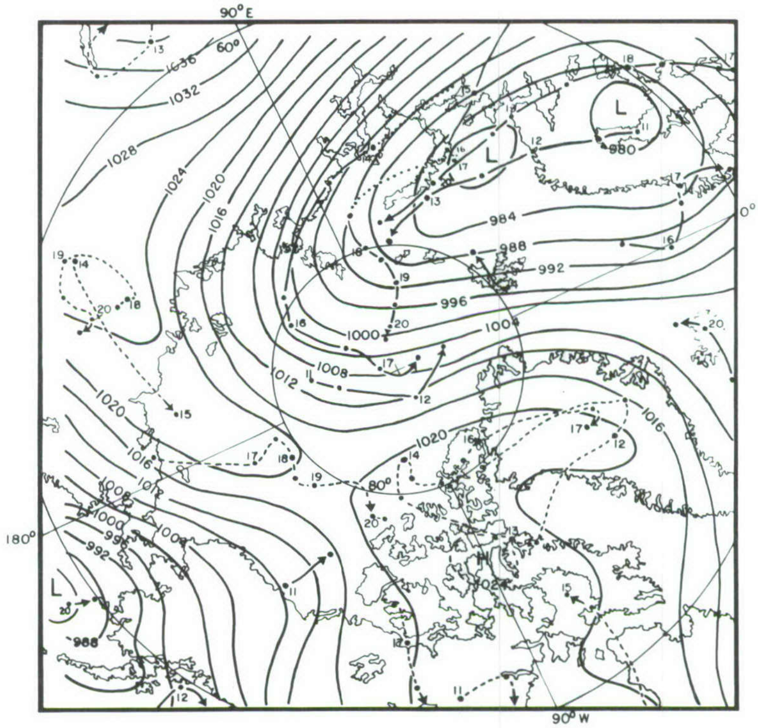

a. Mid-winter, 11 - 20 January, 0630Z.

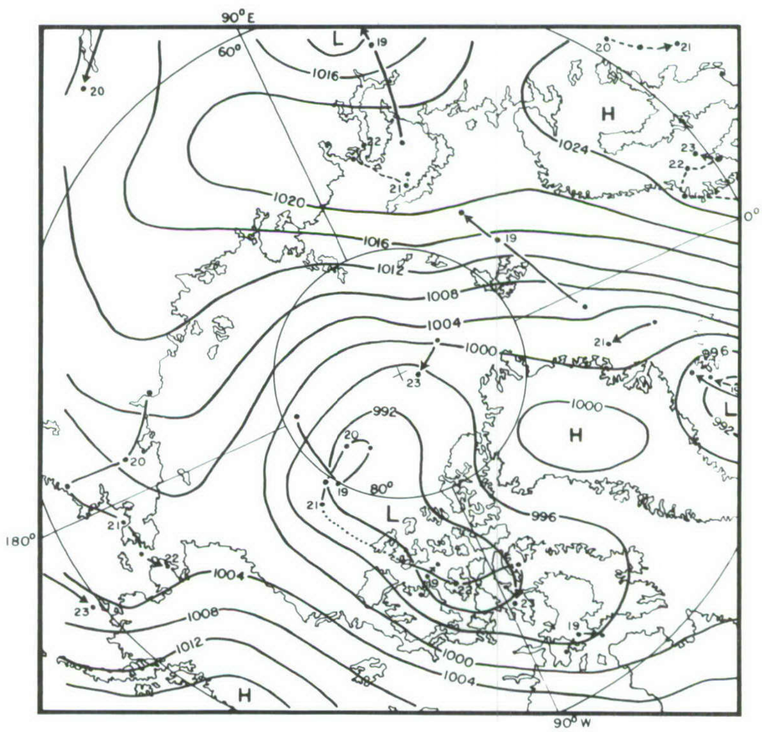

b. Summer, 19 - 23 August, 1230Z.

Figure 13. Persistence of large-scale pressure patterns in 1955 (Wilson, 1958[37]). See Figure 12 for legend.

Surface Weather Associated with High Latitude Pressure Systems

Cold season

The surface weather associated with anticyclones and cyclones is profoundly affected by the high degree of static stability of the lowest layer of the atmosphere, caused by the radiational cooling over the snow and ice cover. The surface weather over much of the Arctic and subarctic depends on the local effectiveness of anticyclonic and cyclonic activity in either intensifying or breaking down this very cold stable layer.

In general the calm clear conditions of the central regions of large persistent anticyclones favor the intensification of the inversion, both by the heating and relative drying of the free atmosphere through subsidence, which characterizes these systems, and by not hindering outgoing radiation from the surface. Consequently very low surface temperatures occur and are maintained. Where local topography prevents the free drainage of the dense cold air, pockets of extreme cold persist; where the surface allows drainage, strong gravity winds are periodically set off. Visibility, normally excellent, can be marred by local ice fog around settlements, and the sharp density gradient in the inversion layer is often responsible for such optical phenomena as mirages. Where leads exist in the ice, the cold air spreading over the warm surface of the water gives rise to "Arctic smoke" or "steam fog."

Warming of the free atmosphere through subsidence or the inflow of warmer air has little influence on the surface temperature unless there is a mechanism to carry the heat to the surface. Strong winds can create sufficient turbulence to bring about this mixing, and under the steep pressure gradients that frequently separate well-developed anticyclonic and cyclonic centers, the inversion is often rapidly destroyed as surface temperatures rise. As the wind abates, the inversion is quickly reestablished and temperatures fall again. Blowing snow can accompany these conditions.

Most of the variety of surface weather - cloud, precipitation, high winds, temperature change – is associated with the presence and passage of cyclonic disturbances. Besides the strong winds that frequently accompany the passage of cyclones, the cloud cover and precipitation effect a rise in the surface temperature through long wave radiation. This rise tends to be slow, but persisting overcast skies together with warm air advection can lead to extended periods of above-normal surface temperatures, as in 1958[32] when Alert recorded a maximum of 0C on January 24. Jackson[12] has commented qualitatively on the sequence of weather at Alert in relation to the synoptic pattern during this month (Fig. 14). Following December 1957, when the persistent surface inversion was associated with temperatures well below the 1951-53 mean, the inversion scarcely existed for much of January 1958.

The sounding for January 4 (Fig 14a) shows a cold, almost isothermal lower layer at about -40C, under clear sky conditions. By January 6, warm air associated with a complex cyclonic circulation system over Greenland and Iceland served to warm the higher layers, but in spite of related overcast skies, quite strong winds and almost continuous light snow the lowest layers remained cold. After a brief interruption on the 9th, renewed flow from the Norwegian Sea on January 10 resulted in a warming to -12C at 1500 m. Late on January 11 the sky became overcast, snow began to fall, winds were moderate and the surface temperature finally rose rapidly from -35C to -14C.

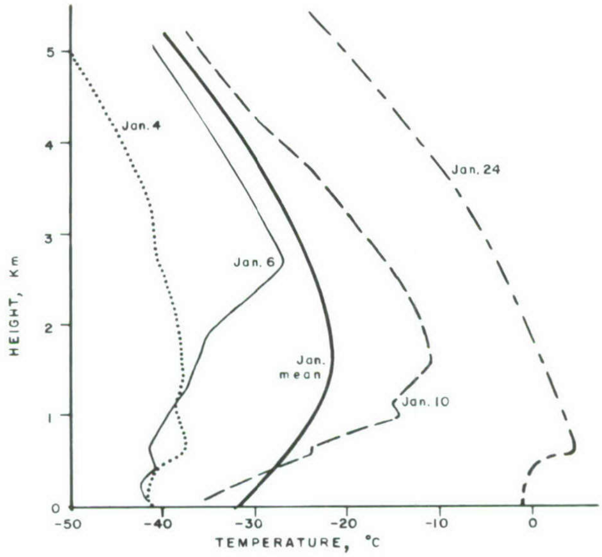

a. Profiles for January 1958 and January mean 1951-1953 (after Jackson, 1960[12]).

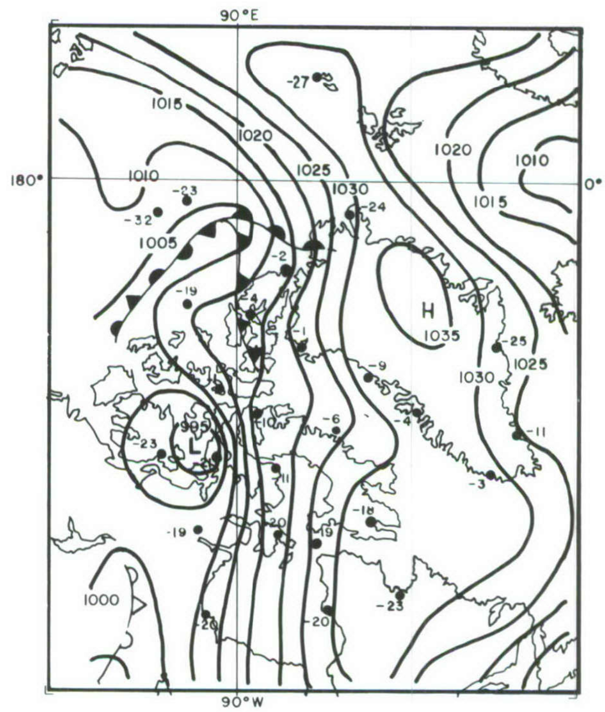

b. Sea level chart for 24 January, 1200Z; temperatures in °C, pressure in mb.

Figure 14. Temperatures and pressures at Alert, N. W. T., January 1958.

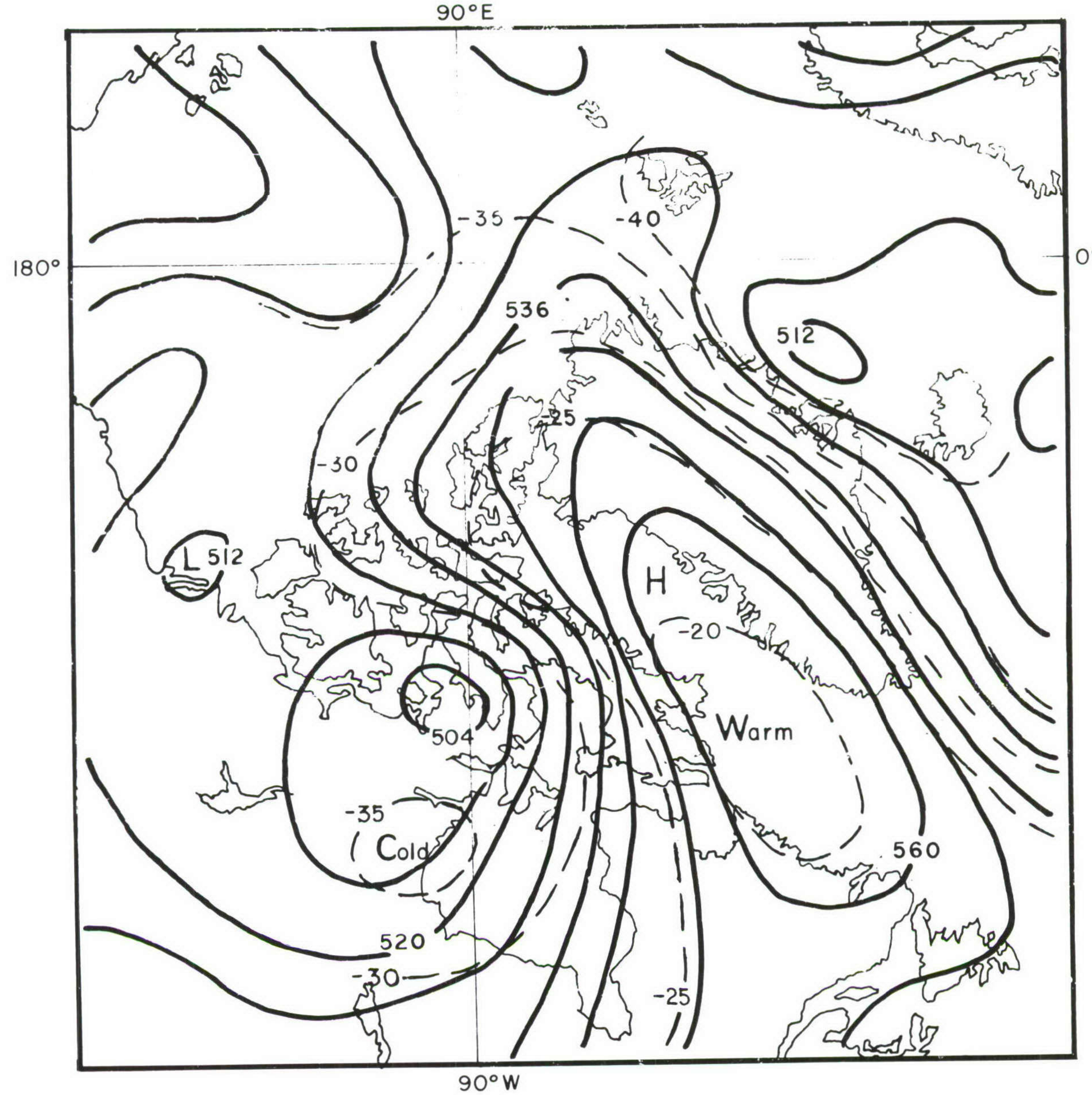

c. 500-mb chart for 24 January, 1200Z; temperatures in °C, contour height in dekameters.

Figure 14 (Cont'd). Temperatures and pressures at Alert, N.W.T., January 1958.

During the last half of the month a very strong blocking high built up over the Davis Strait-Baffin Bay-Greenland area as an upper ridge extended northwards from the Atlantic. To the northwest, a low pressure center north of Alaska moved slowly eastward over the Canadian Archipelago. This situation resulted in a very strong pressure gradient over the eastern Archipelago and a persistent flow of warmer, moister air from the south. Between 0600Z on January 16 and 1500Z on January 18, the lowest wind value at a surface observation was 40 mph and windspeeds reached 80 to 90 mph. The sounding for January 18 is missing, but the temperatures remained high at the surface through the month, culminating in record values from January 23-25, when the blocking high almost reached record intensity. The profile for January 24 contrasts strongly with that of January 6. Figures 14b, c show the synoptic patterns on this occasion; an unusual feature is the clearly defined frontal cyclone over Ellesmere that is being steered around northern Greenland under the strong upper flow.

The weather associated with these cyclonic systems is modified, especially in winter, by the fact that air temperatures are generally so low that the moisture content even at saturation point is too little to give a dense cloud cover[18] and heavy precipitation. Locally, the weather resulting from these storms is influenced by their recent passage over land, water or ice surfaces. Most of the cyclones originate in more southerly latitudes and by the time they reach the Arctic have lost most of their strong temperature contrast, their frontal structure at the surface, and the associated high, middle and low cloud sequences. They are generally weaker and occluded with the warm air lifted to considerable heights. When fronts do exist, they are often ill-defined, with no extensive cloud systems or precipitation. These dying systems often persist aloft as symmetric cold lows and, although the cyclonic circulation at the surface may be weak or absent, the sky is generally overcast beneath the upper center (Fig. 15); occasionally ice needles or traces of snow are reported.

Warm season

With the general break-up of the ice and the disappearance of the snow cover, the surface inversion weakens and is confined to a shallow layer over the pack ice and ice caps. At this season, the differential heating of the land, water and ice, and the local modification of the temperature profile and moisture content of the moving air masses becomes a prime factor affecting surface weather over the Arctic and subarctic regions.

Over the Arctic pack and coastal waters, where the presence of ice holds the surface temperatures near zero C, the high frequency of fogs and heavy low stratus cloud in the 0 to 1500 m layer is closely linked with the inversion itself, and to a large extent independent of the type of circulation system. Condensation occurs when warmer air flows out and is cooled over the cold waters or watery-ice surface. If the windspeed is low, fog forms close to the surface; if the windspeed is high enough the fog is lifted to form a low ceiling of stratus cloud. When the wind direction is favorable, the fog and cloud drift in over the coastal regions, and conditions over coastal airstrips can change rapidly. Drizzle and snow frequently fall from the stratus layer, and temperatures remain low below this pall of cloud. Wherever cloud is present within the temperature range of -30C to 0C there is the possibility of aircraft icing. Moderate to heavy icing has been encountered where cold air passes over open water forming cloud with a large concentration of supercooled droplets; usually this type of cloud does not extend beyond about 1200 m. Inland, the inversion and the stratus layer soon disappear over the heated land surfaces.

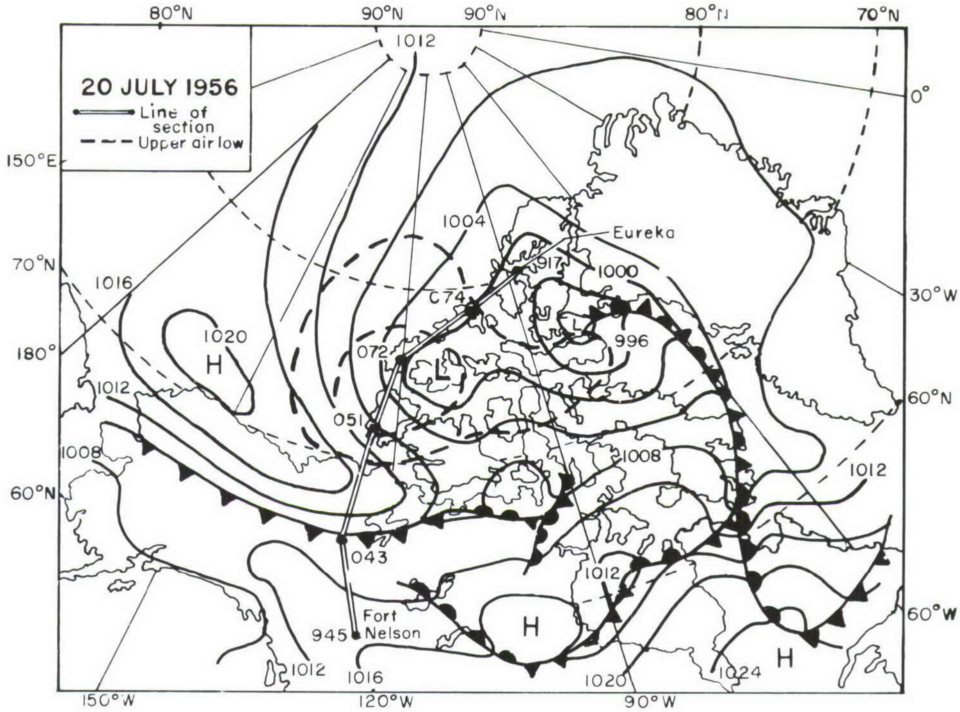

a. Sea level chart for 1230Z; pressure in mb.

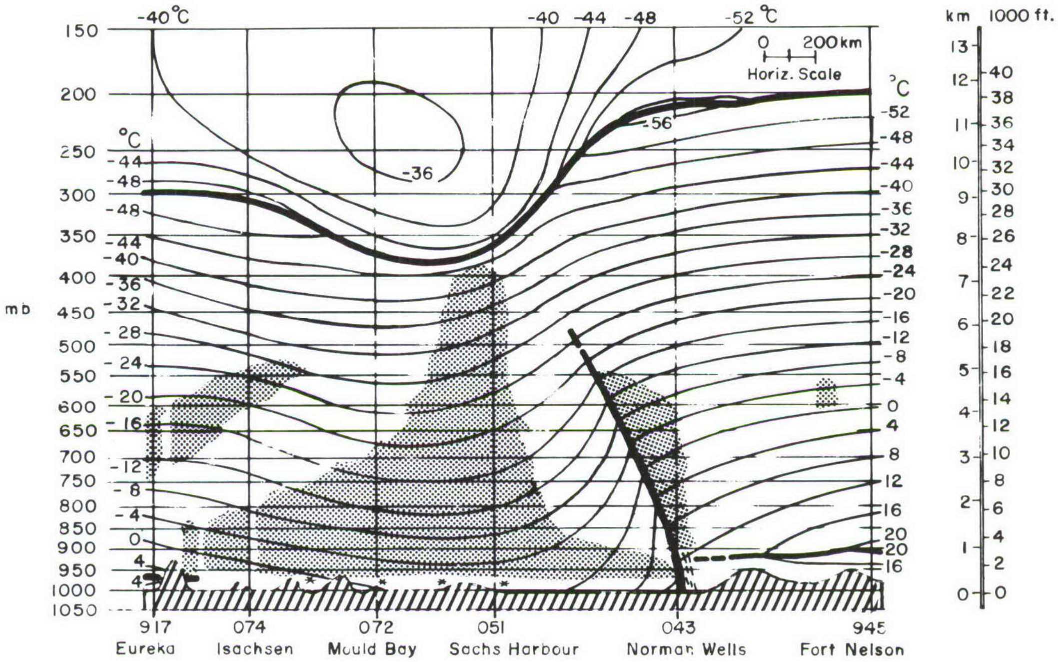

b. Cross section from Eureka to Fort Nelson showing temperature and cloud distribution at 1500Z. Heavy lines are tropopause and frontal and inversion discontinuities. Clouds are depicted by stippling. Short slanting lines represent rain, asterisks - snow.

Figure 15. Cloud over the Canadian Arctic, 20 July 1956 (Reed, 1962[27]).

However, it is the frequent cyclonic activity over the high Arctic in summer which is responsible for the middle and high cloud, the storms, and much of the precipitation. Gaigerov[7] reports cyclones with quite large temperature contrasts, strong winds, well-defined frontal zones, extensive cloud systems and precipitation zones over North Pole IV during the summer of 1955. The vigor of these storms is partly related to the strong thermal contrasts that exist near the Arctic coast at this season. Reed's[25] study of the cloud type and amount in a series of frontal cyclones over the Arctic Basin in July, 1956 suggests that the relationship between cloud amount and type is similar to that in mid-latitudes, where the large-scale upgliding motion of the warm air produces the sequence of cirrus and cirrostratus, lowering to altostratus and altocumulus and finally to nimbostratus with the onset of precipitation. However, the different cloud types often lie in discrete overlapping strata rather than in a single sloping layer. The largest amount of cloud was in the vicinity of the occlusion, where it extended to over 6000 m. Figure 15 illustrates the cloud distribution from Eureka to Fort Smith on July 20, through a cold low and a cold front*. The cloud type in the first 1500 m is stratus associated with the cold surface inversion layer, which gradually dies out over the continent. Strong cumulus development and thunderstorms are rare over the central Arctic.

Once the snow and ice have cleared from the continental subarctic, surface temperatures generally rise rapidly; however, heavy cloud cover and increased precipitation in areas of high cyclonic frequency can do much to delay the rise and the drying out of the surface. Labrador, for example, compares unfavorably in this respect with the lower MacKenzie valley which has a lower cyclone frequency and a correspondingly higher number of sunshine hours. The amount of weather associated with cyclonic activity over the subarctic will again vary according to the temperature contrasts and moisture content of the airmasses involved. These in turn are influenced by surface conditions, from the strong contrasts over land and ocean to local water bodies such as the lakes in the MacKenzie valley, Lake Baikal, or coastal configuration. Great Slave Lake and Great Bear Lake are notorious for the sudden development of storms over them.

Under an anticyclonic regime, the long hours of daylight can produce warm clear weather, with inland temperatures north of the Arctic Circle rising beyond 20 or even 30C. With continued heating of the surface, convection leads to cumulus development and thunderstorms.

Over both the central Arctic and much of the continental subarctic, the precipitation maximum occurs in the warmer half of the year, associated with the passage of frontal cyclones. The low stratus decks give some additional precipitation over the basin, and convective showers occur south of 75°N where continental heating is strong; in northern Alberta, for example, considerable damage can be caused by hailstones. The amount and type of precipitation depends on the temperature and moisture content of the air. Rain can fall anywhere in the Arctic in summer – Rae[24] suggests that nearly 50% of the annual total precipitation over the Canadian Archipelago may fall as rain. Where temperatures are in the vicinity of 0C, it is not easy to predict type of precipitation without a detailed knowledge of local conditions, which are often unknown. Furthermore, since the greater part of the high

---

*Appendix A includes the circumpolar synoptic charts for July 19 and 22, 1956.

Arctic is virtually a desert, a single storm can represent a high percentage of the annual total precipitation. At Thule, on July 22, 1957, 4.75 cm, almost the whole season's rainfall, fell in one day. There is, therefore, considerable variability in the amount from year to year. Local terrain also ensures considerable variation from place to place in the amount of precipitation received from any one storm. Jackson[11] illustrates these points with data from northern Ellesmere (Table II).

Table II. Precipitation, September 1957-August 1958, northern Ellesmere.[11]

Station	Total precipitation (water equivalent in cm)	Total number of days with more than a trace	Total rain (cm)	Number of days with rain
Lake Hazen (inland, in trough)	2.5	39	0.2	3
Eureka (at head of inlet, in mountain country)	5.3	49	0.25	3
Alert (coastal position, mountain backing)	11.5	95	2.1	10

Over coastal regions, the bulk of the precipitation frequently falls at the end of the warm season, when the land surfaces are cooling more rapidly than the open water, and the latter serves as a heat, and moisture, source in modifying the airmasses.[4]

SELECTED BIBLIOGRAPHY

1. Berry, F.A.; Owens, G.V.; and Wilson, H.P. (1954) Arctic track charts, Proceedings of Toronto Meteorological Conference, Royal Meteorological Society and American Meteorological Society, 1953. London: Royal Meteorological Society, p. 91-102.

2. Bodurtha, F.F. (1952) An investigation of anticyclogenesis in Alaska, Journal of Meteorology, vol. 9, p. 118-25.

3. Bryson, R.A. et al. (1957) Normal 500-mb charts for the Northern Hemisphere, annual, seasonal and monthly, with monthly standard deviations, Department of Meteorology, University of Wisconsin, Sci. Report no. 8.

4. Burbidge, F.E. (1951) The modification of continental polar air over Hudson Bay, Quarterly Journal of the Royal Meteorological Society, vol. 77, p. 365-74.

5. Estoque, M.A. (1957) Dynamical prediction of the Arctic circulation, Publication in Meteorology no. 6, McGill University, Montreal.

SELECTED BIBLIOGRAPHY (Cont'd)

6. Flohn, H. (1952) Zur Aerologie der Polargebiete, Meteorologische Rundschau, vol. 5, p. 81-87. Trans. A. M. Kroger, McGill University, Montreal, 1955.

7. Gaigerov, S.S. (1957) Atmospheric processes in the central arctic, Priroda, vol. 12, p. 27-34. Trans. by E.R. Hope, T282R, Defence Research Board, Ottawa, 1958.

8. Hamilton, R.A. (1958a) The meteorology of northern Greenland during the midsummer period, Quarterly Journal, Royal Meteorological Society, vol. 84, p. 142-158.

9. ______________ (1958b) The meteorology of northern Greenland during the midwinter period, Quarterly Journal, Royal Meteorological Society, vol. 84, p. 355-374.

10. Hare, F.K. and Orvig, S. (1958) The arctic circulation, AFCRC, TN-58-486. Publication in Meteorology, no. 12, McGill University, Montreal, with bibliography. (See also F.K. Hare, 1960: "The Westerlies," Geographical Review, vol. 50, p. 345-367.)

11. Jackson, C.I. (1959) Operation Hazen, the meteorology of Lake Hazen, N.W.T., Part I. Analysis of the observations, Publication in Meteorology, no. 15, McGill University, Montreal.

12. ______________ (1960) Operation Hazen, the meteorology of Lake Hazen, N.W.T., Parts II, III, IV. Synoptic influences, local forecasting, bibliography, Publication in Meteorology, no. 16, McGill University, Montreal.

13. Johnson, G.B. (1948) Anticyclogenesis in eastern Canada during the spring, Bulletin of the American Meteorological Society, vol. 29, p. 47-55.

14. Keegan, T.J. (1958) Arctic synoptic activity in winter, Journal of Meteorology, vol. 15, p. 513-521.

15. Klein, W.H. (1957) Principal tracks of cyclones and anticyclones in the Northern Hemisphere, U. S. Weather Bureau Research Paper, no. 40. (See also "Prevailing tracks of lows and highs," Weatherwise, vol. 9, p. 83-87, 128-131, 158-161, 205-209; vol. 10, p. 50-53.)

16. Kunkel, B.A. (1959) A synoptic-climatological study of the arctic circulation in summer, Department of Meteorology and Climatology, University of Washington, Sci. Report No. 7.

17. Lahey, J.F. et al. (1958) Atlas of 5-day normal sea-level pressure charts for the Northern Hemisphere, Department of Meteorology, University of Wisconsin, Sci. Report No. 7.

18. Marshunova, M.S. (1959) Calculation of the longwave radiation balance during an overcast sky in the Arctic. Leningrad: Arkticheskii i Antarkticheskii Nauchno-Issledovatel 'skii Institut, Trudy, 226, p. 109-112. Trans. R.M. Holden for G.R.D., T-R304.

19. Namias, J. (1958) Synoptic and climatological problems associated with the general circulation of the Arctic, Transactions American Geophysical Union, vol. 39, p. 40-51.

SELECTED BIBLIOGRAPHY (Cont'd)

20. Namias, J. (1962) Influence of abnormal surface heat sources on atmospheric behaviour, Proceedings of the International Symposium on Numerical Weather Prediction, Tokyo, November 7-13, 1960, Meteorological Society of Japan, p. 615-628.

21. O'Connor, J.F. (1961) Mean circulation patterns based on 12 years of recent Northern Hemispheric data, Monthly Weather Review, vol. 89, p. 211-227.

22. Petterssen, S. (1958) Introduction to meteorology. New York: McGraw-Hill.

23. Putnims, P. and Shallert, W. (1959) Some aspects of the meteorological dynamics in the Greenland area, U. S. Weather Bureau, Foreign Area Section, Office of Climatology, Washington, D.C. See also: Some meteorological and climatological problems of the Greenland area, 1959; Further circulation studies in the Greenland area based on observed winds, 1960; Some further studies on the meteorology of the Greenland area, 1961; Studies on the meteorology of Greenland, 1962; and Studies on the meteorology of Greenland, 1963.

24. Rae, R.W. (1951) Climate of the Canadian Arctic Archipelago, Canadian Department of Transport, Toronto.

25. Reed, R.J. (1959) Arctic weather analysis and forecasting, AFCRC-TN-58-647. Occasional report no. 11, Department of Meteorology and Climatology, University of Washington.

26. __________ and Kunkel, B.A. (1960) The arctic circulation in summer, Journal of Meteorology, vol. 17, p. 489-506.

27. Reed, R.J. (1962) Arctic forecast guide, U. S. Navy Weather Research Facility, Norfolk, Virginia, NWRF 16-0462-058.

28. Rex, D.G. (1950) Blocking action in the middle troposphere and its effect on regional climate; Part I. An aerological study of blocking action, Tellus, vol. 2, p. 196-211; Part II. The climatology of blocking action, ibid, p. 275-301.

29. __________ (1951) The effect of Atlantic blocking action upon European climate, Tellus, vol. 3, p. 100-112.

30. Rossby, C.G. (1959) "Current problems in meteorology" in The atmosphere and the sea in motion, B. Bolin, Editor. The Rockefeller Institute Press, p. 9-50.

31. Staff Members of the Academia Sinica, Peking (1958) The general circulation over eastern Asia (II), Tellus, vol. 10, p. 58-75.

32. Thomas, M.K. and Titus, R.L. (1958) Abnormally mild temperatures in the Canadian Arctic during January 1958, Monthly Weather Review, vol. 86, p. 19-22.

33. U. S. Navy Weather Research Facility (1961) Jet stream climatology at 500 mb north of 50°N, Navy Weather Research Facility, NWRF 20-0661-045, Norfolk, Virginia.

SELECTED BIBLIOGRAPHY (Cont'd)

34. United States Weather Bureau: Daily series, synoptic weather maps, Part I, Northern Hemisphere sea level and 500 millibar charts.

35. Wexler, H. (1936) Cooling in the lower atmosphere and the structure of polar continental air, Monthly Weather Review, vol. 64, p. 122-36.

36. ________ (1937) Formation of polar anticyclones, Monthly Weather Review, vol. 65, p. 229-36.

37. Wilson, C.V. (1958) The synoptic regimes in the lower arctic troposphere during 1955, AFCRC-TN-58-249; Publication in Meteorology, no. 8, McGill University, Montreal.

38. Winchester, J.W. and Bates, C. C. (1958) Meteorological conditions and the associated sea ice distribution in the Chukchi Sea during the summer of 1955, Polar Atmosphere Symposium, Part I, p. 323-334.

39. Dorsey, H.G. Jr. (1954) Some meteorological aspects of the Greenland Ice Cap, Journal of Meteorology, vol. 2, p. 135-142.

THE HEAT BALANCE

Introduction

Knowledge of the available energy and exchange of energy at the ground-atmosphere interface, and of how changes in these factors affect both ground and atmospheric conditions, are of greatest importance in cold regions where the processes of freezing and thawing add to the inherent complexities of the subject. In an earlier monograph, Scott[130]* discusses the physical aspects of the heat exchange at the ground surface, its measurement and its relationship to engineering. In this report, emphasis is placed on the regional and seasonal distributions of the heat balance of the surface and the atmosphere in the cold regions of the Northern Hemisphere.

The heat balance at the earth's surface can be expressed as

$$R + LE + P + A = 0$$

where R = the radiation balance (net radiation) at the surface = $(Q+q)(1-a)-J$,

$(Q+q)$ = the sum of direct (Q) and scattered (q) incoming solar radiation (insolation) received on a unit horizontal surface,

a = the albedo (reflectivity) of the surface,

J = the effective outgoing long-wave radiation,

LE = the evaporative heat flux,

P = the sensible heat flux between the surface and the lower atmosphere,

A = the heat flux between the surface and subsurface layers. (Heat loss to the surface has a negative sign.)

Observations of the components of the energy budget over the many different types of surface throughout the year are expensive to obtain and existing data are still comparatively few. The closest "network" of actinometric stations was achieved during the IGY. The best coverage in the northern cold regions was in the USSR,[28,76] where about 200 stations† recorded total solar radiation, and most of them net radiation; in addition, several dozen stations measured temperatures, humidity and wind profiles near the ground. In general, the period of regular radiation observations is longest in the Soviet Union. The northern stations include the series of drifting sites[6] in the Arctic Ocean.

Although the total number of stations over the North American section has always been few,** sample heat balance data for different surface and atmospheric conditions are gradually being accumulated. Studies over snow and ice surfaces have been the most numerous[101] (see bibliography), and include recent work under both maritime and continental conditions in Alaska,[66,82,109] on Baffin,[108] Ellesmere[124] and Axel Heiberg[7,60] Islands in the

* Reference numbers refer to the bibliography at the end of each section.

† cf. IGY Microdata cards, W.M.O. Geneva.

** cf. Monthly Radiation Summary, and Monthly Record, Canadian Meteor. Branch, Toronto and Climatological Data, National Summary, U.S.W.B., Washington, D.C.

Canadian Arctic Archipelago, on the elevated Greenland Ice Cap[37] and on Fletcher's Ice Island, T-3[10,47] in the Arctic Ocean. Periglacial conditions have been measured and studied at Camp Tuto,[129] Greenland. For the highly textured vegetation surfaces, reliable measurements are more difficult to obtain; this is especially true of the evaporative and sensible heat fluxes (LE, P). Measurements have been made over high-centered polygons of the tundra at Point Barrow, Alaska;[23,98,99,132] the lichen woodland has been sampled at Knob Lake, Labrador;[34,68,105,110,172] and the subarctic forest at Big Delta, Alaska[184] and Fort Churchill, Manitoba.[183] At Norman Wells, N. W. T.[22] an attempt has been made to measure the surface energy exchange in relation to local differences in the vegetation cover and ground conditions, in connection with permafrost studies. The component of heat flux (A) between the surface and subsurface layers is being systematically measured at a number of sites, most of them in Alaska.[178] Many of these studies are confined to a brief summer period, when the inversion is weak or absent.

Because of the micro-scale in both space and time of significant changes in the heat balance components, obtaining satisfactory integrated values representative of areas, surface types, or even regions over a more extended period of time is a problem, especially complex with respect to a forest cover. Most of the existing climatological work on the heat balance has been attempts to relate the various measured components to standard meteorological data so as to estimate their values. Water surfaces, with their greater homogeneity, have yielded more readily than land areas to the calculation of aerial estimates. Many northern land surfaces are waterlogged during the brief summer and similar techniques may be applicable. In the past few years, however, experimentation with aerial sensing from low flying aircraft has shown considerable promise,[13,24,88] and now satellite data offer further possibilities of obtaining integrated values.[117,171,185] If characteristic values and regimes can be found for various surface conditions in relation to the frequency of major weather types, this would appear to be a particularly valuable climatological approach.

The first climatological study of the heat balance of the earth's surface was the work of Budyko,[27,29] although his first atlas omitted the high Arctic and Antarctic. Maps for the U.S.S.R. of monthly mean values of total radiation and the radiation balance were published by Berliand and Efimova[14] during the same period. In 1963[27,28] Budyko published another world atlas of the heat balance based on the results of the IGY data; again, this study does not extend to the poles. This atlas contains mean monthly and annual charts of total solar radiation, net radiation, heat loss through evaporation, and the evaporative and sensible heat exchange between the earth's surface and the atmosphere. There are also mean annual charts of heat advection by the atmosphere and oceans, the radiation balance between the surface and atmosphere, and the heat released in condensation. The world maps were drawn up from both observed and calculated values; a detailed study of the total and net radiation over the U.S.S.R.,[14,179,180] where the observed data were adequate, served as a check on the calculations and on the variability of the values. A further world map of annual total solar radiation at the surface has recently been published by Landsberg.[81]

A number of studies over high latitudes have been made.[6,9,48,49,50,73,149,169,182] Of these, the most detailed regional distributions have been attempted by Vowinckel and Orvig.[169] Monthly estimates were made at 10° long, 5° lat intervals north of 60°N of: clear-sky radiation, total solar radiation, albedo and absorbed radiation at the surface, cloud cover and type, long-wave radiation emitted by the surface, long-wave radiation received under clear-sky and average cloud conditions, net radiation, the atmospheric radiation balance, and the earth-atmosphere energy balance. Heat used in evaporation and sensible heat flux could only be estimated for the ocean and neighboring seas; final annual and monthly energy budgets were drawn up for the central Polar Ocean, the Kara-Laptev Sea, the East Siberian Sea, the Beaufort Sea and the Norwegian-Barents Sea. A complementary study by Gagnon[49] showed the influence of the type and frequency of weather systems on the regional energy budget.

The Radiation Balance

In the absence of adequate regional data, radiation components can be calculated approximately. Total solar radiation (direct and diffuse) depends on the duration of daylight, solar altitude, the composition of the atmosphere and the cloud cover; the percentage absorbed by the earth itself is mainly a function of its reflectivity – the albedo. Over cold regions this is an important depletion factor. With respect to the effective outgoing long-wave radiation, the thickness of the cloud layer(s) and the temperature of the cloud base are the determining factors.

Length of daylight

The total possible duration of daylight on the 15th of each month for latitudes 60° - 90°N is given in Table IIIa.*[84] The Arctic twilight is prolonged by some 20 days after the setting of the sun at the pole, with complete darkness only from November 12 to January 30. The angle of incidence of the sun's rays is lower than in middle latitudes and the amount of light reflected from the snow surface is greater. Reflected light may be so intense that shadows are obliterated and obstacles and outlines of the landscape cannot be distinguished. Over a water surface, reflectivity increases with increasing angle of incidence, particularly when the angle is greater than 70°. The landing of aircraft under these conditions is not always easy. Table IIIb shows the number of hours on the 15th of each month that the sun is below 20° above the horizon. In winter, the prolonged moonlight and high reflectivity of the snow cover allow most surface activities to continue.

Albedo

The albedo is the ratio of the solar energy which the surface reflects, I_r, to the solar energy incident upon such a surface, I_0, or $A = I_r/I_0$; it is generally expressed as a percentage. Albedo is a function of the texture, wetness and color of the surface, of the angle of incidence of the solar beam, and the amount of atmospheric diffusion. It usually increases with decreasing solar altitude, which is particularly significant with snow and water surfaces at high latitudes. On the other hand, the albedo decreases with increasing wetness. Over a rough wooded surface variation occurs according to the degree of penetration and differing colors of the ground cover and higher vegetation; at lower angles there is generally less penetration and more reflection. By far the highest albedos are over fresh snow surfaces, which can reflect 80% or more of the incoming radiation compared with values of generally less than 20% for non-snow-covered surfaces.

* More detailed tables are included in Appendix B, together with values of solar altitude at noon.

Table IIIa. Total possible duration of daylight on 15th of each month[84] (in hours and minutes, to nearest 15 minutes).

Month/Lat.°	60	65	70	75	80	85	90
January	6.45	4.30	-	-	-	-	-
February	9.00	8.00	7.00	4.15	-	-	-
March	11.45	11.30	11.30	11.00	10.30	8.30	-
April	14.30	15.00	16.00	17.00	23.00	24.00	24.00
May	17.15	18.30	21.45	24.00	24.00	24.00	24.00
June	18.45	22.30	24.00	24.00	24.00	24.00	24.00
July	18.00	20.30	24.00	24.00	24.00	24.00	24.00
August	15.45	16.30	18.00	21.00	24.00	24.00	24.00
September	13.00	13.00	13.30	13.45	14.30	17.30	24.00
October	10.15	9.45	9.00	7.15	4.15	-	-
November	7.30	6.00	3.45	-	-	-	-
December	6.00	3.15	-	-	-	-	-

Table IIIb. Duration of sun below 20° above the horizon[84] (in hours and minutes, to the nearest 15 minutes on the 15th of each month).

Month/Lat.°	60	65	70	75	80	85	90
January	6.45	4.30	-	-	-	-	-
February	9.00	8.00	7.00	4.15	-	-	-
March	8.30	10.00	11.30	11.00	10.30	8.30	-
April	7.15	8.45	10.45	13.45	23.00	24.00	24.00
May	7.00	8.30	11.15	13.00	13.30	14.45	24.00
June	7.00	9.15	10.00	9.15	8.00	4.00	-
July	7.00	8.45	11.00	10.45	10.00	8.15	-
August	6.45	8.30	10.30	14.30	19.00	24.00	24.00
September	7.45	9.15	11.45	13.45	14.30	17.30	24.00
October	9.30	9.45	9.00	7.15	4.15	-	-
November	7.30	6.00	3.45	2.30	-	-	-
December	6.00	3.15	-	-	-	-	-

Total duration below 20°

Total duration below 20°

Outside the U.S.S.R.[76] there is no "network" of albedo stations, and existing observations are few. There is also considerable discrepancy among the existing data owing to the variety of instruments and observational techniques in use. Readings made at the ground and in low flying aircraft [12,34] differ significantly because of the different horizons of the various instruments. In addition, the dependence on highly localized surface and atmospheric conditions as well as solar altitude poses problems in the time and space integration of albedo values.

The present regional estimates of albedo are essentially based on the detailed mapping of surface conditions and cloudiness at various times of the year, and the application of sample data obtained under approximately similar conditions. There are three studies which have reference to Northern Hemisphere cold regions:

(1) Budyko's[27,28,29] global study of the heat balance, in which broad-scale surface types and vegetation zones were considered. Over periods of the order of a month, these "average" values were used:

Stable snow cover of higher latitudes (60° and higher)	80%
Stable snow cover of middle latitudes (below 60°)	70%
Unstable snow cover	45%
Coniferous forest (range 10-15%)	14%
Deciduous forest (range 15-20%)	18%
Tundra	18%
Fresh, dry snow	80-95%
Pure, white snow	60-70%
Polluted snow	40-50%
Sea ice	30-40%

(2) The study by Larsson and Orvig[83,84] on albedo north of 65°N. They attempted to adjust the broad climatological values to local conditions by considering in detail the nature of the surface at each point of a 10° longitude/5° latitude grid, for the middle of each month. This adjusted value has special significance in high latitudes where surface conditions are so variable. For example, there is the effect on the albedo of the wetness of the surface, where drainage is poor in summer. The albedo was estimated at noon.

Over the pack ice, the estimates were based mainly on Russian drifting station data. Table IV gives the average and extreme values of the observations.[19] With a snow cover the difference in albedo under diffuse and direct radiation was considered negligibly small.

In high latitudes, open water is mostly associated with cloudy conditions, but when skies are clear low solar altitude needs to be considered; values range from a very low percentage at high sun to almost 100% when the sun is near the horizon. Under diffuse radiation Houghton's[63] value of 8% was used. For direct radiation a curve was plotted of published observed albedo of wave-covered surfaces versus solar height which was used for estimates in each 5° latitude belt.

The direct and diffuse radiation over vegetation surfaces presented the greatest difficulties, especially over woodland and forest where shadow effects must be considered with low solar heights. Eventually no distinction was made between direct and diffuse radiation and the albedo values were based on all available information for similar vegetation areas. These data include measurements made from the air over snow-free surfaces in Labrador-Ungava by Davies,[34] who suggests the following representative values:

Tundra	< 17%	the best reflecting surface owing to its smoothness, dryness and unconcealed lichen growth.
Burn	> 12%	spruce stripped of bark and dead trees reflect strongly.
Open woodland	> 10%	a great range of values (7-20%) depending on the amount of open lichen cover.
Bog and muskeg	< 10%	the water is hidden from the air.
Closed-crown forest	> 9.9%	before the crowns are completely closed (e.g. in June) the albedo is lower as the surface is not as uniform.

Table IV. The albedo of different surfaces from data of drifting stations North Pole IV, VI and VII, in 1956-57 (north of 75°N)(Briazgin[19]).

Structure	Water content and color	Albedo % Avg	Max	Min
freshly fallen snow	dry bright-white clean	88	98	72
freshly fallen snow	wet bright-white	80	85	80
freshly drifted snow	dry clean loosely packed	85	96	70
freshly drifted snow	moist gray-white	77	81	59
snow, fallen or drifted 2 to 5 days ago	dry clean	80	86	75
snow, fallen or drifted 2 to 5 days ago	moist gray-white	75	80	56
dense snow	dry clean	77	80	66
dense snow	wet gray-white	70	75	61
snow and ice	dry gray-white	65	70	58
melting ice	wet gray	60	70	40
melting ice stamukhas*	moist dirty gray	55	65	36
snow, saturated with water (snow during intense thawing)	light green	35	-	28
melt puddles in last period of thawing	light blue water	27	36	24
melt puddles, 30-100 cm deep	green water	20	26	13
melt puddles, 30-100 cm deep	blue water	22	28	18
melt puddles covered with ice	smooth gray-green ice	25	30	18
melt puddles covered with ice	smooth ice, covered with icy white hoar frost	33	37	21

* ice hummocks

(3) Kung, Bryson and Lenschow's[78] study over North America in which they typed the surface into albedo regions on the basis of airborne observation.

Although the absolute values of the albedos shown in Figure 16[12] are tentative, owing to instrumentation problems* and variable angle of incidence, the relative values show the striking effect on the albedo of the arrival and melting of the seasonal snow/ice cover over various types of surface. The existence of two major levels or seasons of albedo, linked by rapid transitions, is especially marked over the surfaces of Lake Mendota (Fig. 16a) and the smooth, rolling farm land, while the rougher hilly and wooded surfaces have a lower seasonal contrast. When the snow melts and the land is uniformly brown, or when the fields and forest change color in spring and autumn, there is little variation from one area to another. On the average the albedo over the water surface is low.

In the Arctic and subarctic, the seasonal variation in snow cover is the dominant factor. Even in the central Arctic, the albedo drops in summer with the formation of melt pools on the ice and open leads. In the forest tundra area the albedo is approximately twice as large with a snow cover beneath the treas as with an undisturbed vegetation floor of lichens and mosses.[84] The seasonal contrast is even sharper in the tundra zone, from >80% in winter to <20% in summer. In the closed-crown forest, snow does not play such an important role; it may be caught in the canopy for a time but over periods such as a month this effect should hardly be noticeable. Over the Arctic and subarctic, the distribution of albedo can be summarized as follows:[83]

(1) In January, when the region is almost completely snow-covered, differences in albedo between the closed-crown forest and more open woodland show up clearly. Over the oceans, differences depend on the distribution of open water surfaces. There is comparatively little alteration until May, when change in the texture of the snow is accompanied by rapid lowering of its albedo. With the northward migration of the snow cover limits, the closed-crown/open woodland albedo differences are less distinct.

(2) In June, land areas affected by snow cover are considerably reduced and the ablation area of the Greenland Ice Cap becomes evident. The formation of melt water pools on sea ice together with the lower albedo of melting sea ice rapidly reduces the areal albedo of the Arctic Ocean area. During July only those areas covered by ice are affected by snow cover, and areas of open water increase.

(3) By August, albedos are lowest over the Arctic. Large areas of open water occur in the Baffin Bay-Davis Strait area, around Novaya Zemlya and along the Siberian coast.

---

* Both hemisphere and beam instruments were used; in the latter the beam width for the parabolic reflector was 4° and at 150 m an area of only 11 m diameter was sampled. The differences between the two readings were very large, the beam averaging 29% lower over pure snow, 22% over spring farmland and 19% over forest. Over rippled water the average difference was 60%.

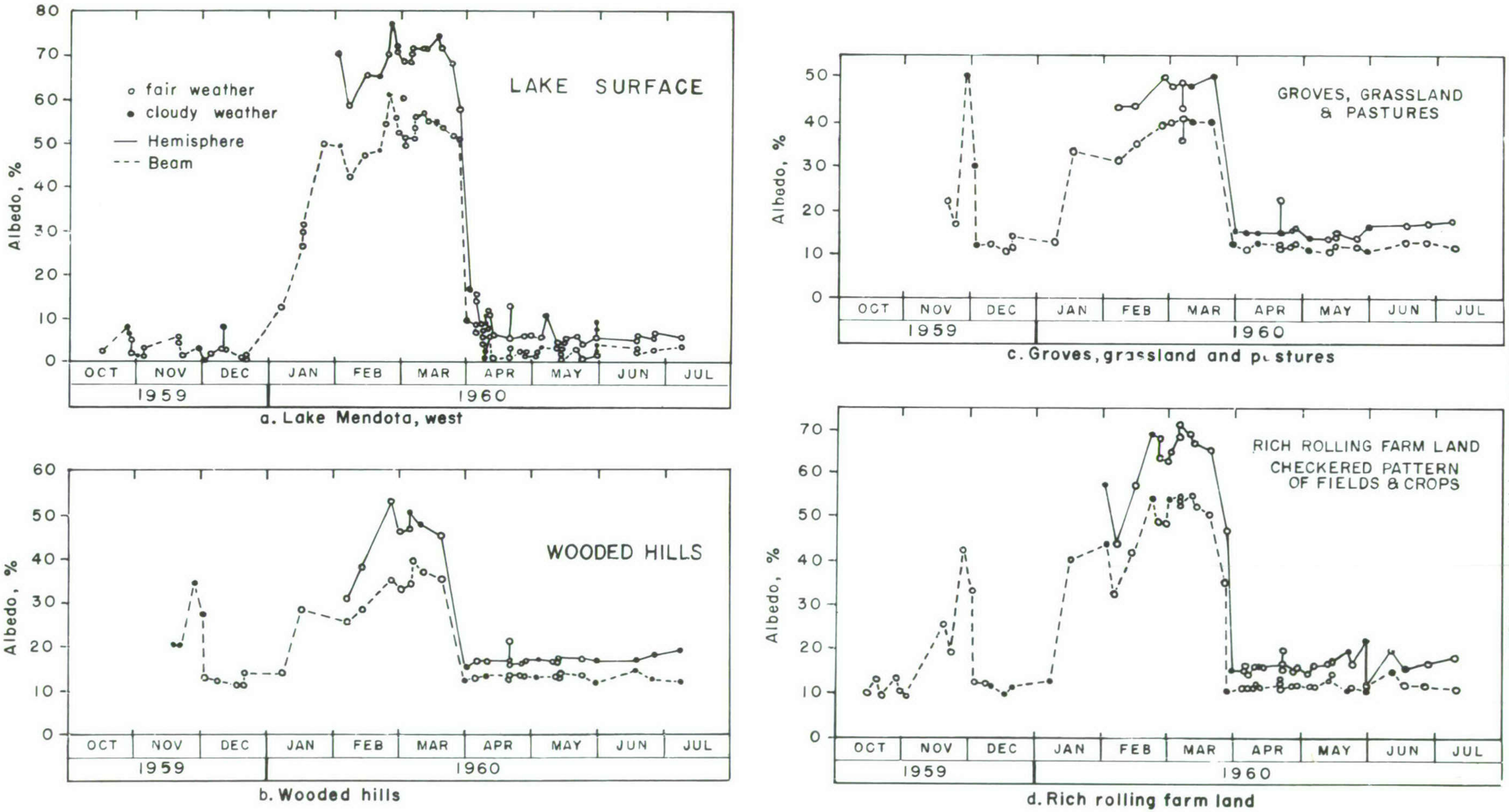

Figure 16. Observed albedo through the year over various surfaces near Lake Mendota, Wisconsin (Bauer and Dutton, 1960[12]).

(4) In September, the southern extension of the snow cover leads to a rapid increase in the albedo values over the central Arctic and the October map already shows the differentiation between forest and open woodland. By November, the major features of the winter pattern are already well-established.

Total solar radiation* and absorbed radiation at the ground

Total solar radiation (direct + diffuse) is the most frequently measured component of the heat balance; these observations can be supplemented by estimating the clear sky radiation and correcting for cloud cover. Available values of clear sky radiation include the tables of Bolsenga,[16] based on Klein's[74] method of computation and the monthly grid point values (and maps) of Vowinckel and Orvig,[158] based on Houghton's[63] work. A major difficulty at high latitudes is the lack of quantitative information on the regional and seasonal distributions of the depletion factors. Preliminary studies of the monthly distribution of type and amount of cloud[156, 157, 159] were made by Vowinckel in order to obtain estimates of total solar radiation received at the surface.† These values were then corrected for albedo to obtain the amount absorbed by the surface.

Table V. Comparison of different types of solar radiation.[158] (Vowinckel and Orvig, p. 26) (Values expressed in % of extraterrestrial radiation.)

		F	M	A	M	J	J	A	S	O	N
	Clear Sky	69	75	80	79	77	74	73	71	69	63
65°N	Insolation	57	64	64	56	52	48	48	39	41	44
	Absorbed	32	35	38	37	42	42	42	34	32	25
	Clear Sky	68	73	80	79	76	74	72	70	66	
70°N	Insolation	46	62	65	61	50	45	40	38	34	
	Absorbed	17	24	26	29	34	36	33	31	19	
	Clear Sky		71	79	79	78	74	72	69	60	
75°N	Insolation		59	62	57	50	43	40	38	27	
	Absorbed		16	18	22	26	30	27	22	10	
	Clear Sky		62	78	79	78	75	71	63		
80°N	Insolation		54	60	49	54	45	42	41		
	Absorbed		12	14	19	23	27	24	18		
	Clear Sky		37	75	80	79	75	71	56		
85°N	Insolation		29	56	61	54	45	42	29		
	Absorbed		9	14	21	24	26	22	12		
	Clear Sky			76	80	79	75	71	52		
90°N	Insolation			57	62	54	42	39	24		
	Absorbed			14	22	24	24	20	10		

Table V offers a comparison of the different types of solar radiation by latitude and by month. Owing to the high albedo of a snow cover, the differences between the total and absorbed radiation become very great towards winter and to the north, and albedo becomes a factor of equal or greater importance than all other depletion factors. Sharp gradients are set up regionally, dependent in general on the seasonal retreat and advance of the snow cover and locally on the continuity of the snow and ice. The closed-crown forest plays a significant role by lowering the winter albedo.

---

* Total solar radiation received on a horizontal surface.

† Values of mean monthly cloudiness and frequency of cloud types are given in the second part of this monograph (IA3b).

The main features of the distribution of total solar radiation and absorbed radiation north of 65°N are summarized below:[158]

Total solar radiation (insolation). "The latitudinal minima of insolation are found, during all months, over the Norwegian Sea with its high cloud amount and density and high atmospheric water vapor content. The maxima are mostly over eastern Siberia between 140° and 160°E. It is remarkable that this eastern Siberian maximum is stable through the whole year, although the (winter) anticyclone disappears during summer. The extreme remoteness from open oceans must be responsible. A secondary radiation maximum is experienced over Canada but without the same degree of stability. At 65°N, the maximum near 150°W is the last northward extension of the clear skies of the prairies. The main Arctic maximum, however, is found farther to the northeast, over the Canadian Archipelago. The main feature of the Polar Ocean is the markedly higher radiation in the western part especially in the Greenland section," (p. 13).[158]

Absorbed solar radiation (retained radiation). "The outstanding feature of all insolation maps is the pronounced minimum over the Norwegian Sea. This minimum disappears completely in the maps of retained radiation. In these maps the main phenomenon is a band of extremely steep gradients which is apparent in all months but especially well developed in spring and early summer. Over the Atlantic Sector this zone of high gradient follows the ice limit, as was to be expected. More complicated conditions exist however over the continental areas. The large zones of coniferous forests with low albedo cause rather higher retained radiation amounts to be found far northwards, beyond the snow line. Over the American continent, where the area examined is essentially north of the tree line, the snow cover becomes significant, with the result that a pronounced maximum of retained radiation is found in the western part of the continent where the coniferous forest reaches the coast. As surface conditions over the Polar Ocean are rather uniform with only slight meridional variations, the wide region with slight radiation gradient in the insolation maps is sustained," (p. 15).[158]

Long-wave radiation

At the outer limits of the atmosphere, incoming short-wave solar radiation is the single energy source, while losses are due to outgoing long-wave radiation from the earth and atmosphere. At the surface, losses are still by long-wave radiation, but the energy received is made up of both short- and long-wave components.[164] As one approaches high latitudes, the long-wave component becomes increasingly important. North of 65°N, this component probably accounts for some 60 to 69% of the total incoming radiation in mid-summer, and approaches 100% during the polar night.[161]

Instrument measurements of long-wave radiation are still unreliable and estimates must be made by applying radiation laws to atmospheric conditions. However, observational material over high latitudes is still inadequate for the evaluation of physical processes on a climatological basis and results must be considered tentative. Vowinckel and Orvig[161] attempted to estimate the long-wave components and their discussion of the problems with respect to high latitudes is summarized below:

Long-wave radiation emitted from the ground. Assuming black-body values for the emissivity of all natural surfaces, the outgoing radiation is a function of surface temperature only, but knowledge of actual surface temperature is scanty. Over the open ocean, the sea surface temperature is comparatively stable in time and space and the marine charts are readily available. Over the pack ice there is still little detailed knowledge of the distribution of open water and thin ice and the temperature of the ice and snow surface was taken as representative. Owing to the interference of the instrument itself and the very sharp gradients above and below the surface, reliable measurements of surface temperature are few. Sverdrup's data[136] from the "Maud" and Yakovlev's[175] at North Pole II were used to obtain a monthly correction factor to convert known air temperatures to surface values over the whole region. A surface value of 0C was assumed on all occasions in summer when positive temperatures were reported. It was also assumed that local differences due to the varying thickness of the ice and snow cover, cloud and wind conditions, and local microtopography would cancel out over reasonably large areas. The error of surface temperature is believed not to exceed 1 to 2C, 5-10 ly/day, or 2% of the outgoing radiation in winter. The continental surfaces are most varied and offer most difficulties. In winter over the flat snow-covered tundra, temperature gradients near the surface appear to resemble those over the Polar Ocean. However, a bias exists in the hilly regions such as northeastern Siberia and Alaska, where most stations are set up in valley bottoms which experience deep inversions, while the hills are less cold. Here, no attempt was made to adjust the air temperature values, which are in any case unrepresentative. Over the woodland and forest, to the south, where the vegetation varies in height and there is the crown area of the trees, the exact determination of the temperatures of the radiating surface becomes even more complicated. Very large errors in the outgoing radiation are likely in winter over these areas. In summer, when the inversion is absent, the air temperature is less affected by topography and representative of larger areas. There is also less temperature difference between the air and surface over the swampy or flooded expanses of tundra. Furthermore, a low, uneven vegetation cover will bring the radiating temperature nearer to that of the air. Near the Arctic Circle, the superadiabatic gradients which build up during the day are counterbalanced by the tendency to inversion at night. With respect to wind and cloud, it is impossible to calculate a correction factor without knowledge of the extent of water and swamp, the amount of bare surface, the amount of overheating plant tissue and the height of the plant surface. However, in the snow-free months the shelter temperature will generally be lower than that of the radiating surface, and from Mather's results at Barrow,[98] correction factors of 3C for June, 4C for July and 1C for August were selected for snow-free surfaces. A resulting probable error over land surfaces is 10 to 20 ly/day.

Long-wave radiation received by the ground. This component can be estimated from the temperature and humidity conditions of the atmosphere and the amount and height of clouds. With the aid of Elsasser's[41] radiation diagram, grid-point values were calculated for clear sky conditions and then corrected for cloud amount and type.[157]

For clear sky conditions, it was assumed that the water vapor content approaches zero by 300 mb (about 9 km) and mean charts of temperature and humidity were used, for a number of levels. Temperature error is more significant than that of the moisture content.

For actual cloud conditions, the assumption was made that the downward radiation of clouds is that of a black body of the same temperature as the cloud base. A difference of 10% or more from black body radiation could be critical for overcast conditions. For thin cirrus cloud, 50% of black body radiation was accepted. There is still little known of the emissive properties of clouds at high latitudes or of the mean height of the cloud base, from which to obtain its temperature. A check on the significance of cloud heights was made over a maritime region (Norwegian Sea) and a continental area (central Siberia). Table VI shows the different regional values due to the presence of the inversion over Siberia, and indicates that only in cyclonic areas with a high cloud frequency will the average ascent approximate reality. In general, assuming an error in cloud temperature of 5C, the mistake in downward radiation will be about 10 ly/day. Evaluations based on weather patterns rather than the month could decrease the error.

Table VI. Relation between cloud height and downward radiation with 10/10 overcast (ref. 161, p. 31).

January	height (m)										
	100	200	300	400	500	1000	1500	2000	3000	4000	5000
65°/0°E	648	645	643	640	637	636	634	630	610	591	573 ly/day
65°/120°E	372	382	387	389	391	401	403	400	396	382	366 ly/day

Fortunately, some of these difficulties are likely to be eased before long. New techniques in measurement of surface temperatures and cloud heights from aircraft[2, 32, 88, 92] and satellites[171, 188] are developing rapidly. These techniques, depending on the radiation emitted by the surface, offer weighted area-mean values with a time constant of the order of milliseconds, while the instrument itself has little or no effect on the environment. With a Tiros satellite in polar orbit, information on cloud cover is rapidly accumulating.

Net radiation at the surface

Table VII shows the net radiation gain or loss as a percentage of the total incoming and outgoing radiation for each latitude.[161] Net radiation calculations are the small residuals of large components. These values are therefore very sensitive to error.

Table VII. Net radiation as a percentage of the total incoming and outgoing radiation, irrespective of sign.[161]

Month/Latitude °N	65	70	75	80	85	90
January	8.5	9.7	10.6	9.4	10.6	11.0
July	13.8	12.6	12.4	14.2	13.2	12.6

The errors in the basic meteorological data will, however, influence incoming and outgoing radiation in the same direction, if the study has been consistent. Areal comparisons and relative magnitudes should therefore be reasonably reliable, even if the absolute numbers are doubtful.

Radiation regimes. Three basic radiation types can be distinguished (Fig. 17).

Type I: The Norwegian Sea type (Fig. 17a) is characteristic of the open ocean north of the Arctic Circle, where a high positive radiation balance in summer is compensated by large negative values in winter. The dominant factor is the open water, whose relatively high surface temperatures in winter result in very high values of outgoing long-wave radiation. Compared with the difference between ice and open water (cf. Davis Strait, Fig. 17a), the effect of a warm or cold surface current is negligible. Open water surfaces in polar regions are therefore very strong "heat sinks" at this season, and although changes in the weather patterns, from cyclonic to anticyclonic conditions, can strengthen this negative value, positive changes in temperature, moisture, and cloud conditions are never strong enough to eliminate this negative balance. The high frequency of cyclones, however, does retard the effect of the radiation loss.

From mid-March to mid-October, the positive radiation balance is determined by the incoming short-wave component, and so at this season the clearer skies associated with anticyclones are most favorable to the balance. However, the large difference between the curves for the clear sky and for the actual radiation received at the surface reflects the cloudiness during these months. The relative coolness and stability of the ocean surface temperature in summer is favorable to the radiation balance, as the emission from the surface is kept low compared to the total

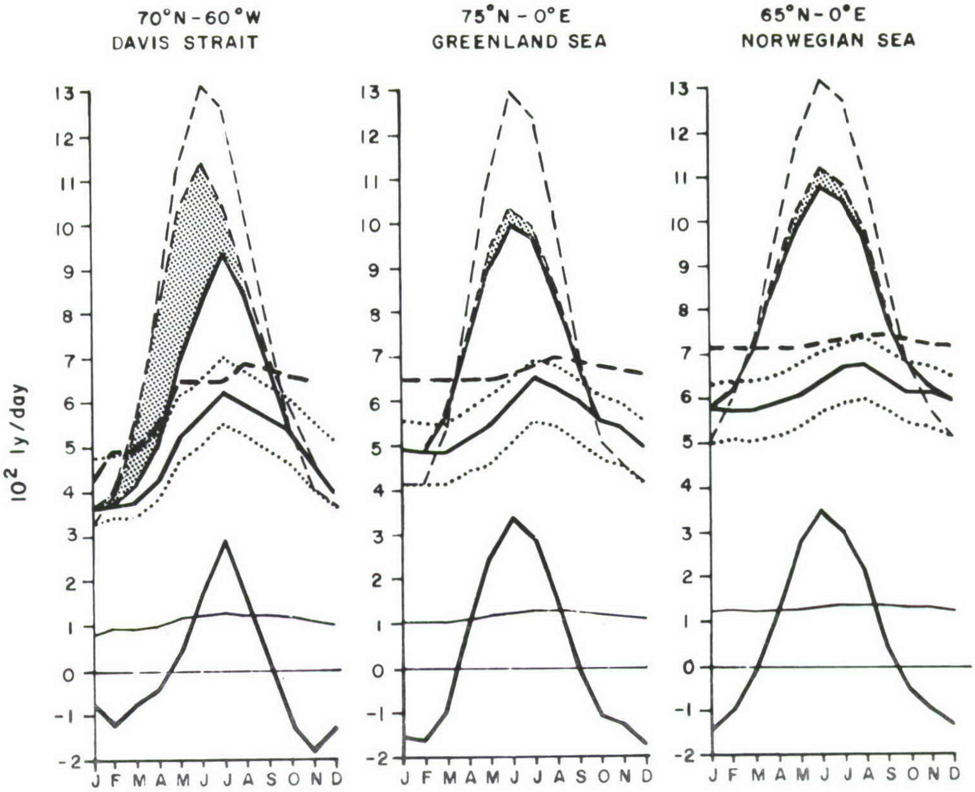

a. Norwegian sea type.

Figure 17. Radiation regime (after Vowinckel and Orvig, 1963[161]). See Fig. 17b for legend.

radiation received. The outgoing long-wave component reaches its maximum in late summer, just when the solar radiation begins to drop of rapidly. July is the only month when, given overcast conditions, a radiation balance is achieved in long-wave components. In general, maritime conditions give a more negative balance in high latitudes, where there is a predominant radiation loss.

Type II: The Continental type (Fig. 17b) is typical of the extreme continental areas of inner Siberia and western Canada; it is characterized by small negative radiation values in winter and low positive values in summer. One interesting feature is that the radiation balance for the Norwegian Sea is 21.8 Kly/year compared with 30.4 Kly/year over east-central Siberia in the same latitude. This higher positive balance for the year is the result of a smaller negative balance in winter, when the very low surface temperature reduces the outgoing radiation. It is the long-wave components which are decisive in this regime. In winter, the ratio of clear sky incoming to outgoing radiation is not very different over the two areas, in spite of the strong inversion over Siberia. This is due to the very low humidities over the continental area. Cloud amounts are low so that the long-wave incoming radiation curves for clear sky and the actual conditions are close together. However, contrary to type I, long-wave radiation received at the ground under overcast conditions is higher than the outgoing radiation from November to March. It follows that significant changes from a negative to a positive radiation balance can be brought about in winter through a change in the circulation and weather pattern, since the inversion is highly effective when associated with cloud and higher humidities, but ineffective when the air is clear and dry.

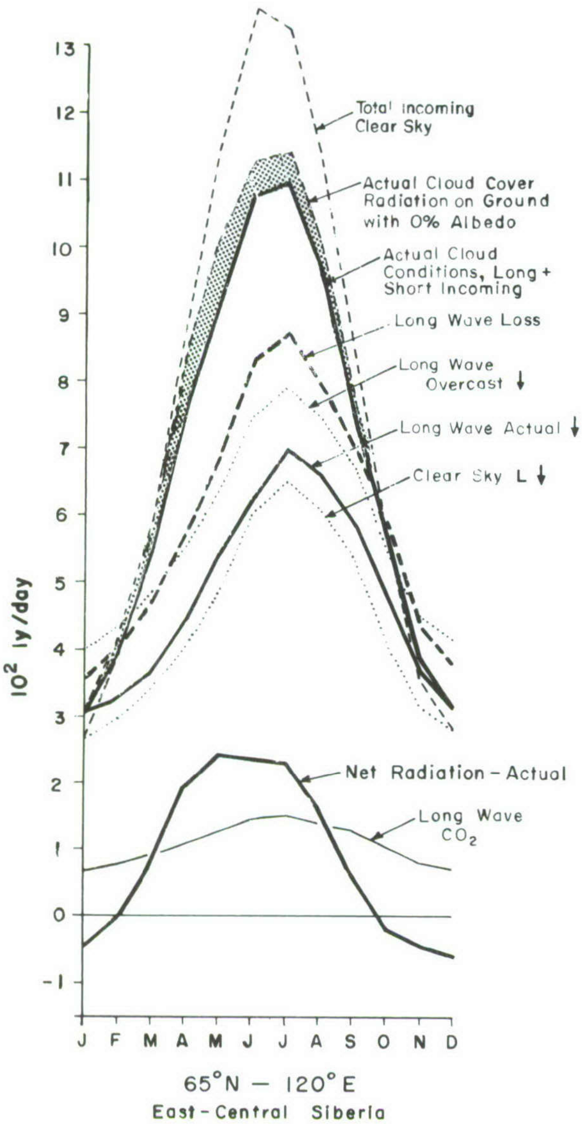

b. Continental type.

Figure 17 (Cont'd). Radiation regime (after Vowinckel and Orvig, 1963[161]).

In summer, the surface temperature increases more rapidly than that of the air and the long-wave balance becomes increasingly negative. Furthermore, at the time when the humidities increase, the winter inversion disappears. During the late winter-spring, when the radiation balance becomes positive, there is a steep rise in the short-wave radiation. Towards May, however, the inversion disappears and moister airmasses with higher cloud amount appear, lessening the increase in short-wave radiation while the outgoing radiation continues to increase. As a result, there is no month with a net radiation maximum and the variation through the summer is small. The details of the type vary from place to place, depending mainly on the rate of increase of surface temperature and the establishment of summer conditions in the free atmosphere.

Type III. The pack ice regime (Fig. 17c) is characteristic of the oceans and seas which are only temporarily free from ice, e. g. Baffin Bay.

This regime lies between the oceanic and continental extremes. In winter, the outgoing radiation from the ice-covered sea surface is not as low as over continental areas, 420 ly/day compared with 700 over the ocean and 350 over the continents; furthermore, the cloud cover is low and ineffective and the inversion less intense, so that even with overcast conditions there is only a brief period with a positive long-wave balance. In fact, the influence of overcast skies on long-wave radiation varies little in space or time over the Polar Ocean, remaining at about 150 ly/day.

With the return of the sun in spring there is no rapid increase in the radiation balance, largely owing to the high albedo values. When these values have decreased by July and August, as the ice eventually clears, the incoming short-wave radiation has already passed its maximum. Moreover, as the albedo decreases there is an increase in cloud cover associated with the open water, which continues the depletion of short-wave radiation. The increase in the incoming long-wave radiation due to cloudiness is relatively little compensation. As a result, the maximum positive radiation balance occurs after the sun has reached its height.

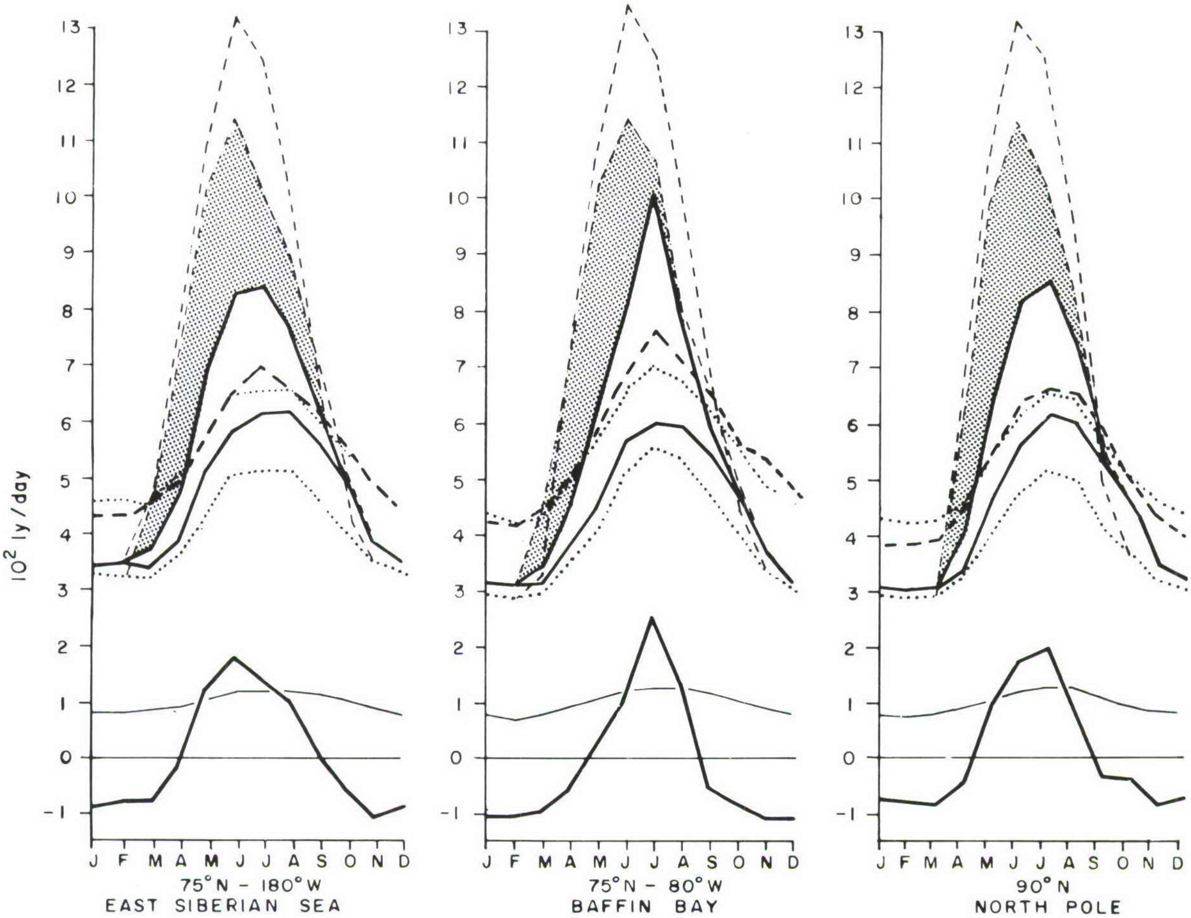

c. Pack ice type.

Figure 17 (Cont'd). Radiation regime (after Vowinckel and Orvig, 1964[161]). See Fig. 17b for legend.

Over the central Polar Ocean, the albedo remains relatively high throughout the polar day and the late summer maximum in the radiation balance is less pronounced. However, the positive radiation balance in summer is not significantly less over the pole because the clouds are thinner and the short-wave radiation less depleted by them, and because the low surface temperatures which do not pass 0C maintain low values of long-wave emission. In autumn the radiation balance is less strongly negative than further south, owing to the rapid freeze-over and lowering of surface temperatures.

Monthly and annual distribution of net radiation. Figures 18 and 19 and Table VIII summarize the regional distribution of net radiation through the year, north of 65°N.

In early winter, the main feature is the high negative values over open water; these tend to increase while the water stays open. Longitudinal differences are therefore pronounced (Table VIIIa), and the western hemisphere generally has a higher energy deficit than Eurasia. A comparison of Tables VIIIb and c shows the influence of the ice-water margin over the Norwegian Sea. Over the Polar Ocean and continents the deficit is only about 50% that of the Norwegian Sea. In spring, regional differences in the transition from a negative to a positive balance depend on the variations in albedo and heat capacity of the surfaces. Steep gradients occur between open water and ice and even steeper gradients between the snow-free continental areas and the northern ocean (Fig. 19b). In summer, the net radiation gain is largely a function of the long-wave emission from the surface; tongues of high values extend up Davis Strait and Baffin Bay and from the Norwegian Sea into the Kara Sea. The smoothest distribution occurs in late summer when the effects of the various surfaces are least differentiated (Fig. 19d).

Table VIII. Annual estimated net radiation (ly/day) at the surface (Vowinckel and Orvig, 1963[161]).

LONGITUDE

	E									180	W							
	0°	20°	40°	60°	80°	100°	120°	140°	160°		160°	140°	120°	100°	80°	60°	40°	20°
J	-138	-96	-65	-67	-64	-46	-52	-71	-49	-91	-49	-49	-72	-65	-83	-58	-107	-92
F	-93	-49	-27	-44	-21	-10	-7	-34	7	-71	-37	-15	-39	-57	-71	-91	-87	-60
M	-5	49	39	-2	62	68	73	15	48	-55	-10	14	20	-29	-66	-81	-40	-5
A	150	167	88	102	166	191	190	125	157	13	50	124	142	100	4	-16	28	166
M	281	273	215	201	223	225	240	224	189	59	193	209	204	77	35	121	115	290
J	357	325	311	281	297	289	234	327	283	185	222	287	285	194	157	269	262	295
J	312	236	400	227	211	225	228	257	239	240	235	215	218	247	211	278	338	254
A	217	167	197	161	157	165	162	186	167	174	162	171	178	169	196	206	245	183
S	44	30	108	26	24	65	53	56	52	35	33	44	34	48	57	53	73	36
O	-57	-36	-9	-30	-25	-15	-21	-42	-21	-29	-38	-38	-35	-26	-26	-65	-31	-36
N	-96	-83	-83	-56	-47	-51	-45	-72	-60	-105	-73	-47	-81	-86	-111	-139	-79	-95
D	-131	-95	-70	-68	-66	-55	-60	-74	-59	-112	-58	-40	-93	-101	-118	-124	-102	-110

a. Along latitude 65°N

LATITUDE

	65°	70°	75°	80°	85°	90N
J	-138	-146	-157	-92	-74	-76
F	-93	-123	-166	-107	-84	-81
M	-5	-39	-98	-91	-89	-85
A	150	91	78	14	-51	-50
M	281	242	252	64	82	90
J	354	290	337	175	177	169
J	312	250	288	208	200	195
A	217	130	146	108	82	85
S	44	23	-3	-43	-35	-36
O	-57	-80	-108	-91	-52	-38
N	-96	-126	-131	-83	-87	-83
D	-131	-142	-176	-100	-79	-71

b. At 0° E longitude (maritime)

	65°	70°	75°	80°	85°	90°N
J	-52	-34	-54	-73	-74	-76
F	-7	-50	-85	-38	-84	-81
M	73	40	-50	-78	-89	-85
A	190	150	-9	-33	-51	-50
M	240	270	78	101	82	90
J	234	266	166	190	177	169
J	228	193	217	200	200	195
A	162	115	118	90	82	85
S	53	25	7	-24	-35	-36
O	-21	-46	-92	-71	-52	-38
N	-45	-52	-85	-89	-87	-83
D	-60	-53	-80	-95	-79	-71

c. At 120° E longitude (continental)

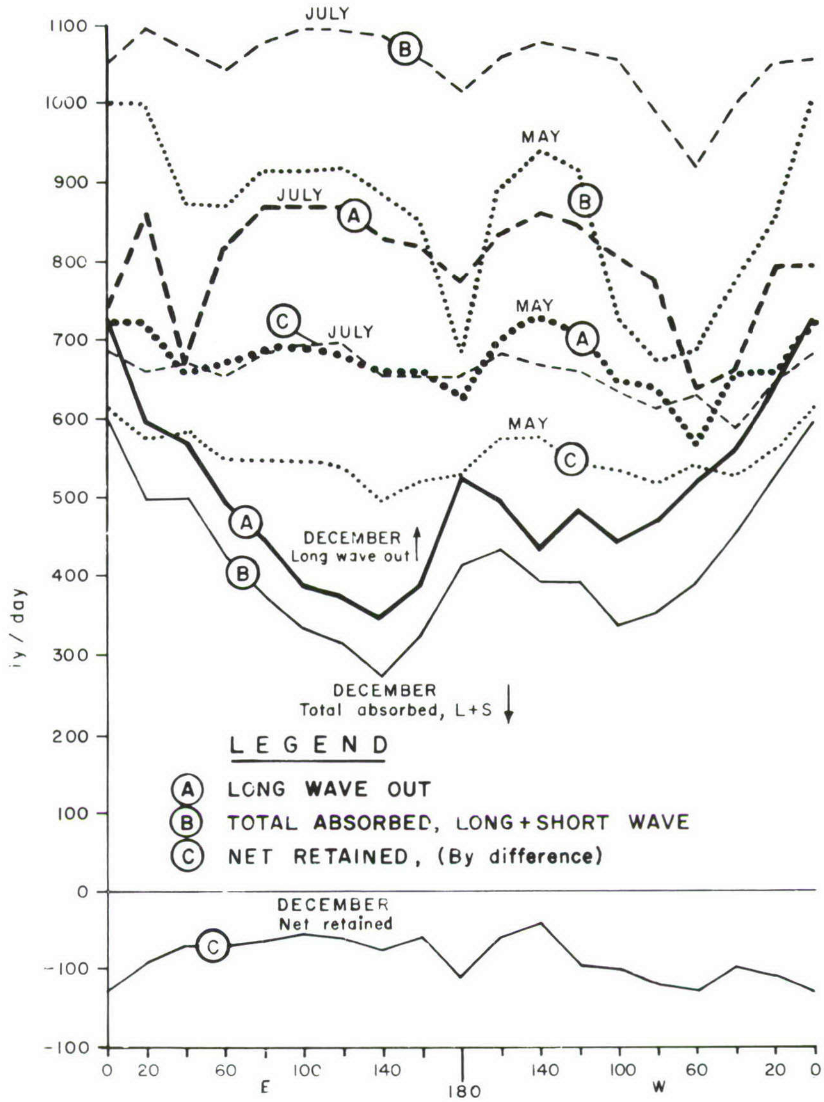

Figure 18. Radiation balance components. Lat. 65°N, December, May and July.

Measurements of net radiation are few compared with those of total daily solar radiation; a working relationship between the two values would therefore be useful. During the summer of 1958 net radiation measurements were made at Knob Lake[110] with a portable "economical net radiometer" developed by Suomi and Kuhn.[134] A regression analysis showed a straight line trend between the total solar radiation received, x, and the mean daytime net flux, Y,

$$Y = -2.84 + 0.01 x.$$

This indicates that at Knob Lake an insolation of > 284 ly/day is required before the net flux becomes positive (directed downwards). Table IX shows that the critical value is passed in March and September. Further measurements at other seasons, and simultaneously at other sites, would suggest whether such an equation can be used as a regional characteristic, from which the approximate mean daytime flux can be estimated from the total daily solar radiation.

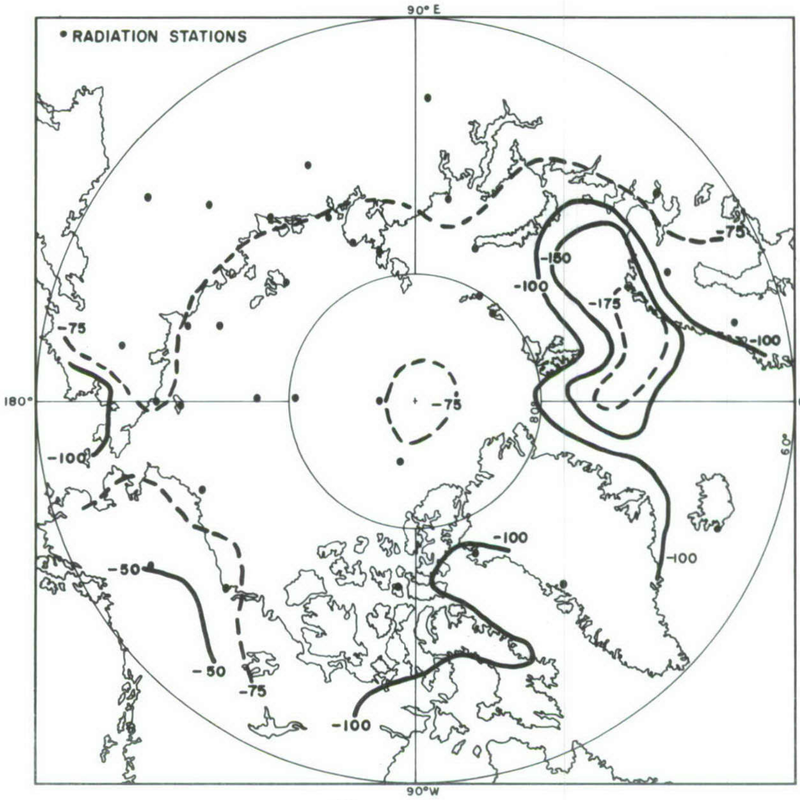

a. December

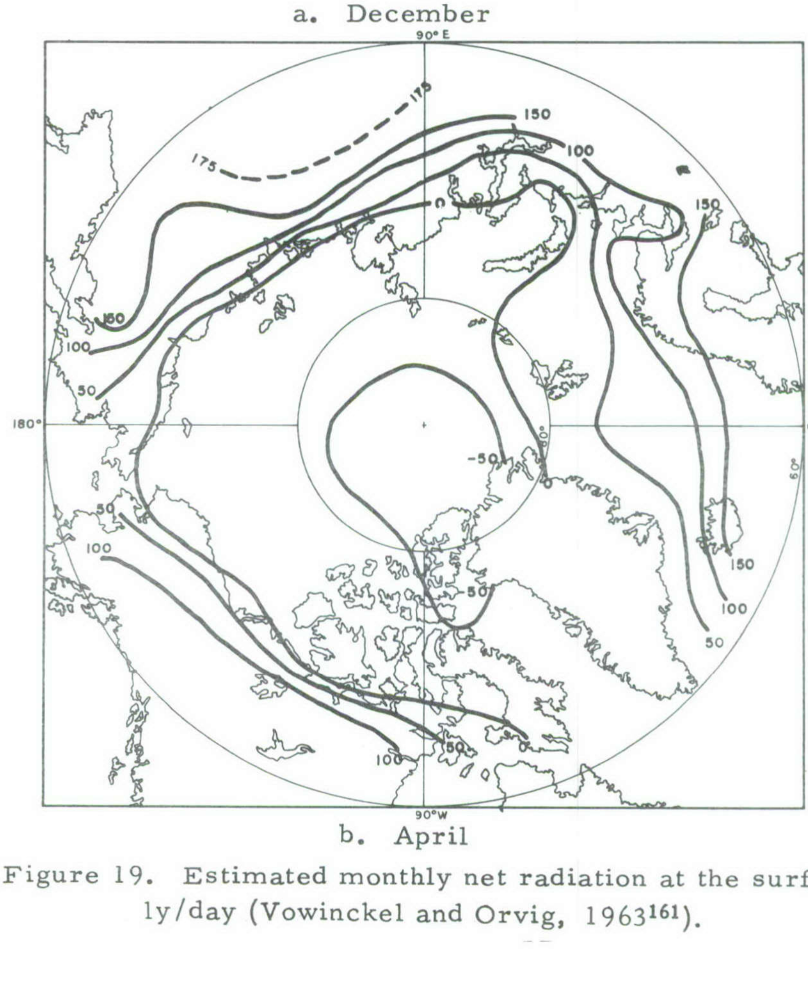

b. April

Figure 19. Estimated monthly net radiation at the surface, ly/day (Vowinckel and Orvig, 1963[161]).

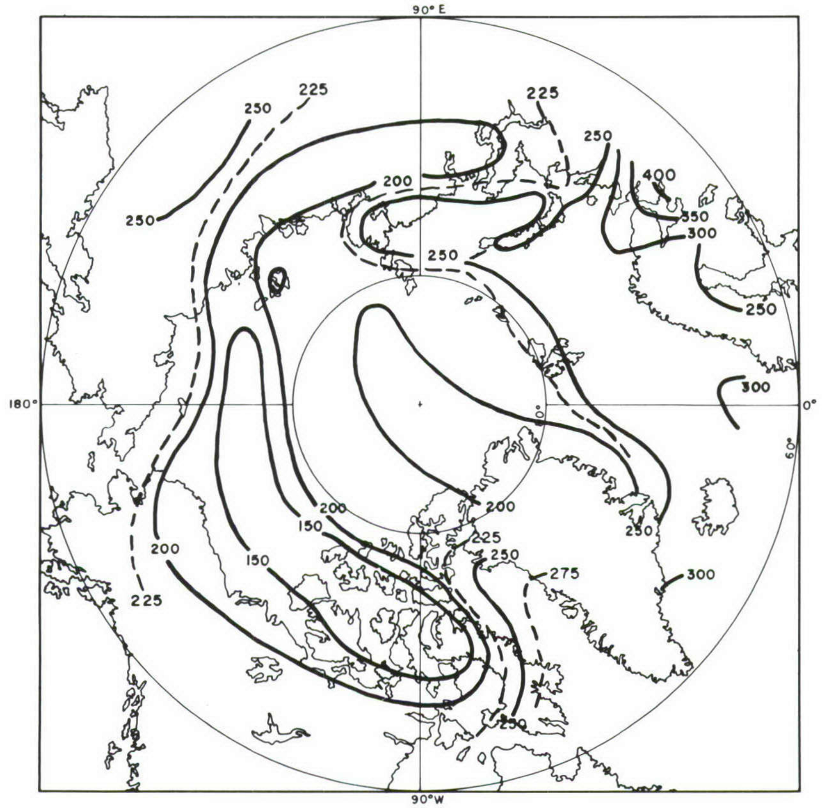

c. July

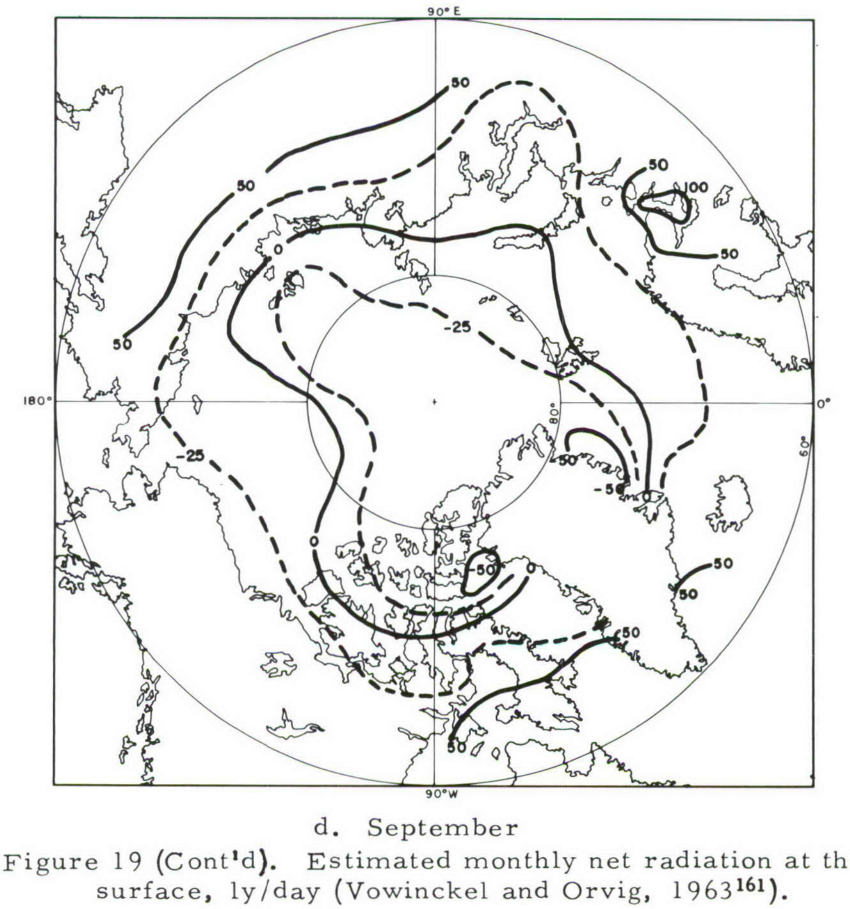

d. September

Figure 19 (Cont'd). Estimated monthly net radiation at the surface, ly/day (Vowinckel and Orvig, 1963[161]).

Table IX. Averages of the monthly means of total daily solar radiation Knob Lake (Orvig[110]).

January	based on 1958, 1959 and 1960	61 ly	
February	based on 1958, 1959 and 1960	127 ly	
March	based on 1958 and 1959	291 ly	
April	based on 1958 and 1959	402 ly	
May	based on 1959	277 ly	– (with additional years this value would probably pass 400 ly)
June	based on 1958 and 1959	439 ly	
July	based on 1957, 1958 and 1959	375 ly	
August	based on 1957, 1958 and 1959	299 ly	
September	based on 1957, 1958 and 1959	277 ly	
October	based on 1957, 1958 and 1959	127 ly	
November	based on 1957, 1958 and 1959	73 ly	
December	based on 1957, 1958 and 1959	52 ly	

The Heat Balance

The final terms in estimating the heat balance include those of non-radiative transfer – essentially the fluxes of evaporative and sensible heat, including the advection of energy into the area by oceanic and atmospheric circulation. These terms are not easy to calculate. One approach is to estimate the net radiation of the atmosphere and of the earth-atmosphere system ; these last values represent the amount of energy which has to be transported into or out of the area by non-radiative processes.

Energy budget of the atmosphere and earth-atmosphere systems

Several evaluations have been made of these budgets[27, 28, 63, 91, 162] but generally by latitude zones, with a view to obtaining hemisphere and global values. Budyko[27, 28] and Kondrat'ev's recent work was based on new observations from actinometric radiosondes, balloons, aircraft and satellites[181] as well as calculated values; a world map of annual values of net radiation for the earth-atmosphere has been published,[27] but it does not extend to the poles. The only regional estimates at higher latitudes are those of Vowinckel and Orvig.[162] These are discussed below.

The gain in radiation to the atmosphere is through the absorption of solar radiation and of long-wave radiation from the surface. Estimates of the short-wave term depend mainly on the accuracy of knowledge of the water vapor content of the atmosphere. The radiation losses are by long-wave radiation to the ground and to space; the last term requires a knowledge of the distribution, height and temperature of cloud tops. The upper limit of the atmosphere was assumed to be the 300 mb surface (about 9 km). In spite of the tentative nature of the resulting values of the net radiation of the lower atmosphere, the following features are suggested:[162]

(1) The net radiation is negative all year. The smallest negative values occur in late spring and early summer, owing to the increased absorption of reflected short-wave radiation from surfaces still covered by snow and ice; the largest deficits occur in late summer and autumn. Individual components show maximum values in summer.

(2) The annual variation is much smaller than at the surface since the short-wave component is minor. The variations in energy loss are mostly brought about by long-wave loss from the atmosphere to the earth.

(3) With respect to the atmosphere, the presence of clouds increases with the negative radiation balance owing to the increased radiation loss from the clouds to the ground, which overcompensates for the reduced loss to space. Exceptions occur in early summer over eastern Siberia and parts of Canada, where the air

is very dry and solar elevation relatively high so that the importance of short-wave absorption is somewhat greater with cloud. Although long-wave radiation to space is generally lower with a cloud cover, in winter over the Arctic the areas of high anticyclonic frequency show a marked increase in radiation loss under cloudy conditions. This is due to the presence of the inversion, where cloud temperatures are higher than those at the earth's surface. Since the downward radiation is also increased, overcast conditions in the Arctic winter anticyclones produce a more negative radiation balance for the system earth-atmosphere as a whole.

(4) The larger portion of the energy exchange is effected by radiative processes. Even during the Arctic winter, non-radiative transfer accounts for only a third of the energy requirements. In summer it is less than 20% (N. B. this refers only to the mode of energy transfer and not to the source of energy).

The radiation balance of the earth-atmosphere system is the difference between the solar radiation absorbed both at the ground and in the atmosphere and the long-wave radiation lost to space. In the polar night this represents almost 100% of the energy expenditure (Table X). Since the latitudinal differences are only slight in winter, it is suggested that either the energy transport by advection in the air is so strong that neither its sensible nor latent heat content is exhausted, or the ocean makes a higher contribution in the north.

Table X. The percentage contribution of non-radiative processes to the turn-over of energy[162].

	J	F	M	A	M	J	J	A	S	O	N	D
65°N, 0°E	100	73	36	4	8	15	10	20	32	62	92	100 %
65°N, 120°E	100	56	20	3	11	14	10	22	27	55	85	100
Pole	100	100	100	48	10	9	22	25	79	100	100	100

Figure 20 and Table XI describe the distribution of the net radiation for the earth-atmosphere system over the northern areas of the cold regions. The distribution is similar to that for the earth's surface; although the regional differences are smoother, there is still a clear distinction between maritime and continental areas.

(1) In winter, latitudinal variation is slight, with maximum negative values over the Atlantic and Davis Strait where long-wave radiation loss from the open water is the decisive factor.

(2) Toward spring with the increasing short-wave radiation, the high albedo of the ground becomes the critical factor in energy depletion and the area of maximum radiation loss shifts to higher latitudes, to the pack ice. Steep gradients develop over the southern Arctic in spring.

(3) From midsummer, the extensive cloud cover over the Polar Ocean becomes the significant factor. In May and June, the maximum loss over Baffin Bay and the Canadian Archipelago can be attributed to the relatively high cloud amount and its comparative opacity. In June, the central Arctic attains a small positive value. The maximum radiation loss does not reach the area around the pole until August. In early summer, differences between land and ocean disappear and by late summer, early autumn the balance approaches the "ideal" with the greatest loss at the pole and a gradual decrease southward.

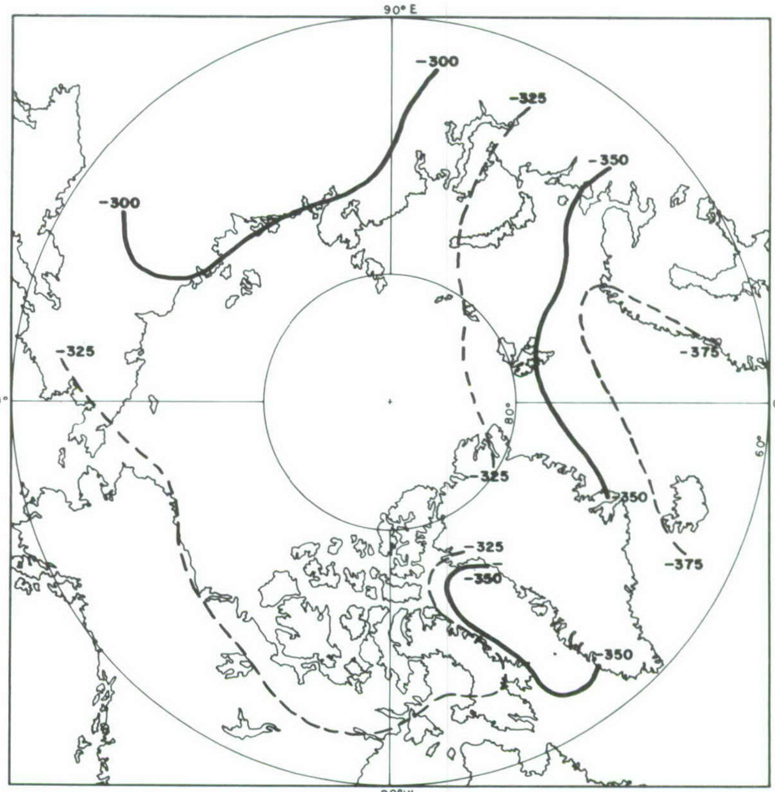

a. December

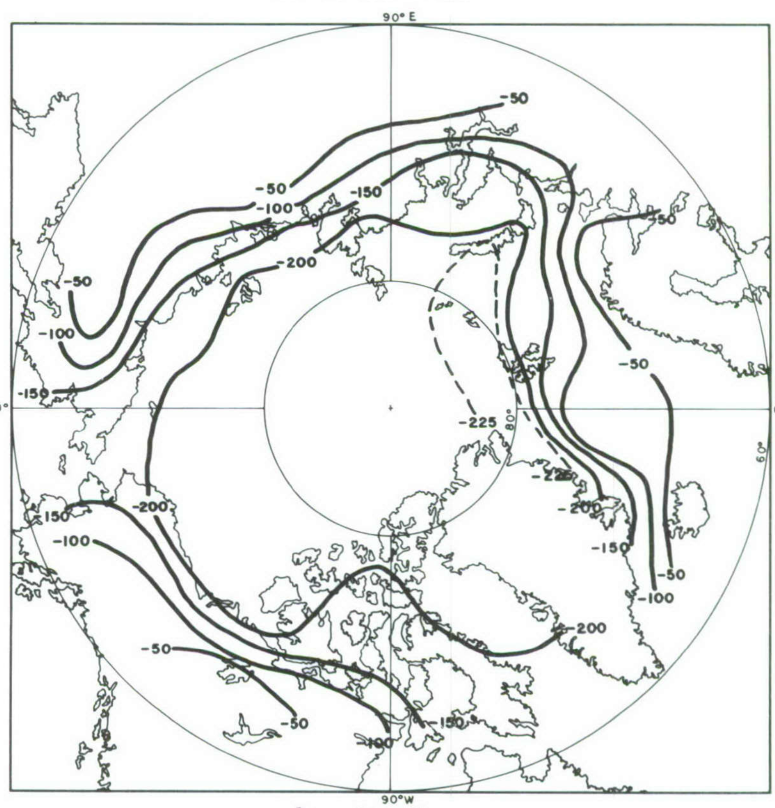

b. April

Figure 20. Estimated monthly net radiation for the earth-atmosphere up to 300 mb, ly/day (Vowinckel and Orvig, 1964[162]).

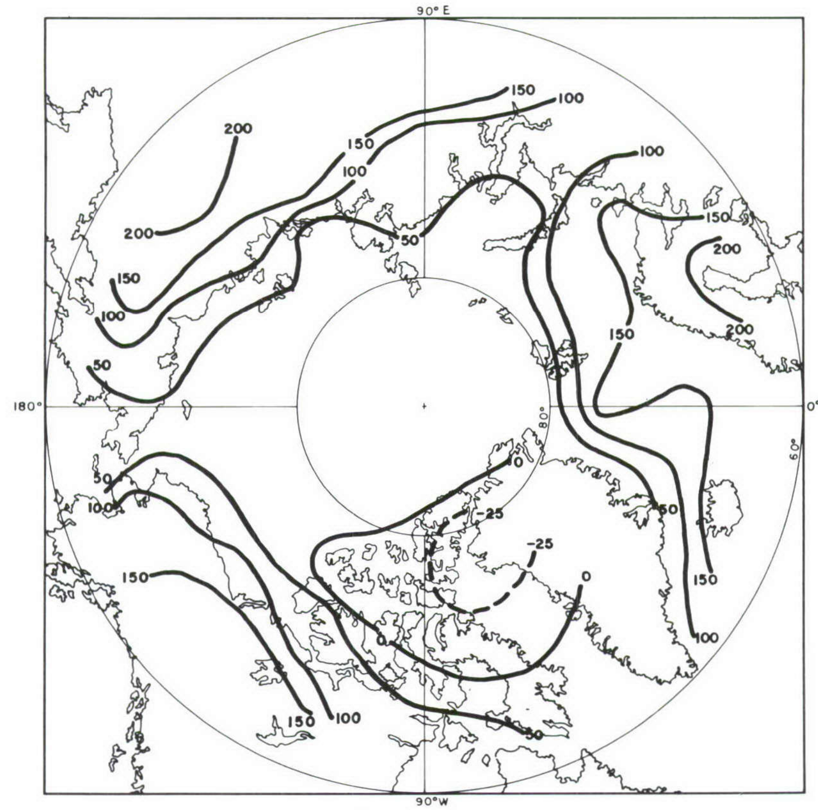

c. June

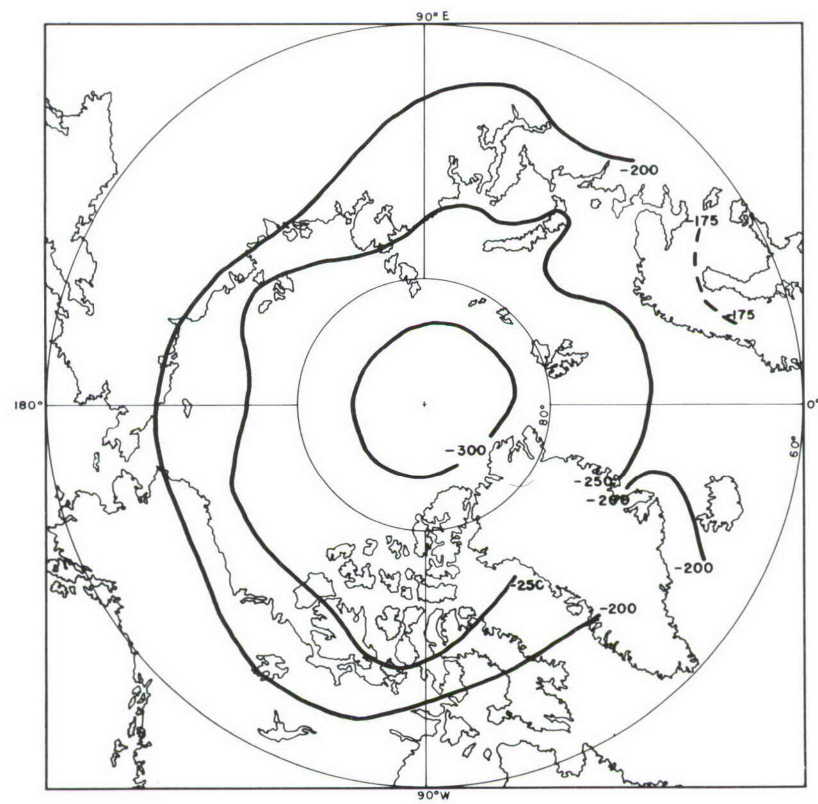

d. September

Figure 20 (Cont'd). Estimated monthly net radiation for the earth-atmosphere up to 300 mb, ly/day (Vowinckel and Orvig, 1964[162]).

Table XI. Annual estimated net radiation (ly/day) in the earth-atmosphere up to 300 mb (Vowinckel and Orvig, 1964[162]).

LONGITUDE

	E 0°	20°	40°	60°	80°	100°	120°	140°	160°	180°	W 160°	140°	120°	100°	80°	60°	40°	20°	0°
J	-390	-355	-340	-332	-311	-286	-275	-297	-303	-339	-344	-333	-323	-297	-306	-330	-361	-365	-390
F	-340	-290	-285	-295	-237	-212	-209	-229	-231	-295	-293	-277	-264	-265	-283	-302	-297	-317	-340
M	-210	-172	-196	-210	-146	-124	-107	-159	-144	-245	-211	-193	-172	-219	-191	-275	-249	-227	-210
A	-33	-11	-76	-79	-3	15	22	-44	-22	-151	-130	-58	-38	-95	-183	-199	-130	-28	-33
M	81	116	20	32	70	93	97	84	39	-101	37	59	61	-89	-22	-38	-37	111	81
J	156	218	145	74	170	163	144	229	173	36	118	179	178	92	50	2	86	185	156
J	100	131	92	83	91	98	104	131	105	82	106	103	59	118	73	3	120	127	100
A	-17	-14	-35	-29	-37	-15	-19	-8	-14	-21	-27	-26	4	-29	1	-15	2	-13	-17
S	-205	-163	-213	-194	-202	-193	-174	-157	-163	-182	-189	-151	-203	-200	-193	-186	-195	-209	-205
O	-328	-299	-297	-283	-266	-250	-243	-248	-255	-267	-270	-274	-284	-287	-274	-294	-284	-306	-328
N	-384	-366	-353	-344	-312	-287	-282	-301	-307	-350	-340	-341	-342	-339	-351	-349	-353	-385	-384
D	-398	-396	-355	-341	-324	-299	-289	-282	-305	-341	-334	-328	-340	-323	-331	-355	-358	-356	-398
J	-390	-355	-340	-332	-311	-286	-275	-297	-303	-339	-344	-333	-323	-297	-306	-330	-361	-365	-390

a. Along latitude 65°

LATITUDE

	65°	70°	75°	80°	85°	90°N
J	-390	-372	-356	-333	-302	-299
F	-340	-349	-351	-335	-299	-297
M	-210	-216	-261	-309	-298	-286
A	-33	-79	-87	-226	-208	-217
M	81	73	-21	-55	-71	-63
J	156	133	159	29	19	15
J	100	55	73	18	-6	-17
A	-17	-82	-71	-101	-143	-156
S	-205	-231	-252	-292	-308	-311
O	-328	-358	-357	-361	-335	-330
N	-384	-392	-362	-357	-321	-320
D	-398	-378	-361	-337	-302	-300
J	-390	-372	-356	-333	-302	-299

b. At 0° E longitude (maritime)

	65°	70°	75°	80°	85°	90°N
J	-275	-282	-300	-301	-302	-299
F	-209	-259	-301	-304	-299	-297
M	-107	-162	-262	-281	-298	-286
A	22	-19	-193	-214	-208	-217
M	97	117	-81	-63	-71	-63
J	144	157	101	26	19	15
J	104	85	-13	-8	-6	-17
A	-19	-72	-100	-145	-143	-156
S	-174	-197	-228	-281	-308	-311
O	-250	-300	-324	-339	-335	-330
N	-282	-305	-320	-323	-321	-320
D	-289	-292	-308	-309	-302	-300
J	-275	-282	-300	-301	-302	-299

c. At 120° E longitude (continental)

The latitudinal distribution of mean annual net radiation for the earth and atmosphere (Table XII) calculated by London [91] shows the transition from positive to negative values at approximately 45°N. Budyko's results were similar. This coincides with the most southerly extension of the cold regions over the high continental interior in North America and Eurasia (Fig. 1). Budyko's annual negative values over the central Arctic were more than 60 K ly/year; for the subarctic, 20 to 50 K ly/year.[27,28]

Table XII. Mean annual radiation balance of the surface-atmosphere system and its components[91] (ly/min).

	30-40	40-50	50-60	60-70	70-80	80-90°N
Absorbed solar radiation	0.341	0.276	0.224	0.169	0.122	0.106
Outgoing radiation	0.327	0.306	0.287	0.270	0.253	0.245
Net radiation	0.014	-0.030	-0.063	-0.101	-0.131	-0.139

The input of energy into the Arctic by oceanic circulation, estimated first of all from the heat flux through the Polar Ocean ice[165] and the open water,[163] then checked by adding together the heat gains through ocean currents,[154] melt water run-off[149] and radiation,[161] probably totals between 8500 and 9000 ly/year. The advection of latent heat by the atmosphere can be calculated by determining precipitation, evaporation and change in storage of atmospheric water vapor.[166] With the exception of the autumn, this term appears to be always positive, contributing as much as 65% of the annual precipitation (see also reference 18). The net sensible heat convection, given by the energy balance equation for the atmosphere,[166] is far more important in high latitudes. The ratio of latent heat to sensible heat advection may be as high as 1:14 over the central Polar Ocean and 1:8 over the Norwegian-Barents Sea.

Evaporation and evapotranspiration

Evaporation depends on the energy available at the evaporating surface, the temperature gradient above the surface and the capacity of the air to remove the vapor - i.e., the saturation deficit of the air, the vapor pressure gradient above the surface, the windspeed and turbulence.

Transpiration from a vegetation surface increases the complexity of the problem;[59] the rate of flow of water from the soil through the plant system and into the atmosphere varies with temperature, humidity, windspeed and light intensity. The nature of the vegetation, the extent and depth to which it occupies the soil, the nature of the soil and the availability of water in the root zone are additional considerations. Furthermore, the vegetation cover intercepts precipitation to a varying degree and direct evaporation takes place from the different surfaces. Thornthwaite has called the combined process evapotranspiration.

Evaporation measurements[35] are still unsatisfactory; it is difficult to sample the environment without disturbing it. Evaporation pans and atmometers are used for open water surfaces, and pans and various types of lysimeters over land.

In the absence of a direct method of sensing evaporation over a broad natural surface, the problem has been approached either by the energy budget method or through the application of the processes of turbulent diffusion in the overlying air.[35,140,99,145]

The ocean areas have lent themselves more rapidly to the regional estimation of evaporation[27,28,163] because of the greater homogeneity of the surface and stability of temperature. Budyko's[27] monthly maps of heat used in evaporation do cover continental areas, but detail is sketchy for the cold regions.

The Arctic Ocean. Estimated evaporation values for the central Polar Ocean, the Laptev and Kara Seas, the East Siberian Sea, the Beaufort Sea and the Norwegian-Barents Seas are given in Appendix C.[163] Separate values are given for ice and open water; the average values were obtained by weighting according to the ice-water distribution for each month. The calculations are based on Sverdrup's evaporation formula,[138]

$$E = K(e_w - e_a) . V, \text{ where}$$

K = coefficient of turbulent exchange
V = wind speed (m/sec)
$e_{w,a}$ = water vapor pressure at the surface, and in the air (mb),

assuming that during the main period of evaporation in summer, the ice surfaces are generally slush and melting ice, with an estimated 42% covered by puddles.[149] An ice surface was considered similar to a water surface if the saturation vapor pressure over ice were used. The formula was adjusted for Arctic wind conditions and a correction was made for salinity.

Figure 21 illustrates some typical seasonal curves of evaporation over these ocean areas:

The Polar Ocean: There is a complete reversal of the annual trend for ice and water surfaces. The curve for an ice surface shows spring and fall maxima. The main minimum is in winter, owing to the predominant surface inversion; the low air temperature and low water content prevent the occurrence of higher negative values. As the inversion gradually disappears in spring, the surface temperature and evaporation increase. The summer minimum is a result of the surface

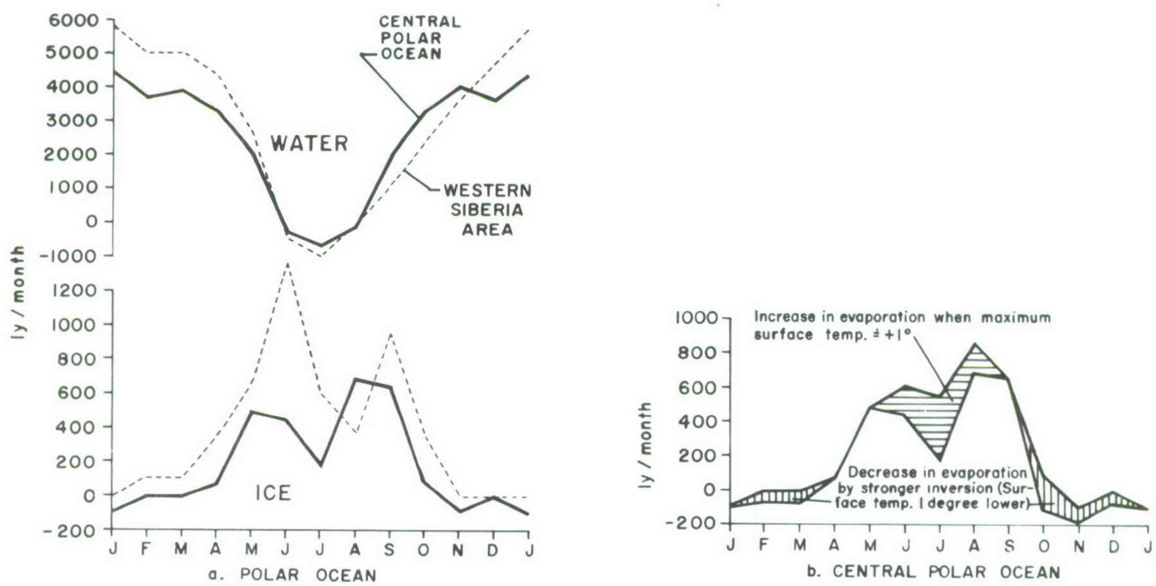

a. Polar ocean. b. Central polar ocean.

Figure 21. Evaporative heat flux from the surface. Typical curves (Vowinckel and Taylor, 1964[163]).

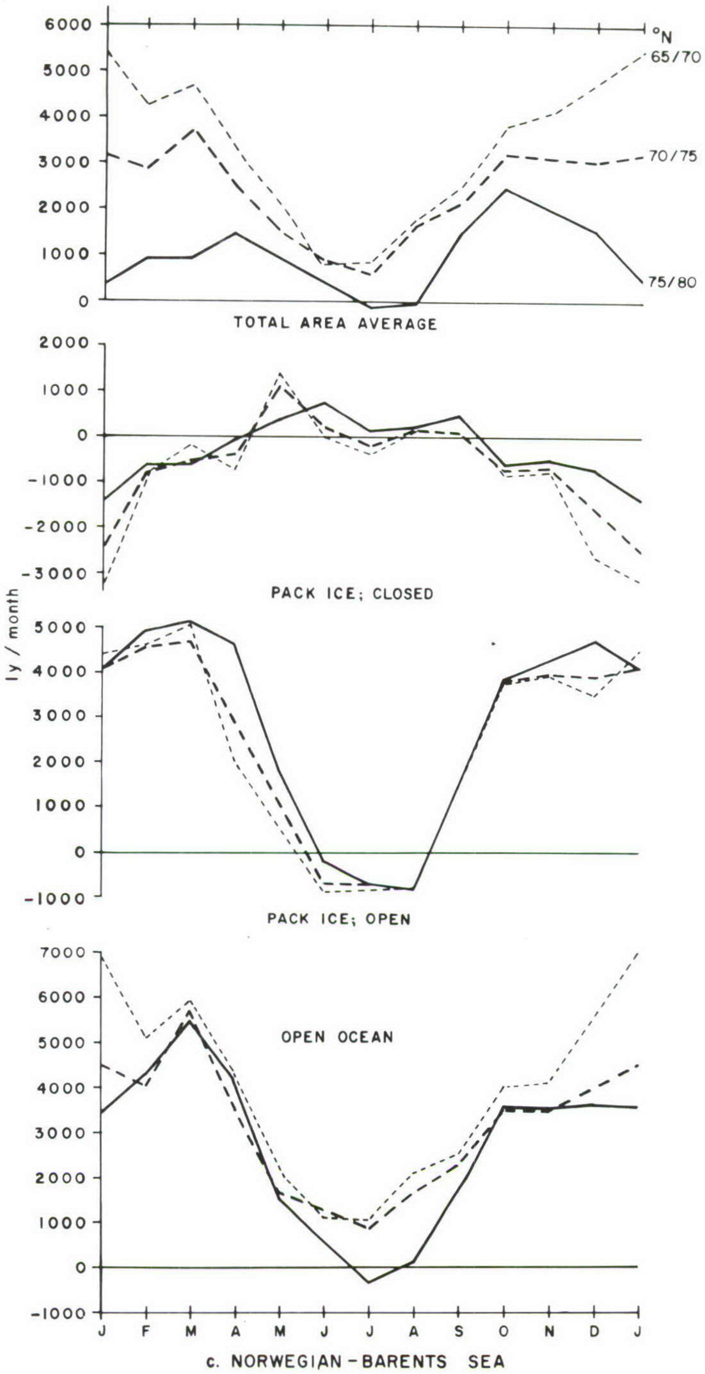

c. Norwegian-Barents Sea.

Figure 21 (Cont'd). Evaporative heat flux from the surface. Typical curves (Vowinckel and Taylor, 1964[163]).

temperature persisting near 0C, while the air temperature increases through advection. In autumn, as the air temperature falls below 0C, evaporation increases once again, to decline to winter values as the surface temperature lowers. The curve for Western Siberia shows a more pronounced summer minimum, owing to the stronger influence of warm air advection in the peripheral areas.

Further calculations confirmed that the summer minimum is due to the low temperature at the melt surface. Figure 21b shows the smoothing of the curve that would result if the water in the puddles on the ice were to rise from 0 to +1C. With an upper limit of +2 C a single maximum and minimum results. The effect of a drop of the winter inversion temperature of 1C is also given. It is mainly associated with condensation.

The evaporation curve over open water shows a pronounced summer minimum, with condensation, and a broad winter maximum. The temperature of the sea surface is conservative, with values lower than the air in summer but very much higher in winter resulting in maximum evaporation. The curve for the Western Siberian sector shows slightly higher values due to the lower relative humidity on the periphery and higher wind speeds at the Eurasian coast. Since the assumption was made that there is no open water in the winter, the open water values are theoretical but important in their implications. A slight inaccuracy in the extent of the ice cover or slight variation from year to year will have a significant influence on the whole energy budget.

The Norwegian-Barents Sea (Fig. 21c): The curves of the areal averages show the gradual transition from the pack ice shape (80°-75°N).to almost undisturbed open water conditions (70°-65°N).

From these results three distinct regimes for Arctic and subarctic regions can be defined:[163]

An oceanic type, with summer minimum and winter maximum.

A continental type with a summer maximum and winter minimum. For example, an area with shallow waters in summer could be substantially heated while the winter freeze up would hold evaporation values down. The swamp areas of high latitudes would fulfill such conditions (cf. Bryson and Kuhn [23,25]).

A transitional type, exemplified by the pack ice of the central Polar Ocean, in which the winter and transition seasons are "continental," and summer, with the incomplete melting, approaches the oceanic pattern.

Arctic and subarctic land surfaces. In the absence of a direct measure, evapotranspiration in cold regions has been based principally on the work of Budyko, Penman and Thornthwaite, who have approached the problem of evaporation over natural surfaces by attempting to estimate the potential evaporation (the upper limit), assuming an unfailing moisture supply. This quantity is then related to the actual conditions of plant cover and soil water.[58,59] Budyko[26,29] uses a turbulent-flux relationship to define potential evaporation or evaporability, where $E = \rho D(q_s - q)$ and

q_s = saturation specific humidity at temperature of evaporating surface,
q = actual specific humidity at 2 m,
ρ = air density,
D = integral coefficient of external diffusion $\int_0^z \frac{dz}{K(z)}$ (cm/sec)
K = coefficient of turbulent exchange at 1 meter (cm^2/sec)
z = height

The basic disadvantage is that the equation involves quantities equally difficult to measure. It does not take into account vegetation or albedo differences. Penman's[111,112,113] approach combines the turbulent-flux and radiation-balance methods.

$$E^* = \left[\frac{R\partial e'}{\gamma\partial T} + f(u)\cdot(e'_a - e_d)\right]\left[\frac{1\partial e'}{\gamma\partial T} + 1\right]^{-1}, \text{ where}$$

E^* = evaporation rate as it applies to an open water surface,
R = mean monthly solar radiation expressed as an evaporation rate,
γ = the psychrometric constant,
e' = saturation vapor pressure,
T = temperature,
e'_a = saturation vapor pressure at 2 meters,
e_d = measured vapor pressure at 2 meters,
$f(u)$ = empirical diffusion coefficient dependent on wind at 2 m.

From this equation, Penman obtains E_p, potential transpiration, by a comparison between open water tank evaporation and turf evaporation. Robertson[120] in Canada has had some success with a similar approach. Penman corrects for daylight, albedo and "oasis" effects (exposure).

Thornthwaite's[141, 147, 148] approach was empirical, though indirectly related to the radiation balance. He incorporated the plant cover. Potential evapotranspiration (PE) is the total water loss from a plant cover that fully shades the floor, where the soil is at or above field capacity. No distinction was made between different vegetation types in transpiration, but albedo was later considered.

$$E_p = 1.6b\left(10T/\sum_{1}^{12}(0.2T')^{1.514}\right)^a, \text{ where}$$

E_p = potential evapotranspiration for a specific period in cm per 30-day month of 12-hour days,
T = mean Celsius temperature for same period at shelter level,
T' = mean Celsius temperature for each month of normal year,
a = constant, a cubic function of $\sum_{1}^{12}(0.2T')^{1.514}$
b = a factor to correct for unequal day length as between months.

In establishing a relationship between the potential and actual evaporation the assumptions of Penman and Thornthwaite concerning the influence of variations in soil moisture differ widely.[58, 59] In actual fact, the measurements made in the cold regions have generally been concerned with potential evapotranspiration, by maintaining the soil moisture in the measuring tanks at field capacity.

For the land areas of the northern USSR, an annual map of "evaporability" is published in the Agricultural Atlas of the USSR (1960), while the following characteristic magnitudes of annual evapotranspiration have recently been given by L'vovich:[93]

1.	Tundra and wooded tundra:	European	21.0 cm
		Siberian	18.5
2.	Boreal Forest:	European	28.0
		West Siberian plain	28.0
		East Siberian mountains	20.0
		Permafrost	22.5
		Amur	29.0

Tentative values for North America, based on Thornthwaite's computed potential evapotranspiration, were put forward by Thornthwaite and Hare[146] in 1955, as a suggested broad-scale subdivision of the northern forest zone.

Forest sub-zone	Annual PE (cm)	Vegetation
Tundra		tundra
	31	
Forest-tundra		tundra on interfluves – wood in valley
	35	
Woodland		lichen – open woodland, closed in isolated groups
	42	
Forest		closed crown forest occupying most of mesic sites
	52	
Mixed temperate forest		

More recently field studies have been made over lichen-woodland and tundra at Knob Lake in Labrador and at Point Barrow, Alaska, in an attempt to measure evapotranspiration over sample surfaces and to gain control data for northern areas with which to refine the computed quantities. At Knob Lake[104, 110, 172] the measured PE from a burn of scattered spruce, dwarf birch and willow, with ground mosses, lichen and small flowering plants, was smaller than the computed PE by a factor of 2 or 3, each year from 1956 to 1957 (Table XIII). Although the albedo of the bright lichen surface may have been underestimated in the calculations, especially with low solar angles, the difference appears to be principally due to the nature of the lichen. Lichen is a non-vascular plant and does not transpire; much of the water loss from this type of vegetation cover is therefore direct evaporation.

Table XIII. Evapotranspiration over lichen-woodland, Knob Lake.[172]

Year	Computed PE (cm)	LE* (cm)	Measured PE (cm)	Measured PE/LE mm/cm³
1956	18.6	13.6	5.4	0.0325
1957	26.5	20.5	11.5	0.0475
1958	24.3	17.6	8.9	0.0425
1959	26.3	23.2	15.6	0.0575
				mean 0.0450

* Latent evaporation, measured by the atmometer (p.96).

The lichen mat* acts as a mulch; as the surface dries out, a barrier is formed between the air and the cool, saturated layer below so that the subsurface water is unavailable for evaporation. Hare[59] stresses the fact that in subarctic areas, the greater part of the ground cover may be non-vascular. Evidence from Finland shows a greater run-off than would be expected from computed PE values, the difference increasing towards the north.

---

*For a description of this vegetation cover see Fraser, E.M., 1957: The lichen-woodlands of Labrador – Ungava, McGill University, Sub-Arctic Research Laboratory, Research Publication No. 1, Montreal.

A comparison of estimated and measured PE for Knob Lake shows the following discrepancies:

According to Thornthwaite's[146] climatic classification	35-42 cm
According to Budyko[31]	32 cm
Mean daily computed PE (Thornthwaite) 1956-59	24 cm
Measured mean daily PE, 1956-59	10 cm.

At Point Barrow, Alaska,[99,132] the tanks were set up in a patterned ground area (high-centered polygons) of the tundra from 1956 to 1958. The measured PE was found to be lower (by a factor of 2) than the computed values. Profiles of wind, temperature and humidity were also measured in the layer above the ground; the evaporative heat flux, which varied from 110 ly/day in July to 0 in November and May, appeared to use only about 40% of the net radiation. In mid-latitudes the comparative value over grassland varies from 80% with a moist soil to 14% when the soil is dry.[145] The effect of the underlying permafrost on the amount of available water in the soil has yet to be studied. Owing to the very variable local distribution of the small total precipitation at Point Barrow, few conclusions could be drawn about the actual amount of ice and snow melt water withdrawn annually from the soil.

Very little is known of the evapotranspiration of the closed-crown forest of the subarctic owing to the problem of measurement. Thornthwaite and Hare[146] have suggested that, with a slightly lower albedo than the grassland, under moist conditions the forest would consume at least as high a proportion of the net radiation; under drought conditions, the deeper-rooted forests would probably maintain a much higher value than the grassland.

Attempts have been made to relate the various evaporation parameters both internally and to radiation and meteorological factors. The most useful relationship in estimating evapotranspiration may be Robertson's[119,120] ratio of measured PE to the "latent" (potential) evaporation (LE) measured by the black Bellani plate atmometer. This ratio was found to be relatively constant at 0.085 mm/cm^3 in southern Canada; measurements at Knob Lake (Table XIII) suggest that the value for lichen-woodland should be much lower.[110,172]

Sensible heat flux

Vowinckel and Taylor[163] have published values for sensible heat flux over the various sectors of the Arctic Ocean. For the Norwegian-Barents Sea region they used the Bowen ratio R which relates sensible heat flux H to evaporation E:

$$R = \frac{H}{E} = 0.66 \frac{P}{1000} \frac{(T_w - T_a)}{(e_w - e_a)}, \text{ where}$$

$T_{w,a}$ = temperature of water, air,

P = pressure,

$e_{w,a}$ = water vapor pressure at the surface and in the air (mb).

For the Polar Ocean, where evaporation values are so small and unreliable, Shuleikin's (1953) formulae which are independent of evaporation were used:

Where water is warmer than air: $H = 30.24\,(T_w - T_a)$; (under unstable conditions convection is the significant factor)

Where water is colder than air: $H = 0.42\,(T_w - T_a) \cdot V$; (under stable conditions wind is decisive).

In Appendix C monthly mean values of sensible heat flux are given for the various ocean sectors, computed by both methods for comparison.

Over the Polar Ocean (Fig. 22a) the results indicate:

(1) The characteristic curves resemble those for evaporation, with the double maxima in spring and fall over the ice. A 1° stronger winter inversion would change the annual flux from about 3370 to 3190 ly.

(2) The importance of the spring and autumn gradients in the energy transfer. Given surface temperatures consistently 1° higher in April – May, the annual value would change from above 3370 to 5350 ly.

(3) The very high sensible heat flux from the restricted open water areas in the Polar Ocean. The 160 Kly total value for open water in the central Polar Ocean (App. C) is similar to that of long-wave radiation. An increase of 1% open water from October to May would change the heat flux from 3.7 Kly/yr to 5.2. Hence the small areas of open water have a great effect on the energy budget.

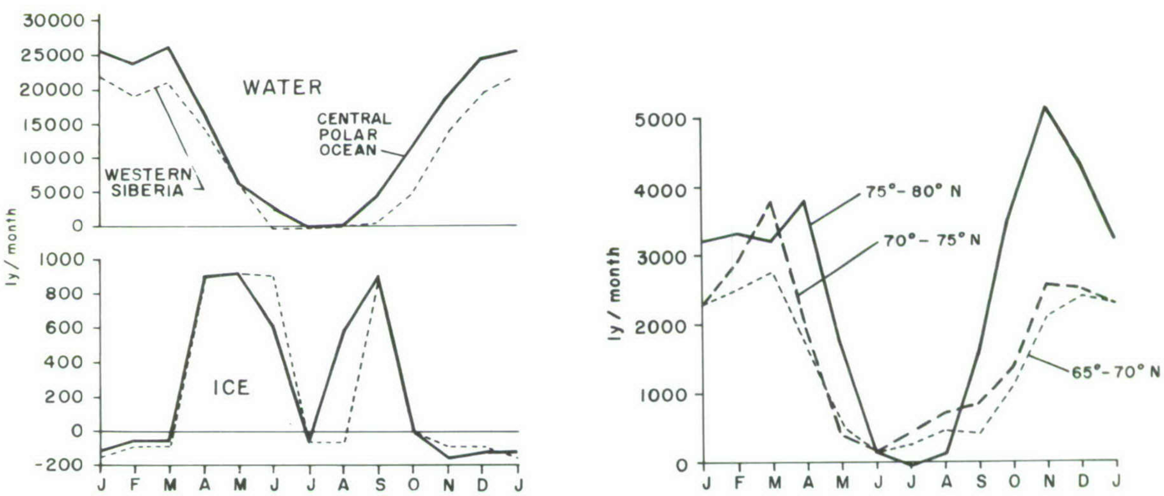

a, Polar ocean. b. Norwegian-Barents Sea.

Figure 22. Sensible heat flux from the surface. Typical curves (Vowinckel and Taylor, 1964[163]).

The curves for the various sectors of the Norwegian-Barents Sea show the sharp decrease in the flux in autumn from north to south, as the air/sea temperature difference becomes less.

Table XIV summarizes the estimated monthly values of the total heat loss (evaporation and sensible heat flux) for the Norwegian-Barents Sea, central Polar Ocean and peripheral Polar Ocean.

Table XIV. Total heat loss by evaporation and sensible heat flux, ly/month (year).[163]

	J	F	M	A	M	J	J	A	S	O	N	D	Year
Norwegian-Barents Sea	5341	5496	6733	4687	2048	178	-129	86	2751	4687	5632	5796	43306
Central Polar Ocean	-217	-56	-62	972	1499	1091	129	1219	1688	93	-150	-63	6143
Peripheral Polar Ocean	-151	-1	8	1229	1578	1809	39	224	1719	2058	214	64	8790

For land areas, few data are available for Arctic and subarctic regions. From the heat balance study made over the polygons at Point Barrow,[98, 99] an annual convective heat flux of 27 ly/day was reported (as against an evaporative heat flux of 19). Bryson[23] found from studying the surface heat budget on clear summer days at Point Barrow that the Bowen ratio could be estimated for a wet surface, such as the tundra, by using surface temperature only. Considering the region from Norman Wells, N.W.T., to Fort Smith, N.W.T., a lake-studded waterlogged forest – tundra region, Bryson and Kuhn[25] found the convective heat transfer at the air-ground interface to be 129 ly/day in July (with the evaporative term 438 ly/day*). In January the corresponding figures for the ice- and snow-covered surface were 192 ly/day and 175 ly/day*. Unfortunately, values are not given for the critical periods of spring and fall.

Variations in the energy budget

Figure 23 summarizes the annual energy budget for the earth-atmosphere system over the central ocean and Norwegian-Barents Sea;[168] monthly and annual values for the various sectors of the central ocean and the Norwegian-Barents Sea are given in reference 168. Regional budgets are not available for other areas in the northern cold regions.

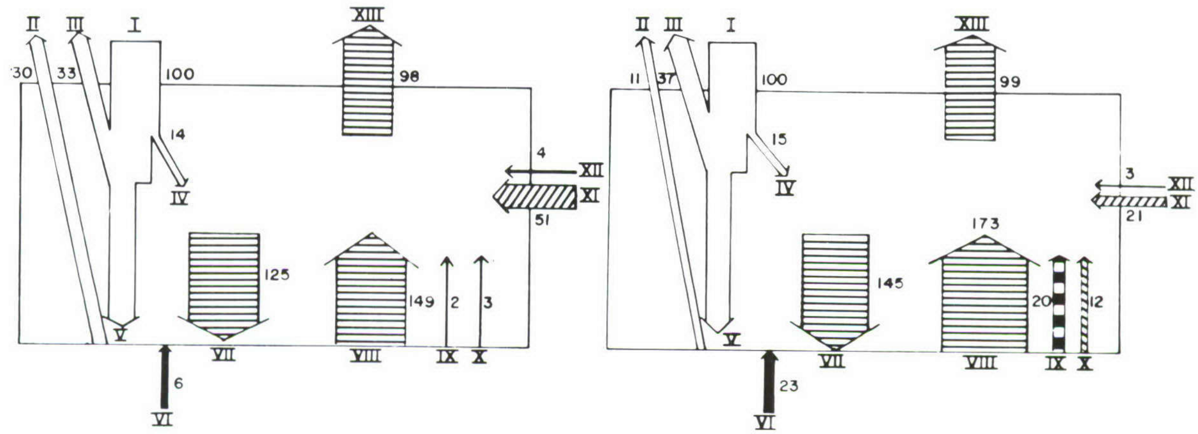

a. Central polar ocean. b. Norwegian-Barents Sea.

Figure 23. Annual energy budget (Vowinckel and Orvig, 1965[168]).

I. Extraterrestrial radiation
II. Reflected solar radiation (from surface)
III. Upward scattered solar radiation
IV. Absorbed solar radiation (in atmosphere)
V. Global radiation
VI. Heat flux below surface
VII. Counterradiation from atmosphere
VIII. Terrestrial radiation
IX. Flux of latent heat
X. Flux of sensible heat
XI. Advection of sensible heat
XII. Advection of latent heat
XIII. Upward flux of atmospheric radiation

Budyko[31] has published climatological estimates of the heat balance for ocean and land surfaces by 10° latitudinal belts (Table XV). In assessing these values he has assumed that, over land areas, the evaporative heat loss (LE) can be determined from the precipitation minus the run-off, that the soil heat-flux becomes zero in the long term mean, and that the turbulent heat exchange (P) is the residual from the net radiation (R). Over the ocean he retains the term A, the redistribution of heat by ocean currents.

*This is in agreement with Vowinckel and Taylor's "continental type" cf. p. 93 .

Table XV. Mean latitudinal values of components of the heat balance in K ly/year, (Budyko[31]).

Latitude	Oceans R	Oceans LE	Oceans P	Oceans A	Land R	Land LE	Land P	Earth R	Earth LE	Earth P	Earth A
70°-60°	23	33	16	-26	20	14	6	21	20	9	- 8
60°-50°	29	39	16	-26	30	19	11	30	28	13	-11
50°-40°	51	53	14	-16	45	24	21	48	38	17	- 7
Earth as a whole	82	74	8	0	49	25	24	72	59	13	0

The study only extends to 70°N, but a comparison of the ocean values for the 70-60° latitudinal band with those of Vowinckel and Taylor (Table XVI) shows agreement with the magnitude of the evaporative and sensible heat terms at 70-65°N over the Norwegian-Barents Sea.

Table XVI. Yearly averages of evaporation (heat) and sensible heat flux in K ly/year for the Arctic Ocean (Vowinckel and Taylor, 1964[163]).

Norwegian-Barents Sea: Latitude	Evap. flux	Heat flux	Polar Ocean: Sector	Evap. flux	Heat flux
80-75°N	12.5	13.3	Central Ocean	2.4	3.7
75-70°N	28.8	21.6	W. Eurasia	4.8	4.3
70-65°N	38.6	16.1	E. Eurasia	3.6	4.1
			Alaska	3.5	3.3
Area average	27.4	16.6	Area average	3.1	3.8

Table XVI also shows the relatively greater importance of the sensible heat flux over the polar regions compared with more southerly latitudes. This is largely due to the coldness of the air and to the presence of open water areas in association with the frozen expanses, which give strong surface-air temperature gradients.

Over the land, Budyko's values are rather more difficult to interpret because the zonal belts contain varying proportions of highly contrasting surface conditions. The 70-60° belt over Eurasia for example includes large expanses of lichen-woodland and forest, whereas over the Western Hemisphere there are extensive areas of tundra and the ice sheet of southern Greenland. Budyko's average value for the evaporation flux as 70% of the net radiation (70-60°N) would seem rather large compared with the findings for tundra at Point Barrow, 71°N (Table XVII) and lichen-woodland at Knob Lake (51°N).

A climatological discussion of the heat balance over the land presupposes detailed knowledge of the nature and distribution of types of surface conditions and the integrated effect of these factors on the radiation and heat fluxes. Here the problem is to find representative spatial mean values for the components of the energy budget for each surface type. Aerial sensing and photography promise new solutions in this field. A project of particular interest has been undertaken by the University of Wisconsin,[23,24] in which the terrain – climate interrelationships are being studied along the forest-tundra transition in the Northwest Territories of Canada.

Table XVII. Average annual heat balance, 1957-58, Point Barrow.[99]

Component	ly/day	Kly/year	Remarks
Convective flux	27	10	Small net transfer from soil to air
Evaporative heat flux	19	7	Small net loss to evaporation
Soil heat flux	0	0	Winter 7 months of loss of energy from soil just balanced by energy received May-August.
Total	46	17	Small net receipt of solar energy fully used for convective and soil heat flux; only about 40% used in evaporative heat flux.
Net radiation	44	16	

In addition to spatial variations in the heat balance terms, there are the important time variations on a scale of less than a month, due to the dominance of various broad-scale atmospheric circulation patterns or weather types. The temperature and water content of the air can vary widely according to these different situations (Fig. 24), and hence the varying frequency of these types from one season to another and from year to year can create considerable fluctuation in the energy budget. For the Norwegian Sea area Gagnon[49] isolated five circulation patterns covering 90% of all days during the month of January, 1959-1962. For the period under each regime he has calculated separate energy budgets. Some of his results are shown in Figures 25-26 and Tables XVIII and XIX.

Figures 25a, b show the energy budget and components for two extreme circulation types, both well-developed meridional situations that tend to be persistent. In the first case (Type 1), there is a ridge over Greenland, a low over Scandinavia and flow is to the south, cold and relatively dry; this type was present on 31.4% of all days. In the second case (Type 5, 16.9% of all days), the ridge is over Scandinavia and warm maritime air flows from the south; cyclones tend to be fast moving, giving an almost uninterrupted flow of warm air over the North Atlantic Drift. These types account for the extremes of the frequency curve of temperature and dew point values for the four months of January studied (Fig. 24). The magnitude of each term in the energy budget and the net deficit along 5°W for each situation is given in Table XVIII. This can be considered a representative trajectory both for the southerly (towards the south) flow of Type 1 and the northerly airstream of Type 5.

A brief discussion of the individual terms of the heat budget and the net values for these two circulation types is given below.

The radiation balance. Since the short-wave radiation can be neglected for January as far south as 65°N, the radiation budget is confined to the long-wave components. The outgoing long-wave term ($L\uparrow$) depends on the highly constant sea surface temperature and the distribution can therefore be considered constant for all types. As most of the energy immediately available to the atmosphere comes from ($L\uparrow$), the incoming long-wave component ($L\downarrow$) also tends to follow the sea surface isotherms, but here the contrasting temperature and moisture properties of the northerly and southerly airstreams influence the magnitude and the strength of the north-south gradient. The radiation balance ($L\uparrow$ - $L\downarrow$) for Type 1 thus shows deficits 2 to 3 times greater than Type 5.

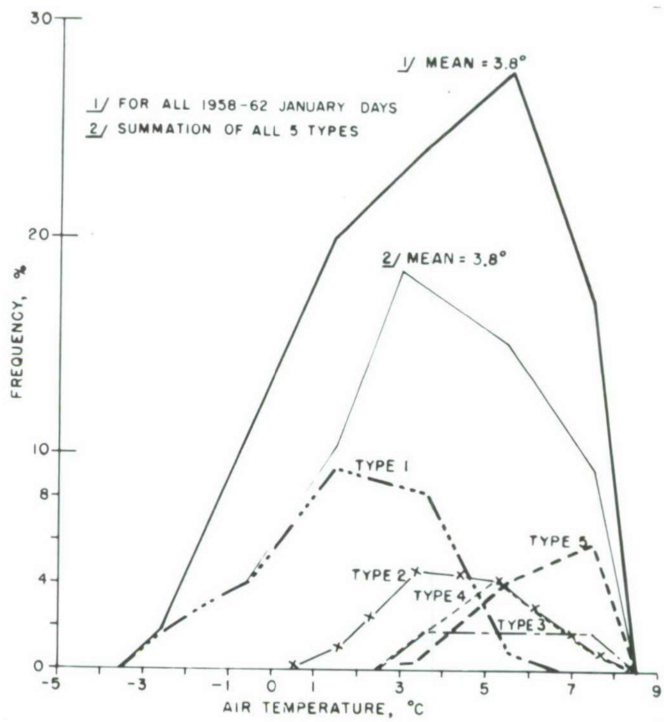

a. Air temperature.

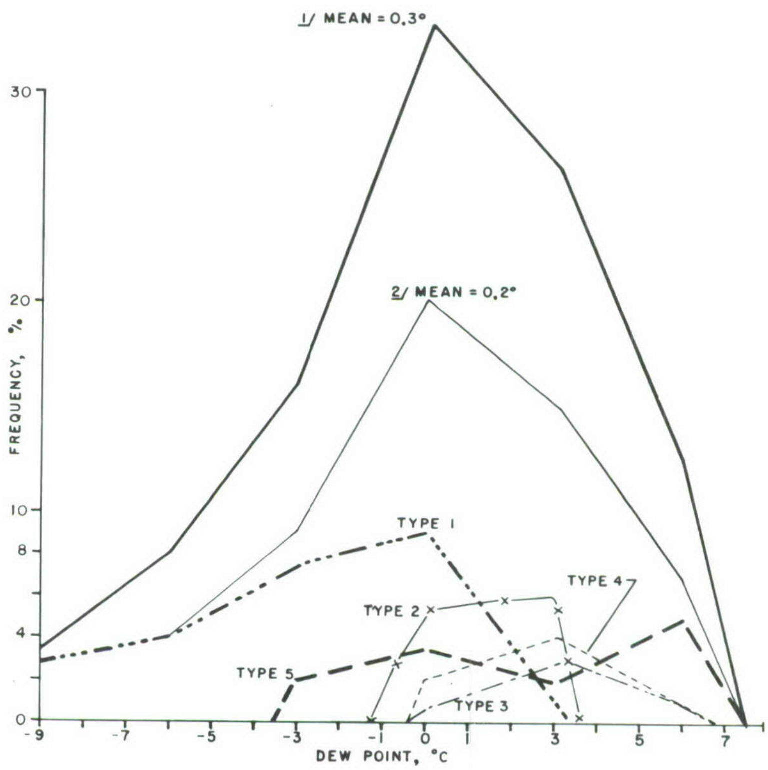

b. Dew point temperature.

Figure 24. Frequency distributions of air temperature and of dew point temperature at Ship M Weather Station according to circulation types (Gagnon, 1964[49]).

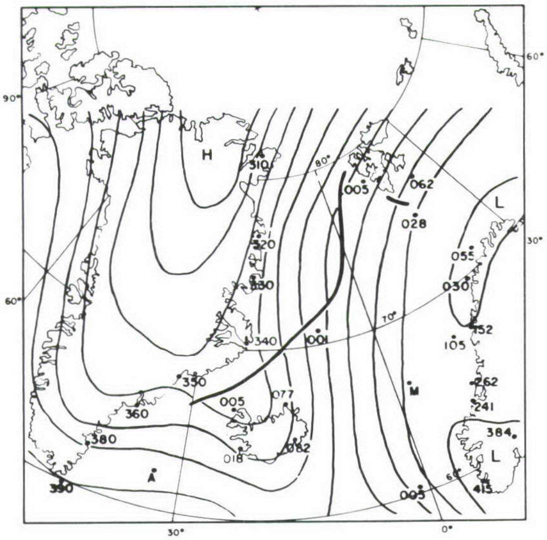

1. circulation

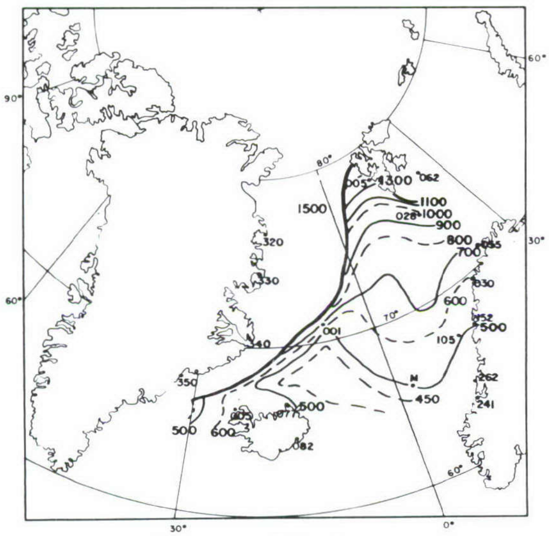

2. sensible heat

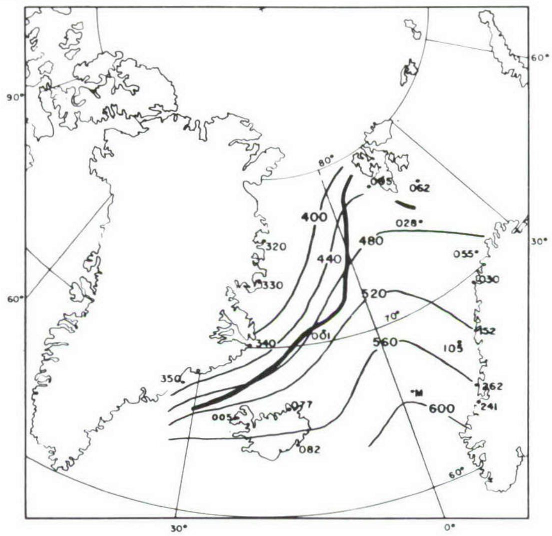

3. long wave incoming radiation

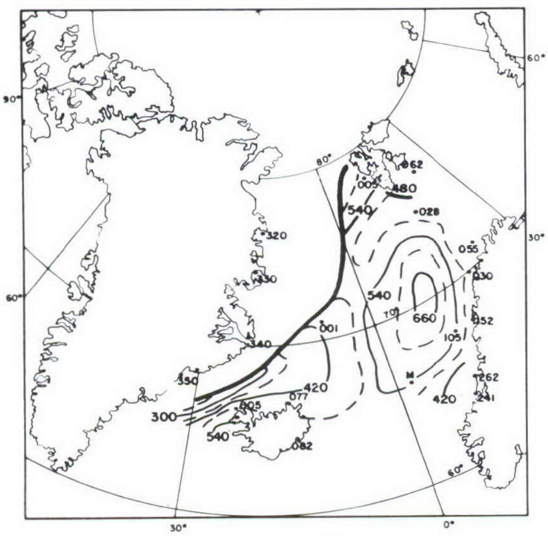

4. evaporation

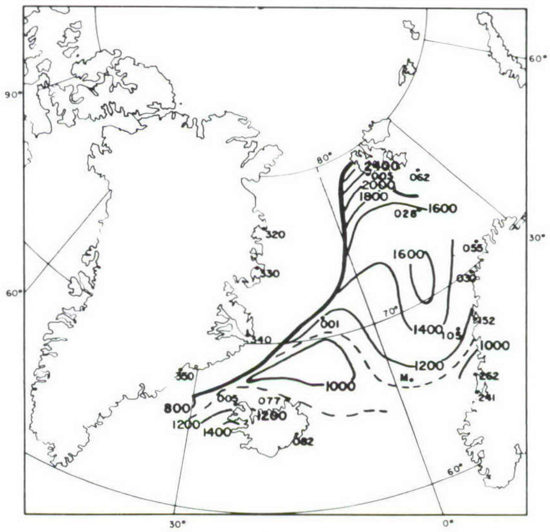

5. net outgoing energy

a. Circulation type 1.

Figure 25. January energy budget over the Norwegian Sea, ly/day (Gagnon, 1964[49]).

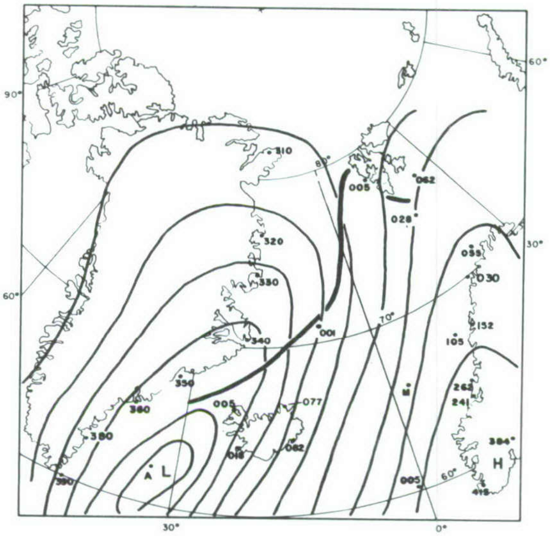

1. circulation

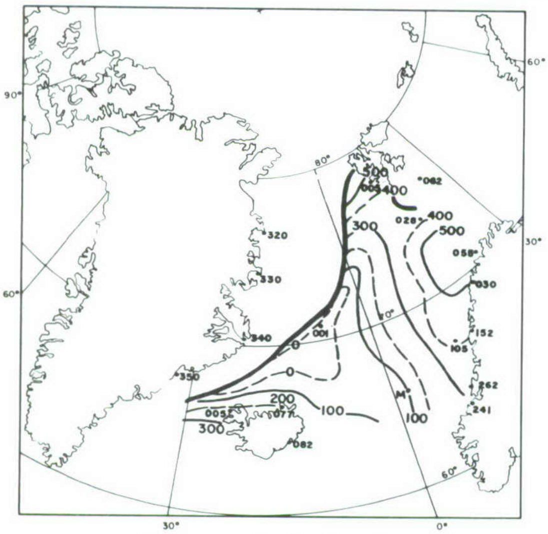

2. sensible heat

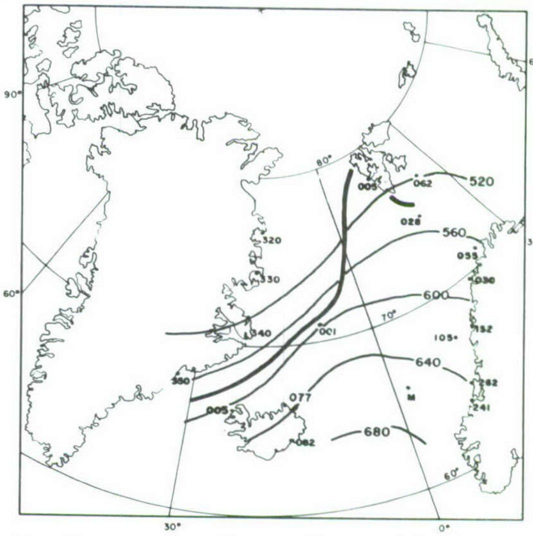

3. long wave incoming radiation

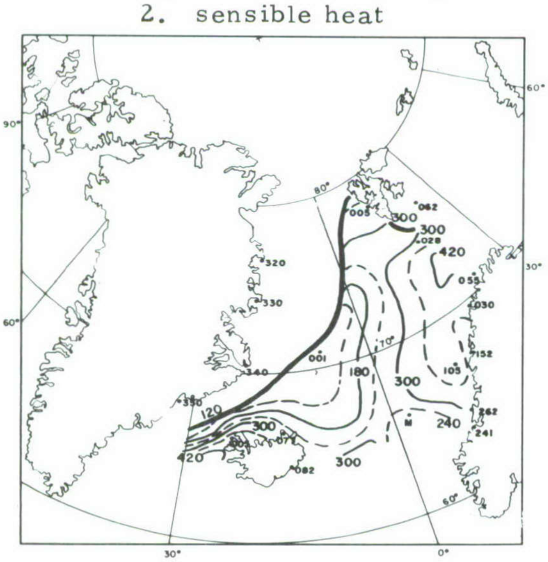

4. evaporation

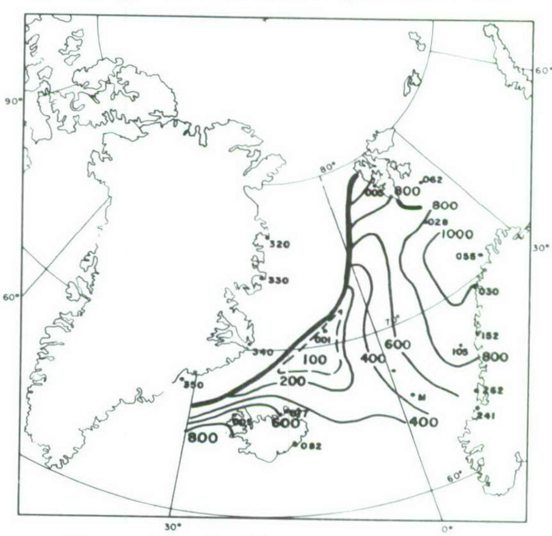

5. net outgoing energy

b. Circulation type 5.

Figure 25. January energy budget over the Norwegian Sea, ly/day (Gagnon, 1964[49]).

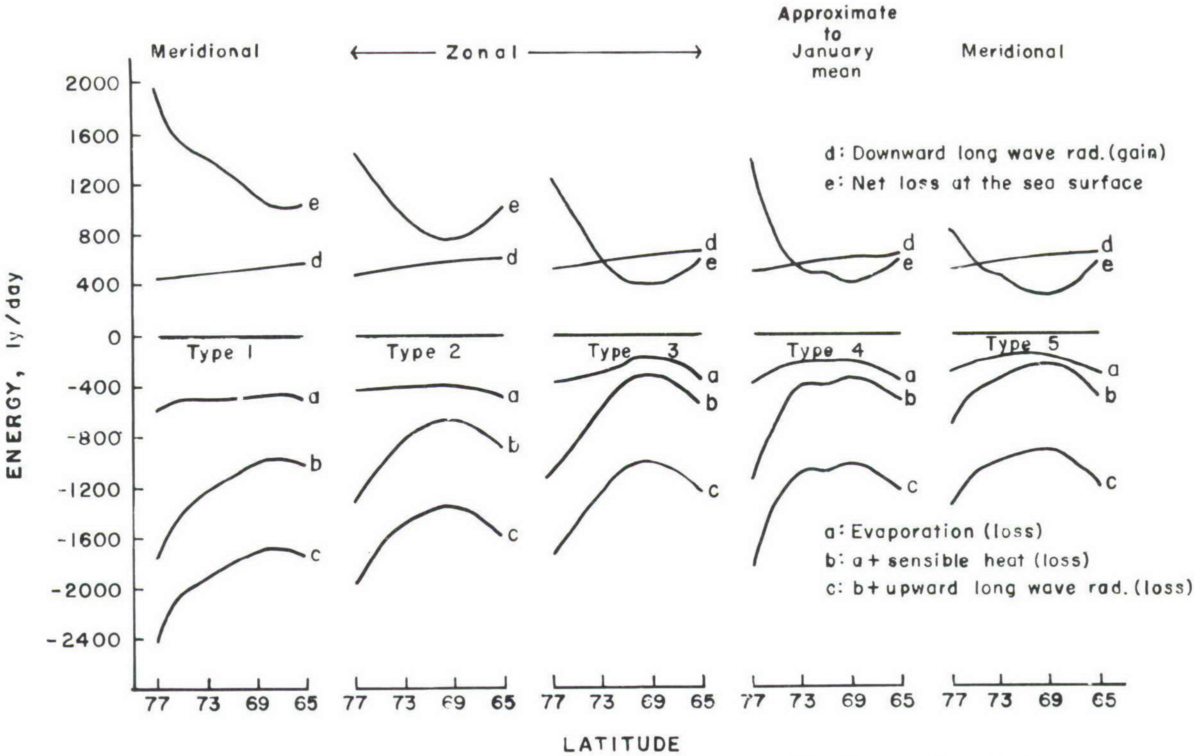

Figure 26. Surface-energy exchange components. Various circulation types (after Gagnon, 1964[49]).

Table XVIII. Energy components and net deficit along 5° W for two circulation types[49] and % of the total outgoing energy ($Q_E + Q_H + L\uparrow$).

Lat °N	Q_E	%	Q_H	%	$L\uparrow$	%	$L\downarrow$	$L\uparrow - L\downarrow$	Net Deficit
Type 1									
72.3	589	27.9	877	41.5	645	30.6	490	155	1621
72.0	426	23.6	730	40.4	650	36.0	498	152	1308
71.0	452	27.1	552	33.0	666	39.8	520	146	1150
69.0	474	28.3	509	30.5	686	41.1	548	138	1121
67.0	476	29.3	447	27.5	699	42.8	564	134	1058
65.0	530	30.9	465	27.1	721	42.1	592	129	1124
Type 5									
72.3	70	9.8	-86	-12.0	645	90.2	572	73	57
72.0	61	8.1	-34	- 4.9	650	92.7	580	70	97
71.0	118	14.7	18	2.2	666	83.0	600	66	204
69.0	158	18.2	23	2.7	686	79.2	632	54	235
67.0	179	20.0	18	2.0	699	78.0	656	43	240
65.0	343	29.2	110	9.4	721	61.4	674	47	500

Non-radiative transfer. The basic pattern of the evaporative heat flux (Q_E) is dictated by the sea surface isotherms, with maximum values over the Gulf Stream and minimum over the eastern branches of the East Greenland current, but between Types 1 and 5 there is a great difference in the magnitude of the flux. The instability set up by the flow from the north of cold, dry air over the warmer ocean surface in Type 1 results in higher evaporation values; in contrast, the warmer moister air from the south tends to become progressively stable to the north, and evaporation is discouraged. At latitude 72.3°N (Table XVIII), the evaporative heat loss is 589 ly/day for Type 1 compared with only 70 for Type 5. (The only synoptic factor that could possibly change the basic pattern is the wind.) However, it is the sensible heat flux that is the prime differentiator between the types. In this case both the pattern and numerical value change. The temperature gradient between the surface and air is the basic factor. In Type 1 this is shown clearly in the sharp rise in values towards the ice margin in the north, where the temperature contrasts are highest. Further south, the air becomes modified by its passage over open water and the gradient decreases. The flux is least over the cold surface of the branch of the East Greenland current. Table XVIII illustrates the remarkable difference in the transfer of sensible heat between the generally unstable conditions of Type 1 and Type 5, where there is warm air advection. Over the East Greenland current, there is actually a loss from the air to the surface.

The energy budget. Since the sea surface temperature plays such a large role in each term, this pattern is imposed on the budget distribution for each type, the distinction lying in the magnitudes involved. The balance is negative for all types.

Although the long-wave outgoing radiation does not change numerically, it becomes the dominant term under northerly flow (Type 5), whereas the non-radiative terms dominate under southerly flow. The table also reemphasizes the fact that under Arctic conditions, the sensible heat flux rather than the evaporative term predominates.

The striking contrast in the net budget values for the two atmospheric regimes is especially marked at the ice-water margin, where at latitude 72.3°N the deficit for Type 1 is about 1620 ly/day as against 60 ly/day for Type 5.

Gagnon's remaining three types are intermediate (Fig. 24). Types 2 and 3 are more zonal in pattern with predominantly westward continental flow; the flow in Type 3 has a stronger southward component. Type 4 is closest to the January mean pattern with moist warm air in the south and cold air from the pack ice in the west and north. Table XIX gives the areal values for the heat budget for each case while Figure 26 summarizes the mean north-south variation.

Table XIX. Mean values of the January net energy budget and the individual terms, for Norwegian Sea area, with their ratio (%) to the total outgoing energy flux.[49] Means are in ly/day. (Gagnon, 1964).

	Type	Q_E	%	Q_H	%	L	%	L	(L-L)	Net
dry cold	1	483	27.8	564	32.5	690	39.7	541	149	1196
air	2	425	29.1	347	23.7	690	47.2	548	102	874
generally	3	247	21.9	190	16.9	690	61.2	631	59	496
warm	4	257	23.1	165	14.8	690	62.1	607	83	505
moist air	5	217	21.2	118	11.5	690	67.3	619	71	406

Although the sea surface conditions in January control the regional pattern of the energy deficit, the circulation types determine the intensity of the pattern.

It is interesting to note that the extreme Types 1 and 5, the most frequent and persistent of the circulation patterns in these four Januaries, correspond to blocking situations over the Greenland-Davis Strait area and Scandinavia respectively.

Rex* found that blocking was most frequent off Scandinavia (Type 5) during the years 1932 to 1950, which would imply a minimum heat loss over the Norwegian Sea, but more recently Namias* and O'Connor have pointed out that one of the most notable changes in the Arctic circulation in the past decade has been the increasing frequency of blocking high pressure areas over Greenland and the Davis Strait (Type 1). Gagnon's study now demonstrates the enormous heat loss involved in any change towards higher frequency of Type 1. So far this approach has not been extended systematically to the other seasons or to the various continental surfaces, which do not have the high heat capacity of water. It is clear that the location of the blocking ridges in the circumpolar vortex with respect to land and open water in the winter is an important factor, not only in regional climate, but also in secular and perhaps longer climatic change. It is largely during the well-developed meridional circulation patterns that the exchanges take place that maintain hemispheric and global heat balance despite the radiation imbalance between the poles and the equator.

SELECTED BIBLIOGRAPHY

1. Air Ministry (1959) Monthly meteorological charts and sea surface currents of the Greenland and Barents Sea, London, H.M.S.O., MO 575.
2. Albrecht, F. (1952) Mikrometeorologische Temperaturemessungen vom Flugzeug aus, Ber. deut. Wetterd, U. S. Zone, 38, p. 332-339.
3. Ahlmann, H.W. (1948) Glaciological research on the North Atlantic coasts, Royal Geographical Society (London), Research series, no. 1.
4. Allen, C.W. (1958) Solar radiation, Quarterly Journal of Royal Meteorological Society, vol. 84, p. 307.
5. American Meteorological Society (1957) Meteorological abstracts and bibliography, vol. 8, no. 7.
6. Andreeva, N.N. and Piatnenkov, B.A. (1959) Certain characteristics of the radiation balance in the central Arctic, Problemy Arktiki, no. 7, p. 79-87. Trans. C.E. Townsend 1960, T-R 321+, Geophysics Research Directorate, Bedford, Mass. and the American Meteorological Society (containing the results of actinometric observation of the drifting stations North Pole II-VII, 1950-58).
7. Andrews, R.H. (1964) Meteorology and heat balance of the ablation area, White Glacier, Canadian Arctic Archipelago - summer 1960, Axel Heiberg Island research reports, Meteorology, no. 1, McGill University, Montreal (with bibliography).
8. Angstrom, A. (1925) Albedo of various ground surfaces, Geografiska Annaler, vol. 7, p. 323-342.
9. Badgley, F.I. (1961) Heat balance at the surface of the Arctic Ocean, Proceedings of the Western Snow Conference, p. 101-104.
10. Banks, H.C., and Partanen, E.N. (1959) Meteorological observations, scientific studies at Fletcher's Ice Island, T-3, 1952-1955, U. S. Air Force, Geophysical Research Paper, no. 63, vol. 2, p. 1-6, and appendix Ib, p. 49-73.
11. Barrett, E. and Brodin, G. (1955) The acidity of Scandinavian precipitation, Tellus, vol. 7, p. 251-257.

* Second section: references 28, 29, 19, and 21.

SELECTED BIBLIOGRAPHY (Cont'd)

12. Bauer, K.G. and Dutton, J.A. (1960) Flight investigations of surface albedo, Technical Report No. 2, Department of Meteorology, University of Wisconsin.

13. ______________ (1962) Albedo variations measured from an airplane over several types of surface, Journal of Geophysical Research, vol. 67, p. 2367-2376.

14. Berliand, T.G. and Efimova, N.A. (1955) Monthly charts of global radiation balance in the U.S.S.R., Trudy Glav-Geof. obs. Leningrad, 50, p. 48-82. (See also, Morskoi atlas, vol. 2, 1963, U.S.S.R. and Agricultural atlas of the U.S.S.R., Moscow, 1960.)

15. Bernhardt, F. and Philipps, H. (1958) Die raumliche und zeitliche Verteiling der Einstrahlung, der Ausstrahling und der Strahlungsbilanz im Meeresniveau, Teil I: Die Einstrahlung, Abh. Met. und Hydr., Dienst. Deut. Dem. Rep. No. 45, Akademie Verlag, Berlin, 227 p.

16. Bolsenga, S.J. (1964) Daily sums of global radiation for cloudless skies, U. S. Army Cold Regions Research and Engineering Laboratory, Research Report 160.

17. Bowen, I.S. (1926) The ratio of heat losses by conduction and by evaporation from any water surface, Physical Review, vol. 27, p. 779-787.

18. Boyes, G.A. (1963) Meridional advection of moisture in the Arctic, Publication in Meteorology, No. 57, McGill University, Montreal.

19. Briazgin, N.N. (1959) The problem of the albedo on the surface of drifting ice, Problemy Arktiki i Antarktiki, No. 1, p. 33-39; trans. R.M. Holden, 1960, T-R-310+, Geophysics Research Directorate, Bedford, Mass. and the American Meteorological Society.

20. Brooks, F.A. (1952) Atmospheric radiation and its reflection from the ground, Journal of Meteorology, vol. 9, p. 41-52.

21. Brown, J. and Johnson, P.L. (1965) Pedo-ecological investigations, Barrow, Alaska, USA CRREL, Technical Report 159.

22. Brown, R.J.E. (1965) Some observations on the influence of climatic and terrain features on permafrost at Norman Wells, N.W.T., Canada, Canadian Journal of Earth Sciences, vol. 2, no. 1, p. 15-31.

23. Bryson, R.A. (1956) Preliminary estimates of the surface heat budget, summer, clear days, at Point Barrow, Alaska, mimeographed report, Department of Meteorology, University of Wisconsin, Madison.

24. __________ (1961) A reconnaissance study of certain aspects of heat cycles in lakes, semi-annual report (contract Nonr. 1202/07), Department of Meteorology, University of Wisconsin, Madison (see also annual summary report, 1959).

25. __________ and Kuhn, P.M. (1962) Some regional heat budget values for Northern Canada, Geographical Bulletin No. 17, Department of Mines and Technical Surveys, Ottawa, p. 57-65.

26. Budyko, M. (1948) Evaporation in natural conditions, Gidrometeorizdat, Leningrad.

27. __________ (1955) Atlas of heat balance, Hydromet. Service, U.S.S.R., Leningrad. Trans. of text by Moira Dunbar, 1960. Publication in Meteorology, no. 19, McGill University, Montreal. (New atlas based on IGY data published in 1963: Atlas teplovogo balansa zemnogo shara, Moscow.)

SELECTED BIBLIOGRAPHY (Cont'd)

29. Budyko, M.I. (1956) Heat balance of the earth's surface, Leningrad. Trans. 1958 by N. A. Stepanova, U. S. Weather Bureau, Washington, D.C.

30. __________ (1961) The heat balance of the earth's surface, Soviet Geography, April 1961, p. 3-14.

31. __________ et al. (1962) The heat balance of the surface of the earth, Soviet Geography, May 1962, p. 3-15.

32. Combs, A.C. (1961) Techniques and results of infrared surface temperature measurements in New Jersey and Greenland, U.S.A. Signal Research and Development Laboratory, Technical Report 2193, DA Task 3A99-07-001-01, Fort Monmouth, N. J.

33. Cook, F.A. (1955) Near surface soil temperature measurements at Resolute Bay, Northwest Territories, Arctic, vol. 8, no. 4, p. 237-249.

34. Davies, J.A. (1962) Albedo measurements over sub-Arctic surfaces, McGill Sub-Arctic Research Papers, No. 13, Publication in Meteorology, No. 52, McGill University.

35. Department of Northern Affairs and National Resources, Water Resources Branch (1961) Evaporation, Proceedings of Hydrology Symposium No. 2, Toronto, March 1 and 2. Ottawa: Queen's Printer.

36. Diamond, M. (1953) Evaporation or melt of a snow cover, U. S. Army Snow Ice and Permafrost Research Establishment, Research Report No. 6.

37. __________ and Gerdel, R.W. (1956) Radiation measurements on the Greenland Ice Cap, U. S. Army SIPRE, Research Report 19. Also published in 1958 as IUGG, International Association of Scientific Hydrology, Publication no. 46, p. 404-423.

38. __________ (1960) Air temperature and precipitation on the Greenland ice sheet, Journal of Glaciology, vol. 3, no. 27, p. 558-567.

39. Dickson, R.R. (1964) Synoptic characterization of the thermal nature of the earth's surface, Monthly Weather Review, vol. 22, p. 195-201.

40. Dutton, J.A. (1962) Space and time response of airborne radiation sensors for the measurement of ground variables, Journal of Geophysical Research, vol. 67, p. 193-205.

41. Elsasser, W.M. and Culbertson, M.F. (1960) Atmospheric radiation tables, Meteorological Monographs, vol. 4, no. 23, 43 p.

42. Fonselius, S.; Koroleff, F. and Buch, K. (1955) Microdetermination of CO_2 in the air, with current data for Scandinavia, Tellus, vol. 7, p. 258-265 (CO_2 values for Scandinavia are published periodically in Tellus).

43. Franssila, M. (1962) On the temperature conditions in a large Aapa bog area in Finnish Lapland, Finnish Meteorological Office, Contribution No. 52, Helsinki.

44. Fritz, S. (1948) The albedo of the ground and atmosphere, Bulletin of the American Meteorological Society, vol. 29, p. 303-312.

45. ________ (1951) "Solar radiant energy and its modification by the earth and its atmosphere," in Compendium of meteorology, p. 13-33.

46. ________ (1958) Solar radiation measurements in the Arctic Ocean, Polar Atmosphere Symposium, Part I, Pergamon Press.

SELECTED BIBLIOGRAPHY (Cont'd)

47. Fritz, S. (1959) Solar radiation measurements in the Arctic Ocean, Scientific Studies at Fletcher's Ice Island, T-3, 1952-1955, U. S. Air Force, Geophysical Research Paper, no. 63, vol. 2, p. 6-10 and appendix II, p. 74-80.

48. Gaevskii, V.D. (1959) Certain features of the radiation regime of the central Arctic, Leningrad, G.R.D. translation, R.M. Holden, 1960, T-R-303+.

49. Gagnon, R.M. (1964) Types of winter energy budgets over the Norwegian Sea, Publication in Meteorology, No. 64, McGill University, Montreal.

50. Gavrilova, M.K. (1959) Total radiation in the Soviet and foreign Arctic, Trudy Arkt. Inst., vol. 217, p. 139-156.

51. Geiger, R. (1961) Das Klima der bodennahen Luftschicht (The climate near the ground), Braunschweig Friedr. Vickwej und Sohn. (English edition, 1965, Harvard University Press.)

52. Gerdel, R.W.; Diamond, M. and Walsh, K. J. (1954) Nomographs for computation of radiation heat supply, U. S. Army SIPRE, Research Paper 8.

53. Gerdel, R.W. (1961) A climatological study of the Greenland ice sheet, Folia Geographica Danica, vol. 9, p. 84-106.

54. Griffiths, T.M. (1960) Glaciological investigations in the Tuto area of Greenland, U. S. Army SIPRE, Technical Report 47.

55. Hamilton, H.I. (1962) Spatially continuous measurements of temperature profiles through an air-water interface, University of Wisconsin, Department of Meteorology, Annual Report, Contract DA-039-SC-80282, p. 47-68.

56. Hanson, K.J. (1961) The albedo of sea-ice and ice islands in the Arctic Ocean Basin, Arctic, vol. 14, p. 188-196.

57. Hare, F.K. (1954) The boreal conifer zone, Geographical Studies, vol. 1, no. 1, p. 4-18.

58. ________ (1959) Evaporation in fact and controversy, mimeographed paper, McGill University.

59. ________ (1960) The evapotranspiration problem, mimeographed paper, McGill University.

60. Havens, J.M. (1964) Meteorology and heat balance of the accumulation area, McGill ice cap, Canadian Arctic Archipelago - summer 1960, Axel Heiberg Island research reports, Meteorology, no. 2, McGill University (with bibliography).

61. Hoinkes, H. (1955) Measurements of ablation and heat balance on alpine glaciers, Journal of Glaciology, vol. 2, no. 17.

62. Houghton, D.M. (1958) Heat sources and sinks at the earth's surface, Meteorological Magazine, vol. 87, p. 132-143.

63. Houghton, H.G. (1954) On the annual heat balance of the Northern Hemisphere, Journal of Meteorology, vol. 11, p. 3-9.

64. Houghton, J.T. (1958) The emissivity of the earth's surface, Quarterly Journal of the Royal Meteorological Society, vol. 84, p. 448-450.

65. Hubley, R.C. (1955) Measurements of diurnal variations in snow albedo on Lemon Creek Glacier, Alaska, Journal of Glaciology, no. 2, p. 560-563.

66. ________ (1957) An analysis of surface energy during the ablation season on Lemon Creek Glacier, Alaska, Transactions, American Geophysical Union, vol. 38, no. 1.

SELECTED BIBLIOGRAPHY (Cont'd)

67. Jackson, C.I. (1959) Insolation and albedo, Publication in Meteorology, no. 13, McGill University.

68. ______ (1960) Estimates of total radiation and albedo in sub-arctic Canada, Archiv fur Meteorologie, Geophysik und Bioklimatologie, Series B, vol. 10, no. 2, p. 193-199.

69. Johnson, J.C. (1954) Physical meteorology, New York: John Wiley and Sons.

70. Kasten, F. (1962) Table of solar altitudes for geographical latitudes ±77° 10', USA CRREL, Special Report 57.

71. ______ (1966) Albedo and sky radiance measurements in Greenland, USA CRREL, Research Report 180.

72. Kelley, J.J.Jr. (1964) An analysis of carbon dioxide in the atmosphere at Point Barrow, Alaska, 1961, 1962, 1963, University of Washington, Department of Atmospheric Sciences.

73. ______ (1964) Radiative energy exchange over Arctic land and sea, Part I, data 1962, University of Washington, Department of Atmospheric Sciences.

74. Klein, W.H. (1948) Calculation of solar radiation and the solar heat load on man, Journal of Meteorology, vol. 5, p. 119-129.

75. Kondrat'ev, K. (1954) The radiant energy of the sun, Gidromet, Leningrad, Chap. IX; "Albedo of the underlying surface and clouds." English summary by A. Kurlents and P. Larsson, McGill University, for Geophysics Research Directorate, Bedford, Mass.

76. ______ (1965) Radiative heat exchange in the atmosphere, Pergamon Press.

77. Kramer, P.J. (1950) Plant and soil water relationships, New York: McGraw Hill, 374 p.

78. Kung, E.C.; Bryson, R. and Lenschow, D.H. (1964) Study of a continental surface albedo on the basis of flight measurements and structure of the earth's surface cover over North America, Monthly Weather Review, vol. 22, p. 543-564 (with bibliography).

79. LaChapelle, E. (1959) Annual means and energy exchange on the Blue Glacier, Journal of Geophysical Research, vol. 64, no. 4, p. 443-449.

80. Landsberg, H.E. (1943) Physical climatology, Pennsylvania State University.

81. ______ (1961) Solar radiation at the earth's surface, Solar Energy, vol. 5, no. 3.

82. Larsson, P. (1960) A preliminary investigation of the meteorological conditions on the Chamberlin Glacier, 1958, Arctic Institute of North America, Research Paper, no. 2, 89 p.

83. ______ and Orvig, S. (1961) Atlas of mean monthly albedo of Arctic surfaces, Publication in Meteorology, no. 45, McGill University.

84. ______ (1962) Albedo of Arctic surfaces, Publication in Meteorology, no. 54, McGill University.

85. Larsson, P. (1963) The distribution of albedo over Arctic surfaces, Geographical Review, vol. 53, p. 572-579.

SELECTED BIBLIOGRAPHY (Cont'd)

86. Lemon, E.R.; Glasser, A.H. and Satterwhite, L.E. (1957) Some aspects of the relationship of soil, plant and meteorological factors to evapotranspiration, Soil Science Society of America Proceedings, vol. 21, no. 5, p. 464-468.

87. Lenschow, D.H. (1962) Technique and results of surface-temperature determination with the aid of an airborne bolometer, University of Wisconsin, Department of Meteorology, Annual Report, Contract DA-36-039-SC-80282, p. 81-98.

88. ______________ and Dutton, J.A. (1964) Surface temperature variations measured from an airplane over several surface types, Journal of Applied Meteorology, vol. 3, p. 65-69.

89. Lettau, H. (1957) "Computation of heat budget constituents of the earth/air interface" in Exploring the atmosphere's first mile, VI, London, p. 305-327.

90. Lister, H. and Taylor, P.F. (1961) Heat balance and ablation on an Arctic glacier, Meddelelser om Grønland, bd. 158, no. 7.

91. London, J. (1957) A study of the atmospheric heat balance, Final report for G.R.D., Project No. 131, Contract No. AF 19 (221)-165, Department of Meteorology and Oceanography, New York University, (with bibliography).

92. Lorenz, D. (1962) Messungen der bodenoberflachentemperatur vom hubschrauber aus, Ber. Deut. Wetterd. 11, no. 82, 25 p.

93. L'vovich, M.I. (1962) The water balance and its zonal characteristics, Izvestiya Akademii Nauk S.S.S.R., Seriya geograficheskaya, no. 5, p. 3-13, Trans. in Soviet Geography, p. 37-50.

94. Marshunova, M.S. (1959) Calculation of the longwave radiation balance during an overcast sky in the Arctic, Leningrad. American Meteorological Society, translation by R. M. Holden for G.R.D., TR-304.

95. Mateer, C.L. (1955) A preliminary estimate of the average insolation in Canada, Canadian Journal of Agricultural Science, vol. 35, p. 579-594.

96. ____________ (1955) Average insolation in Canada during cloudless days, Canadian Journal of Technology, vol. 33, p. 13-22.

97. Mather, J.R. (1955) Investigation of Thornthwaite's evapotranspiration formula and procedure, Publications in Meteorology, vol. VII, no. 1, The Johns Hopkins University, Centerton, N.J.

98. ____________ and Thornthwaite, C.W. (1956) Microclimatic investigations at Point Barrow, Alaska, Drexel Institute of Technology, Publications in Climatology, Vol. IX, no. 1, 51 p.

99. ______________________________ (1958) Microclimatic investigations at Point Barrow, Alaska, 1957-58, Drexel Institute of Technology, Publications in Climatology, Vol. XI, no. 2.

100. McKee, H.G. (1961) Atmospheric ozone in north Greenland, Southwest Research Institute, San Antonio, Texas.

101. Mellor, M. (1964) Snow and ice on the earth's surface, U. S. Army CRREL, Cold Regions Science and Engineering, II-C1.

102. Mosby, H. (1932) "Sunshine and radiation" in The Norwegian North Polar Expedition with the "Maud," 1918-1925, Scientific Results, vol. 1, no. 7, Bergen, Geofysisk Institutt.

SELECTED BIBLIOGRAPHY (Cont'd)

103. Mosby, H. (1962) Water, salt and heat balance of the north Polar Sea and of the Norwegian Sea, Geof. Publ., vol. 24, p. 289-313.

104. Nebiker, W.A. (1957) Evapotranspiration studies at Knob Lake, June - September, 1956, Publication in Meteorology, no. 11, McGill University.

105. ______________ and Orvig, S. (1958) Evaporation and transpiration from an open lichen woodland surface, Comptes Rendus et Rapports, UGGI, Assemblée Générale 1957, III, p. 379-384.

106. Nobles, L.H. (1960) Glaciological investigations on the Nunatarssuaq ice ramp, N.W. Greenland, U. S. Army SIPRE, Technical Report 66.

107. Orvig, S. (1951) The climate of the ablation period on the Barnes ice cap in 1950, Geografiska Annaler, vol. 33, no. 3-4, p. 166-209.

108. ________ (1954) Glacial-meteorological observations on ice caps in Baffin Island, Geografiska Annaler, vol. 36, pt. 3, 4, p. 193-318.

109. ________ ed. (1961) McCall Glacier, Alaska: meteorological observations, 1957-1958, Arctic Institute of North America, Research Paper, No. 8 (and data).

110. ________ (1961) Net radiation flux over sub-arctic surfaces, Journal of Meteorology, vol. 18, p. 199-203.

111. Penman, H.L. (1948) Natural evaporation from open water, bare soil and grass, Royal Society, London, Proceedings, Series A, 193, p. 120-145.

112. _____________ (1956) Evaporation: an introductory survey, Netherlands Journal of Agricultural Science, vol. 4, no. 1, p. 9-29.

113. _____________ (1963) Vegetation and hydrology, Harpenden, London.

114. Petterssen, S.; Jacobs, W.C. and Haynes, B.C. (1956) Meteorology of the Arctic, Naval operations for polar projects (OP-O3A3).

115. Piatnienkov, B.A. (1959) Influence of albedo on the influx of radiation in the Arctic, Arkt. Inst. Trudy, vol. 217.

116. Powell, J.M. (1961) The vegetation and micro-climate of the Lake Hazen area, northern Ellesmere Island, N.W.T., Publication in Meteorology no. 38, McGill University, Defence Research Board, Ottawa, Report D. Phys. R. (G) Hazen 14.

117. Rap, P.K. and Winston, J.S. (1963) An investigation of some synoptic capabilities of atmospheric "window" measurements from satellite Tiros II, Journal of Applied Meteorology, vol. 2, p. 12-23.

118. Reed, R.J. (1962) Arctic forecast guide, U. S. Navy Weather Research Facility, Norfolk, Virginia, NWRF 16-0462-058.

119. Robertson, G.W. (1954) Latent evaporation: its concept, measurement and application, Original paper presented January 29 at the regular weekly seminar of the Field Husbandry, Soils and Agricultural Engineering Division, Ottawa.

120. _______________ (1955) The standardization of the measurement of evaporation as a climatic factor, W.M.D. Technical Note 11, no. 42, TP 16.

121. Robinson, E. (1955) Some instances of unstable surface temperature conditions during the Arctic winter, Arctic, vol. 8, p. 148-157.

122. Romanov, V.V. (1956) A hydrodynamic method for calculating the water balance of swamps, Pochvovedenie, Moscow, 8, p. 49-56.

SELECTED BIBLIOGRAPHY (Cont'd)

123. Rossby, C.G. and Egner, H. (1955) On the chemical climate and its variation with the atmospheric circulation pattern, Tellus, vol. 7, p. 118-134.

124. Sagar, R.B. (1960) Glacial-meteorological observations in northern Ellesmere Island during phase III, "Operation Hazen," May - August 1958, Publication in Meteorology No. 29, McGill University.

125. Sanderson, M. (1950) Measuring potential evapotranspiration at Norman Wells, 1949, Geographical Review, vol. 40, no. 4. p. 636-645.

126. Sauberer, F. and Dirmhirn, I. (1951) The influence of the radiation factor on the growing and shrinking of glaciers, U. S. Army SIPRE, Translation no. 51-1.

127. Schytt, V. (1955) Glaciological investigations in the Thule ramp area, U. S. Army SIPRE, Technical Report 28.

128. Scott, R.F. (1957) Estimation of the heat transfer coefficient between air and the ground surface, Transactions of the American Geophysical Union, vol. 38, p. 25-32.

129. __________ (1959) Study and report of micrometeorological data obtained in 1957-1958 at Tuto, Greenland, Report to Arctic Construction and Frost Effects Laboratory, U. S. Army Engineer Division, New England.

130. __________ (1964) Heat exchange at the ground surface, U. S. Army CRREL, Cold Regions Science and Engineering II-A1.

131. Shaw, R.H. (1956) A comparison of solar radiation and net radiation, Bulletin of the American Meteorological Society, vol. 37, p. 205-207.

132. Shellabear, W.H. (1959) Evapotranspiration at Point Barrow, Alaska during summer 1956, M.Sc. thesis, McGill University.

133. Shuleikin, V.V. (1953) Molecular physics of the sea, Trans. U. S. Navy Hydrographic Office, 1957.

134. Suomi, V.E. and Kuhn, P.M. (1958) An economical net radiometer, Tellus, vol. 10, p. 160-163.

135. Sutton, O.G. (1953) Micrometeorology, New York: McGraw Hill.

136. Sverdrup, H.U. (1933) The Norwegian North Polar expedition with the "Maud," 1918-1925, Bergen, Geofysisk Institutt.

137. __________ (1935) Ablation of Isachsen's Plateau and on the Fourteenth of July Glacier in relation to radiation and meteorological conditions, Geografiska Annaler, vol. 17.

138. __________ (1951) Evaporation from the oceans, Compendium of Meteorology, Americal Meteorological Society, p. 1071-1081.

139. __________; Johnson, M.W. and Fleming, R.H. (1954) The oceans, New York: Prentice-Hall, 1087 p.

140. Swinbank, W.C. (1951) The measurement of vertical transfer of heat and water vapor by eddies in the lower atmosphere, Journal of Meteorology, vol. 8, p. 135-145.

141. Thornthwaite, C.W. (1948) An approach toward a rational classification of climate, Geographical Review, vol. 38, p. 55-94.

SELECTED BIBLIOGRAPHY (Cont'd)

142. Thornthwaite, C.W. (1954) Estimating soil tractionability from climatic data, Publication in Meteorology, VII, no. 3, The Johns Hopkins University, p. 369-447.

143. ________________ and Halstead, M.H. eds. (1954) Final report, micrometeorology of the surface layer of the atmosphere, the flux of momentum, heat and water vapor, Publications in Climatology, vol. 7, no. 2, Johns Hopkins University, Laboratory of Climatology.

144. ________________ and Mather, J.R. (1954) The computation of soil moisture, Publications in Meteorology, VII, no. 3, The Johns Hopkins University, p. 397-402.

145. ________________ et al. (1954) Micrometeorology of the surface layer of the atmosphere, the flux of momentum, heat and water vapor, Publications in Climatology, VII, no. 2, The Johns Hopkins University.

146. ________________ and Hare, F.K. (1955) Climatic classification in forestry, UNASYLVA, vol. 9, p. 49-59.

147. ________________ and Mather, J.R. (1955) The water balance, Drexel Institute of Technology, Publication in Climatology, vol. VIII, no. 1.

148. ____________________________ (1957) Instructions and tables for computing potential evapotranspiration and the water balance, Drexel Institute of Technology, Publication in Climatology, vol. X, no. 3.

149. Untersteiner, N. (1961) On the mass and heat budget of the Arctic sea ice, Archiv Met. Geophys. Bioklimat, Serie A, p. 151-182.

150. U. S. Government Printing Office (1955) Water, The Yearbook of Agriculture.

151. U. S. Hydrographic Service (1957-58) Oceanographic atlas of the Polar Seas, Washington, D.C.

152. Van der Bijl, W. (1956-57) The evapotranspiration problem, Contract No. CWB-88-6, Kansas State College.

153. Veihmeyer, F.J. and Hendrickson, A.H. (1955) Does transpiration decrease as soil moisture decreases?, Transactions of the American Geophysical Union, vol. 36, p. 425-448.

154. Vowinckel, E. and Orvig, S. (1961) Water balance and heat flux of the Arctic Ocean, Publication in Meteorology, no. 44, McGill University (containing extensive bibliography).

155. ______________________ (1961) Water balance and heat flow of the Arctic Ocean, Arctic, vol. 15, p. 205-223.

156. ______________________ (1962) Relation between solar radiation income and cloud type in the Arctic, Publication in Meteorology, no. 48, McGill University.

157. Vowinckel, E. (1962) Cloud amount and type over the Arctic, Publication in Meteorology, no. 51, McGill University.

158. ____________ and Orvig, S. (1962) Insolation and absorbed solar radiation at the ground in the Arctic, Publication in Meteorology, no. 53, McGill University.

159. ______________________ (1962) Relation between solar radiation income and cloud type in the Arctic, Journal of Applied Meteorology, vol. 1, p. 552-559.

SELECTED BIBLIOGRAPHY (Cont'd)

160. Vowinckel, E. (1963) Ice transport between Greenland and Spitzbergen, and its causes, Publication in Meteorology, no. 59, McGill University.

161. ____________ and Orvig, S. (1963) Long-wave radiation and total radiation balance at the surface of the Arctic, Publication in Meteorology, no. 62, McGill University.

162. ________________________ (1964) Radiation balance of the troposphere and of the earth-atmosphere system in the Arctic, Publication in Meteorology, no. 63, McGill University.

163. Vowinckel, E. and Taylor, B. (1964) Evaporation and sensible heat flux over the Arctic Ocean, Publication in Meteorology, no. 66, McGill University.

164. ____________ (1964) The greenhouse effect of the Arctic atmosphere, Publication in Meteorology, no. 67, McGill University.

165. ____________ (1964) Heat flux through the Polar Ocean ice, Publication in Meteorology, no. 70, McGill University.

166. ____________ (1964) Atmospheric energy advection in the Arctic, Publication in Meteorology, no. 71, McGill University.

167. ____________ (1965) The inversion over the Polar Basin, Publication in Meteorology, no. 72, McGill University.

168. ____________ and Orvig, S. (1965) The heat budget over the Arctic Ocean, Publication in Meteorology, no. 74, McGill University.

169. ________________________ (1964) Energy balance of the Arctic, Archiv fur Meteor. Geophys. und Biokl., Serie B, vol. 13, no. 3, p. 352-377. Further articles on the heat balance study are due to appear in vol. 13, no. 4 and vol. 14, no. 1 and 2.

170. Wallen, C.G. (1948-49) Glacial-meteorological investigations on the Karsa Glacier in Swedish Lapland, 1942-48, Geografiska Annaler.

171. Wark, D.Q. et al. (1962) Methods of estimating infrared flux and surface temperature from meteorological satellites, Journal of Atmospheric Science, vol. 19, p. 369-384.

172. Watts, D.; Galloway, J.H. and Grenier, A. (1960) Evapotranspiration studies at Knob Lake in the summers of 1957, 1958 and 1959, Publication in Meteorology, no. 22, McGill University.

173. Weaver, J.E. and Clements, F.E. (1938) Plant ecology, New York: McGraw Hill, 601 p.

174. Wilson, R.K. (1959) An attempt to measure the water vapor divergence over Greenland by direct application of radiosonde data, Department of Meteorology and Climatology, University of Washington, Sc. Report no. 3.

175. Yakovlev, G.N. (1955) "The thermal regime of the ice cover" in Observational data of the scientific research drift station 1950-51, by M.M. Somov, vol. 2, Section 7, p. 1-18 and tables.

176. Kasten, F. (1964) A new table and approximation formula for the relative optical air mass, U. S. Army CRREL, Technical Report 136.

177. MacDonald, V. (1963) An atlas of total ozone distribution, October 1958-September 1959, Publication in Meteorology, no. 61, McGill University.

SELECTED BIBLIOGRAPHY (Cont'd)

178. Aitken, G.W. (1962 to 1964) Ground temperature observations Fort Yukon, Aniak, Galena, McGrath, Big Delta and Northway, Alaska, USA CRREL, Technical Reports 100-104 and 107.

179. Pivovarova, Z.I. (1961) Radiation regime of the territory of the USSR, Gidrometeorizdat, Leningrad.

180. ______________ (1962) Characteristic of the radiation regime in the territory of the USSR in the period of IGY, Institute of Geology and Geography, Academy of Science Lith.S.S.R., Scientific Proceedings, XIII, p. 227.

181. Kondrat'iev, K.Y.; Gaevskaya, G.N. and Nicolsky, G.A. (1963) Experimental investigations of the radiation balance in the free atmosphere, Problems of Atmospheric Physics, p. 17, Leningrad State University.

182. Marshunova, M.S. (1961) Main regularities of the radiation balance of the underlying surface and the atmosphere in the Arctic, Proceedings of Arctic and Antarctic Institute, 229, p. 5.

183. DePercin, F. and Falkowski, S. (1956) Topoclimatic study, Fort Churchill, Canada, H.Q. Quartermaster Research and Engineering Command, U. S. Army Technical Report EP-38, Natick, Mass.

184. DePercin, F. (1960) Microclimatology of a sub-arctic spruce forest and a clearing at Big Delta, Alaska, H.Q. Quartermaster Research and Engineering Command, U. S. Army Technical Report EP-130.

185. Nordberg, W. (1965) Geophysical observations from Nimbus I, Science, vol. 150, no. 3696, p. 559-572.

January 11-14, 1959: Penetration of cyclones into the Siberian Arctic from the Sea of Okhotsk and central Europe (Fig. A1)

From January 6, with the development of the largest cell of the vortex over Eastern Asia, successive cyclones "jumped" over northeastern Siberia from the Sea of Okhotsk into the Arctic Basin, under the strong southerly flow aloft; over the northern coast of Siberia they deepened, moved in below the upper cold centers and soon disappeared from the surface chart. These sequences continued until the middle of the month. These charts for January 11-14 illustrate the situation.

The cyclone over the central Arctic on January 11 previously entered from the Pacific. By January 12 it has filled at the surface and a new low is in the process of crossing northeastern Siberia. Deepening on January 13, it then wobbles towards the west, under the vortex center, and has lost its identity by January 16.

Cyclones associated with the European trough move across northern Siberia. On January 12, as the Siberian anticyclone begins to intensify, the storms move into the Barents Sea and along the Siberian coast beyond Novaya Zemlya to give a belt of cyclonic activity, contrasting with the predominantly anticyclonic conditions of the North American Arctic. Weak disturbances cross the American subarctic, but by January 14, a strong anticyclonic center is again located over the Yukon.

January 19-21, 1959 (Fig. A2)

The charts show strengthening zonal flow over Eurasia, with the jet stream to the north of 50°N and associated with strong cyclonic activity over Siberia and northwest Europe. Over the Western Hemisphere strong meridional conditions are predominant. The strong ridge over Alaska is reflected in the surface anticyclone centered over the Yukon on January 19, with a shift to the Beaufort Sea on January 21, where it persists for several days. The deep vortex center over North America caps a deep cold surface low on January 19, which is stalled between the Pacific and Atlantic ridges. Although the January 21 charts show a weakened situation, a well-developed frontal cyclone moving round the trough from Texas feeds in and rapidly regenerates this low in the next two days. The Atlantic ridge, firmly entrenched over Greenland since early January, is weakening and gradually shifting eastward towards Scandinavia. By January 24, the North American low center has also moved eastward with an extension over southern Greenland into the North Atlantic and for the first time this month cyclones move northeastward across the Atlantic into the Arctic basin.

February 15-17 (Fig. A3)

Two features are outstanding on these 500-mb and sea-level charts: first, the severe contraction of the circumpolar vortex with strong westerly flow over Arctic and subarctic regions – this is well-defined at 500 mb on February 17; and second, the accompanying intense cyclonic activity over the inner Arctic, the storms entering in quick succession from the western Atlantic.

Towards the end of January the persistent Atlantic ridge over Greenland at last weakened and shifted eastward to western Europe resulting in a strong southwesterly airstream aloft over the North Atlantic below which storms were directed into the Arctic basin. These synoptic maps show a sequence of such storms. In this example, the cyclones are particularly intense as the vortex is contracted with the belt of strongest westerly flow in high latitudes and the strong temperature contrasts over the pack ice and warm Atlantic waters serve to revitalize the systems.

Over the Pacific weak storms are crossing the Bering Strait and northwestern Alaska into the central Arctic under the strong upper flow between the Asian trough and Alaskan ridge. The sea level charts for February 15 and 16 show these weak frontal systems moving down over northern Alaska and the Barren Grounds towards the extreme north of the Labrador peninsula, where on February 16 a small cold low is in evidence at 500 mb. At the same time low systems are crossing the Rockies over southern Canada, deepening over Alberta in the lee of the mountains, and then moving rapidly northeastwards towards Ungava, where by February 17 a deep cold upper low has developed.

On February 17 there is truly a circumpolar vortex, with cyclonic activity dominating the Arctic Basin, and anticyclones centered over western Europe and northwestern North America in association with the Atlantic and Pacific ridges.

July 19-22, 1956* (Fig. A4)

During July 1956, a well-defined upper vortex center lay over the Arctic Basin, making a complete rotation within the month. The frequency and position of the storm tracks over the Arctic and subarctic depended on the nature of its progression. In the first three days of July there was a rapid shift in emphasis from the Atlantic quadrant towards the East Siberian Sea, where it remained quasi-stationary until the middle of the month, then deepened and drifted over the Beaufort Sea. Here it oscillated until July 19 when there was a weakening and an eastward move towards Greenland, July 22. By July 26, the center was again oriented towards northeast Siberia and on July 31 a single major center again lay over the East Siberian Sea.

The surface charts show a high frequency of storm tracks along the coastal and subarctic regions of northeastern Siberia, Alaska and northwestern Canada with a maximum frequency of centers over the Arctic ocean to the north (180° longitude). During the entire month, high pressure dominated the area from Greenland over the Barents Sea to the Taimyr Peninsula.

The charts for July 19 and 22 illustrate a period of change during the month, when the vortex center lay off the Canadian coast. Concomitant with the eastward shift of this center is the relaxing of the upper ridges over the Atlantic and western North America, and the subsequent southward shift of the storm tracks over northeastern Siberia, Alaska and the MacKenzie Basin. The surface map of July 22 also illustrates two frequent features of the summer pressure distribution: the high center over the Beaufort Sea and lower MacKenzie, and the low system over Baffin Bay.

* Reed has made a special study of the circulation and weather over the North American Arctic in July 1956, published in the Reports of the Department of Meteorology and Climatology, University of Washington, under AF contract 19(604)-3063, 1959.

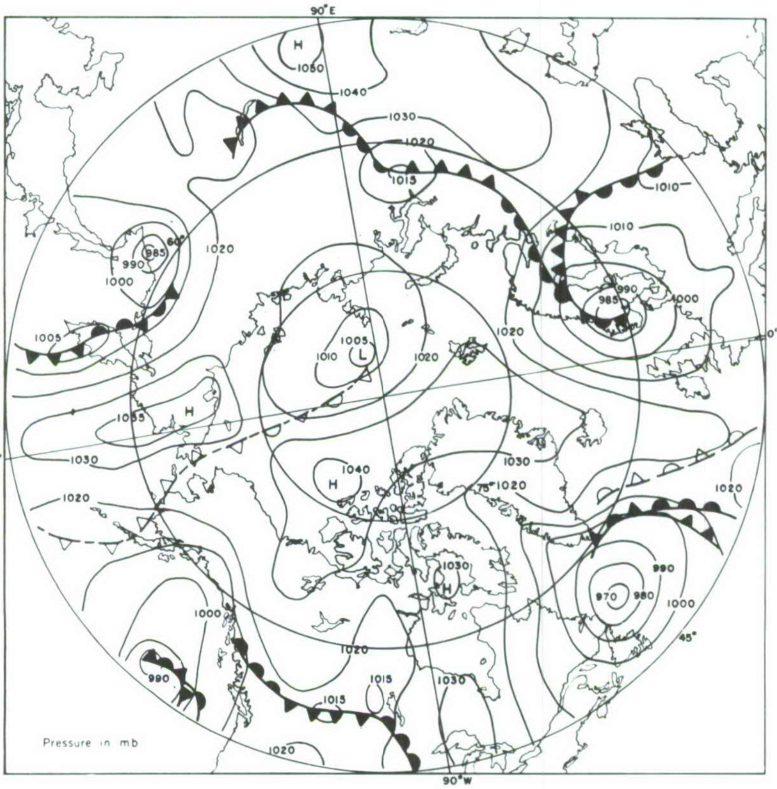

a. Sea level, 1230Z, 11 January 1959.

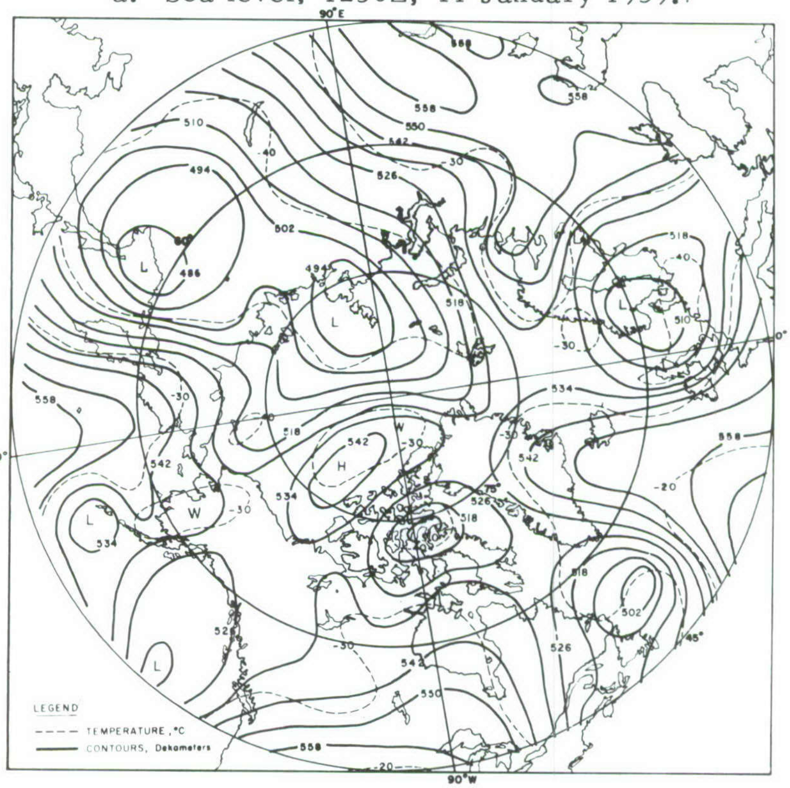

b. 500 mb, 1200Z, 11 January 1959.

Figure A1. Examples of movements of weather systems, 11-14 January 1959.

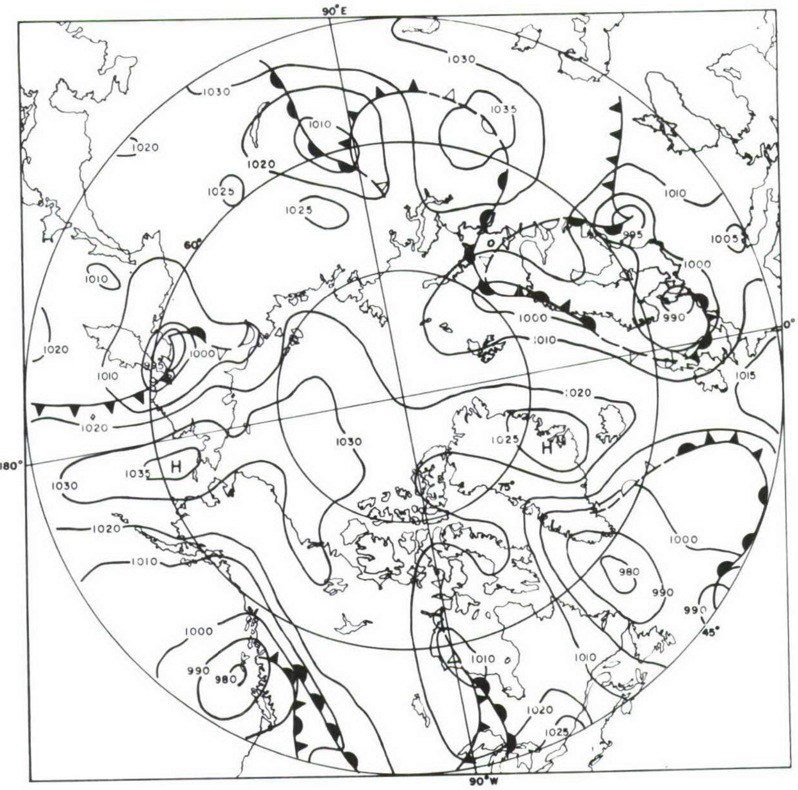

c. Sea level, 1230 Z, 12 January 1959.

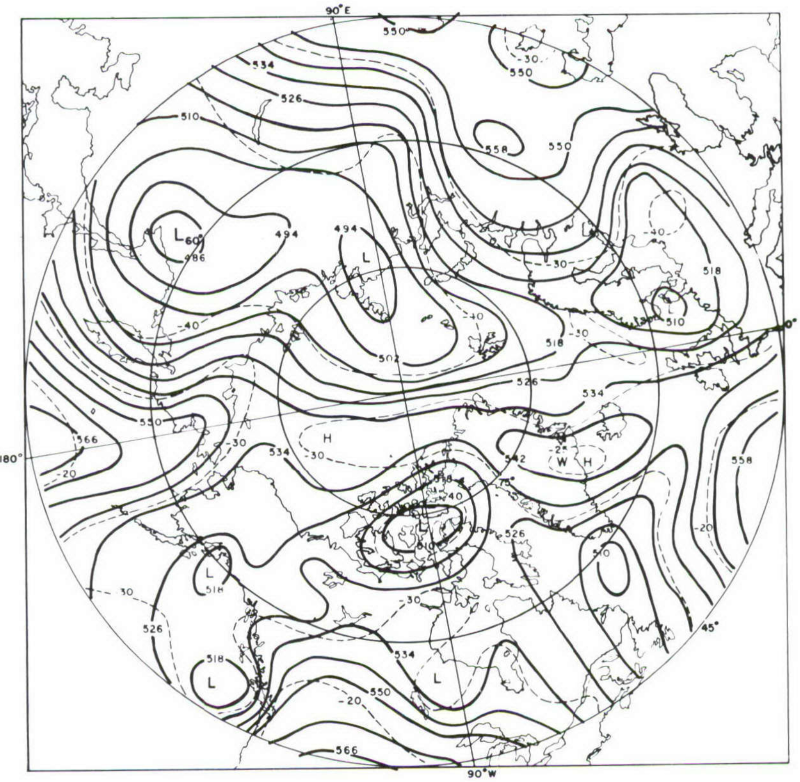

d. 500 mb, 1200 Z, 12 January 1959.

Figure A1 (Cont'd). Examples of movements of weather systems, 11-14 Jan 1959.

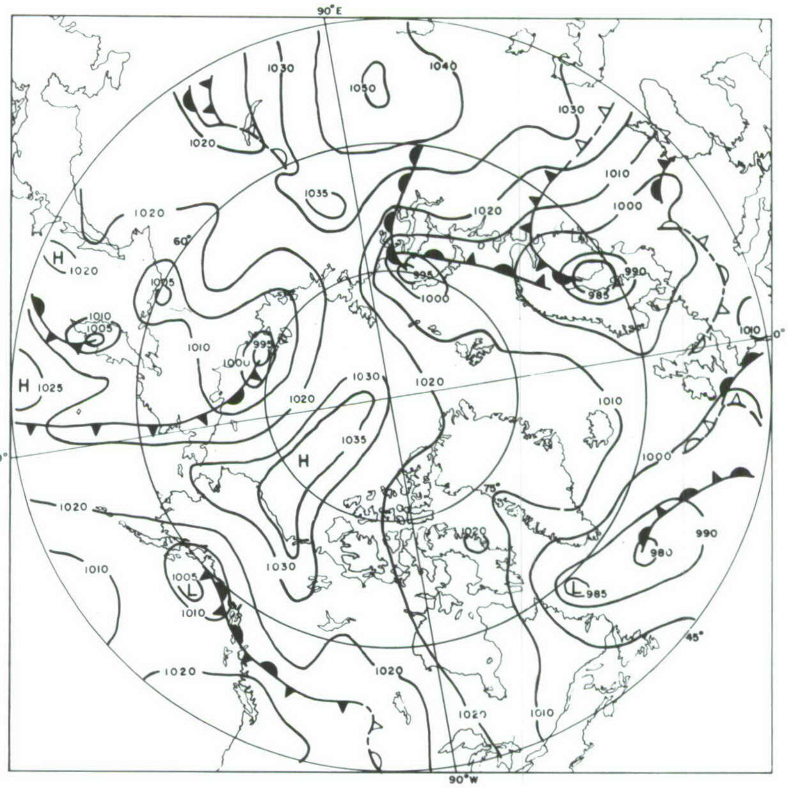

e. Sea level, 1230Z, 13 January 1959.

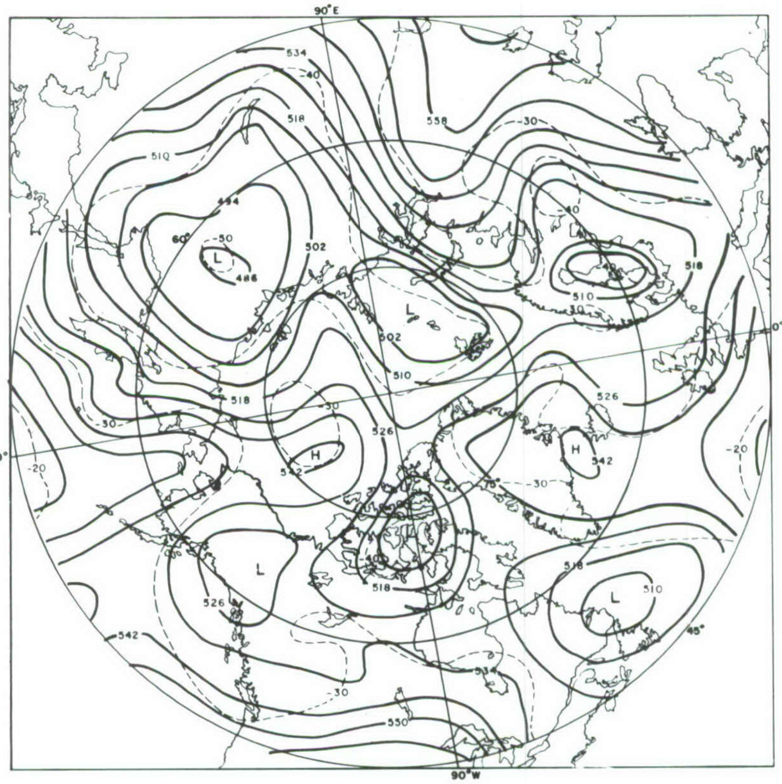

f. 500 mb, 1200Z, 13 January 1959.

Figure A1 (Cont'd). Examples of movements of weather systems, 11-14 Jan 1959.

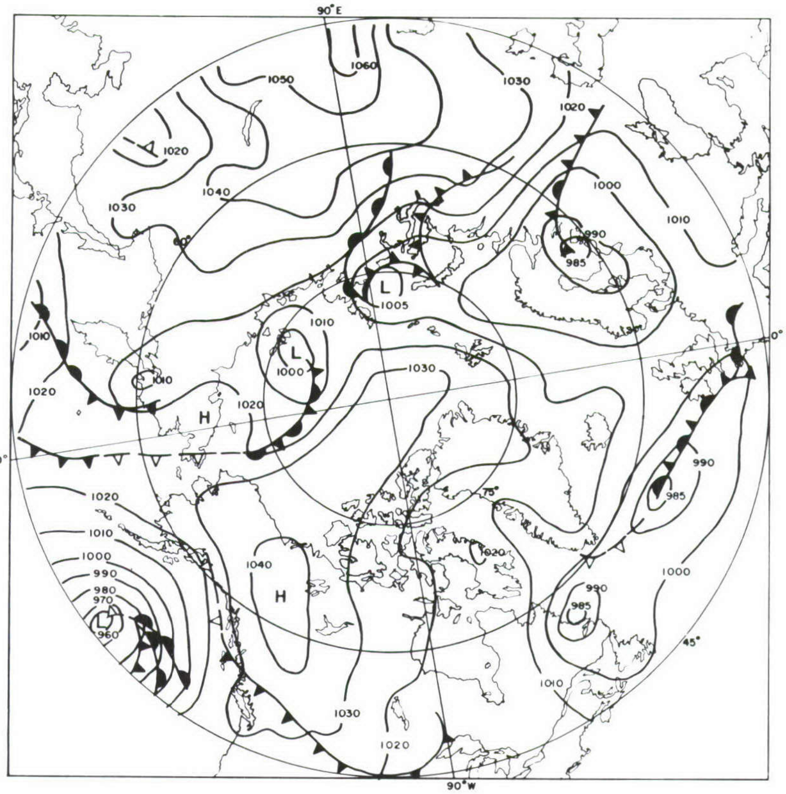

g. Sea level, 1230Z, 14 January 1959.

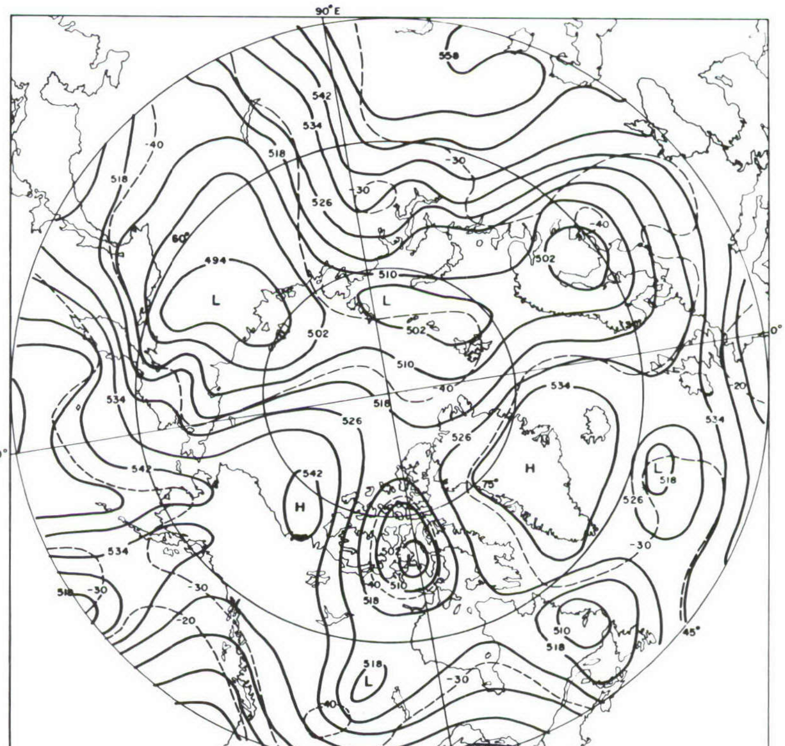

h. 500 mb, 1200Z, 14 January 1959.

Figure A1 (Cont'd). Examples of movements of weather systems, 11-14 Jan 1959.

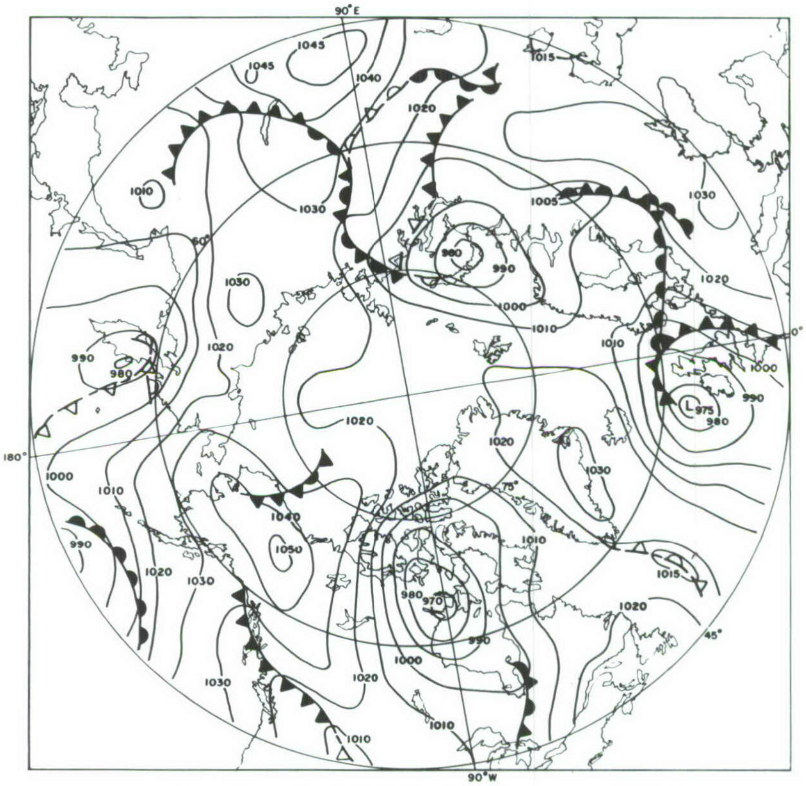

a. Sea level, 1230Z, 19 January 1959.

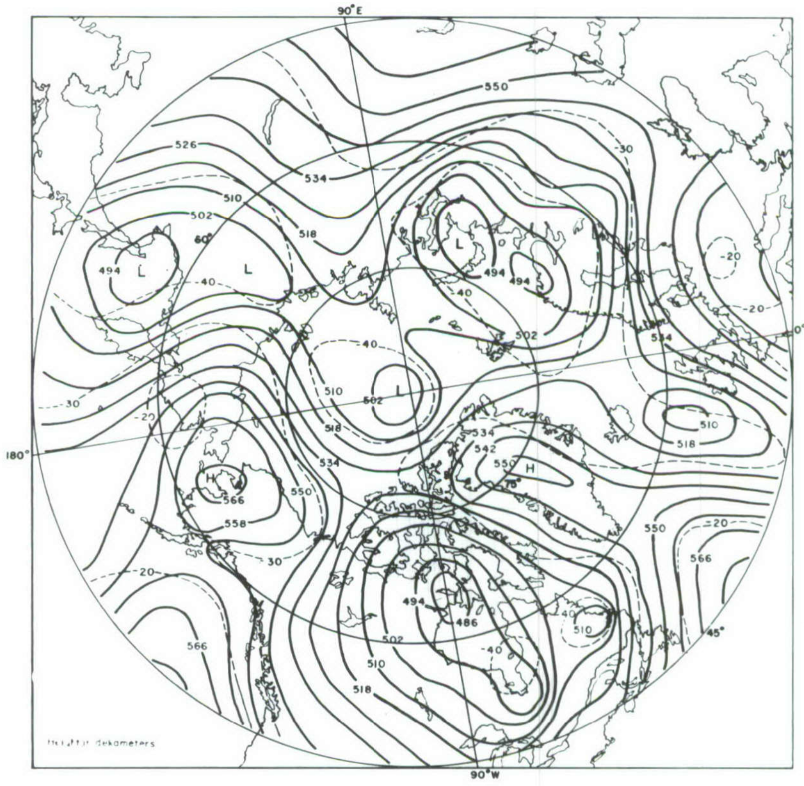

b. 500 mb, 1200Z, 19 January 1959.

Figure A2. Examples of movements of weather systems, 19-21 January 1959.

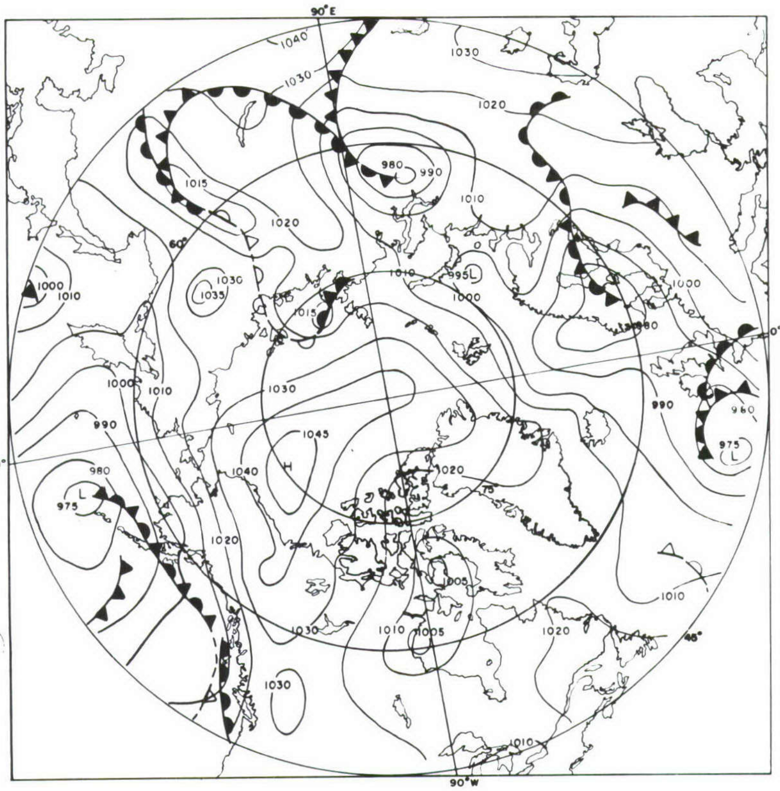

c. Sea level, 1230Z, 21 January 1959.

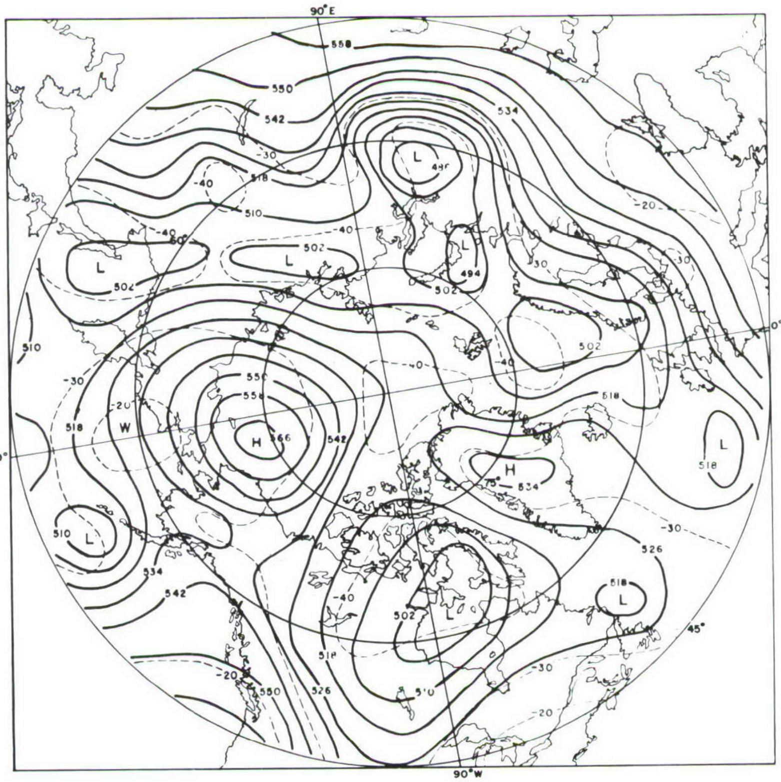

d. 500 mb, 1200Z, 21 January 1959.

Figure A2 (Cont'd). Examples of movements of weather systems, 19-21 Jan 1959.

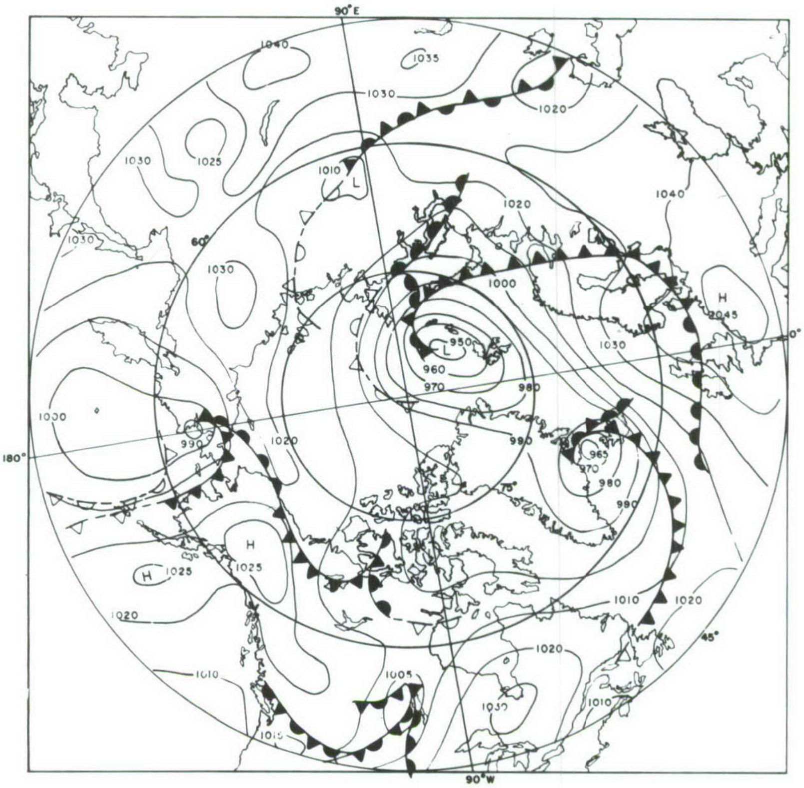

a. Sea level, 1230Z, 15 February 1959.

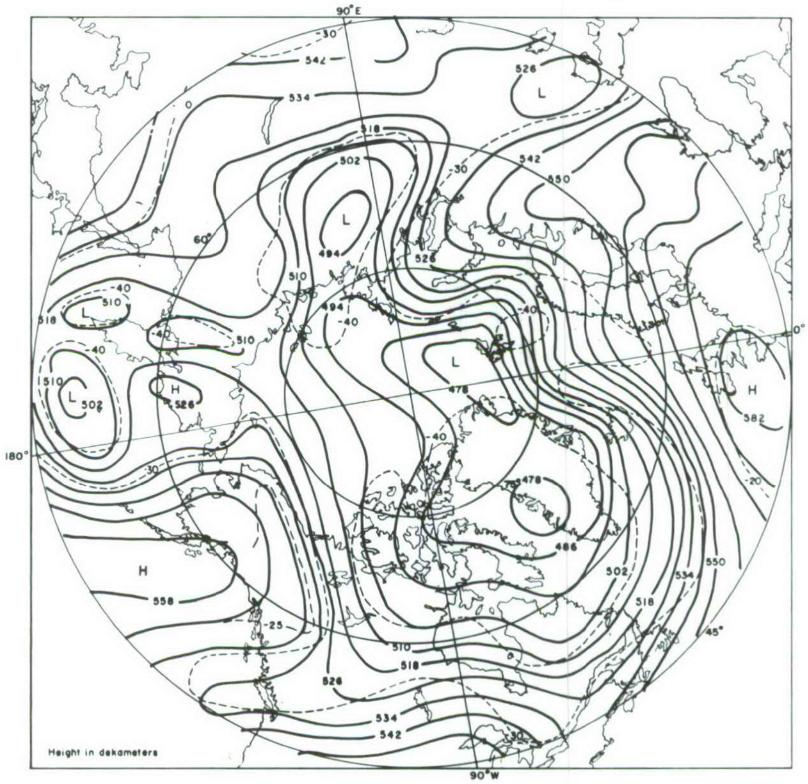

b. 500 mb, 1200Z, 15 February 1959.

Figure A3. Examples of movements of weather systems, 15-17 February 1959.

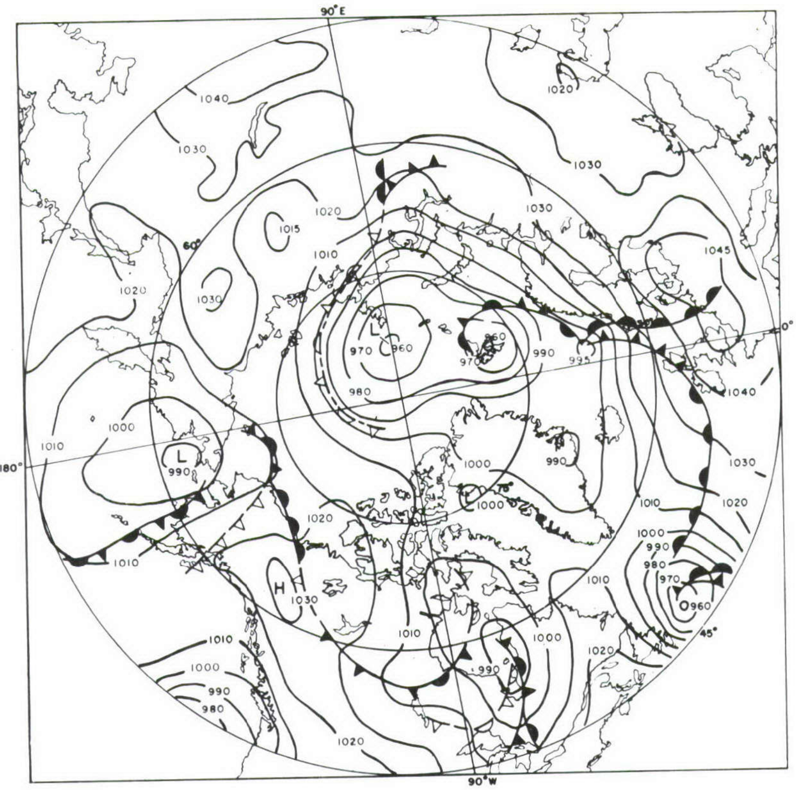

c. Sea level, 1230Z, 16 February 1959.

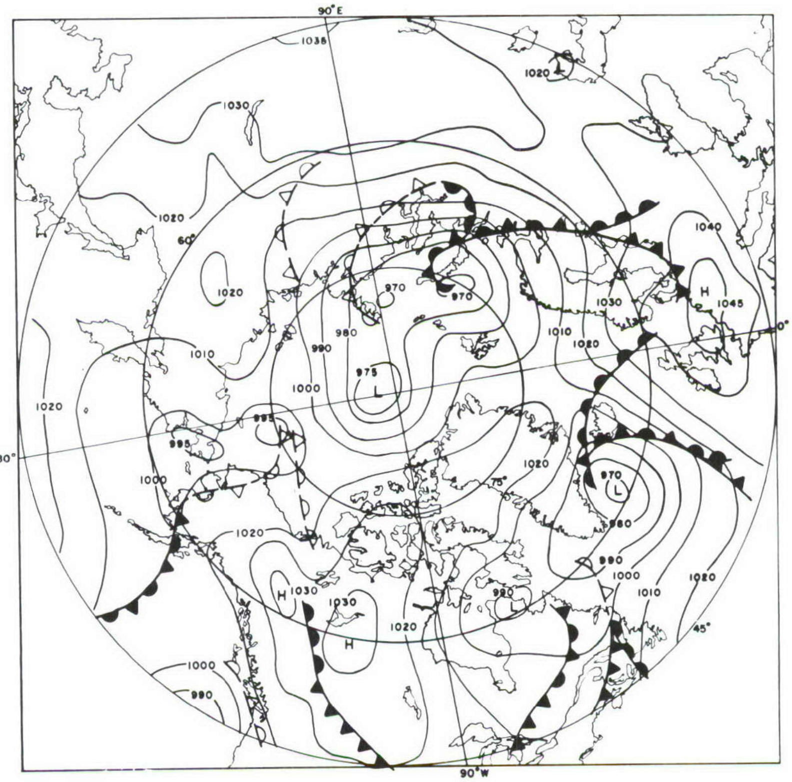

d. Sea level 1230Z, 17 February 1959.

Figure A3 (Cont'd). Examples of movements of weather systems, 15-17 Feb 1959.

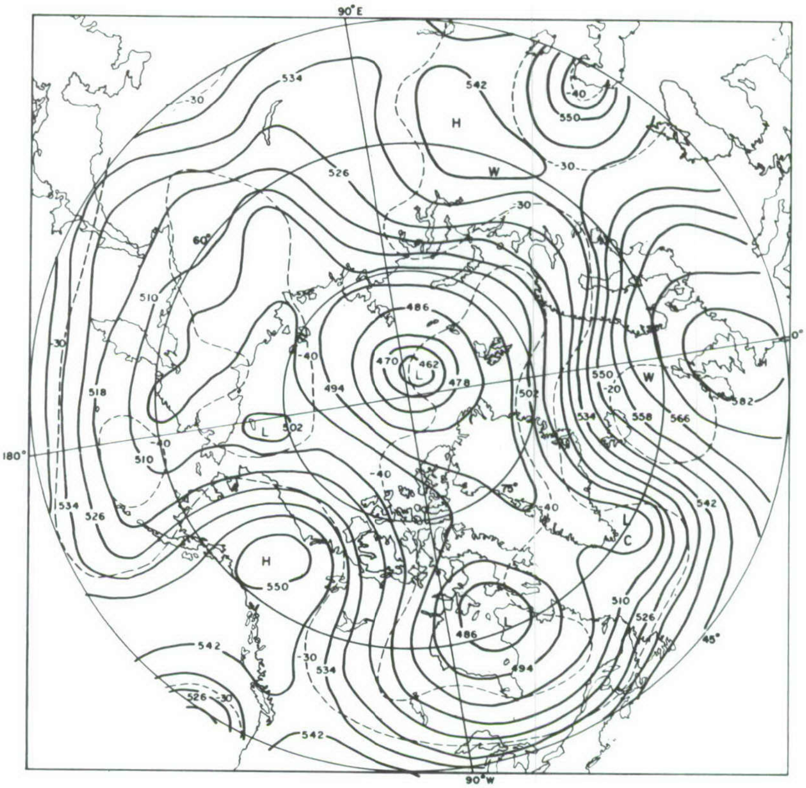

e. 500 mb, 1200Z, 17 February 1959.

Figure A3 (Cont'd). Examples of movements of weather systems, 15-17 Feb 1959.

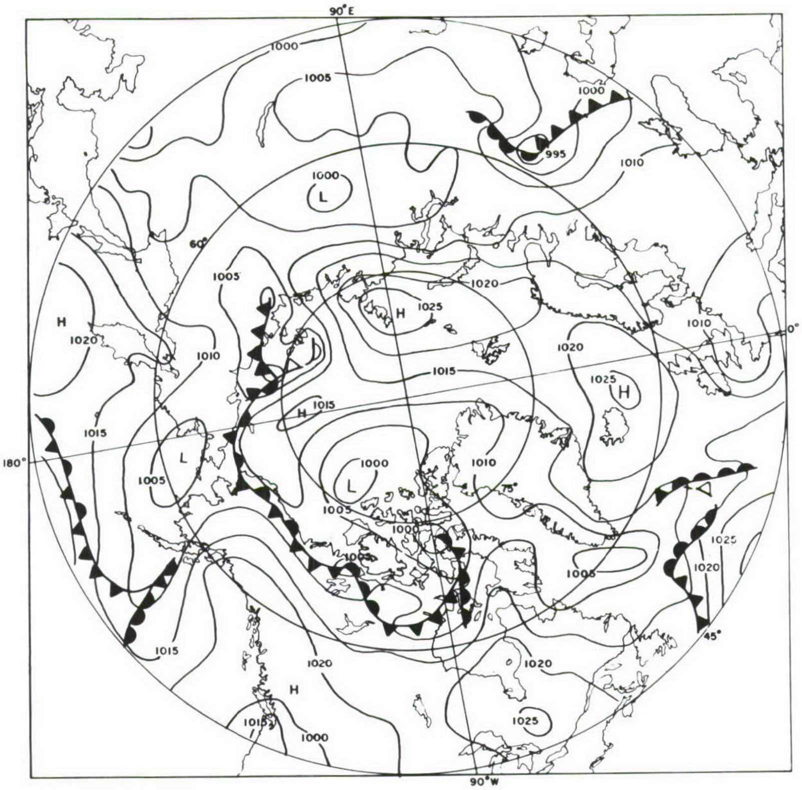

a. Sea level, 1230Z, 19 July 1956.

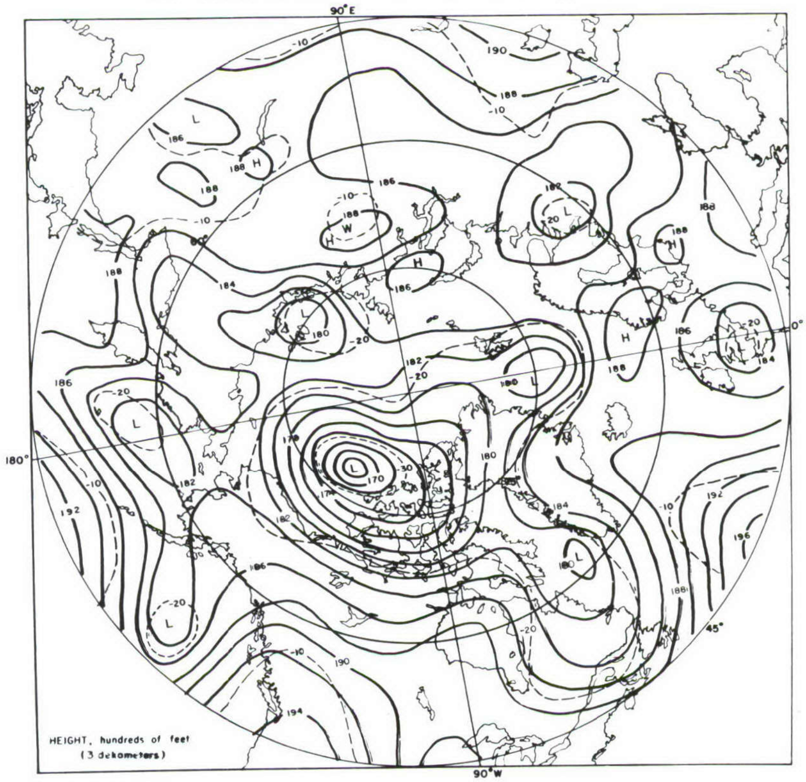

b. 500 mb, 1500Z, 19 July 1956.

Figure A4. Examples of movements of weather systems, 19-22 July 1956.

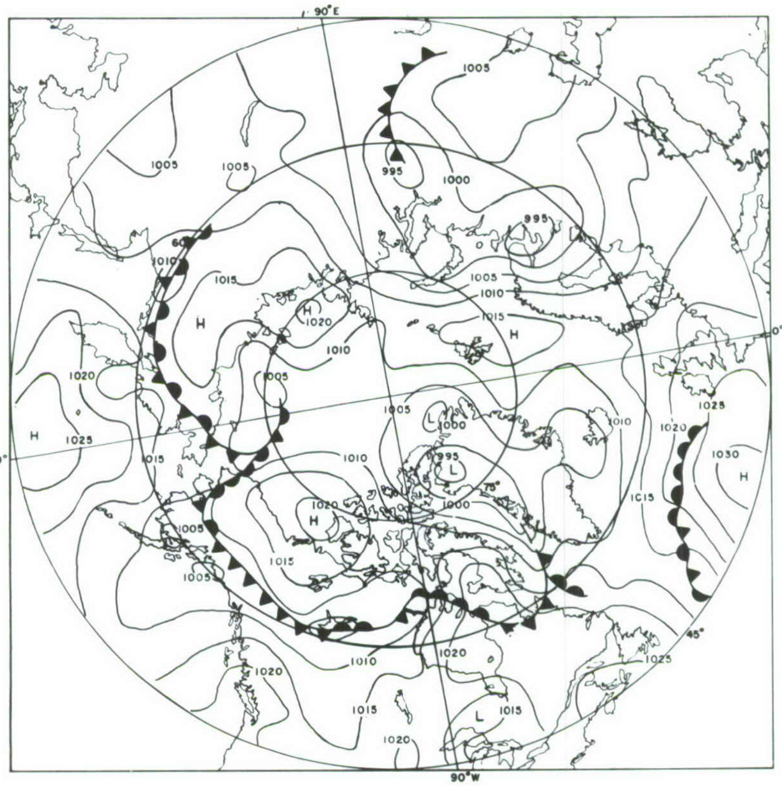

c. Sea level, 1230Z, 22 July 1956.

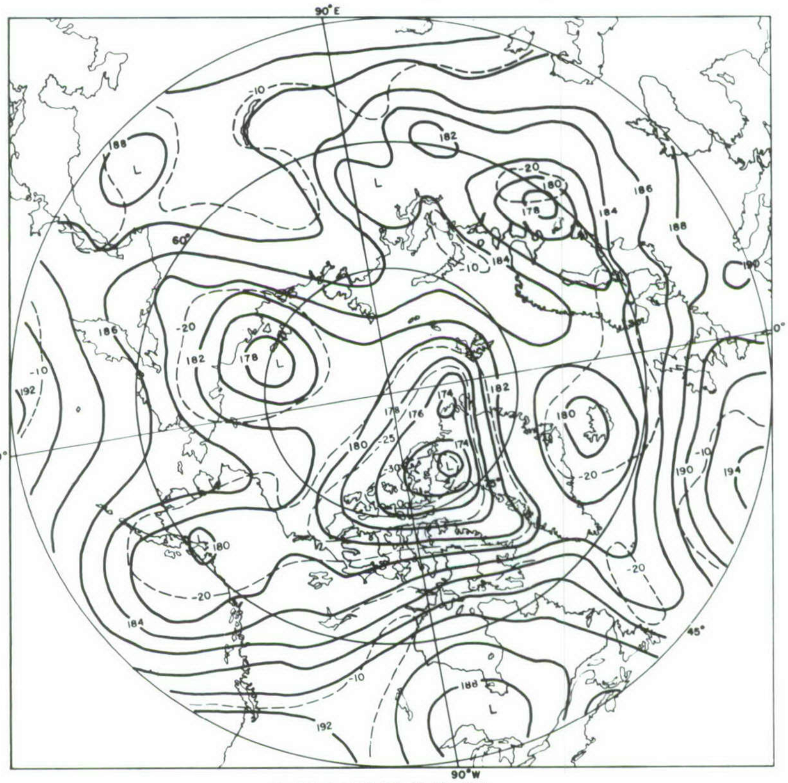

d. 500 mb, 1500 GMT, 22 July, 1956

d. 500 mb, 1500Z, 22 July 1956.

Figure A4 (Cont'd). Examples of movements of weather systems, 19-22 July 1956.

APPENDIX B: DURATION OF DAYLIGHT AND SUN'S ALTITUDE, FROM 60°N TO THE POLE

(After P. Larsson and S. Orvig (1962) Albedo of arctic surfaces, Publication in Meteorology No. 54, McGill University, Montreal.)

60°N

Month	Date	Altitude*	Duration of daylight† hr.	min.	Duration of sun below 20° hr.	min.	Duration of sun above 20° hr.	min.
Jan	1	6° 54'	6	00	6	00	0	00
	15	8 40	6	45	6	45	0	00
Feb.	1	12 34	8	00	8	00	0	00
	15	16 55	9	00	9	00	0	00
March	1	22 20	10	30	9	30	1	00
	15	27 47	11	45	8	30	3	15
	21	30 09	12	00	8	00	4	00
April	1	34 28	13	15	7	45	5	30
	15	39 41	14	30	7	15	7	15
May	1	45 01	16	00	7	00	9	00
	15	48 49	17	15	7	00	10	15
June	1	52 01	18	15	7	00	11	15
	15	53 18	18	45	7	00	11	45
	21	53 26	19	00	7	00	12	00
July	1	53 08	18	45	7	00	11	45
	15	51 34	18	00	7	00	11	00
August	1	48 05	16	45	7	00	9	45
	15	44 08	15	45	6	45	9	00
Sept.	1	38 22	14	15	7	30	6	45
	15	33 07	13	00	7	45	5	15
	23	30 01	12	00	8	00	4	00
Oct.	1	26 54	11	30	8	30	3	00
	15	21 34	10	15	9	30	0	45
Nov.	1	15 38	8	45	8	45	0	00
	15	11 34	7	30	7	30	0	00
Dec.	1	8 14	6	30	6	30	0	00
	15	6 45	6	00	6	00	0	00
	22	6 33	5	45	5	45	0	00

* Elevation of the sun above the horizon at noon.

† Approximate duration of daylight (upper limb of the sun apparently on or above the astronomical horizon).

65°N

Month	Date	Altitude	Duration of daylight hr.	min.	Duration of sun below 20° hr.	min.	Duration of sun above 20° hr.	min.
Jan.	1	11° 54'	3	45	3	45	0	00
	15	3 40	4	30	4	30	0	00
Feb.	1	7 34	6	15	6	15	0	00
	15	11 55	8	00	8	00	0	00
March	1	17 20	9	45	9	45	0	00
	15	22 47	11	30	10	00	1	30
	21	25 09	12	00	9	00	3	00
April	1	29 28	13	15	9	00	4	15
	15	34 41	15	00	8	45	6	15
May	1	40 01	17	00	8	30	8	30
	15	43 49	18	30	8	30	10	00
June	1	47 01	20	15	8	30	11	45
	15	48 18	22	30	9	15	13	15
	21	48 26	22	45	9	30	13	15
July	1	48 08	22	15	9	15	13	00
	15	46 34	20	30	8	45	11	45
August	1	43 05	18	30	8	30	10	00
	15	39 08	16	30	8	30	8	00
Sept.	1	33 22	14	45	8	45	6	00
	15	28 07	13	00	9	15	3	45
	23	25 01	12	00	9	30	2	30
Oct.	1	21 54	11	15	10	15	1	00
	15	16 34	9	45	9	45	0	00
Nov.	1	10 38	7	45	7	45	0	00
	15	6 34	6	00	6	00	0	00
Dec.	1	3 14	4	30	4	30	0	00
	15	1 45	3	15	3	15	0	00
	22	1 33	3	00	3	00	0	00

70°N

Month	Date	Altitude	Duration of daylight hr.	Duration of daylight min.	Duration of sun below 20° hr.	Duration of sun below 20° min.	Duration of sun above 20° hr.	Duration of sun above 20° min.
Jan.	1	- 3°06'	0	00	-	-	0	00
	15	- 1 20	0	00	-	-	0	00
Feb.	1	+ 2 34	4	15	4	15	0	00
	15	6 55	7	00	7	00	0	00
March	1	12 20	9	15	9	15	0	00
	15	17 47	11	30	11	30	0	00
	21	20 09	12	00	12	00	0	00
April	1	24 28	13	45	11	15	2	30
	15	29 41	16	00	10	45	5	15
May	1	35 01	18	15	10	30	7	45
	15	38 49	21	45	11	15	10	30
June	1	42 01	24	00	10	45	13	15
	15	43 18	24	00	10	00	14	00
	21	43 26	24	00	10	00	14	00
July	1	43 08	24	00	10	00	14	00
	15	41 34	24	00	11	00	13	00
August	1	38 05	22	00	11	30	10	30
	15	34 08	18	00	10	30	7	30
Sept.	1	28 22	15	30	11	00	4	30
	15	23 07	13	30	11	45	1	45
	23	20 01	12	00	12	00	0	00
Oct.	1	16 54	11	15	11	15	0	00
	15	11 34	9	00	9	00	0	00
Nov.	1	5 38	6	45	6	45	0	00
	15	1 34	3	45	3	45	0	00
Dec.	1	- 1 46	0	00	-	-	0	00
	15	- 3 15	0	00	-	-	0	00
	22	- 3 27	0	00	-	-	0	00

75°N

Month	Date	Altitude	Duration of daylight hr.	Duration of daylight min.	Duration of sun below 20° hr.	Duration of sun below 20° min.	Duration of sun above 20° hr.	Duration of sun above 20° min.
Jan.	1	- 8° 06'	0	00	-	-	0	00
	15	- 6 20	0	00	-	-	0	00
Feb.	1	- 2 26	0	00	-	-	0	00
	15	+ 1 55	4	15	4	15	0	00
March	1	7 20	8	00	8	00	0	00
	15	12 47	11	00	11	00	0	00
	21	15 09	12	00	12	00	0	00
April	1	19 28	13	45	13	45	0	00
	15	24 41	17	00	13	45	3	15
May	1	30 01	22	00	14	45	7	15
	15	33 49	24	00	13	00	11	00
June	1	37 01	24	00	10	30	13	30
	15	38 18	24	00	9	15	14	45
	21	38 26	24	00	9	15	14	45
July	1	38 08	24	00	9	30	14	30
	15	36 34	24	00	10	45	13	15
August	1	33 05	24	00	13	30	10	30
	15	29 08	21	00	14	30	6	30
Sept.	1	23 22	16	45	14	15	2	30
	15	18 07	13	45	13	45	0	00
	23	15 01	12	00	12	00	0	00
Oct.	1	11 54	10	45	10	45	0	00
	15	6 34	7	15	7	15	0	00
Nov.	1	0 38	2	30	2	30	0	00
	15	- 3 26	0	00	-	-	0	00
Dec.	1	- 6 46	0	00	-	-	0	00
	15	- 8 15	0	00	-	-	0	00
	22	- 8 27	0	00	-	-	0	00

80°N

Month	Date	Altitude	Duration of daylight hr.	Duration of daylight min.	Duration of sun below 20° hr.	Duration of sun below 20° min.	Duration of sun above 20° hr.	Duration of sun above 20° min.
Jan.	1	-13° 06'	0	00	-	-	0	00
	15	-11 20	0	00	-	-	0	00
Feb.	1	- 7 26	0	00	-	-	0	00
	15	- 3 05	0	00	-	-	0	00
March	1	+ 2 20	5	30	5	30	0	00
	15	7 47	10	30	10	30	0	00
	21	10 09	12	00	12	00	0	00
April	1	14 28	15	30	15	30	0	00
	15	19 41	23	00	23	00	0	00
May	1	25 01	24	00	18	00	6	00
	15	28 49	24	00	13	30	10	30
June	1	32 01	24	00	9	30	14	30
	15	33 18	24	00	8	00	16	00
	21	33 26	24	00	8	00	16	00
July	1	33 08	24	00	8	15	15	45
	15	31 34	24	00	10	00	14	00
August	1	28 05	24	00	14	15	9	45
	15	24 08	24	00	19	00	5	00
Sept.	1	18 22	20	00	20	00	0	00
	15	13 07	14	30	14	30	0	00
	23	10 01	12	00	12	00	0	00
Oct.	1	6 54	10	00	10	00	0	00
	15	1 34	4	15	4	15	0	00
Nov.	1	- 4 22	0	00	-	-	0	00
	15	- 8 26	0	00	-	-	0	00
Dec.	1	-11 46	0	00	-	-	0	00
	15	-13 15	0	00	-	-	0	00
	22	-13 27	0	00	-	-	0	00

85°N

Month	Date	Altitude	Duration of daylight hr.	Duration of daylight min.	Duration of sun below 20° hr.	Duration of sun below 20° min.	Duration of sun above 20° hr.	Duration of sun above 20° min.
Jan.	1	-18° 06'	0	00	-	-	0	00
	15	-16 20	0	00	-	-	0	00
Feb.	1	-12 26	0	00	-	-	0	00
	15	- 8 05	0	00	-	-	0	00
March	1	- 2 40	0	00	-	-	0	00
	15	+ 2 47	8	30	8	30	0	00
	21	5 09	12	00	12	00	0	00
April	1	9 28	19	30	19	30	0	00
	15	14 41	24	00	24	00	0	00
May	1	20 01	24	00	24	00	0	00
	15	23 49	24	00	14	45	9	15
June	1	27 01	24	00	7	15	16	45
	15	28 18	24	00	4	00	20	00
	21	28 26	24	00	3	45	20	15
July	1	28 08	24	00	4	30	19	30
	15	26 34	24	00	8	15	15	45
August	1	23 05	24	00	16	30	7	30
	15	19 08	24	00	24	00	0	00
Sept.	1	13 22	24	00	24	00	0	00
	15	8 07	17	30	17	30	0	00
	23	5 01	12	00	12	00	0	00
Oct.	1	1 54	7	15	7	15	0	00
	15	- 3 26	0	00	-	-	0	00
Nov.	1	- 9 22	0	00	-	-	0	00
	15	-13 26	0	00	-	-	0	00
Dec.	1	-16 46	0	00	-	-	0	00
	15	-18 15	0	00	-	-	0	00
	22	-18 27	0	00	-	-	0	00

90°N

Month	Date	Altitude		Duration of daylight		Duration of sun below 20°		Duration of sun above 20°	
				hr.	min.	hr.	min.	hr.	min.
Jan.	1	-23°	06'	0	00	-	-	0	00
	15	-21	20	0	00	-	-	0	00
Feb.	1	-17	26	0	00	-	-	0	00
	15	-13	05	0	00	-	-	0	00
March	1	- 7	40	0	00	-	-	0	00
	15	- 2	13	0	00	-	-	0	00
	21	+ 0	09	24	00	24	00	0	00
April	1	4	28	24	00	24	00	0	00
	15	9	41	24	00	24	00	0	00
May	1	15	01	24	00	24	00	0	00
	15	18	49	24	00	24	00	0	00
June	1	22	01	24	00	0	00	24	00
	15	23	18	24	00	0	00	24	00
	21	23	26	24	00	0	00	24	00
July	1	23	08	24	00	0	00	24	00
	15	21	34	24	00	0	00	24	00
August	1	18	05	24	00	24	00	0	00
	15	14	08	24	00	24	00	0	00
Sept.	1	8	22	24	00	24	00	0	00
	15	3	07	24	00	24	00	0	00
	23	+ 0	01	24	00	24	00	0	00
Oct.	1	- 3	06	0	00	-	-	0	00
	15	- 8	26	0	00	-	-	0	00
Nov.	1	-14	22	0	00	-	-	0	00
	15	-18	26	0	00	-	-	0	00
Dec.	1	-21	46	0	00	-	-	0	00
	15	-23	15	0	00	-	-	0	00
	22	-23	27	0	00	-	-	0	00

APPENDIX C: EVAPORATION AND SENSIBLE HEAT FLUXES OVER THE POLAR OCEAN AND NORWEGIAN-BARENTS SEA

(From E. Vowinckel and B. Taylor (1964) Evaporation and sensible heat flux over the Arctic Ocean, Publication in Meteorology No. 66, McGill University, Montreal. See also references 165 and 166).

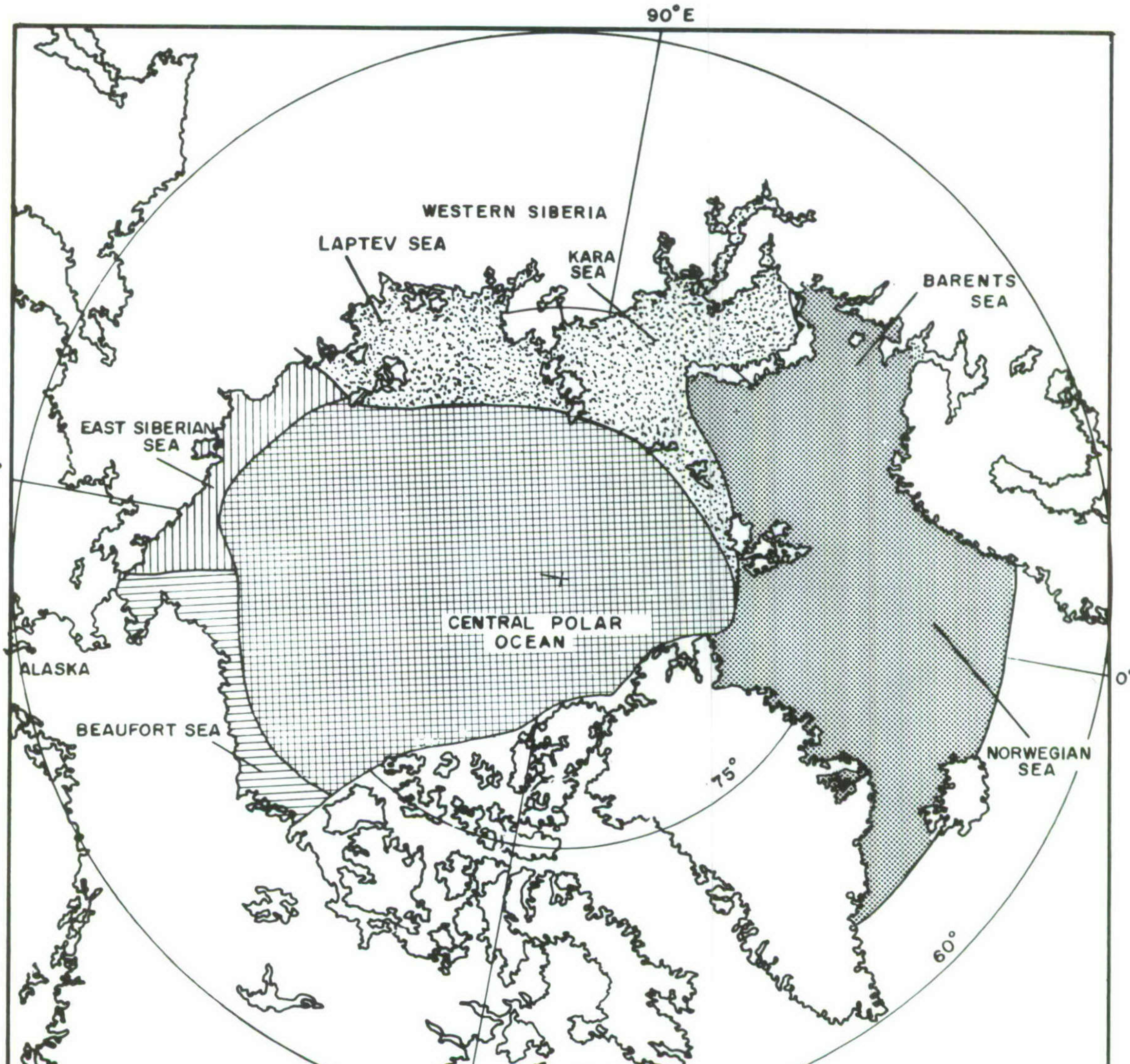

Figure C1. Key map to the study of the evaporation and sensible heat flux over the Arctic Ocean (Vowinckel and Taylor, 1964[163]).

Evaporation (heat) over the Polar Ocean, ly/month (year).

	J	F	M	A	M	J	J	A	S	O	N	D	Year
Central Polar Ocean													
ice	-93	0	0	72	484	450	186	688	648	93	-90	0	2438
water	4427	3679	3943	3258	2009	-270	-651	-93	1872	3329	3996	3683	29182
average	-43	0	0	72	502	437	164	664	693	93	-90	0	2442
West Eurasia													
ice	0	101	112	342	670	1350	614	372	954	372	0	0	4887
water	5831	5032	5041	4446	2650	-360	-948	-78	1073	2421	3672	4697	33477
average	0	101	112	342	670	1307	137	161	1007	901	85	0	4823
East Eurasia													
ice	0	0	0	342	521	486	205	1172	486	316	0	0	3528
water	4873	4032	4166	3438	2083	-198	-205	632	594	2678	3924	3962	29979
average	0	0	0	342	521	481	77	632	584	971	0	0	3608
Alaska													
ice	0	0	74	234	632	252	614	93	918	279	0	74	3170
water	4334	3528	3943	3096	1283	-414	539	186	1098	967	3816	3608	25984
average	0	0	74	234	632	107	587	154	1098	513	0	74	3473
Total Polar Ocean													
average	-66	22	26	146	543	618	169	536	771	315	46	2	3128

Evaporation (heat) over the Norwegian-Barents Sea, ly/month (year).

	J	F	M	A	M	J	J	A	S	O	N	D	Year
80°/75°N													
open ocean	3627	4248	5506	4212	1637	504	-372	74	1728	3608	3636	3720	32128
pack ice water	4111	4855	5171	4590	1693	-234	-651	-911	1404	3776	4176	4594	32574
pack ice	-1399	-588	-595	-72	409	666	56	205	540	-614	-540	-670	-2602
areal average	447	890	911	1512	930	378	-149	-56	1476	2455	2052	1655	12501
75°/70°N													
open ocean	4520	3982	5580	3582	1693	1206	781	1655	2250	3497	3528	3850	36124
pack ice water	4055	4603	4762	2970	1042	-738	-651	-781	1440	3757	3924	3794	28177
pack ice	-2530	-806	-465	-360	1209	234	-186	93	108	-818	-594	-1693	-5808
areal average	3236	2789	3757	2466	1544	900	651	1572	2178	3311	3222	3124	28750
70°/65°N													
open ocean	6863	5107	5915	4320	2213	1098	986	2120	2538	3869	4176	5487	44692
pack ice water	4427	4553	5096	2196	670	-936	-818	-781	1440	3157	3924	3385	26913
pack ice	-3199	-874	-242	-720	1395	-36	-279	93	108	-818	-594	-2790	-7956
areal average	5468	4335	4724	3294	2083	810	763	1827	2502	3850	4068	4874	38598
Total area average	3191	2767	3279	2471	1549	724	464	1197	2088	3249	3174	3290	27443

Sensible heat flux for the Polar Ocean after Shuleikin formulae, ly/month (year).

	J	F	M	A	M	J	J	A	S	O	N	D	Year
Central Polar Ocean													
ice	-124	-56	-62	900	930	630	-31	558	900	0	-150	-124	3371
water	25536	23800	26350	17070	6572	1350	-155	-93	4350	11253	18960	24552	159545
areal average	-124	-56	-62	900	997	654	-35	555	995	0	-60	-63	3701
Kara-Laptev Sea													
ice	-155	-84	-93	900	930	900	-62	-62	900	0	-90	-93	2991
water	21855	19292	21359	14880	6107	-120	-186	-93	690	4650	13410	19313	121157
areal average	-155	-84	-93	900	930	867	-119	-106	806	1200	220	-93	4273
East Siberian Sea													
ice	-155	-56	-62	900	930	900	-124	0	900	0	-60	-62	3111
water	23467	21084	23343	14430	5704	-150	-155	0	90	6572	15240	20894	130519
areal average	-155	-56	-62	900	930	892	-172	0	163	1820	-60	-62	4138
Beaufort Sea													
ice	-124	-56	-62	900	930	-60	-274	-93	900	0	-150	-124	1782
water	23436	30328	22506	14160	2914	-240	0	1209	1080	1395	15690	21266	133744
areal average	-124	-56	-62	900	930	-112	-279	695	1080	474	-60	-62	3324
Total Polar Ocean average	-132	-62	-68	900	978	683	-66	396	926	343	1	-69	3830

Sensible heat flux for the Polar Ocean after Bowen ratio, ly/month (year).

	J	F	M	A	M	J	J	A	S	O	N	D	Year
Central Polar Ocean													
ice					527	390	- 341	372	600				
water	16306	13496	13746	9330	3596	870	-1426	-837	2880	7533	12150	12927	90589
Kara-Laptev Sea													
ice				720	713	780	- 715	-620	690				
water	18476	15624	15655	11520	4495	- 900	-1798	-868	540	3875	10020	13795	90434
East Siberian Sea													
ice				540	558	630	- 992	-124	630				
water	15965	13412	13454	8520	3410	-1380	-1488	-124	60	4619	10290	12276	79014
Beaufort Sea													
ice				510	496	- 420	-3658		600				
water	14446	11508	12679	7740	1612	-2010	- 124	775	690	930	10080	11191	69517

Sensible heat flux for the Norwegian-Barents Sea after Shuleikin formulae, ly/month (year).

	J	F	M	A	M	J	J	A	S	O	N	D	Year
80/75°													
open ocean	8835	10584	12772	7740	2418	120	31	248	1740	4991	7830	7285	64594
pack ice water	11656	13496	13547	10140	3007	-120	- 186	-217	1620	6417	11700	12245	83305
pack ice	-155	-84	-93	900	930	420	- 93	-155	900	0	-60	-62	2448
areal average	3216	3330	3185	3726	1678	154	- 66	93	1566	3736	5177	4356	30151
75/70°													
open ocean	2790	3724	5332	1890	341	240	527	775	870	1364	2580	2790	23223
pack ice water	5425	8064	7967	4350	682	-270	- 217	-248	900	4588	10440	5983	47664
pack ice	- 217	- 112	-93	900	682	-150	- 124	-155	900	0	-60	-93	1478
areal average	2328	2901	3783	1795	430	142	439	726	872	1361	2553	2511	19841
70/65°													
open ocean	2697	2856	3317	1770	527	210	341	558	390	1054	2010	2573	18303
pack ice water	3007	6020	6682	1920	- 93	-300	- 248	-248	900	4588	9720	2449	34597
pack ice	- 279	- 112	-93	900	682	-180	- 155	-155	900	0	-60	-86	1362
areal average	2316	2501	2740	1610	535	130	255	478	400	1089	2123	2378	16545
Total area average	2572	2888	3271	2274	815	141	237	463	910	1936	3147	2984	21638

Sensible heat flux for the Norwegian-Barents Sea after Bowen ratio, ly/month (year).

	J	F	M	A	M	J	J	A	S	O	N	D	Year
80/75°													
open ocean	2585	5342	8221	2718	577	72	- 372	- 93	-846	2120	2844	2589	25757
pack ice water	9170	12230	12927	10098	2251	-666	-1674	-2335	1260	6268	9630	10621	69790
pack ice	-1637	-864	-967	918	670	54	- 539	-1116	504	0	-756	-800	-4533
areal average	368	1694	1707	2877	992	-103	- 745	- 655	799	1941	2287	2099	13261
75/70°													
open ocean	3553	4586	6919	2466	391	-216	- 242	205	828	1414	2790	3050	25744
pack ice water	5859	8635	8835	4266	93	-2070	-1990	-2492	720	4892	8640	5822	41210
pack ice	-2530	-1008	-1097	918	409	-1134	- 874	- 539	342	0	-774	-893	-7180
areal average	2528	3293	4572	2175	374	511	348	281	814	1413	2658	2621	21588
70/65°													
open ocean	4148	3511	4650	1872	316	- 684	- 558	- 223	360	1004	2304	2995	19695
pack ice water	5320	7493	8909	1890	-930	-3222	-2288	-2492	720	4892	8640	3385	32317
pack ice	-3199	-1170	-1172	972	-186	-1458	-1469	- 539	342	0	-774	-1060	-9713
areal average	3216	2942	3629	1702	226	- 965	- 753	- 359	370	1043	2370	2714	16135
Total area average	2150	2729	3459	2216	499	- 546	- 593	- 411	663	1438	2458	2506	16568

Unclassified

Security Classification

DOCUMENT CONTROL DATA - R&D

(Security classification of title, body of abstract and indexing annotation must be entered when the overall report is classified)

1. ORIGINATING ACTIVITY (Corporate author) U. S. Army Cold Regions Research and Engineering Laboratory, Hanover, N.H.	2a. REPORT SECURITY CLASSIFICATION Unclassified 2b. GROUP

3. REPORT TITLE

COLD REGIONS CLIMATOLOGY. INTRODUCTION. NORTHERN HEMISPHERE I

4. DESCRIPTIVE NOTES (Type of report and inclusive dates)

Monograph

5. AUTHOR(S) (Last name, first name, initial)

Wilson, Cynthia

6. REPORT DATE	7a. TOTAL NO. OF PAGES	7b. NO. OF REFS
June 1967	147	323

8a. CONTRACT OR GRANT NO.	9a. ORIGINATOR'S REPORT NUMBER(S) CRSE I-A3a
b. PROJECT NO. c. DA Project 1VO25001A130 d.	9b. OTHER REPORT NO(S) (Any other numbers that may be assigned this report)

10. AVAILABILITY/LIMITATION NOTICES This document is available to U.S. government agencies and their contractors from: Defense Documentation Center. Microfilm or photocopy of this document is available at cost of reproduction from: Clearinghouse for Federal Scientific and Technical Information.

11. SUPPLEMENTARY NOTES	12. SPONSORING MILITARY ACTIVITY U. S. Army Cold Regions Research and Engineering Laboratory

13. ABSTRACT

A review summary of the climatological environment of the Northern Hemisphere contains a general introduction to the cold regions and a discussion of geographic controls and meteorological aspects including: 1) the hemisphere surface in terms of configuration and relief, vegetation zones and permanent and seasonal ice and snow; 2) the general circulation and weather system dealing with the circumpolar vortex, sea-level pressure and cyclonic frequency, circulation system persistence, and surface weather associated with high latitude pressures; 3) the net radiation and heat balance. Selected bibliographic references are given.

DD FORM 1 JAN 64 1473

Unclassified

Security Classification

14. KEY WORDS	LINK A ROLE	LINK A WT	LINK B ROLE	LINK B WT	LINK C ROLE	LINK C WT
Climatology--Northern Hemisphere Atmospheric circulation--Northern Hemisphere Heat transfer--Arctic regions Geography--Arctic regions						

INSTRUCTIONS

1. ORIGINATING ACTIVITY: Enter the name and address of the contractor, subcontractor, grantee, Department of Defense activity or other organization *(corporate author)* issuing the report.

2*a*. REPORT SECURITY CLASSIFICATION: Enter the overall security classification of the report. Indicate whether "Restricted Data" is included. Marking is to be in accordance with appropriate security regulations.

2*b*. GROUP: Automatic downgrading is specified in DoD Directive 5200.10 and Armed Forces Industrial Manual. Enter the group number. Also, when applicable, show that optional markings have been used for Group 3 and Group 4 as authorized.

3. REPORT TITLE: Enter the complete report title in all capital letters. Titles in all cases should be unclassified. If a meaningful title cannot be selected without classification, show title classification in all capitals in parenthesis immediately following the title.

4. DESCRIPTIVE NOTES: If appropriate, enter the type of report, e.g., interim, progress, summary, annual, or final. Give the inclusive dates when a specific reporting period is covered.

5. AUTHOR(S): Enter the name(s) of author(s) as shown on or in the report. Enter last name, first name, middle initial. If military, show rank and branch of service. The name of the principal author is an absolute minimum requirement.

6. REPORT DATE: Enter the date of the report as day, month, year; or month, year. If more than one date appears on the report, use date of publication.

7*a*. TOTAL NUMBER OF PAGES: The total page count should follow normal pagination procedures, i.e., enter the number of pages containing information.

7*b*. NUMBER OF REFERENCES: Enter the total number of references cited in the report.

8*a*. CONTRACT OR GRANT NUMBER: If appropriate, enter the applicable number of the contract or grant under which the report was written.

8*b*, 8*c*, & 8*d*. PROJECT NUMBER: Enter the appropriate military department identification, such as project number, subproject number, system numbers, task number, etc.

9*a*. ORIGINATOR'S REPORT NUMBER(S): Enter the official report number by which the document will be identified and controlled by the originating activity. This number must be unique to this report.

9*b*. OTHER REPORT NUMBER(S): If the report has been assigned any other report numbers *(either by the originator or by the sponsor)*, also enter this number(s).

10. AVAILABILITY/LIMITATION NOTICES: Enter any limitations on further dissemination of the report, other than those imposed by security classification, using standard statements such as:

(1) "Qualified requesters may obtain copies of this report from DDC."

(2) "Foreign announcement and dissemination of this report by DDC is not authorized."

(3) "U. S. Government agencies may obtain copies of this report directly from DDC. Other qualified DDC users shall request through
______________________________."

(4) "U. S. military agencies may obtain copies of this report directly from DDC. Other qualified users shall request through
______________________________."

(5) "All distribution of this report is controlled. Qualified DDC users shall request through
______________________________."

If the report has been furnished to the Office of Technical Services, Department of Commerce, for sale to the public, indicate this fact and enter the price, if known.

11. SUPPLEMENTARY NOTES: Use for additional explanatory notes.

12. SPONSORING MILITARY ACTIVITY: Enter the name of the departmental project office or laboratory sponsoring *(paying for)* the research and development. Include address.

13. ABSTRACT: Enter an abstract giving a brief and factual summary of the document indicative of the report, even though it may also appear elsewhere in the body of the technical report. If additional space is required, a continuation sheet shall be attached.

It is highly desirable that the abstract of classified reports be unclassified. Each paragraph of the abstract shall end with an indication of the military security classification of the information in the paragraph, represented as *(TS)*, *(S)*, *(C)*, or *(U)*.

There is no limitation on the length of the abstract. However, the suggested length is from 150 to 225 words.

14. KEY WORDS: Key words are technically meaningful terms or short phrases that characterize a report and may be used as index entries for cataloging the report. Key words must be selected so that no security classification is required. Identifiers, such as equipment model designation, trade name, military project code name, geographic location, may be used as key words but will be followed by an indication of technical context. The assignment of links, rules, and weights is optional.

Errata - Cold Regions Science and Engineering, Part I, Sect. A3a

p. 1, line 16: for "... temperature of 10C." read "... temperature $\geq$ 10C."

p. 2, Figure 1a legend: after "Southern limit of NORTHERN COLD REGIONS" add "(D + E climates)"
after "Southern limit of ARCTIC CLIMATE" add "(E climates)"

p. 16, para. 4, line 1: for "(Fig. 1b)" read "(Fig. 2a)"

p. 54, Figure 10: add to caption: "(After Reed and Kunkel.[26])"

p. 63, lines 2 and 3 from bottom: for "... 1200 m." read "... 1200 m.[27]"

p. 71, para. 2, line 10: for "... applicable." read "... applicable.[23,25]"

p. 75, line 12: for "> 9.9%" read "> 9%"

p. 99, para. 1, line 7: for "1956 to 1957" read "1956 to 1959"